51559

ACTA UNIVERSITATIS SZEGEDIENSIS

ACTA MINERALOGICA-PETROGRAPHICA

Tomus XXXVII.

SZEGED, HUNGARIA
1996

NOTE TO CONTRIBUTORS

General

The Acta Mineralogica–Petrographica publishes original studies on the field of geochemistry mineralogy and petrology, first of all studies Hungarian researches, papers resulted in by cooperation of Hungarian researches and those of other countries and, in a limited volume, papers from abroad on topics of global interest.

Manuscripts should be written in English and submitted to the Editor-in-chief, Institute of Mineralogy, Geochemistry and Petrography, Attila József University, H–6701 Szeged, Pf. 651 Hungary.

The authors are responsible for the accuracy of their data, references and quotations from other sources.

Manuscript

Manuscript should be typewritten with double spacing, 25 lines on a page and space for 50 letter in a line. Each new paragraph should begin with an indented line. Underline only words that should be typed in italics.

Manuscript should be generally be organized in the following order:

Title
Name(s) of author(s) and their affiliations, in foot-note the address of the author to whom the correspondence should be sent
Abstract
Introduction
Methods, techniques, material studied, description of the area investigated, etc.
Results
Discussion or conclusions
Acknowledgement
Explanation of plates (if any)
Tables
Captions of figures (drawings, photomicrographs, etc.)

Abstract

The abstract cannot be longer than 500 words.

Tables

The tables should be typewritten on separate sheets and numbered according to their sequence in the text, which refers to all tables.

The title of the table as well as the column headings must be brief, but sufficiently explanatory.

The tables generally should not exceed the type-area of the journal, i.e. 12,5x18,5 cm. Foldouts can only exceptionally be accepted.

(continuation on the inner side of verso)

ACTA UNIVERSITATIS SZEGEDIENSIS

ACTA MINERALOGICA-PETROGRAPHICA

Tomus XXXVII.

SZEGED, HUNGARIA
1996

CONTENTS

Acta Mineralogica-Petrographica, Szeged, XXXVII, 5–33, 1996

CASE HISTORIES OF SOME TRANSYLVANIAN GLAUCONIES

D. POP*

I. BEDELEAN*

Department of Mineralogy-Petrometallogeny
Babeş-Bolyai University

ABSTRACT

Several Romanian glaucony-bearing units (Cretaceous, Eocene, Oligocene and Miocene) from the Transylvanian Depression and, for comparision, one Cretaceous outcrop from the post-tectonic cover of the Southern Carpathians were studied from mineralogical, lithological and sedimentological point of view. The study focused on the morphological (as noticed under binocular, polarizing microscope, SEM and TEM-replica method) and the X-ray powder diffraction characteristics of the glauconitic grains.

The general lithological and sedimentological context, as well as data supplied by the mineralogical study of glauconies made possible a preliminary genetical characterization of the green grains (sensu AMOROSI 1993a).

Both Eocene occurrences, Luna de Sus and Ortelec (e.g. samples GE 2, GE 3 resp. GE 5) contain the most evolved glauconies under study: they consist of highly evolved, ordered glauconites (1M). They are considered authigenic, possibly perigenic glauconies.

The Miocene samples (e.g. GM 2, GM 7) from Tihău display a mineralogical variability: GM 2 represents transition from the ordered to the moderately disordered species (1Md) and GM 7 shows the features of moderately disordered glauconite (1Md). Both samples reflect the evolved stage of glauconitization. They are assumed to be perigenic glauconies.

The Cretaceous glauconies from Sebeşel are moderately disordered glauconites (1Md), with a maturity degree between slightly evolved to evolved glauconies (e.g. GC 28). The genetic type is either authigenic or perigenic. The other Cretaceous glauconies from Râşnov (e.g. GC 3) have a more opened and disordered structure: they contain extremely disordered glauconites (1Md) and represent the less evolved glauconies under study (slightly evolved stage). We assume a perigenic origin of these glauconies.

The Oligocene sample (GO 1) from Var displays XRD features which characterize also the extremely disordered glauconites (1Md), but the green grains show an intermediate glauconitization stage, between slightly evolved and evolved. They are transported (detrital/perigenic) glauconies.

INTRODUCTION

The Fe^{3+}-rich phyllosilicate species which form the family of glauconitic minerals are characterized by lamellar or lath-like crystallites (1—6 μm), which generally agglomerate in grains (pellets, or peloids, sensu BATHURST 1975, in FISCHER 1987), of a diameter usually between 100—1000 μm. Very rarely, other facies of glauconitic minerals (such as film habit or diffuse habit) develop, case in which the mineralogical identification is difficult.

* RO-3400 Cluj-Napoca, Kogălniceanu St. 1, Romania

Since the '70s, especially the papers of ODIN underlined the distinction which should be taken between the glauconitic facies — for which the term "glaucony" (plural "glauconies") (ODIN and LÉTOLLE 1978, ODIN and MATTER, 1981) was suggested, and the mineral species of the glauconitic group. The term "glauconite" is strongly recommended to be used only for defining the mineralogical species.

In 1978 the AIPEA Nomenclature Commission established the classifying criteria and redefined the species glauconite (BAILEY 1980). In agreement with this, the glauconitic minerals presented by ODOM (1984) are:

Glauconite s.s. (glauconitic mica, or ordered glauconite) is a dioctahedral, highly Fe^{3+} and K mica, with a generalized chemical formula:

$$K(R^{3+}_{1,33} R^{2+}_{0,67}) (Si_{3,67} Al_{0,33}) O_{10} (OH)_2,$$

where $Fe^{3+} >> Al$ and $Mg > Fe^{2+}$

The structure is of illitic-type, with less than 10 % expandable layers (exp.).

The disordered glauconites (glauconitic mixtures) are interlayered structures of Fe^{3+}-illitic and smectitic type, with 10—20 % exp., and usually 1Md polytype.

The interstratified glauconite/smectite is characterized by low K content, highly disordered structure (1Md or <1Md polytypes) and exp. between 20—60 %.

These minerals reflect the degree of maturity, i.e. the stage reached by the crystallization process. Glauconitic minerals form by neoformation or transformation. The semi-restrictive microenvironment in which the slow cation exchanges led to the glauconitization process are provided by an organic substrate or other minerals (ODIN 1975, ODIN and MATTER 1981).

SAMPLES

Sample selection; geological outline

A wide variety of glauconitic occurrences are to be found in the Transylvanian Depression, located in the central area of Romania (*Fig. 1*).

The Transylvanian Depression represents the result of the superposition of distinctive basins, starting their evolution in the Upper Permian, as a consequence of the existence of several different geological settings (BALINTONI 1996, in press). The glauconitic grains occur in sedimentary sequences formed during three distinctive evolutionary stages:

- the post-Gosau (post-Mediteranean) basin (Upper Cretaceous), displaying generally flysch-type deposits;
- the post-Laramic (Eocene—Oligocene) basin, in which mainly continental and epicontinental sediments formed on the Preapulian craton;
- the post-Meseș basin (Lower Miocene), characterized by marine deposits (Chechiș Beds), followed by molassic formations (Hida Beds).

The final stage of evolution of the Transylvanian Depression is represented by a molassic basin formed subsequently to Hida Beds (Medium Miocene—Pleistocene), in connection with an extension in the Pannonian Basin.

Samples representing this variety of stratigraphic ages, host-rock lithologies and general mineralogic features were collected and studied.

There is only one Cretaceous occurrence belonging to the Transylvanian Depression, the one near Sebeșel, Alba distr. For comparison, Upper Cretaceous samples from the post-Austric tectonic cover of the Southern Carpathians, near Râșnov, Brașov distr. were also studied.

Eocene samples were collected from two profiles of the almost 70 km long glauconi-ny-bearing Căpuşu Formation (Luna de Sus, Cluj distr. — as an extreme south-eastern end; Ortelec, Sălaj distr. — as the north-western end). More samples from the Luna de Sus profile were selected due to the distinctive lithology of the host-rock.

Oligocene age is represented among the samples by the isolated glauconitic occurrence in Var, Sălaj distr.

The most recent glauconitic level under study belongs to the basal part of the Chechiş Beds (Lower Miocene). It outcrops almost continuously from Coruş (Cluj distr.), through Tihău, to Surduc (Sălaj distr.), on about 70 km, as a 0.5–3.5 m thick stratigraphic marker (ŞURARU 1967).

This selection of samples (*Fig. 1*) is representative for the geological and mineralogical complexity of the various Transylvanian glauconitic occurrences. From the 79 studied samples 8 reference samples (Table 1) were selected for further, more detailed investigations (such as FTIR, Mössbauer spectroscopy, wet chemical analyses, REE content and others). The results of these studies will be published elsewhere.

Sample separation

In all the studied samples glauconies display dominantly granular facies, which enables a more accurate separation methodology and, subsequently, a more precise mineralogical investigation of them.

Principally, the procedure suggested by ODIN (1969) was performed (see also POP and BEDELEAN, 1996). The pure glauconitic loose A granulometric fractions (160—500 μm), magnetically separated and finally hand-picked, were submitted to further mineralogic investigations.

METHODS; NOMENCLATURE

The basic mineralogical data on glauconies were obtained using stereoscopic and polarizing microscopy, electron microscopy (SEM, TEM) and X-ray powder diffraction (XRD). Thus, the morphologic features of the green grains and the mineralogical aspects could be noted.

The study under binocular of loose A fractions evidenced the morphological types (as defined by TRIPLEHORN 1966 and completed by MCCONCHIE and LEWIS 1980), the colour and the surface features of the glauconitic grains. The internal structure (fabric) of the crystalline aggregates, following the same classifications as mentioned above, was studied in thin sections of the host-rock.

The SEM studies were carried out using a TESLA BS 340 unit, on gold-covered samples (Babeş-Bolyai University, Cluj-Napoca) and on uncovered samples, on a variable pressure HITACHI S-2360 unit (Eötvös L. University, Budapest).

Powdered glauconitic grains from the A magnetic fractions were examined using the TEM replica-method on a JEOL 100U device, at Eötvös L. University. As far as we know, this method is new for the description of the crystallites of the glauconitic minerals.

X-ray powder diffraction was used for identification of the glauconitic minerals and for the characterization of their ordering degree. The powder diffractograms of the magnetic loose fraction A of the samples were obtained on a SIEMENS D-500 unit with a Cu anticathode and graphite monochromator (Eötvös L. University, Budapest). The peaks were indexed as suggested by WARSHAW (WARSHAW 1957 in ODOM 1984).

Oriented samples of the clay fraction separated from the host-rock were studied by a DRON 3 diffractometer (Cu anticathode, at Babeş-Bolyai University, Cluj-Napoca) in order to evidence the possible relationship with the glauconitic grains (sensu BELL and GOODELL 1967).

We followed the main classification patterns proposed by BURST (1958), HOWER (1961) and BENTOR and KÄSTNER (1965, cf. ODOM 1984). The X-ray patterns were grouped according to the following criteria:

(1) ordered glauconite (glauconite s.s., glauconitic mica) — less than 10 % exp., 1M polytype, d(001) = 10.1 Å, d(003) = 3.3 Å represented by symmetric and sharp peaks;

(2) disordered glauconite (glauconitic mixtures) — 10—20 % exp., 1Md polytype, low intensity or absent 112, 112 peaks and d(001) after glycolation between 10.1—15 Å.

For a better distinction among the disordered glauconites, we used the suggestion of MCCONCHIE and LEWIS (1980), who separate two sub-species:

a) moderately disordered — X-ray diffraction pattern showing sometimes some peak asymmetry, and less than 40 % exp.;

b) extremely disordered glauconite — the same limit for the exp. content, but the X-ray diffraction pattern generally is showing pronounced peak asymmetry.

(3) interstratified glauconite-smectite (or interlayered glauconite, defined by MCCONCHIE and LEWIS 1980 with more than 40 % exp.) — in the AIPEA classification between 20—60 % exp., 1Md or <1Md polytypes, irregularly interstratified structure, and d(001) after glycolation between 10—17 Å.

The ordering degree (as a measure of the structural ordering of the interstratified illitic-and smectitic-type layers) was evaluated by comparing the intensities of 112, 003 and 112 peaks (BENTOR and KÄSTNER 1965, cf. ODIN 1975). The opening degree (suggesting the amount of exp.) was estimated using the shapes and ratios of the intensities of 001/003 peaks (ODIN 1975). The Ø opening index (as defined by ODIN 1975), depending on the intensity (mm), width (mm) and position (Å) of the 001 peak was also calculated.

CASE HISTORIES

CRETACEOUS GLAUCONIES

RÂŞNOV (BRAŞOV DISTRICT)

Geological data

The oldest glauconitic samples were collected from the profile on the Ghimbăşel Brook, near Râşnov, Braşov distr. (Table 1). They are hosted by the most deformed and lithified rocks under study, thus some diagenetic changes of the glauconies might be assumed.

Our study is the first focusing on the glauconitic facies in the area. Within the profile three lithological facies alternate: clayey limestones (which dominate the upper part of the profile), laminated clays and terrigenous limestones, which particularly host the glauconitic grains (*Fig. 2*). The terrigenous limestones intercalations (usually 0.5—3 cm thick) contain stratified levels of green grains concentrated in the basal part of the intercalation, where they constitute about 15—20 % of the rock (the average content is 5 %). The deposits are of Cenomanian–Coniacian(?) age (JEKELIUS 1938, Zărneşti map 1:50000).

In thin section the terrigenous limestones consist of two major petrographic types: packstone (biomicrite) with a siltic (subordinately arenitic) matrix and grainstone/ packstone (biosparite/biomicrite) with terrigenous, mainly arenitic content. Bioclasts, like planktonic foraminifera (Pithonella ovalis, Globotruncana sp., etc.), radiolarians, sponge spicules are abundant and suggest a basinal environment of sedimentation (200—400 m depth). The glauconitic grains are generally associated with the arenitic clasts (quartz, muscovite, biotite, feldspars) — sometimes forming laminated structures, which characterize the grainstones/packstones.

The mineral association of the clay fraction (Table 1) may characterize the external shelf (ANASTASIU 1988).

Glauconies morphology

Glauconies from Râșnov evidence the common granular habit. The grains are light green (the lightest shade among the grains under study) and display a porous, earthy surface. The main morphological types are listed in Table 2. Foraminifera moulds as substrates of glauconitization are the most characteristic feature of this occurrence (Pl. I–Fig. 1). The neoformation of glauconitic minerals affected the clay matrix which filled the fossil tests. The presence of the basinal species of foraminifera suggests an open sea paleoenvironmnet (GIRESSE et al. 1980). Morphological similarities with the recent glauconies forming in foraminiferal oozes on the south-eastern Atlantic shelf of United States (BELL and GOODELL 1967) can be noticed.

Organic inclusions (sponge spicules, radiolarians) or small detrital quartz grains caught in the glauconitic mass (Pl. I–Fig. 2) suggest that spheroidal-ovoidal grains might have had also agglutinated clays as substrates.

The TEM-replica images of sample GC 3A show lamellar xenomorphic crystallites, ranging between 0.3 to 0.7 μm. Sometimes the crystallites associate in poorly-developed rosettes; fan-like aspects are also noticeable. The irregular shape and the small sizes of the crystallites indicate a slightly evolved glauconitic mineral (Pl. V–Fig. 1).

Glauconies mineralogy

The diffractometric features (*Fig. 5*, Table 3) indicate extremely disordered glauconite, the less evolved glaucony under study.

Glauconies genesis

The clay mineral association, as well as the bioclasts included in the host-rock and the significant amount of foraminifera internal moulds as substrates of glauconitization suggest an external shelf, in which probably the neoformation of glauconitic minerals took place. The internal moulds of the microfossils confered the semi-restrictive microenvironment only until the dissolution of the thin tests of planktonic microorganisms. The open sea environment, geochemically less favourable for the glaucony formation, determined a slower evolution (slightly evolved to evolved stage). Diagenetic alterations might also be assumed.

As far as the genetic types of glauconies are concerned, the relative thick level in which glauconies occur and the lithological features (the rhythmic intercalations) indicate transport versus deeper waters, in a turbiditic facies. We assume that the Cretaceous green grains from Râșnov represent transported — probably perigenic (intrabasinal, intra-sequential) — sensu AMOROSI (1993a) glauconies.

SEBEŞEL (ALBA DISTRICT)

Geological data

The glauconitic samples belong to the Upper Cretaceous deposits (Table 1). The green grains are hosted by the basal part (Coniacian) of the Săsciori Beds (MARINCAŞ 1965), which represent a locally shallower facies developed in the south—south-eastern part of the region.

The outcrop in the Gorganu Hill (first mentioned by MAREŞ and TODIRIŢĂ-MIHĂILESCU 1970) preserved very badly, so that a profile is hard to sketch (*Fig. 2*). The basal part of the outcrop consists of coarser sandstones (poorly cemented, with quartzitic gravels) and silty sands (partly oxidized; containing green, altered biotite). Glauconitic grains first occur in the profile in form of nests and lenses or filling the bioturbations. In the subsequent strata they are distributed homogeneously in the rock. The glauconitic level, of 2.5 m thickness, contains about 70 % green grains (e.g. in sample GC 28). The glaucony concentration decreases towards the top of the outcrop.

In thin section the host-rock is represented by a sublithic sandstone with micritic, basal-type carbonate cement. The lithoclasts are represented mainly by carbonate and quartzitic rocks. Rare small hypidiomorphic pyrite crystals are present in some samples (e.g. GC 28). Quartz clasts are sometimes corroded by neoformed calcite.

The mineral association of the clay fraction is dominated by montmorillonite (Table 1).

Glauconies morphology

Table 2 shows the morphological characteristics of the glauconitic grains.

In thin section, the most remarkable are the vermicular grains (10 %), with linear or curved shapes, and micaceous fabrics (Pl. I–Figs. 3–4). Signs of various degrees of oxidation of the glauconitic grains are present, but not generalized; the most susceptible seem to have been the vermicular glauconies, in which films of iron oxi-hydroxides develop along the cleavages (Pl. I–Fig. 3).

Uncovered samples of the vermicular grains were studied in a variable pressure SEM (Pl. III–Figs. 1–2). The micaceous cleavages are still visible; the glauconitic minerals develop as new, authigenic phases between the cleavage planes (Pl. III–Fig. 3), which act as favourable semi-restrictive microenvironments (ODIN 1972). Patches of neoformed crystallites develop in quasi-parallel laminae, oblique to the relic micaceous phase (Pl. IV–Figs. 1–2). Another SEM image (Pl. IV–Fig. 3) shows a microfossil mould which was glauconitized and caught in a glauconitic mass.

TEM-replica images show crystallites of the size similar to those of the Râşnov samples (0.2–1.5 μm) but the lamellae are thicker and more irregular in shape; the margins are curved and folded (Pl. V–Fig. 2). The association of crystallites sometimes resembles dendritic aggregates; the individual lamellae develop quasi-parallel or fan-like (Pl. V–Fig. 3). Some granular structures might indicate mineral impurities inside the glauconitic grains. The general features show a slightly evolved to evolved glaucony.

Glauconies mineralogy

XRD studies (*Fig. 5*) indicate disordered glauconite, respectivelly a moderately disordered sub-species. The glauconitization surpassed the slightly evolved stage and reached the evolved maturity degree (Table 3).

Glauconies genesis

The general lithological context indicates a shallow water paleoenvironment, in which an increased alkalinity was registered.

The mechanism of biotite–chlorite–glauconite transformation is possible to have been more extended than it might be proved by the presence of vermicular grains (about 10 % of the glauconies), thus signifying a tectonically active continental margin (FISCHER 1987).

The fragile morphologies of the abundant lobate and mammillated glauconitic grains plead for an authigenic origin (TRIPLEHORN 1966), but a local transport towards deeper waters can not be excluded (perigenic origin), as proved by the significant amount of smectite with a high crystallinity in the clay association (BELL and GOODELL 1967). The lack of a representative outcrop does not allow a more detailed interpretation.

EOCENE GLAUCONIES

The Eocene of the Transylvanian Depression provides one of the most complex case of glaucony formation: the diversity of stratigraphic levels and geographic repartition of the occurrences is still a "puzzle" which needs further investigations.

The richest and most extended glaucony-bearing levels are the Sokolowia eszterhazyi and Nummulites perforatus ones. They are included in the Căpuşu Formation (Upper Lutetian, RUSU 1987, Terminal Lutetian—Bartonian, RUSU 1995). At the S. eszterhazyi level glauconies indicate a deeper paleoenvironment, as compared to the north-westwards one in which some oolitic ironstones formed (VINOGRADOV et al. 1963, STOICOVICI and MUREŞAN 1964, POPESCU et al. 1978), as a result of a progressive transgression of the Medium Eocene sea.

LUNA DE SUS (CLUJ DISTRICT)

Geological data

In the profile at Dâmbu Rotund Hill (first described by MAREŞ and TĂTĂRÎM 1967) glauconies were collected from both S. eszterhazyi and N. perforatus (the basal N. striatus lumachell) levels.

The deposits consist of intercalations of limestones with massive clays (*Fig. 3*). Sample GE 2 is hosted by a clayey silt (about 10 % green grains) with rare Sokolowia shells and GE 3 by a bioclastic packstone with a microsparitic cement, displaying frequent bioturbations and containing N. striatus, lamellibranchiate debris and algae (about 15—20 % green grains) (Table 1). The profile ends with nummulitic limestone interbedded with clays.

The mineral association in the clay fraction is presented in Table 1.

Glauconies morphology

These samples contain the darkest glauconitic grains under study (Table 2); their morphology and colour suggest favourable paleoenvironmental conditions.

In thin section, about 20 % of the glauconitic grains in sample GE 3 are broken and display fragmentary morphologies.

Light yellowish-green glauconitic(?) films formed inside the chambers of some microfossil tests (Pl. II–Figs. 1–2), probably substituting an argillaceous substrate. In some cases granular glauconies were transported inside broken organic tests, before the diagenetic cement crystallized (Pl. II–Fig. 3).

SEM studies on covered samples (POP and BEDELEAN, 1996) indicate that faecal pellets could provide, at least partially, the substrates for the spheroidal-ovoidal grains. Meanwhile, organic debris (echinoderms?) could supply the substrates of the tabular-discoidal grains (e.g. sample GE 3A). The shape, size and types of aggregates of crystallites reflect mainly the slightly evolved and evolved stages of glauconitization.

In TEM-replica images the crystallites are the largest in size (0.3–2.5 μm) among the samples studied. They are represented by xenomorphic, thin curved lamellae, with a "compact" distribution (sample GE 3A). The lamellae form quasi-parallel alignments which develop in larger fan-like aggregates (Pl. VI–Fig. 3). The general aspect is a rosette-like structure which indicates, together with the size of the crystallites, a highly evolved stage reached in the process of neoformation by the Eocene glauconies.

Glauconies mineralogy

The X-ray powder patterns indicate more closed, micaceous structures than the previous ones (*Fig. 5*, Table 3); in spite of that, the glauconitic minerals seem to have a reduced ordering degree. The samples are ordered glauconites, the most evolved green grains under study (highly evolved glauconies).

Glauconies genesis

The peculiar features of this occurrence are the presence of two distinctive host-rocks for the glauconies and the association of the green grains with the green films inside the foraminifera tests. The clay mineral association in sample GE 3, together with the dark green glauconies resemble the recent mollusc shell gravels cemented by carbonate in which evolved glauconies formed on the south-eastern Atlantic shelf of United States (BELL and GOODELL 1967).

The similitudes between the well crystallized illite and the highly evolved glauconies and the horizontal constance of the morphologies and mineralogical species on extended areas (AMOROSI 1993b) suggest an authigenic origin of the Eocene glauconies, especially at the S. eszterhazyi level (samples GE 2, GE 5). The paleoenvironment of formation must have been an open sea (shelf domain).

A possible transport due to paleocurrents might be responsible for the agglomeration of the microfossils and glauconitic grains in more protected areas, with reduced sedimentation rates, where both the granular glauconies and the pellicular ones could evolve. In this way, a perigenic (intrabasinal, intrasequential) origin — particularly in the case of N. perforatus level (GE 3) cannot be excluded, as suggested by the fragmentary grains and the clusters of bioclasts and glauconitic grains.

The shallower facies of the oolitic ironstones and the high degree of maturity of the glauconitic grains may indicate the presence of a paleodelta of a large Eocene river, which contributed with important terrigenous iron supply. Some changes of the sea level, eustatically or tectonically- controlled, can also be assumed.

ORTELEC (SĂLAJ DISTRICT)

Geological data

The stratigraphy of the outcrop in Răpaosului Valley was described by RUSU (1967, 1987), who also mentioned the presence of glaucony. The lithologic sequence consists of: fluvial/coastal plain varriegated clays, yellowish-greyish limestone, evaporitic breccia, condensed rhythmic intercalations of clay and carbonate deposits with Anomya –

suggesting a very reduced terrigenous supply (*Fig. 3*). Detrital glauconitic deposits and nummulitic lumachelles end the succession. The general trend is of shallowing-upward.

The green grains are concentrated on the stratification planes or form lenticular nests in a poorly consolidated silty clay, with rare fragments of S. eszterhazyi (Table 1).

The clay fraction mineral association shows a lower crystallinity, as compared to the Luna de Sus samples.

Glauconies morphology

The green grains from Ortelec show similar morphologies as compared with those from Luna de Sus (Table 2).

About 5–10 % of the glauconies consist of composite grains, usually containing quartz inclusions and displaying patch-oriented microcrystalline fabrics, which suggest an inhomogeneous substrate (McCONCHIE and LEWIS 1980).

A generalized oxidation affected both the clayey matrix of the rock and the glauconitic grains. The substitution is progressive, and several steps are visible. The complete substitution of about 10–20 % of the glauconitic grains led to the formation of goethite peloids.

Glauconies mineralogy

An ordered glauconite (*Fig. 5*, Table 3) with a relative higher amount of exp. layers, as compared with Luna de Sus samples was evidenced in the XRD pattern. The evolutionary stage is highly evolved glaucony.

Glauconies genesis

The similarities of the morphologies and the size of the green grains, as well as the common clay mineral association at Luna de Sus and Ortelec indicate the maintenance of similar micro- and paleoenvironments during the Upper Lutetian. The changes of the sea level might be responsible for the subsequent oxidation (RIGGS et al. 1989); meanwhile, the oolitic ironstone level is missing in the north-western area of the Transylvanian Depression.

The lithological and mineralogical features of the other Eocene occurence indicate an authigenic origin for the glauconies included in the Căpuşu Formation. The accumulation of the green grains in lenses or nests may be the result of intrabasinal transport, thus a perigenic origin may also be assumed.

OLIGOCENE GLAUCONIES

VAR (SĂLAJ DISTRICT)

Geological data

The glauconies are hosted by the shallow marine (littoral to internal shelf) deposits of the Var Sandstone (Upper Rupelian–Chattian, RUSU 1977, RUSU et al. 1978). In the basal part, a normal marine level with Cyprinids, representing the NP25 zone is worth to mention (N. MÉSZÁROS, personal communication).

The outcrop in village Var contains the Ileanda Beds shales, followed by the basal part of the Var Sandstone, consisting of a yellowish clayey silt (*Fig. 4*). The green grains form lenses, nodules (in some cases surrounding quartz clasts) or laminae, or they fill the frequent horizontal and oblique bioturbations. Iron oxi-hydroxides are frequent.

The clay fraction consists of an uncommon association of kaolinite with smectite, and subordinate illite (Table 1), all showing high crystallinity. The presence of kaolinite in the

basal part of the Var Sandstone must be connected with the quartzitic-kaolinitic sands which occur in significant amounts towards the top of the unit.

Glauconies morphology

Morphologic similarities with the Eocene glauconies are listed in Table 2. The particular features are represented by the relatively frequent fragmentary grains (about 40 %) and by the dissolution(?) pits at the surface of the green grains – as a result of a chemical attack of a more acidic environment.

In thin section, a hydrodinamic sorting of the whole sediment is noticeable: the spheroidal-ovoidal grains are hosted by the coarser, arenitic clasts, while the small, fragmentary or spheriodal grains (below 50 μm) grouped in the finer, silty fraction.

The crystallites, as shown in the TEM-replica images are very similar with those which form the Cretaceous glauconies from Sebeşel. The xenomorphic lamellae are thick, curved and folded (Pl. VI–Fig. 1). Their sizes range between 0.2–1 μm. The aggregates are poorly developed. Some granular structures are also visible. The low crystallinity and the small size of the lamellae suggest a slightly evolved glauconitic mineral.

Glauconies mineralogy

The X-ray diffraction pattern indicates an opened structure, with low structural ordering degree (*Fig. 5*, Table 3), thus an extremely disordered glauconite. The stage of glauconitization is slightly evolved to evolved.

Glauconies genesis

The case of the Oligocene glauconies is the most complex one.

The significant amount of well crystallized kaolinite in in the clay fraction, the rests of a brackish fauna and the presence of coal in the upper part of the Var Sandstone indicate an internal shelf environment, possibly placed near a river-mouth. The paleoenvironment seems to have been very unfavourable for the authigenic glaucony formation. Meanwhile, the well-sorted clayey silt indicates a post-depositional size sorting which affected also the glauconitic grains. All these features contribute in assigning an allochtonous (perigenic/detrital) origin to the Oligocene glauconies.

Morphological similitudes with the Eocene glauconies, as well as the less evolved stage of maturity, which could signify a possible re-working and chemical depletion in K and Fe, could indicate an Eocene glauconitic level as the source of the green grains. In this case, the Oligocene glauconies would be detrital (intrabasinal, extrasequential). Meanwhile, the presence of a normal marine environment in the basal part of the Var Sandstone could be a possible argument for a perigenic (intrabasinal, intrasequential) origin. Further study is still requested.

MIOCENE GLAUCONIES

The most extended glauconitic level in the Transylvanian Depression was formed in the Lower Miocene (Eggenburgian) (MÉSZÁROS et al. 1978). It represents the basal part of the Chechiş Beds and signifies a well defined transgression stage on the whole north-western border of the depression.

From tectonic point of view, the Chechiş Beds overlap the Meseş thrust (Table 1), which was the first signal in Romania of the north-eastwards tectonic escape of the North-Pannonian block (BALINTONI 1996, in press).

TIHĂU (SĂLAJ DISTR.)

Geological data

The Cornul Corbilor Hill, near Tihău, Sălaj distr. is one of the best outcrops of the Eggenburgian glauconitic level (RUSU 1977). The profile (*Fig. 4*) starts with a littoral facies, the Coruş Beds: massive fossiliferous conglomerates and sandstones with Pectinids, displaying trough cross beddings (TCB) and ripple marks. A gravel-containing clay with dominant quartz (GM 1) forms the border between the Coruş and Chechiş Beds. The subsequent glauconitic level (about 3.5 m thick) consists of a heterogeneous, poorly sorted glauconitic silty sand. Quartz clasts are abundant in argillaceous matrix (GM 2); bioturbations are present. The upper part of the level is partially laminated (GM 7) (Table 1).

In some thin sections (e.g. GM 2, GM 7) iron oxi-hydroxides are frequent in the matrix of the rock, but they also occur as inclusions in the glauconitic grains. Their granular and quasi-rhombohedral shape may refer to pseudomorphs after siderite(?) or marcasite(?) (Pl. I–Fig. 6). Heavy minerals (titanite, magnetite) occur rarely.

The clay fraction mineralogy is dominated by montmorillonite and illite (Table 1).

Glauconies morphology

The Miocene glauconies are light green and, as in the case of the Cretaceous glauconies from Râşnov, their surface is mat and porous. Spongy morphologic type dominates (Table 2).

In thin section heterogeneous morphologies and internal fabrics are visible (POP and BEDELEAN, 1996). Granular facies is dominant, but also the film habit is present. In a few cases organic substrates (e.g. relic mollusc) may be assumed. They are included in the glauconitic mass, or affected partially by "verdissement" (e.g. sample GM 11 from Baica, Sălaj distr.; Pl. I–Fig. 5). The internal fabric is, in this case, the "zebra" type.

Green films inside quartzitic clasts were evidenced in thin sections of the loose fraction larger than 500 μm; the internal structure is random microcrystalline or oriented (Pl. II–Figs. 4–6). Due to optical similitudes, we assume a glauconitic nature of the green film. Some other mineral grains (feldspars) were also partially glauconitized.

SEM images on covered samples evidence mostly spheriodal-ovoidal morphologies. A microscopic "friction lens" and parallel scratches suggest mechanic impact during a possible transport (POP and BEDELEAN, 1996).

In TEM-replica images (sample GM 2A) the size and the mode of association of crystallites are similar to those of the Eocene glauconies (sample GE 3A). Quasi-parallel aggregates are visible, but also poorly developed dendritic associations of crystallites were noticed. The crystallites are xenomorphic lamellae, 0.4–2.5 μm in size; they are thicker than the Eocene ones, and more irregular in shape (Pl. VI–Fig. 2). An intermediate stage of neoformation between the slightly evolved glauconies (GC 3A, GO 1A) and highly evolved ones (GE 3A) is suggested.

Glauconies mineralogy

Differences in the XRD patterns of samples GM 2A and GM 7A indicate that the two samples are of very similar, but still not of the same structure (*Fig. 5*, Table 3).

GM 2A represents an intermediate case between ordered and disordered glauconites; due to the strictness of classification, we included GM 2A at the ordered glauconites. It represents an intermediate stage between the evolved and highly evolved glauconies.

GM 7A has a more opened structure, with more interstratified exp. layers. The mineral sub-species is moderately disordered glauconite. From the point of view of the glauconitization process, it is an evolved glaucony.

Glauconies genesis

Several controversal features meet in the reconstruction of the Miocene paleoenvironment of glaucony formation. The horizontal uniformity of the glaucony-containing basal part of the Chechiș Beds, pleads for a certain maintenance of a favourable paleoenvironment. Moreover the "verdissement" process, which finally led to the formation of glauconies was generalized, having affected all the possible types of substrates (mineral debris, organic fragments, clay aggregates etc.). Under these constant circumstances distinctive mineralogical types of evolved glauconites formed: in the basal part more closed structures, representing a transition from the ordered to the disordered glauconites (sample GM 2A) and more opened, disordered glauconites at the top of the glauconitic level. A mineralogical heterogenity within the same stratigraphic level (ODOM 1984) cannot be excluded either. The predominance of the spongy morphologic type suggests important diagenetic contribution.

Alternating geochemical environments led to the formation of siderite(?) or marcasite(?) followed by the substitution with iron oxi-hydroxides. The glauconitization process could benefit of an important iron supply resulting from these changes of Eh conditions.

The sedimentary sequence is connected with an important transgressive event.

A perigenic (intrabasinal, intrasequential) origin for the Miocene glauconies is assumed.

CONCLUSIONS

In our study the Cretaceous glauconies near Râșnov (Brașov distr.), the Eocene ones from Ortelec (Sălaj distr.), the Oligocene occurrence from Var (Sălaj distr.) and the Miocene level (mainly the outcrop near Tihău, Sălaj distr.) were studied for the first time from a mineralogical-genetical point of view.

Generally, classical TEM images on the less than 2 μm fraction of the glauconitic minerals were rarely provided by specialized papers (BURST 1958). The TEM-replica method was applied now for the first time – as far as we know – for the description of the morphology of the glauconitic crystallites. Thus, the interpretation of the images is informative and constitues a possible starting point for further studies.

New interpretations on the mineralogy of the Eocene and Miocene samples are presented (see POP and BEDELEAN, 1996), due to more accurate investigations and to the possibility of comparison between several mineralogical species of glauconies.

The values of the Ø opening index calculated by ODIN (1975) on XRD patterns range between 1.5 (for opened, disordered structures) and 7.5 (for closed, ordered structures); in our case, values between 3.72 and 10.1 were obtained. We assumed the same structural signification, e.g. the highest the value is the more closed and ordered the structure is, when defining the mineralogical characteristics.

Finally, the lithological and sedimentological data, as well as the informations supplied by the morphological and mineralogical study of the glauconitic grains allowed us to discuss some of the genetical features of each occurrence.

ACKNOWLEDGEMENT

We are grateful to Dr. Tamás G. WEISZBURG from Eötvös L. University in Budapest for very useful discussions, as well as for the detailed revising of the manuscript. Several colleagues from the Babeş-Bolyai University in Cluj contributed to the interpretation of the analyses: Prof. L. GHERGARI, Prof. I. BUCUR, Lecturer A. HOSU, or provided helpful discussions: Prof. L. GHERGARI, Prof. I. BALINTONI, Lecturer A. HOSU – who also reviewed the manuscript. We thank P. RĂCĂTOIANU for the photos on thin sections and M. GUZU for revising the English version of the manuscript. We express our thanks to Dr. GY. A. LOVAS and to Prof. I. GYURJÁN and Dr. Z. KRISTÓF, Eötvös L. University for the access to XRD resp. variable pressure SEM investigations, as well as to Ms. L. RUDNYÁNSZKY for the TEM-replica photos and to R. ZEMPLÉN for her support in performing the analyses.

The analytical work was supported by the Departments of Mineralogy at Babeş-Bolyai University (Cluj-Napoca) and Eötvös L. University (Budapest), in the latter case (XRD, SEM and TEM investigations) under the auspices of the Agreement of Understanding between the two Universities and the generous help of Dr. GY. BUDA, Head of Department.

One of the authors (DP) was sponsored by the interuniversity scientific exchange programme of the Babeş-Bolyai and the Eötvös L. Universities.

We thank all the Romanian and Hungarian friends who contributed in creating a stimulating and co-operative atmosphere.

REFERENCES

AMOROSI, A. (1993a): Use of glauconies for stratigraphic correlatios: review and case histories. Giornale di Geologia, ser. 3. **55/1**, 117-138.

AMOROSI, A. (1993b): Intérêt des niveaux glauconieux et volcano-sédimentaires en stratigraphie: exemple de dépôts de bassins tectoniques miocènes des Apennins et comparision avec quelques dépôts de plate-forme stable. Thèse Doct., Univ. P. et M. Curie Paris. Mémoires Sciences de la Terre. **93/12**, 194.

ANASTASIU, A. (1988): Petrologie sedimentară. Ed. Tehn., Bucureşti, 365.

BAILEY, S. W. (1980): Summary of recommendations of AIPEA Nomenclature Committee. Clays and Clay Minerals. **28/1**, 73-79.

BALINTONI, I. (1994): Once again about tectonic problems of the Crystalline Mesozoic Zone of the South Carpathians, around Braşov Curvature. Studia. **1-2** (in press).

BALINTONI, I. (1996): Transilvania — depresiune şi bazine. Sesiunea de Comunicări a cadrelor didactice şi studenţilor, Facultatea de Biologie şi Geologie, Universitatea Babeş-Bolyai, Cluj, 17—18 mai, 1996 (in press).

BELL, D. L., GOODELL, H. G. (1967): A comparative study of glauconite and the associated clay fraction in modern marine sediments. Sedimentology. **9**, 169-202.

BIELZ, E. A. (1889): Die Gesteine Siebenbürgens. Eine Systematische Aufzählung der in diesen Lande vorkommenden Mineralien und Fels arten mit ihren Fundorten und ihrem Vorkommen. II Auflage. Separatbuch. Buchdruckerei der G. von Closius, Hermannstadt, 82.

BURST, J. F. (1958): Mineral heterogenity in glauconite pellets. American Mineralogist. **43/5-6**, 481-497.

FISCHER, H. (1987): Excess K-Ar ages of glauconite from the Upper Marine Molasse and evidence for glauconitization of mica. Geologische Rundschau. **76/3**, 885-902.

GIRESSE, P., LAMBOY, M., ODIN, S. (1980): Évolution géométrique des supports de glauconitisation; application à la réconstitution du paléoenvironnement. Oceanologica Acta. **3/2**, 251-260.

HAUER, F., STACHE, G. (1863): Geologie Siebenbürgens. Ed. W. Braumüller, Wien, 636.

HOFMANN, K. (1879): Bericht über die im östlichen Theile des Szilágyer Comitates während der Sommer-campagne 1878 vollfürten geologischen Specialaufnahmen. Földtani Közlöny. **IX/5-6**, 231-283.

HOWER, J.(1961): Some factors concerning the nature and origin of glauconite. American Mineralogist. **46/3-4**, 313-334.

JEKELIUS, E. A. (1938): Das Gebirge von Braşov. Anuarul I.G.R. **XIX**, 379-408.

KOCH, A. (1883): Bericht über die Klausenburger Randgebirge und in dessen Nachbarschaft im Sommer 1882 ausgeführte geologische Special-Aufnahme.Földtani Közlöny. **13**, 117-140.

KOCH, A. (1900): Die Tertiärbildungen des Beckens des siebenbürgischen Landestheile. II. Neogene Abtheilung. Druck des Franklin Vereins. Budapest. 369.

MAREŞ, I., TĂTĂRÎM, N. (1967): Studiul glauconitului din depozitele eocene din regiunea Cluj (Luna de Sus–Lita). Analele Univ. Buc. Geol, Geogr. **16/2**, 25-48.

MAREŞ, I., TODIRIŢĂ-MIHĂILESCU, V. (1970): Asupra prezenţei glauconitului în depozitele neocretacice din regiunea Sebeşel–Săsciori. Analele Univ. Buc. Geol., Geogr. **19**, 61-68.

MARINCAŞ, V. (1965): Studii geologice în regiunea Sebeş–Cîlnic–Săsciori–Răchita–Pianu de Sus–Cioara, cu privire specială asupra stratigrafiei depozitelor cretacice. Teză de doctorat. Univ. Babeş-Bolyai, Cluj. 323.

MCCONCHIE, D. M., LEWIS, D. W. (1980): Varieties of glauconite in late Cretaceous and early Tertiary rocks of the South Island of New Zealand, and new proposals for classification. Journal of Geology and Geophysics. **23/4**, 413-438.

MÉSZÁROS, N., IANOLIU, C., PION, N. (1978): Nannoplanctonul stratelor de Chechiş şi paralelizarea lor cu depozite similare ca vîrstă din Carpaţii Orientali. Anuarul Muzeului de Ştiinţele Naturii Piatra Neamţ, 3, 213-218.

ODIN, G. S. (1969): Méthode de séparation des grains de glauconie. Intérêt de leur étude morphologique et structurale. Révue de Géographie Physique, Géologie Dynamique **11/2**, 171-176.

ODIN, G. S. (1972): Obsérvations nouvelles sur la structure de la glauconie en accordeon ("vermicular pellets"); déscription du processus de génese de ces granules par néoformation. Sedimentology. **19**, 285-294.

ODIN, G. S. (1975): De glauconarium: constitutione, origine, aetateque. Thèse, Univ. P. et M. Curie, Paris. 280.

ODIN, G. S., LÉTOLLE, R. (1978): Les glauconies et aspects voisins ou confondus; signification sédimentologique. Bulletin de la Societé géologique Française **20/4**, 553-558.

ODIN, G. S., MATTER, A. (1981): De glauconarium origine. Sedimentology. **28**, 611-641.

ODOM, E. I. (1984): Glauconite and celadonite minerals. In: S. W. BAILEY (Editor): Micas. Reviews in Mineralogy. **13**, 545-572.

POP, D., BEDELEAN, I. (1996): Glauconites from the Transylvania Basin: New Mineralogical Data. Romanian Journal of Mineralogy. 78 (in press).

POPESCU, B., BOMBIŢĂ, G. RUSU, A., IVA, M., GHEŢA, N., OLTEANU, R., POPESCU, D., TĂUTU, E. (1978): The Eocene of the Cluj—Huedin Area. Dări de Seamă, IV. **64/4**, 295-358.

RIGGS, S. R., SNYDER, S. W. O'BRIEN, W. G., COOK, P. J., HEGGIE D. T. (1989): Sedimentology of the Neogene to modern glauconite–goethite–phosphate system: East Australian continental margin between 29° and 32° south latitude. Sciences Géologiques. Bulletin. **42/3**, 186-204.

RUSU, A. (1967): Studiul geologic al regiunii Moigrad (nord-vestul bazinului Transilvaniei). Dări de Seamă Com. Stat Geol. **53/1**, 427-455.

RUSU, A. (1977): Stratigrafia depozitelor oligocene din nord-vestul Transilvaniei (regiunea Tresnea–Hida–Poiana Blenchii). Anuarul I.G.G. **51**, 69-224.

RUSU, A. (1987): Ostreina biohorizons in the Eocene of the NW Transylvania (Romania). In: I. PETRESCU (Editor-in-chief): The Eocene from the Transylvania Basin. University of Cluj-Napoca. 175-182.

RUSU, A. (1995): Eocene formations in the Călata region (NW Transylvania): a critical review. Romanian Journal of Tectonics and Regional Geology. **76**, 59-72.

RUSU, A., POPESCU, A., RĂDAN, S., GHEORGHIAN, M., IVA M., POPESCU G., CIOFLICA, G. OLTEANU, R., GHEŢA, N., JIPA, D. (1978): Studiul lito-biostratigrafic al forajului 34601 de la Zimbor (NW-ul Transilvaniei). Dări de Seamă I.G.G. **LXIV/4**, 359-376.

SĂNDULESCU, M. (1975): Essai de synthèse structurale des Carpathes. Bulletin de la Societé géologique de France, 7 ser., **XVII/3**, 299-358.

STOICOVICI, E., MUREŞAN, I. (1964): Studiul zăcămîntului de limonit oolitic şi de glauconit din formaţiunile eocene ale Bazinului Transilvaniei (1, 2). Studia Univ. Babeş-Bolyai, ser. Geol., Geogr. **1**, **2**, 7-16, 17-29.

ŞURARU, N. (1967): Beiträge zur Kenntnis des Burdigals im nord-westlichen Teil des Siebenbürger Beckens zwischen Cluj und Surduc (Rumänien). Neues Jahrbuch für Geologie und Paläontologie. Mhf. **8**, 489-497.

TRIPLEHORN, D. M. (1966): Morphology, internal structure and origin of glauconite pellets. Sedimentology. **6**, 247-266.

VINOGRADOV, C., BARBU, I. Z., HESSELMAN, A. (1963): Contribuţii la cunoaşterea zăcămîntului sedimentar de fier de la Căpuş (reg. Cluj). Studii şi Cercetări de Geologie. **VIII/2**, 235-252.

* * * (1972) : Harta geologică 1:50.000 , foaia Zărneşti (110b). Institutul Geologic Bucureşti.

Manuscript received 6. Sep. 1996.

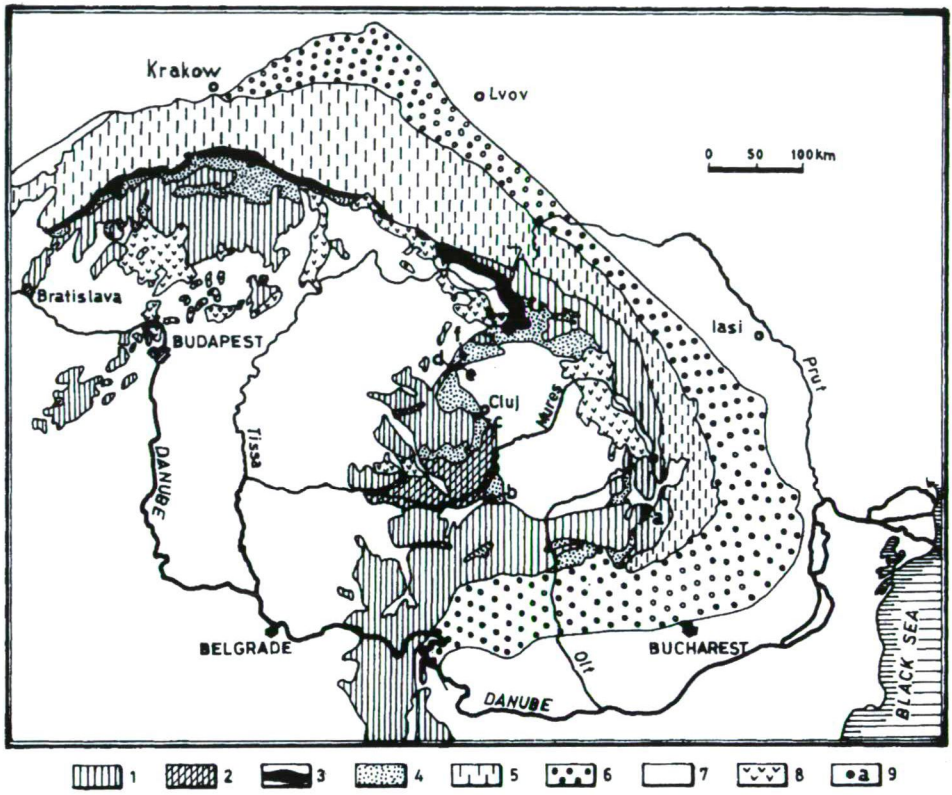

Fig. 1. The main structural units in the Carpathian area (1 - 8) (after SĂNDULESCU 1975, with modifications) and the glauconitic occurrences under study (a - f).

Legend: 1 - Dacides; 2 - Transylvanides; 3 - Pienides; 4 - Post-tectonic covers; 5 - Moldavides; 6 - Foreland basin; 7 - Depressions; 8 - Neogene volcanics; 9 - Glauconitic occurrences: a - Râşnov (Braşov distr.); b - Sebeşel (Alba distr.); c - Luna de Sus (Cluj distr.); d - Ortelec (Sălaj distr.); e - Var (Sălaj distr.); f - Tihău (Sălaj distr.).

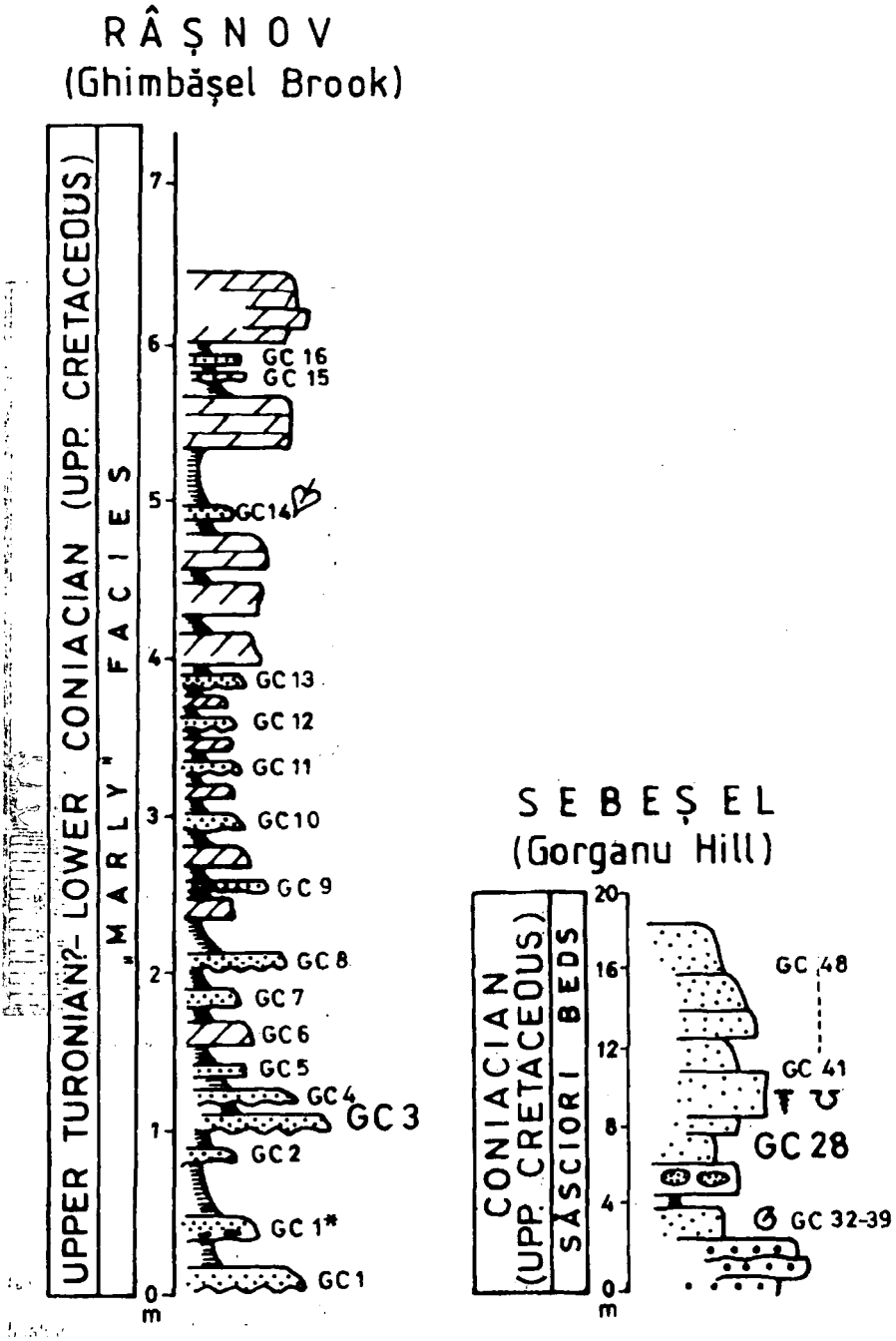

Fig. 2. The profiles of the Cretaceous outcrops from Râșnov and Sebeșel (see explanations in the text).

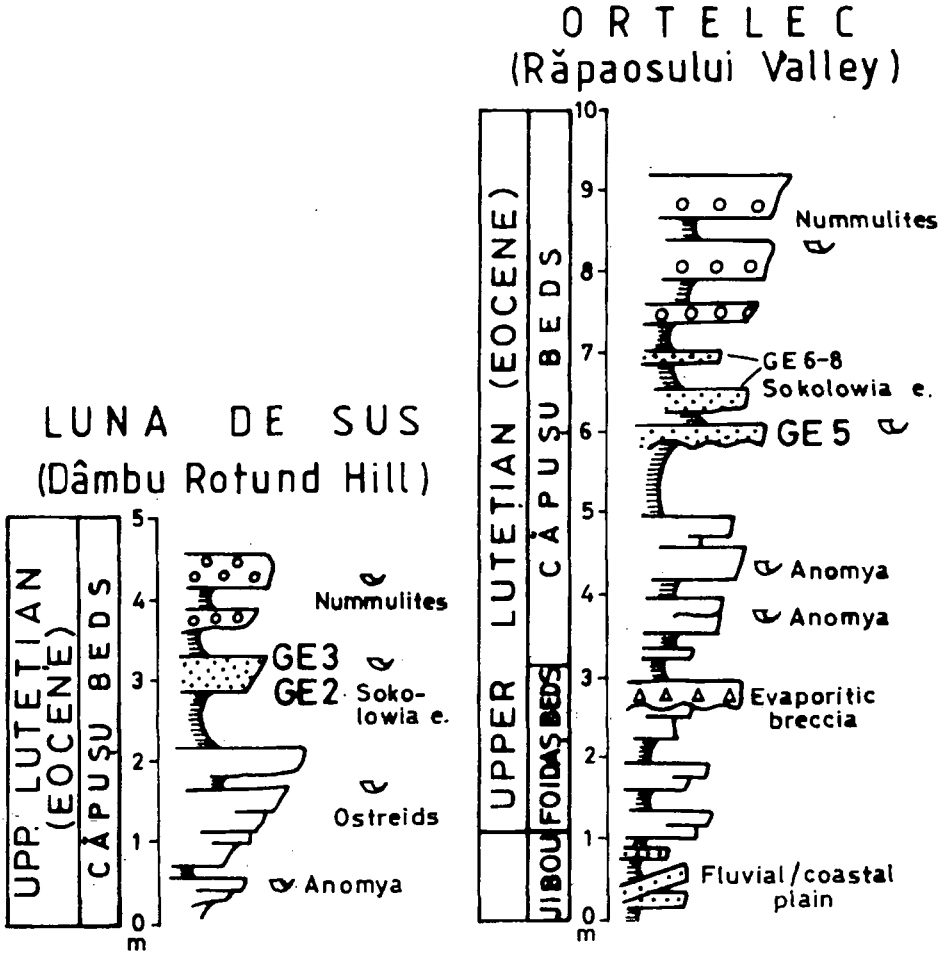

Fig. 3. The profiles of the Eocene outcrops from Luna de Sus and Ortelec (see explanations in the text).

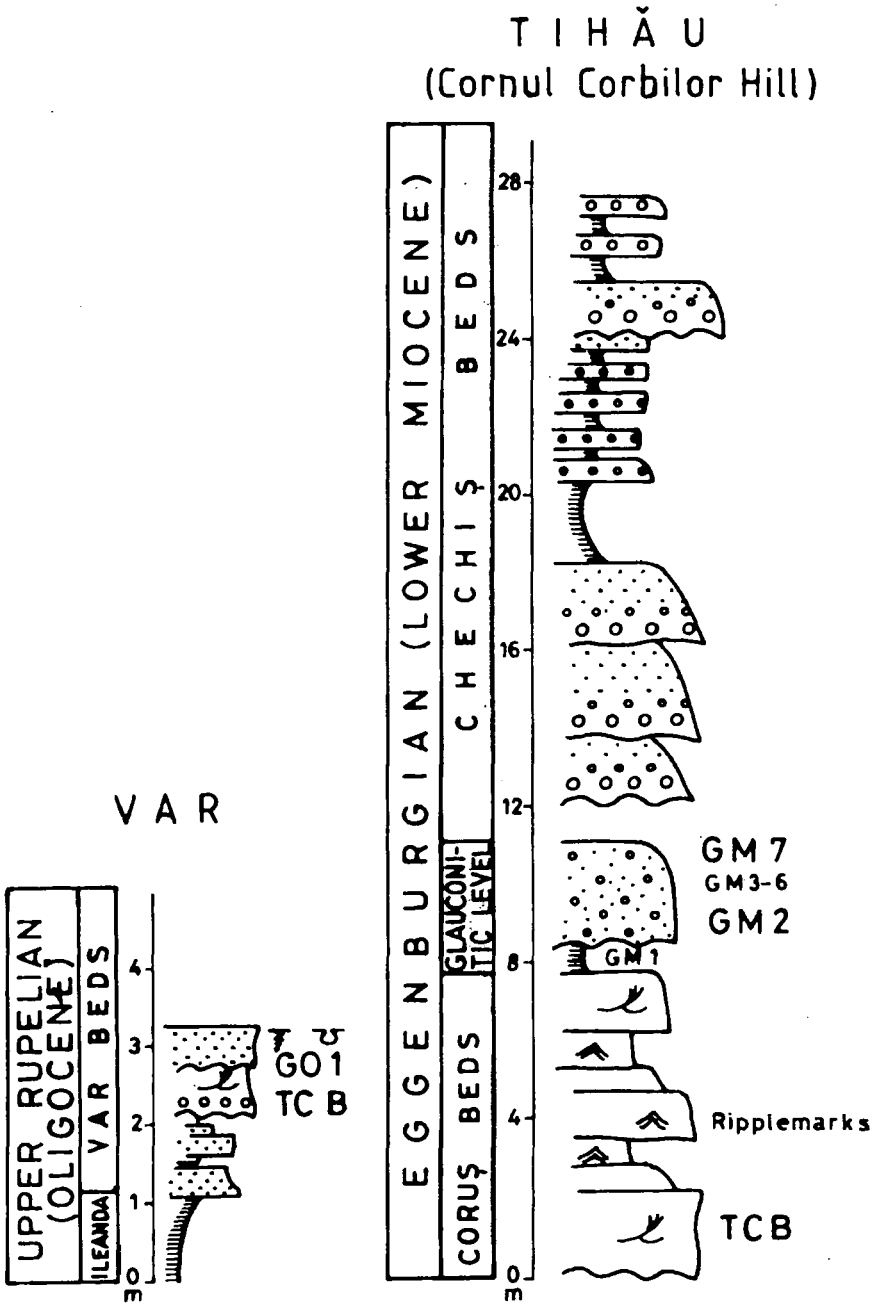

Fig. 4. The profiles of the Oligocene (Var) and Miocene (Tihău) outcrops (see explanations in the text; TCB - trough cross beddings).

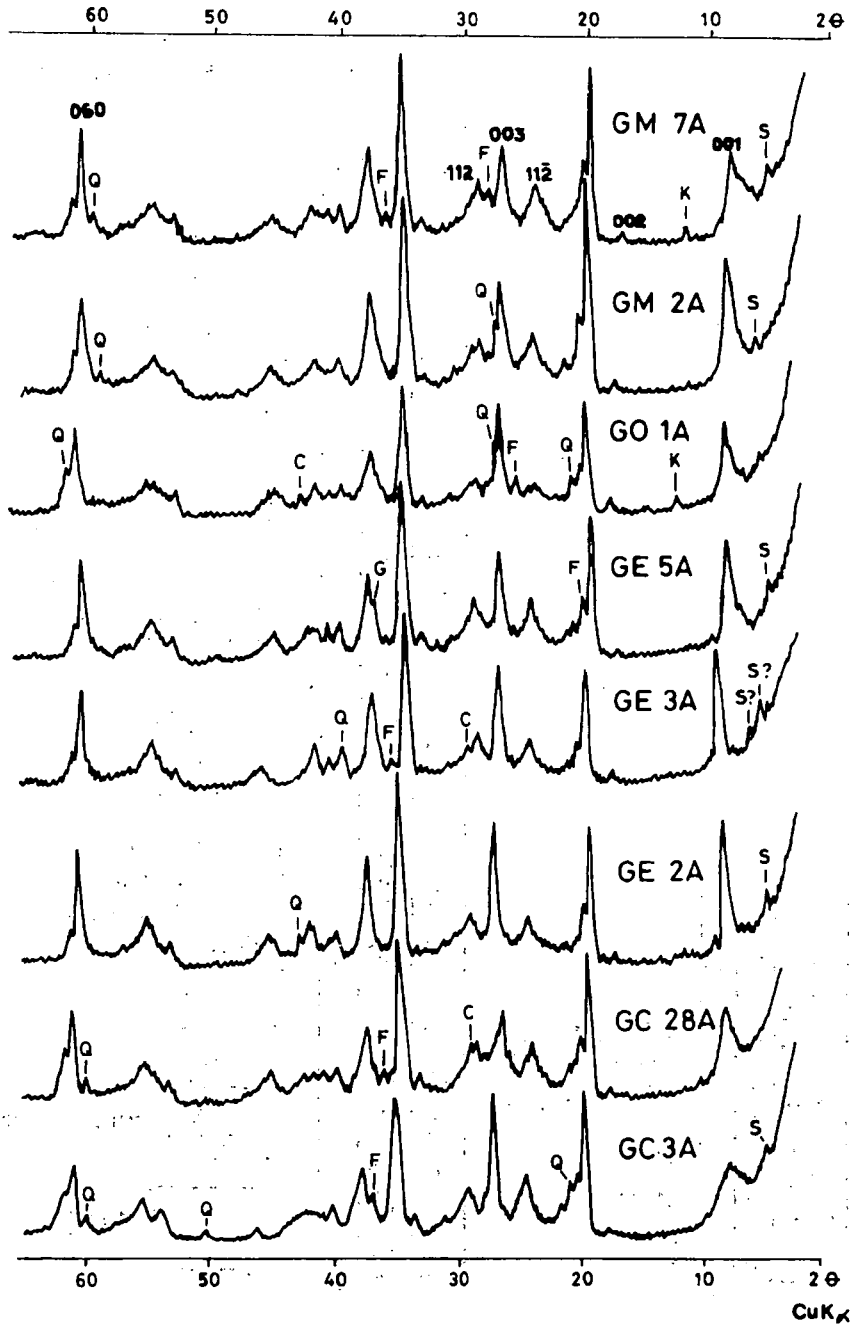

Fig. 5. X-ray powder diffractograms of the reference glauconite samples under study.
Legend: Q - quartz; F - feldspars; K - kaolinite; C - calcite; S - smectite.

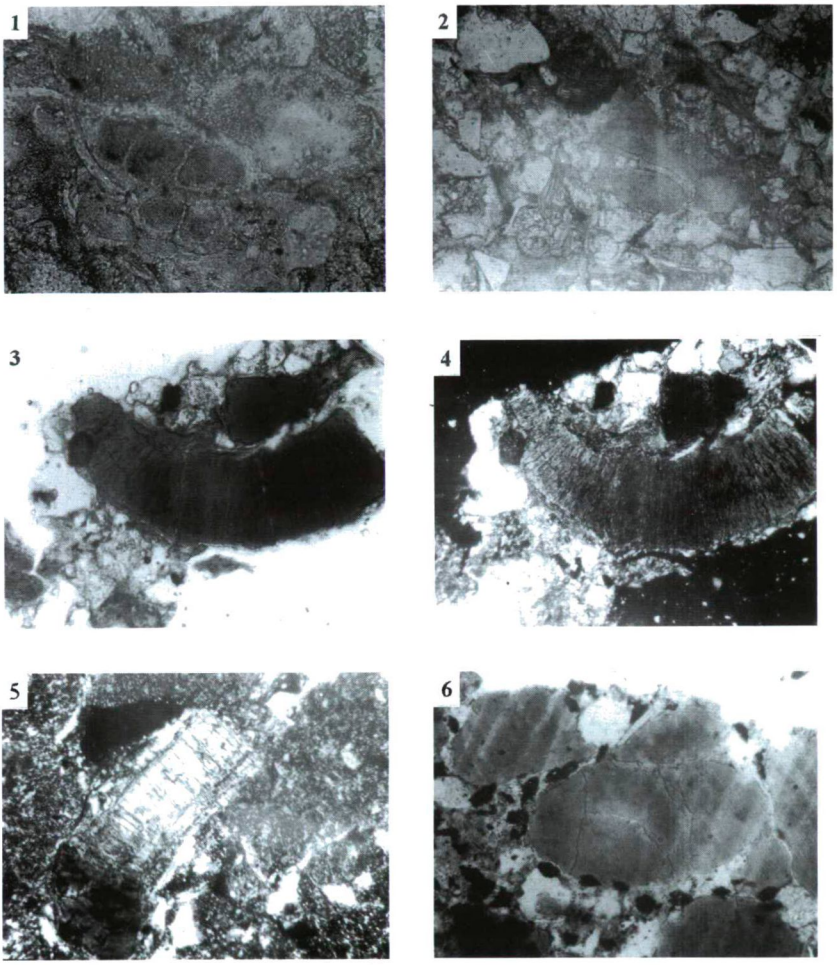

PLATE I

Pl. I–Fig. 1. Microfossil internal mould filled with glaucony (GC 11, Râşnov, 1N, x 190)
Pl. I–Fig. 2. Bioclast included in an ovoidal glauconitic grain (GC 11, Râşnov, 1N, x 100).
Pl. I–Fig. 3. Curved vermicular glauconitic grain; iron oxi-hydroxides develop on the micaceous cleavages and glauconitic cortex surrounds the grain (GC 27, Sebeşel, 1N, x 100).
Pl. I–Fig. 4. idem; micaceous microcrystalline internal fabric (N+).
Pl. I–Fig. 5. "Zebra" internal structure of a glauconitized mollusc relic(?) (GM 11, Baica, Chechiş Beds, N+, x 100).
Pl. I–Fig. 6. Iron oxi-hydroxides pseudomorphs after siderite(?) or marcasite(?) in the matrix of the rock and partially included in spheriodal-ovoidal glauconitic grains (GM 2, Tihău, 1N, x 100).

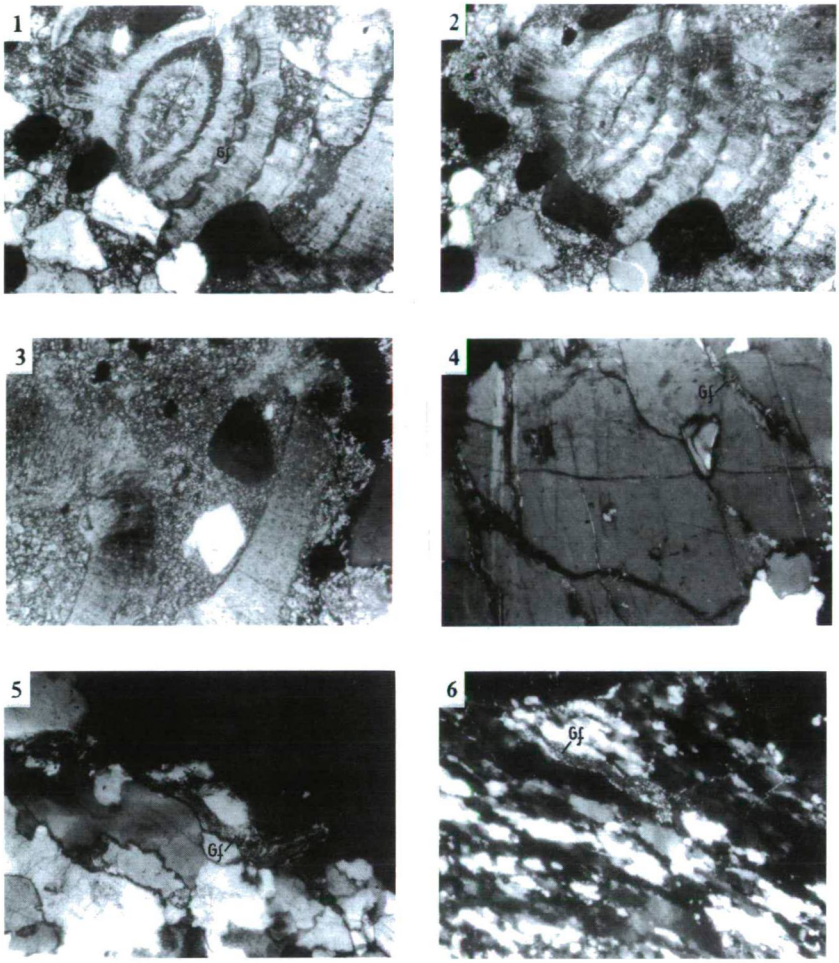

PLATE II
GREEN GLAUCONITIC (?) FILMS (Gf)

Pl. II–Fig. 1. Green fillings of Nummulites tests and granular glauconies agglomerated in transport structures (GE 3 -loose fraction > 500 μm, Luna de Sus, 1N x 65).
Pl. II–Fig. 2. idem (N+).
Pl. II–Fig. 3. Rounded glauconitic grain and subangular detrital quartz included in Nummulites tests and cemented by microsparite (GE 3, Luna de Sus, N+, x 100).
Pl. II–Fig. 4. Green film filling the fissures of quartzitic crystalloclast (GM 3 - loose > 500 μm fraction, Tihău, N+, x 65).
Pl. II–Fig. 5. Random and oriented microcrystalline internal fabric of green infilling in the fissures of quartzitic lithoclast (GM 3 - loose > 500 μm fraction, Tihău, N+, x 65).
Pl. II–Fig. 6. Random microcrystalline internal fabric of a green film formed between the crystals, in a quartzitic lithoclast (GM 3 - loose > 500 μm fraction, N+, x 65).

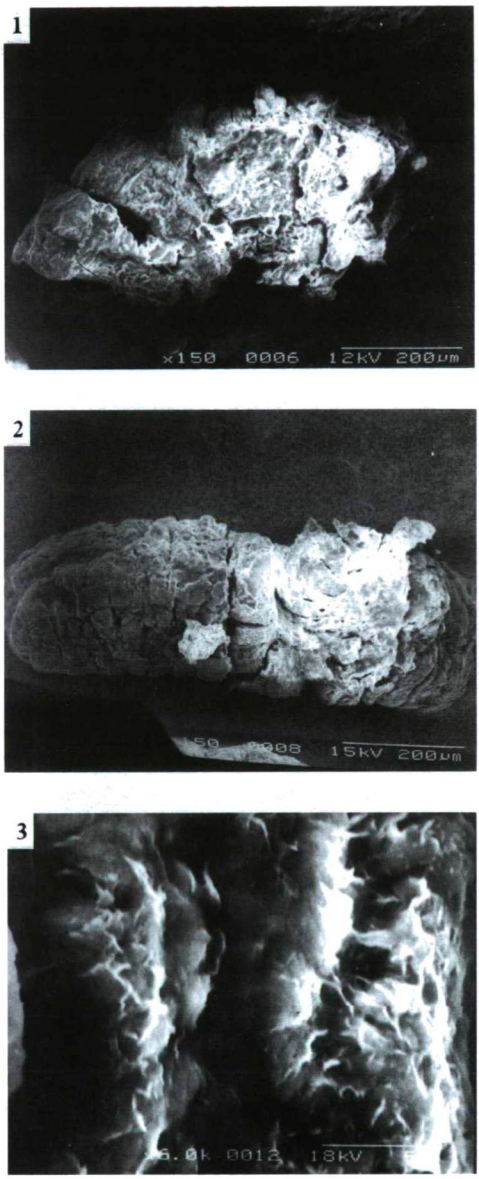

PLATE III
SEM IMAGES OF UNCOVERED SAMPLES.
Vermicular grains in sample GC 28A (Sebeşel, Upper Cretaceous)

Pl. III–Fig. 1. Curved vermicular grain.
Pl. III–Fig. 2. Crushed surface of an elongated vermicular grain; perpendicular cleavages are visible.
Pl. III–Fig. 3. Detail of Fig. 2; flaky crystallites develop in the cracks that follow the cleavage planes (scale bar: 5 µm).

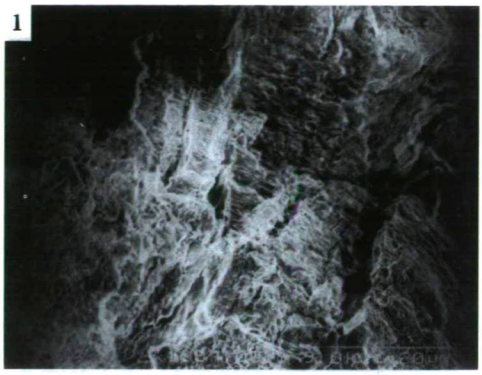

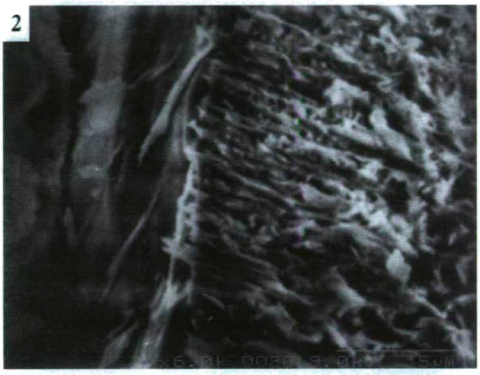

PLATE IV
SEM IMAGES OF UNCOVERED SAMPLES
Sample GC 28A (Sebeşel, Upper Cretaceous)

Pl. IV–Fig. 1. Detail of a vermicular grain, in which cracks following the cleavage planes and quasi-parallel lamellae can be noticed (scale bar: 20 μm).
Pl. IV–Fig. 2. Detail of Fig. 1; the glauconitic quasi-parallel lamellae are oblique to the cleavage planes; relic(?) structures are visible (scale bar: 5 μm)
Pl. IV–Fig. 3. Glauconitized foraminifera mould caught in a mass of neoformed glauconitic lamellae (scale bar: 15 μm).

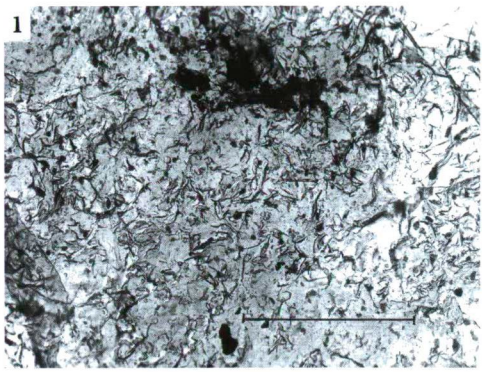

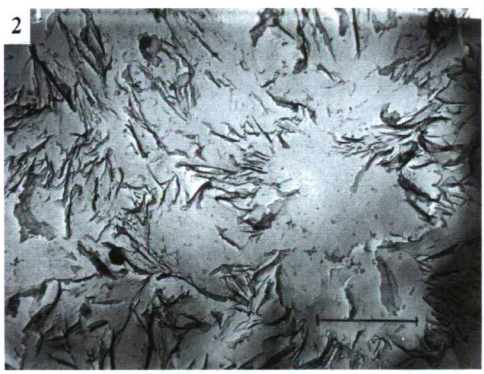

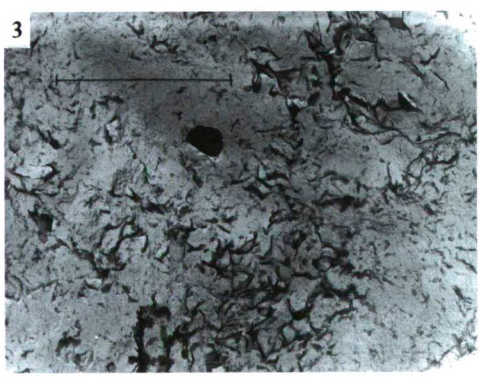

PLATE V
TEM-REPLICA METHOD

Fig. 1. GC 3A sample (scale bar: 5 μm)
Fig. 2. GC 28A sample (scale bar: 1 μm) — Slightly evolved glauconies
Fig. 3. GC 28A sample (scale bar: 5 μm)

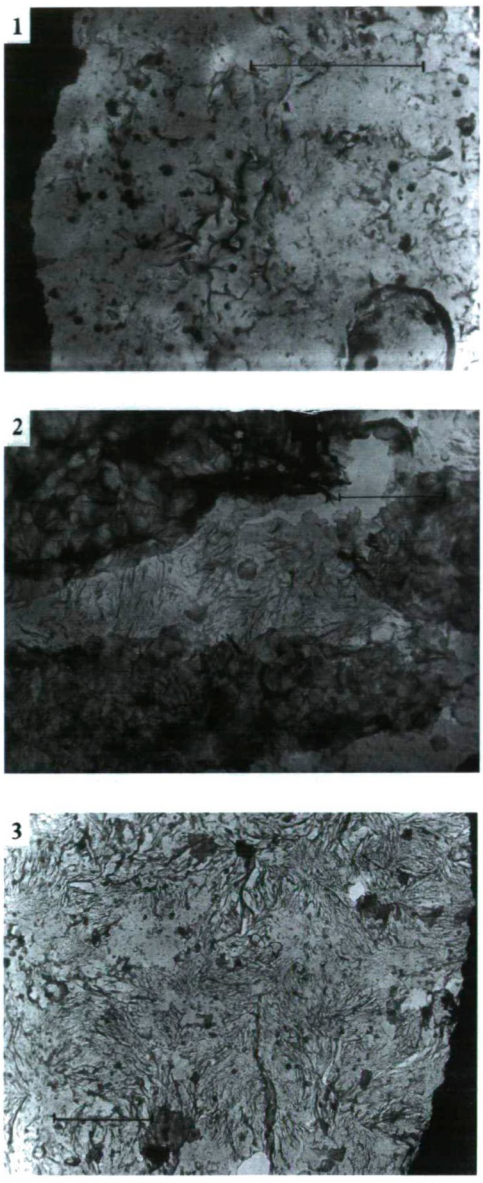

PLATE VI
TEM - REPLICA METHOD

Fig. 1. GO 1A sample (scale bar: 5 μm) Slightly evolved glaucony

Fig. 2. GM 2A sample (scale bar: 5 μm) Evolved glaucony

Fig. 3. GE 3A sample (scale bar: 5 μm) Highly evolved glaucony

TABLE 1

Geological and lithological characteristics of selected glauconitic samples

Sample	Age	Occurrence	Stratigraphy	Geological setting*	Selected references	Host-rock	Clay fraction mineralogy	Observations
GM 7	Miocene (Eggenburgian)	Tihău (Sălaj distr.)	Chechiș Beds	Post-Meseș tectonic cover	Hofmann (1879) Koch (1900) Șuraru (1967) Rusu (1977)	Sandy silt (75% G)	Ca-M+I/S (55%) I (45%)	- laminations -iron oxi-hydroxide pseudomorphs
GM 2	"	"	"	"	"	Silty sand (75% G)	Ca-M+I/S (60%) I(40%) better crystallized	-poorly sorted
GO 1	Oligocene (Upper Rupelian-Chattian)	Var (Sălaj distr.)	Var Sandstone	Post-Laramic tectonic cover of the Transylvanids	Rusu (1977)	Clayey silt (20% G)	Ca-M+I/S (50%) K (40%) I (10%)	-post-depositional sorting -transport structures
GE 5	Eocene (Upper Lutetian - Bartonian?)	Ortelec (Sălaj distr.)	Căpușu Formation (S. eszterhazyi level)	"	Hauer and Stache (1863) Rusu (1967, 1987)	Silty clay (75% G)	I (65%) Ca-M+I/S (35%)	-medium sorted -G nests, laminae
GE 3	"	Luna de Sus (Cluj distr.)	Căpușu Formation (N. perforatus level)	"	Hauer and Stache (1863) Koch (1883) Mareș and Tătărîm (1967)	Bioclastic packstone (15% G)	I (60%) Ca-M (40%)	-transport structures
GE 2	"	"	Căpușu Formation (S. eszterhazyi level)	"	"	Clayey silt (10% G)	Ca-M+I/S (60%) I (35%) C (5%)	-poorly sorted
GC 28	Cretaceous (Coniacian)	Sebeșel (Alba distr.)	Săsciori Beds	Post-Gosau tectonic cover of the Transylvanids	Marincaș (1965) Mareș and Todiriță-Mihăilescu (1970)	Sublithic sandstone (70% G)	Ca-M (75%) I (20%) K (5%)	-transport structures (basal part) -quartz corroded by calcite
GC 3	Cretaceous (Cenomanian - Coniacian?)	Râșnov (Brașov distr.)	"Marly" facies	Post-Austric tectonic cover of the Median Dacides (Southern Carpathians)	Bielz (1889) Jekelius (1938)	Grainstone/ packstone (5% G)	I (50%) Ca-M+Na-M (50%)	-turbiditic deposits -planktonic foraminifers -G associated with arenitic clasts

Legend: glauconies (G); illite-type structure (I); Ca-montmorillonite (Ca-M); Na-montmorillonite (Na-M); kaolinite (K); chlorite (C); randomly interstratified illite-smectite with small amounts of illite layers (I/S). * after BALINTONI (1994, 1996)

TABLE 2

Glauconies morphology

Sample	Colour	Surface features	Morphologic types	Internal structure (fabric)	Observations
GM 7A	light-green	mat, porous	S(85%), M(10%), C(5%)	r (rarely z, m, o)	- organic substrates -green films inside quartzitic clasts
GM 2A	"	"	S(80%), M(15%), C(5%)	"	"
GO 1A	light-yellowish green	glassy, "dissolution pits"	O-S(60%), F(37%), M(3%)	r	-possible transport of G -size sorting of the sediment and G
GE 5A	intense "grass-green"	smooth, glossy	O-S(95%), M(5%)	r (rarely p)	-generalized oxidation
GE 3A	dark-green to black	"	O-S(55%), T-D(25%), F(20%)	r (rarely "corona" structures)	-rarely, green films inside foraminifera tests
GE 2A	"	"	O-S(80%), M(15%), S(5%)	r	
GC 28A	dark yellowish "grass-green"	"	M(75%), V(10%), O-S(7%), T-D(5%), IM(3%)	r, m	-possible biotite-chlorite-glauconite transformation
GC 3A	light-green	earthy, porous	IM(45%), M(35%), S(15%), O-S(5%)	r (rarely c)	-basinal paleoenvironment of G formation (IM)

Legend: Morphologic types: ovoidal-spheroidal (O-S); mammillated (M); tabular-discoidal (T-D); composite (C); vermicular (V); internal moulds (IM); spongy (S); fragmentary (F). Fabric: random microcrystalline (r); composite (c); oriented (o); micaceous (m); patch-oriented (p); "zebra" structures (z)

TABLE 3 .

Glauconies mineralogy

Sample	XRD-characteristics						Mineralogic species	Maturity degree	Genetic type
	d (001) (Å)	d(060) (Å)	b (Å)	Ø	Ordering degree	Polytype			
GM 7A	10.36 (broad)	1.513	9.08	3.72 (opened)	moderate	1Md	MDG	E	P
GM 2A	10.23 (sharp)	1.516	9.10	8.01 (relatively closed)	moderate	1M/1Md	OG	E/HE	P
GO 1A	10.00 (relatively sharp)	1.517	9.11	6.79 (opened)	low	1M	EDG	SE/E	D/P
GE 5A	10.38 (broad)	1.518	9.11	7.68 (relatively opened)	moderate	1M	OG	HE	A/P
GE 3A	10.1 (sharp)	1.521	9.12	9.02 (closed)	moderate	1M	OG	HE	A/P
GE 2A	10.1 (sharp)	1.521	9.12	10.1 (closed)	moderate	1M	OG	HE	A
GC 28A	10.37 (broad)	1.515	9.09	5.06 (opened)	moderate	1Md	MDG	SE/E	A/P
GC 3A	10.8 (broad)	1.514	9.08	5.01 (opened)	low	1Md	EDG	SE	P

Legend: Mineralogic species: ordered (OG); moderately disordered (MDG); extremely disordered (EDG). Maturity degree: slightly evolved (SE); evolved (E); highly evolved (HE). Genetic type: authigenic (A); perigenic (P); detrital (D).

Acta Mineralogica-Petrographica, Szeged, XXXVII, 35–40, 1996

Project No. 384
Spherulites
(micrometeorites)
in Europe

THE POSSIBLE ROLE OF CLAY MINERALOGY IN THE STUDY OF MICROSPHERULES OF COSMIC ORIGIN

I. VICZIÁN*

Hungarian Geological Institute

ABSTRACT

In this short review the clay mineralogy of rocks of cosmic or impact origin and of their enclosing sediments are discussed.

In cosmic matter (meteorites, rocks of the Moon) clay minerals, even hydrous layer silicates are extremely rare (very minor amounts in some Apollo 11 lunar samples and in carbonaceous chondrites). The hydrous layer silicate serpentine is relatively abundant in the zone of asteroids and among the satellites of the planets Jupiter and Saturn.

The non-sedimentary, first phase products (suevites) of the Ries impact crater at Nördlingen contain fresh glassy components. Clay mineral formations starts first during the subsequent post-impact sedimentary history. Examples are given from the Miocene crater lake of the Ries structure, the Cretaceous/Tertiary boundary in a peat-forming environment of western North America and marine deposits of the Eastern Alps as well as Jurassic/Cretaceous boundary formations near an impact structure in the Barents Sea.

Mineralogical analysis may contribute to the reconstruction of the conditions of sedimentation, alteration and diagenesis of rocks containing cosmic or impact-derived material. Examples from the study of Hungarian sedimentary formations are given (Anisian of Mecsek Mts., Uppar Cretaceous of Bakony Mts. and Pannonian of the Little Hungarian Plain).

INTRODUCTION

Microspherules are spherical particles of microscopic size found in sedimentary rocks and Recent sediments. They have either glassy silicatic, or magnetic iron-rich composition. They are supposed to be of cosmic origin. Because of their small size they are normally not accessible for traditional determinative methods of mineralogy. These methods, however, including the determination of clay minerals, can help to elucidate the circumstances of the formation of the rocks that contain the particles. The aim of the present short review is to discuss these possibilities.

COSMIC DISTRIBUTION OF CLAY MINERALS

Clay minerals, similarly to the phenomenon of life seem to be restricted to the surface of the planet Earth. As it was stated by SZÁDECZKY-KARDOSS in one of his essays in 1975, "they are known only on the Earth' surface" and from the "preentrance" of terrestrial life

* H-1143 Budapest, Stefánia út 14. Hungary

(p. 163). One exception from this rule can be the surface of the planet Mars. On the basis of measurements of the Viking program BANIN (1980) supposed that "smectite clays are abundant in the soil of Mars". In the IR spectra of the interstellar dust the lines of clay minerals such as chlorite, montmorillonite and serpentinite could be identified (BÉRCZI 1991, Fig. 72).

Clay minerals or even hydrous layer silicates are completely absent or represent extreme rarity in cosmic materials accessible for direct mineralogical measurements. In the Apollo 11 lunar samples only extremely rare di- and trioctahedral phyllosilicates could be detected by electron diffraction study (DREVER et al. 1970) which were not more closely specified. Among the meteorites the carbonaceous chondrites may contain clay mineral-line phases. In the Orgueil meteorite minor amounts of "pseudo-chlorite" (ORCEL et al. 1972), in the Allende carbonaceous chondrite intergrown mica and montmorillonite and a serpentine-like phase were found (TOMEOKA, BUSECK 1982a,b).

Contrary to true clay minerals the hydrous layer silicate serpentine is relatively abundant in the Solar System in the zone of asteroids and among the satellites of Jupiter and Saturn. Serpentine constitutes e. g. essential part of the 4 Galilean satellites of Jupiter. Its occurrence is typical in a zone which occupies intermediate position between plantes constituted mainly by silicates, e. g. Earth, Moon, Mars and those containing much water like Jupiter and Saturn. Serpentine may be a constituent of carbonaceous chondrites and is supposed to occur in comets (BÉRCZI 1991).

Microspherules of cosmic origin can remain fresh over verly long periods of time. In glassy microspherules found in Carboniferous of Upper Silesia no water contents could be detected by IR method (MANECKI and SKOWRONSKI 1970). On the other hand, glauconite-bearing microspherules proved to be of diagenetic, not of impact origin in the layers near the Cretaceous/Tertiary boundary at Gubbio, Italy (NASLUND et al. 1986).

THE LACK OF CLAY MINERALS IN IMPACT PRODUCTS

Clay minerals are practically absent in particles and rocks formed from terrestrial material by the effect of impact of cosmic bodies.

Tektites and micro-tektites consist of glassy silicate material which may contain also particles of pure SiO2 glass (lechatelierete) but are devoid of primary crystallites (GLASS 1990). No hydrous devitrification and transformation of the glass into clay minerals could be observed.

The infilling of the impact crater of Ries at Nördlingen, Germany, was extensively studied (FÜCHTBAUER et al. 1977, LEMCKE 1981). The rocks on the basis of the sequence, called suevite, show effects of shock and melting phenomena but no evidence of subsequent clay mineral formation was found. The same is true for the majority of the overlying so called Graded Unit which is most probably the product of the subaeric fall of the cloud of suevite debris produced by the impact. Alteration products of glass such as montmorillonite, zeolites and calcite appear first in the fine-grained groundmass of the upper part of the Graded Unit (JANKOWSKI 1977b, FÜCHTBAUER et al. 1977) introducing a subsequent lacustrine sedimentation in the crater basin.

CLAY MINERALS IN SEDIMENTARY ROCKS CONTAINING IMPACT OR COSMIC MINERAL

There is a great variety of composition of rocks hosting impact-derived material or particles of cosmic origin.

In the lacustrine sequence of the Ries impact crater near Nördlingen, Germany, various sediments are present (SALGER 1977, JANKOWSKI 1977a, 1980, 1981). In the lower part of the sequence glassy detrital material derived from the crater walls predominate in the sediments which has been altered into montmorillonite and zeolites. Diagenetic transformation produced illite from montmorillonite in hypersaline periods of the lake. Detrital clay minerals such as micas, chlorite, kaolinite and montmorillonite derived by weathering of micas, appear only in the upper portion of the sedimentary sequence.

In a distance of about 80 km south from the Ries crater sporadic debris derived from the impact products can be found in the fluviatile layers of the Upper Freshwater Molasse horizon of the Molasse Basin. In the molasse sediments of this zone normal terrigene detrital clay minerals were found (e. g. near Augsburg, see VICZIÁN 1984), no traces of the impact material can be detected. There are, however, restricted bentonite layers in the molasse sequence of the area, the glassy components of which are remarkably synchronous with the Ries event (Ries: 14.7±0.4 Ma, bentonite: 14.4–14.6 Ma). They were connected with the impact event by several authors (GENTNER and WAGNER 1969, see HEROLD 1970 and VOGT 1980). No direct mineralogical evidence supporting this theory was found except the very sporadic occurence of diaplectitic plagioclase glass (?) in the sediments (HARR 1976). Recently, however, the connection of the Bavarian bentonites with the Ries event was questioned and the source area was located to the Carpathian volcanic region (UNGER, NIEMEYER 1985).

The Cretaceous/Tertiary boundary is being extensively studied because the theory of a catastrophic impact event on this boundary is widely accepted.

In the western Interior of North America a few cm thick clay layer represents this boundary (POLLASTRO, BOHOR 1993). It was deposited in a peat-forming environment. The clay minerals differ from those found in marine K/T boundary sequences due to special circumstances of deposition and alteration which prevailed in this region. The layer consists of two subunits depending from the mechanism of the impact: the lower one, called the "melt ejecta layer" underwent kaolinitic alteration of glassy fragments including hollow spherules (microtektites). The upper one, called "fireball layer" has been altered into smectite. These impact-derived layers differ significantly from other clays found in the sequence, namely from tonsteins and detrital shales.

In a marine K/T transition sequence of the Northern Calcareous Alps the boundary clay differs from other clay layers in the sequence. It contains remarkably little quartz and detrital minerals such as plagioclase, micas and chlorite while it is rich in "expandable clays" and kaolinite which are the devitrification products of fine-grained vitric material derived by the impact (PREISINGER et al. 1986, LAHODYNSKY 1994).

The Jurassic/Cretaceous transition beds were studied in a borehole drilled in the Barents Sea which penetrated a marine shelf succession of clay- and siltstones (DYPVIK et al. 1995). The upper part of this sequence above the Early Volgian (=Tithonian) beds contains enhanced quantities of smectite. The authors think that smectite may be the devitrification product of glassy particles derived from the closely located Mjølnir Structure, a possible extraterrestrial impact crater.

In Hungary glassy and magnetic microspherules were found in several stratigraphic horizons ranging from Triassic to Recent sediments (DETRE et al. 1995). The clay minerals of the particular host rocks are not yet known. In some instances, however, clay minerals were investigated from the same stratigraphic formation but from another localities. Even so, some conclusions can be drawn concerning the mode of formation of these samples. A few examples are given here:

One of them is the *Lower Anisian Vöröshegy Dolomite Member in the Mecsek Mts.* (RÁLISCH-FELGENHAUER 1995). In this member there is a transition between two clay mineral associations (VICZIÁN 1993). The lower one is illite+Mg-chlorite+corrensite formed in a restricted basin environment, the upper one is detrital illite typical of shallow marine sedimentation.

In the *Upper Cretaceous of the Bakony Mts.* microspherules were found in alluvial sediments of the non-marine Csehbánya Formation as well as in the Ajka Coal Formation and in the marine Polány Marl Formation (SZARKA 1994, BODROGI 1994, 1995, SIEGL-FARKAS and WAGREICH 1994). According to clay mineral analyses Csehbánya Formation and clastic intercalations of the Ajka Coal Formation are characterised by the detrial association of illite+chlorite (VICZIÁN 1988). The Polány Marl is similar but contains more smectite which is a sign of the open marine conditions of sedimentation (VICZIÁN 1987). The possible contribution of a volcanogenic component (VASKÓ-DÁVID 1994) is not yet clear.

Spherules were found in the *Upper Pannonian* deposits of the borehole Nagylózs 1 in the *Little Hungarian Plain* (SZÖÖR and RÓZSA 1995). No clay minerals analysis was performed from this well. Stratigraphically equivalent sediments from another borehole contain detrital terrigeneous polymineralic clay mineral association of illite+chlorite in the bulk rock and highly expandable illite/smectite in the <2 μm fraction (borehole Szombathely II, VICZIÁN 1990).

It is planned to investigate the mineralogy of the samples themselves which contain spherules in order to study the particular conditions of their formation.

CONCLUSIONS

1. Meteorites and micrometeorites of cosmic origin usually contain no clay minerals, even hydrous layer silicates are rarity. Ejecta produced from terrestrial material by impact of a cosmic body are in most cases of fresh unaltered glassy composition.

2. Diagnostic features of cosmic or impact origin can be detected mainly by morphological or geochemical studies rather than by bulk mineralogical methods.

3. The clay minerals formed later of the cosmic or impact-produced particles reflect the circumstances of sedimentation, alteration and diagenesis of this material. The same is true for sedimentary rocks hosting microspherules or rather particles produced by a cosmic event. Bulk mineralogical methods such as X-ray analysis may contribute to the reconstruction of the geological history of these formations.

ACKNOWLEDGEMENTS

The work was supported by the OTKA Grant No. T 014958.

REFERENCES

BANIN, A. (1980): Smectite clays in the Martian soil: evidence for their presence and their effect on the Viking biology results. – 4th Meeting of the European Clay Groups, Freising, 1980, Abstracts 11–12.

BÉRCZI, Sz. (1991): Kristályoktól bolygótestekig (From crystals to planetary bodies). – Akadémiai Kiadó, Budapest.

BODROGI, I. (1994): *Spherulites and microtektites in the ?Coniacian – Lower Maastrichtian of the Bakony Mts.* (Hungary) – a preliminary report (abstract). – Abstracts of the International Meeting Spherulites (micrometeorites) in the Carpathian Basin, Budapest, 1994, 21.

BODROGI, I. (1995): Spherulites and microtektites in the ?Coniacian – Upper Campanian of the Bakony Mts. (Hungary) – a preliminary report. – Annales Univ. Sci. Eötvös, Sect. Geol. (in prep.).

DETRE, CS. H., GY. DON, L. DOSZÁLY, E. RÁLISCH-FELGENHAUER and Á. SIEGL-FARKAS (1995): The possibilities of geological correlation on the basis of extraterrestrial spherules occuring in Hungary (abstract). – Third Symposium on Mineralogy, Baia Mare, 1995. Abstract Volume. Romanian J. Min. 77, Suppl. 1, 15.

DREVER, J. I., R. W. FITZGERALD, S. S. LIANG and G. ARRHENIUS (1970): Phyllosilicates in Apollo 11 samples. – (Proc. Apollo 11 Lunar Sci. Conf. 1, Min. Petr.) Geoch. Cosmoch. Acta 34, Suppl. 1, 341–345.

DYPVIK, H., R. E. FERREL JR. and A. MØRK (1995): Clay mineralogical variations across the Jurassic/Cretaceous boundary, the Barents Sea (abstract). – EUROCLAY '95, Leuven, 1995. Book of Abstracts 411–412.

FÜCHTBAUER, H. et al. (1977): Tertiary lake sediments of the Ries, research borehole Nördlingen 1973 – a summary. – Geol. Bavarica **75**, 13–19.

GLASS, B. P. (1990): Tektites and microtektites: key facts and inferences. – Tectonophysics **171**, 393–404.

HARR, K. (1976): Mineralogisch-petrographische Untersuchungen an Bentoniten in der Süddeutschem Molasse. – Dr. Dissertation, Universität Tübingen.

HEROLD, R. (1970): Sedimentpetrographische und mineralogische Untersuchungen an pelitischen Gesteinen der Molasse Niederbayerns. – Dr. Dissertation, Universität München.

JANKOWSKI, B. (1977a): Die Postimpakt-Sedimente in der Forschungsbohrung Nördlingen 1973. – Geol. Bavarica **75**, 21–36.

JANKOWSKI, B. (1977b): Die gradierte Einheit oberhalb des Suevits der Forschungsbohrung Nördlingen 1973. – Geol. Bavarica **75**, 155–162.

JANKOWSKI, B. (1980): Alluvial fan, playa and lake sediments of the Miocene Ries Crater in SW-Germany. – IAS 1st European Meeting, Bochum, 1980, Abstracts 71–75.

JANKOWSKI, B. (1981): Die Geschichte der Sedimentation im Nördlinger Ries und Randecker Maar. – Bochumer geol. u. geotechn. Arb. 6, 1–315.

LAHODYNSKY, R. (1994): The Cretaceous/Tertiary boundary in the Elendgraben section (Northern Calcareous Alps/Austria). Excursion guide. – Erlanger geol. Abh. **122**, 71–75.

LEMCKE, K. (1981): Das Nördlinger Ries: Spur einer kosmischen Katastrophe. – Spektrum der Wissenschaft 1981 Januar, 111–121.

MANECKI, A., A. SKOWROŃSKI (1970): Materiał gruboziarnisty i pyły kosmiczne ze skał montmorillonitowych karbonu górnośląskiego z Milowic. – Prace Min. **22**, 45–72.

NASLUND, H. R., C. B. OFFICER and G. D. JOHNSON (1986): Microspherules in Upper Cretaceous and Lower Tertiary clay layers at Gubbio, Italy. – Geology **14**, 11, 923–926.

ORCEL, J., S. CAILLÈRE and Y. BENKHEIRI (1972): Données nouvelles sur la nature minéralogique du constituant phylliteux de la météorite d'Orgueil. – C. R. Ac. Sci. Paris, Sér. D. 274, 1, 9–12.

POLLASTRO, R. M., B. F. BOHOR (1993): Origin and clay-mineral genesis of the Cretaceous/Tertiary boundary unit, Western Interior of North America. – Clays Clay Min. **41**, 1, 7–25.

PREISINGER, A., E. ZOBETZ, A. J. GRATZ, R. LAHODYNSKY, M. BECKE, H. J. MAURITSCH, G. EDER, F. GRASS, F. RÖGL, H. STRADNER and R. SURENIAN (1986): The Cretaceous/Tertiary boundary in the Gosau Basin, Austria. – Nature **322**, 794–799.

RÁLISCH-FELGENHAUER, E. (1995): Microspherules of unidentified origin in the Middle Triassic of the Mecsek Mountains, SE-Transdanubia, Hungary (abstract). – Third Symposium on Mineralogy, Baia Mare, 1995. Abstracts Volume. Romanian J. Min. **77**, Suppl. 1, 38–39.

SALGER, M. (1977): Die Tonminerale der Forschungsbohrung Nördlingen 1973. – Geol. Bavarica **75**, 67–73.

SIEGL-FARKAS, Á., M. WAGREICH (1994): Palynological and nannoplankton correlation of spherulite-bearing Senonian formations in Hungary (abstract). – Abstracts of the International Meeting Spherulites (micrometeorites) in the Carpathian Basin, Budapest, 1994, 23.

SZÁDECZKY-KARDOS, E. (1975): Geochemical-biological equilibria and the clay mineral cycle. – Acta Geol. Hung. 19, 1–2. 157–177.

SZARKA, A. (1994): First remarks on the occurence of extraterrestrial magnetic spherulites in the Senonian alluvial sediments of southern Bakony, Hungary (abstract). – Third Symposium on Mineralogy, Baia Mare, 1995. Abstracts Volume. Romanian J. Min. 77, Suppl. 1, 44.

TOMEOKA, K., P. R. BUSECK (1982): Intergrown mical and montmorillonite in the Allende carbonaceous chondrite. – Nature **299**, 5881, 326–327.

TOMEOKA, K., P. R. BUSECK (1982): An unusual layered mineral in chondrules and aggregates of the Allende carbonaceous chondrite. – Nature 299, 5881, 327–329.

UNGER, H. J., A. NIEMEYER (1985): Die Bentonite in Ostniederbayern. Entstehung, Lagerung, Verbreitung. – Geol. Jb. D **71**, 3–58.

VASKÓ-DÁVID, K. (1994): Opac spherulites and microlapillis from the Polány Marl Formation samples of Nagygörbő 1 borehole (abstract). – Abstracts of the International Meeting Spherulites (micrometeorites) in the Carpathian Basin, Budapest, 1994, 22.

VICZIÁN, I. (1984): Clay mineralogy of pelitic sediments of the South German Molasse Basin. – 9th Conference on Clay Mineralogy and Petrology, Zvolen, 1982, 101–105. Univerzita Karlova, Praha.

VICZIÁN, I. (1987): Agyagásványok Magyarország üledékes kőzeteiben (Clay minerals in sedimentary rocks of Hungary). – Akadémiai doktori értekezés (D. Sc. Thesis), Budapest.

VICZIÁN, I. (1988): Az Ajkai Kőszén Formáció pélites kőzeteinek műszeres vizsgálata az Ajka-Magyarpolányi területen (Instrumental mineralogical investigations of pelitic rocks of the Ajka Coal Formation in the Ajka-Magyarpolány area). – Unpublished report, Hung. Geol. Inst., Budapest.

VICZIÁN, I. (1990): A Szombathely-II. sz. fúrás mintáinak röntgendiffrakciós vizsgálata (X-ray diffraction investigations on samples of the borehole Szombathely-II). – Unpublished report, Hung. Geol. Inst., Budapest.

VICZIÁN, I. (1993): Clay mineralogy of Middle Triassic evaporitic and carbonate rocks, Mecsek Mts. (southern Hungary). – 11th Conference on Clay Mineralogy and Petrology, Č. Budějovice, 1990, 135–144. Univerzita Karlova, Praha.

VOGT, K. (1980): Bentonite deposits in Lower Bavaria. – Geol. Jb. **D** 39, 47–68..

Manuscript received 11. Jan. 1996.

Acta Mineralogica-Petrographica, Szeged, XXXVII, 41–50, 1996

THE EXAMINATION OF SUEVITE FROM THE BOSUMTWI IMPACT CRATER (GHANA)

G. HEGYMEGI KISS*

Bessenyei György Teachers College Nyíregyháza (Hungary)

ABSTRACT

That meteorite has probably been hitted one million years ago – which created the Bosumtwi Meteoritic Crater in Ghana. Because of the hit suevite stone came into being and it can be found there today, too. It is a supposition that an ferro meteorite hitted but it was proved only indirectly according to literary sources.

A Hungarian searching group went to the crater and we examined the gathered suevite stonesamples. The original supposition is proved by the meltability research, the surface-research and microanalisis by scanning electronmicroscope and the results of X-ray diffraction research.

THE ORIGIN OF ROCK SAMPLES

The Bosumtwi Meteoritic Crater (Ghana) can be found 30 kilometers from Kumasi town into the South–East. The crater is nearly like a circle, its extension is 11 kms in North–South and 10 kms in East–West. There is a lake in the crater, its deepest point is about 80 m. The edge of the crater is nearly 250–300 ms above the surface of the water (JONES et al. 1981).

The crater was probably made by a 300 m of diameter meteorite at about one million years ago. Its speed was 24,6 km/s (SHOEMAKER, 1977). It was counted that its mass was 10^8 t, the kinetic energy $3x10^{19}$ joules. An immense heat occured because of the bumping against the earth and the blowing up of meteorite. The earthly material had melted and the meteorite together with its material flew about 300 kms while tektites appeared (BARNES, 1961; and COHEN, 1963). The mass of microtektites in Ivory Coast – ivorites – is about $2x10^7$ t (GLASS, 1979). It is one scale smaller than the mass of the hitted meteorite.

Because of the hit, the enormous heat and the effect of pressure suevite stone appeared, and it can be found in spots to the North–South extension from the crater. The geographical place of the crater and the occurences of suevite are shown in the *Fig. 1.*

Suevite is a dark-grey stone similar to pumiceous tuff. It contains coesite – a SiO_2 variety coming into being under high strain (LITTER, 1962), nickel-iron spherules (EL GORESY, 1966), crumbled quartz (CHAO, 1968), melted ilmenite – $FeTiO_3$ – and zircon decomposed into baddeleyite (EL GORESY, 1968).

A group of Hungarian researchers has gone to Ghana in 1993 to examine the meteorite crater of Bosumtwi. I have got a sample from suevite stone and we examined the meltabling, surface, chemical composition and quantity of the components, and the crystallinity.

* H-4400 Nyíregyháza, Hungary

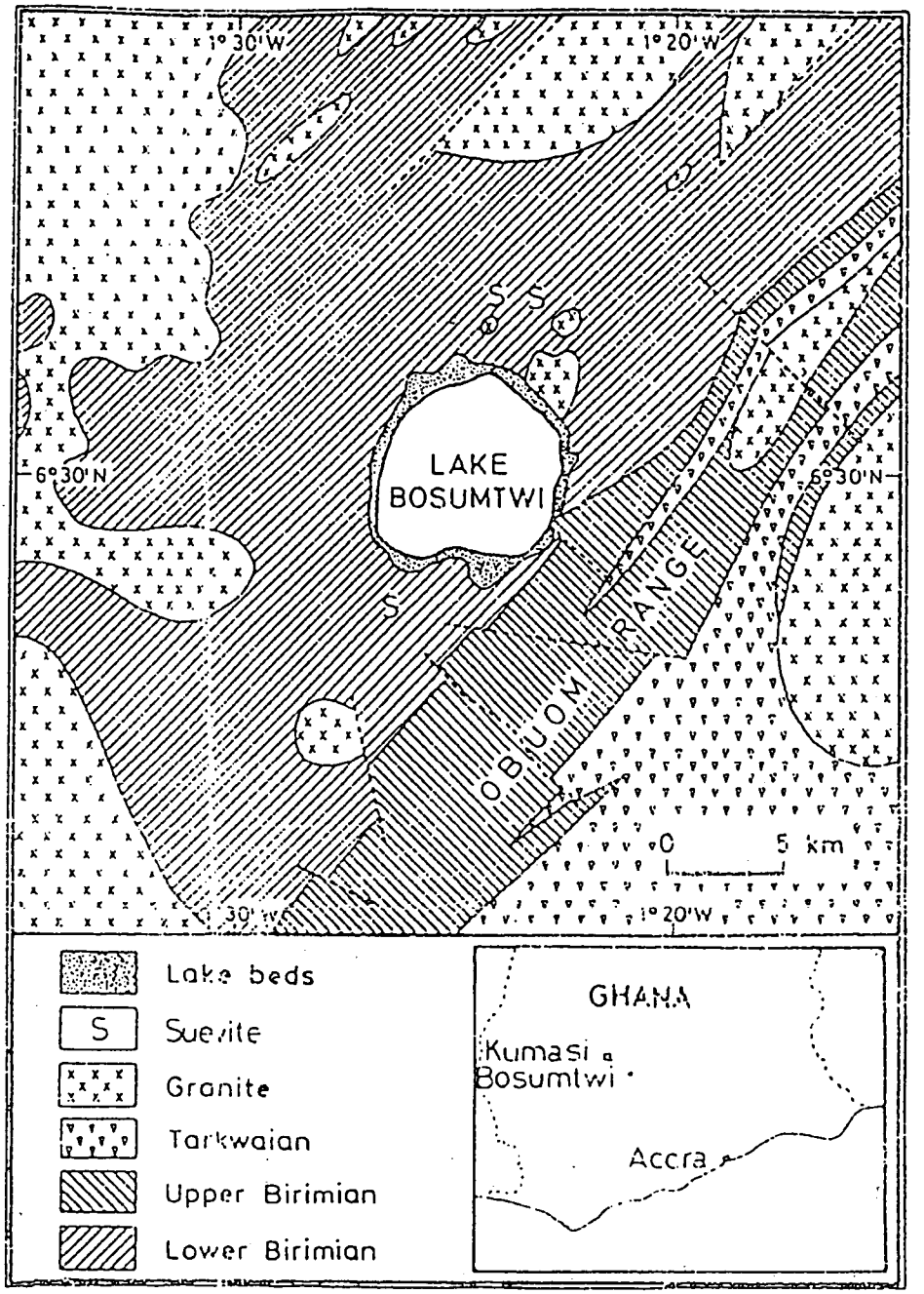

Fig. 1. The Bosumtwi impact crater (Ghana). Quarries of suevite.

MELTABILITY RESEARCH

As the suevite came into being in high temperature I did the meltability research, too. I broke a small chip of some mms piece from the examined material. I put it onto a platinum loop and hot by a jet flame. I made the examine by a precision apparatus working by butan gas so 1500 °C can be reached.

Before and after heating for some minutes I examined the surface in a 30 times enlargement with a SUNRISE hand-microscope considering the peaked parts. I discovered that the sample-piece melted in this temperature but it was not shriveled into a ball. The originally blistering surface did not bulk but its colour became darker.

RESEARCH WITH ELECTRONMICROSCOPE

Surface-research

We made the examination by scanning electronmicroscope. The equipment works in the University of Miskolc, in the Metallurgical Chair and is an American AMRAY 1830 I. type. We broke 3 pieces of some millimeters in expansion chips. To get well – perceptible photoes we made the surface electronically conductor by vapouring a thin gold layer. The secunder electrons gave sharp and large disintegrated pictures from the relief of our sample. The pictures were big profoundnessly sharp and made stereoscopic. The photographs showed it quite well (*Fig. 2a, 4a, 4b*).

The sizes of photos are 100 mm x 65 mm. The text below contains the measure of enlargement, the accelator voltage of electron gun, the measure rate, the name, the time of photo and the serial number.

The Evaluation of Photographs

It was visible to the naked eyes that the stone-sample is not homogeneous. The inner part is porous, like tuff while the outer side remembers to a conglomerate. One side of the sample was rudely polished. Opposite to the mentioned polished side one can see that the stone material is nearly homogeneous in structure.

Outer side of the sample is characterized by three photos. *Fig. 2b* shows that the structure is cracked, it remembers to a conglomerate. On the *Fig. 3b* the structure is porous, on the surface of blister sheeted separation can be found. It was examined the smooth melted surface and the separated sheet by microbougie. On the *Fig. 4b* it can be seen that the balls would melt; the inside part is porous. Increase of the enlargement has not given new informations.

Inner side of the sample is also characterized by three photos. *Fig. 2a* shows that the structure is porous. It is visible on the *Fig. 4a* that the structure is spongy, the melting part was blistered before cooling by gas. Surface of the fracture was examined by microbougie. It can be seen well on the *Fig. 3a* that in the inner surface of the blister there is a cover. The 1st and 2nd points were examined by microbougie. Increase of the enlargement has not given new informations.

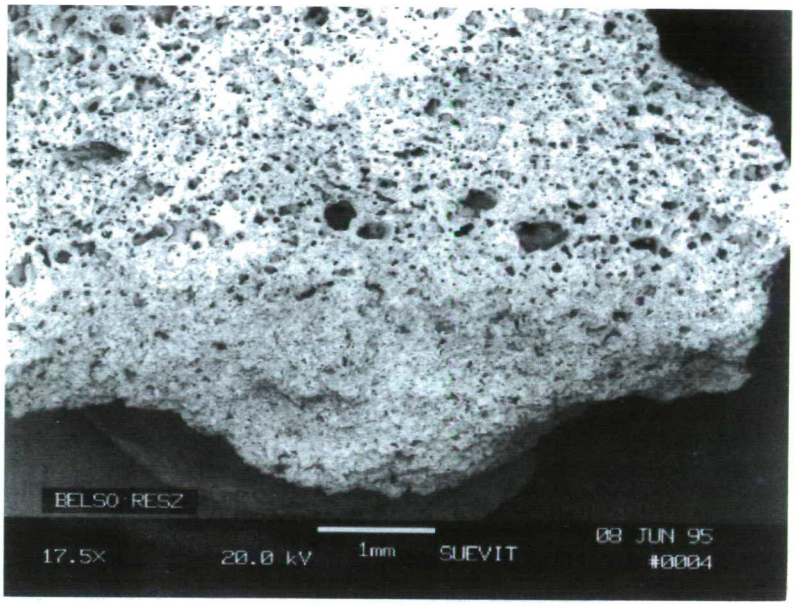

Fig. 2a. Inner part of the sample

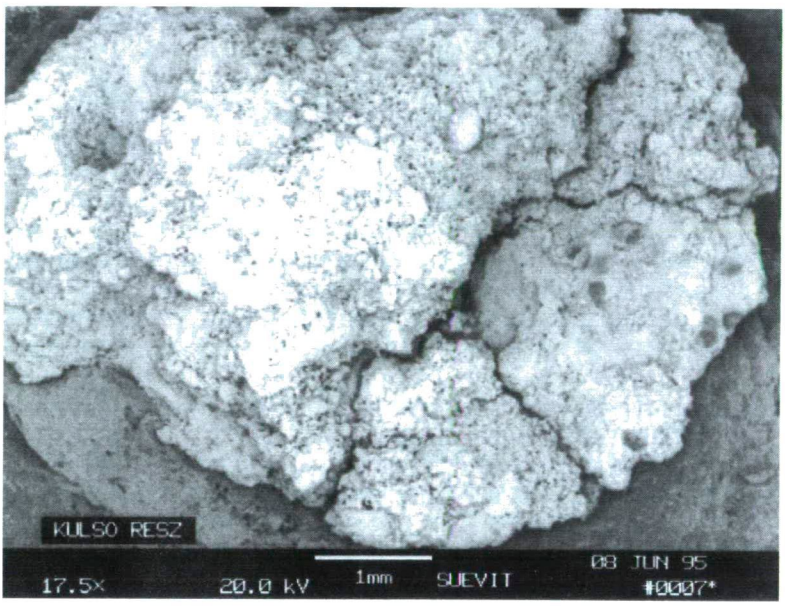

Fig. 2b. Outer part of the sample

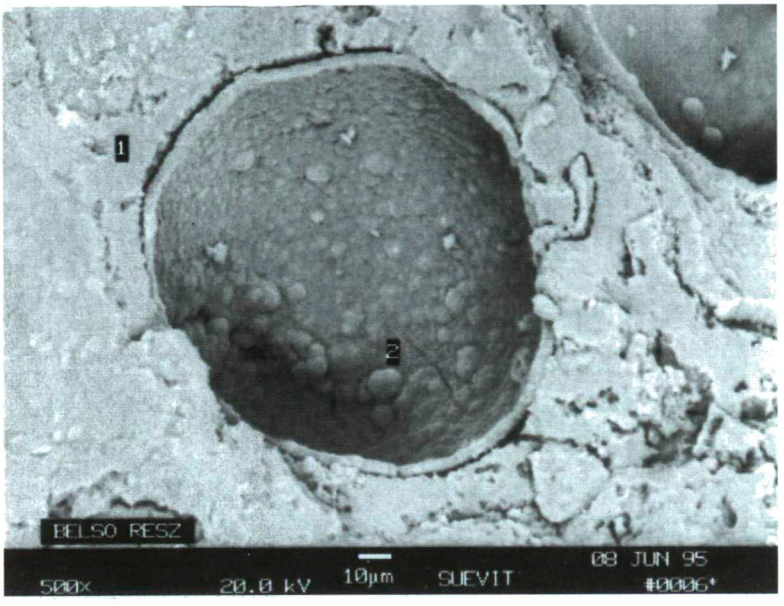

Fig. 3a. The inner surface of blister

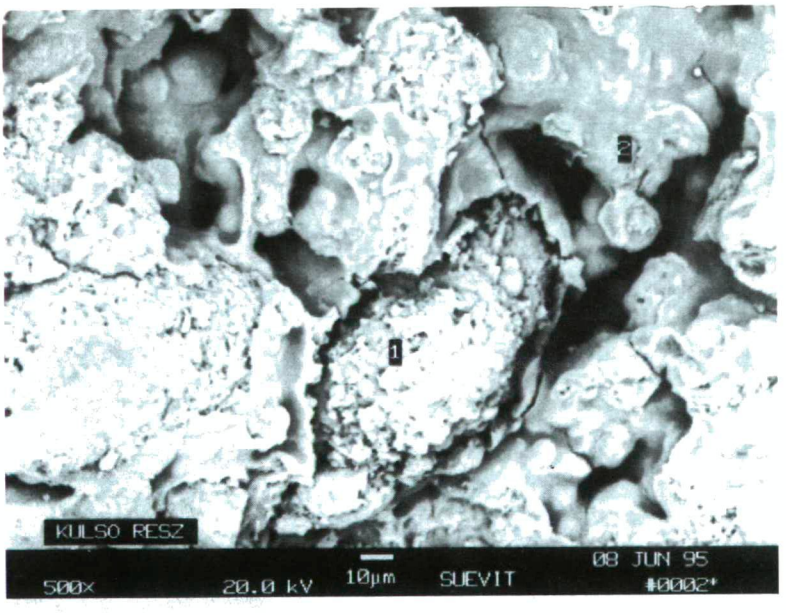

Fig. 3b. On the surface of blister sheeted separation can be found

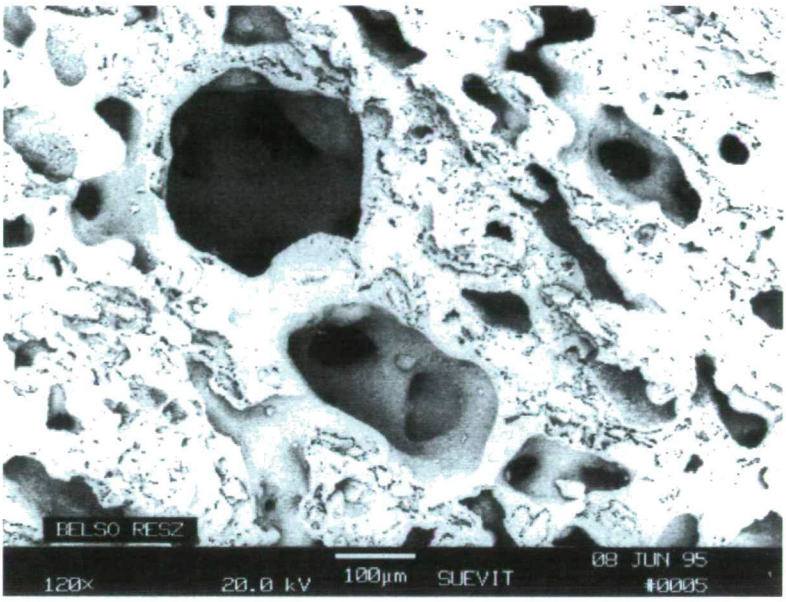

Fig. 4a. The structure is spongy

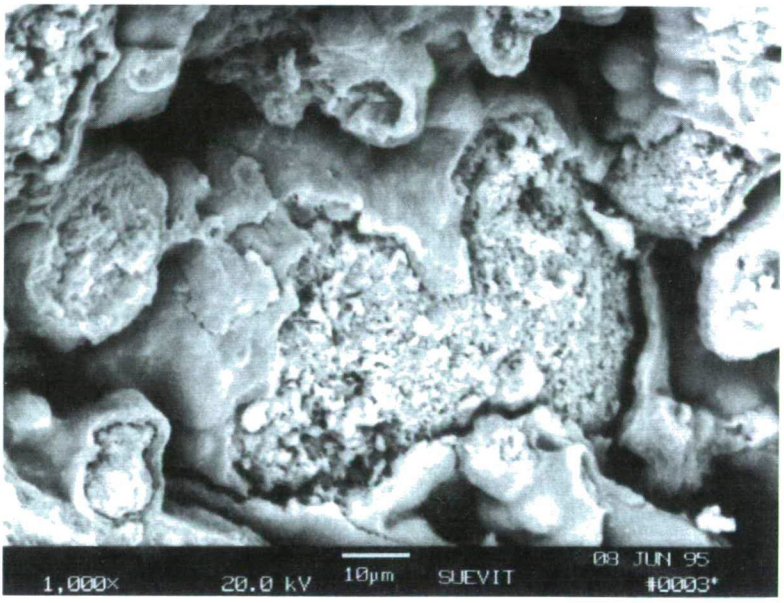

Fig. 4b. As the balls would have melted

CHEMICAL COMBINATION RESEARCH BY MICROBOUGIE

Used electronmicroscope can be utilized as electronray microanalyser (electron-microbougie) over the research of surface. The research was carried out by spread-back electrons. (We broke through the depth of 0,1–1 μm). With the help of energy-dispersive microbougie the given sample can be examined from serial number of 11 to 92. That means, there was no possibility to determine the carbon, nitrogen and oxygen content.

We add the microbougie spectrum made from the marked points of *Fig. 3a (Fig. 5)* and one can read: The disintegration of horizontal shaft 10 electron V/pipe, the researching time was 40 sec by measuring points.

The combination converted into their oxyds in the measuring points are summarized in the Table 1.

TABLE 1

Component	Fig. 4a %	Fig. 3a/1 %	Fig. 3a/2 %	Fig. 3b/1 %	Fig. 3b/2 %
SiO_2	53.57	54.76	32.33	61.02	59.16
Al_2O_3	33.85	30.53	19.46	21.18	30.03
FeO	9.30	11.20	48.21	13.42	10.19
CaO	–	–	–	1.81	0.35
K_2O	3.28	3.52	–	0.73	0.28
TiO_2	–	–	–	1.83	–

X-RAY DIFFRACTION RESEARCH

We worked with a TUR M-62 type diffractometer made in Germany – in the University of Miskolc, the Mineralogical Department. The ray source had been CoK_α, the filtering had been a thin iron sheet, the speed of goniometer 1°/min. The voltage of X-ray tube 30 kV, the currant intensity had been 20 mA during measuring. Putting the diffractograms that are characteristic of the crystal phases of suevite stones is shown on the Fig. 6. The d value belonging to the summits is the distance between the grated flats in mm, what is characteristic to the identified crystal phase. Identification was carried out by the base of ASTM catalogue.

In this way: d=0,426 nm quartz d=0,334 nm quartz
d=0,404 nm cristobalite d=0,319 nm feldspar

Other values by the catalogue were not identified.

CONCLUSIONS

Since the component-research by microbougie shows that the SiO_2 (53–61%) and Al_2O_3 (30–33%) in contents are high, the FeO content is 9–13%, in addition, the inner surface of blisters there is a high, 48,2% FeO settling; outer part of the spongy has 1,8% TiO_2 content; consequently, the hitted meteorite was ferrometeorite or stone-ferrometeorite.

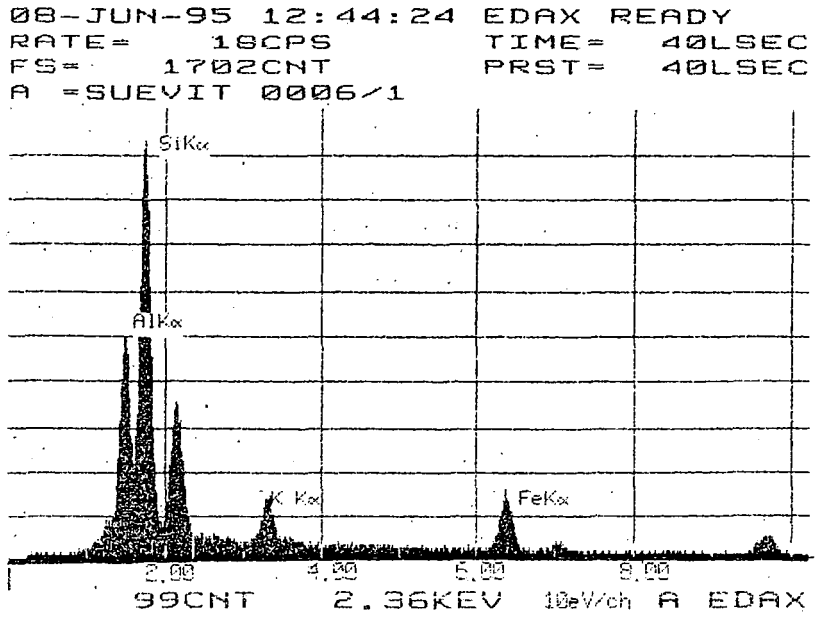

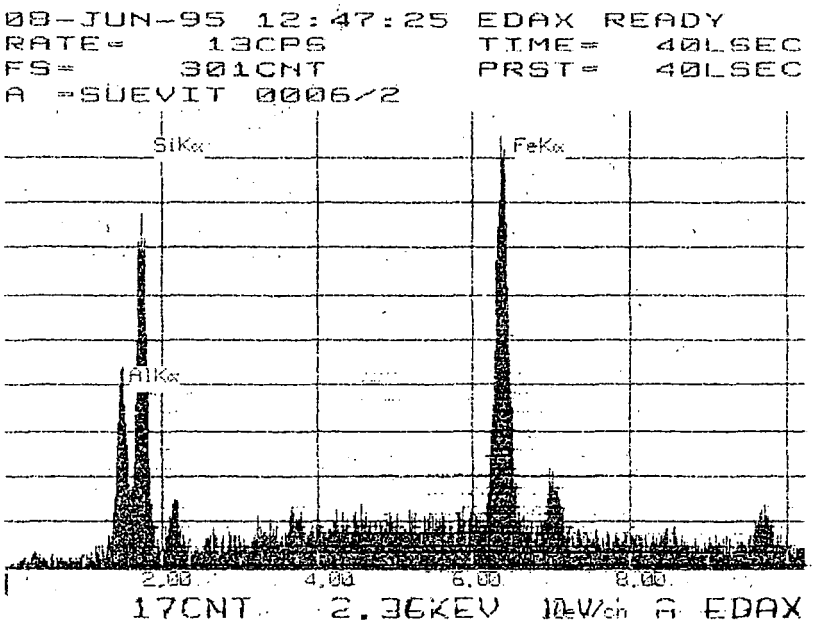

Fig. 5. Microbougie spectrums

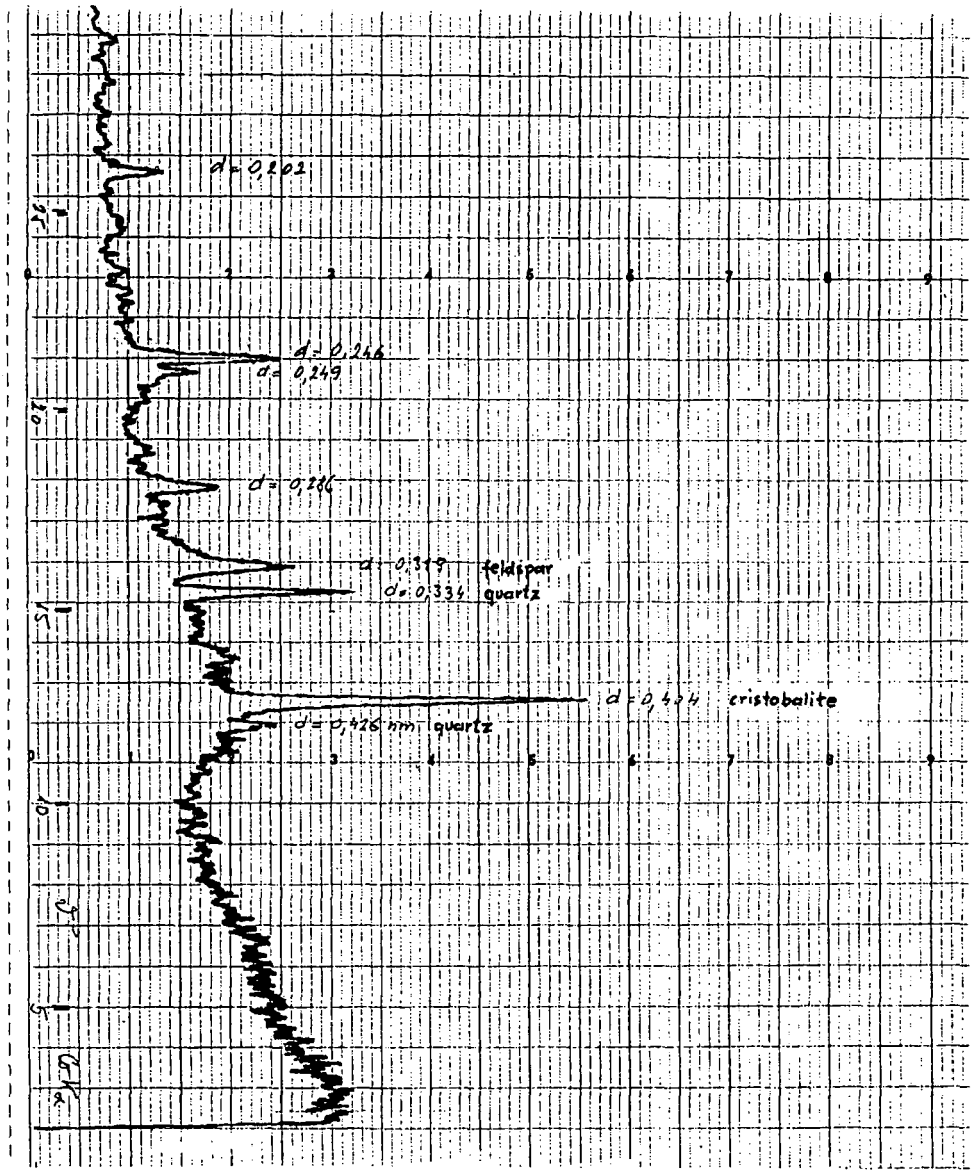

Fig. 6. X-ray diffractogram of Bosumtwi suevite

Mineralogically, the suevite samples contain mostly quartz variations and feldspar. X--ray diffractograms detected cristobalite as high temperature SiO_2 polymorph, only. No signs of the existence of coesite or stishovite in the investigated samples are observed.

In connection to its hitting the meteorite probably melted and from a part of the shooted rock material tektite came into being. It would be very interesting to compare these results to that of Ivory Coast tektites.

ACKNOWLEDGEMENTS

The author is very grateful and many thanks to Prof. L. GÖŐZ for his kind help and to the Dept. of Metallurgy as well as Dept. Mineralogy and Petrography of Miskolc University for the laboratory works.

REFERENCES

BARNES, V. E. (1961): Tektites: Scientific American. **205**, 58–65.

CHAO, E. C. T. (1968): Pressure and temperature histories of impact metamorphosed rocks – Based on petrographic observations. In: FRENCH, B. M., and others, eds. Shock metamorphism of natural materials: Baltimore, Mono Book Corp., 135–158.

COHEN, A. J. (1963): Asteroid or comet-impact hypothesis of tektite origin: The moldavite strown fields. In: O'KEEFE, J., ed., Tektites: Chicago, Illinois, University of Chicago Press, 189–211.

CSANÁLOSI S. és LEHMANN A. (1992): Ásvány- és kőzettani gyakorlatok. Általános természeti földrajzi gyakorlatok. Szerk.: Boros L. Tankönyvkiadó, Budapest, 34–35.

EGERER F. és KERTÉSZ P. (1993): Bevezetés a kőzetfizikába. Akadémiai Kiadó, Budapest, 392–395.

EL GORESY, A. (1966): Metallic spherules in Bosumtwi crater glasses: Earth and Planetary Science Letters. **1**, 23–24.

EL GORESY, A. (1968): The opaque minerals in impactite glasses. In: FRENCH, B. M., and others, eds. Shock metamorphism of natural materials: Baltimore, Mono Book Corp., 531–554.

GLASS, B. P., SWINCKI, M. B., and ZWART, P. A. (1979): Australasian, Ivory Coast and North American tektite strewn fields: Size, mass and correlation with geomagnetic reversals and other Earth events: 10^{th} Lunar and Planetary Science Conference Proceedings, 2535–2545.

JONES, W. B., BACON, M. and HASTINGS, D. A. (1981): The Lake Bosumtwi impact crater, Ghana, Geological Society of America Bulletin. 342–349.

LITTER, J., FAHEY, J., DIETZ, R. S., and CHAO, E. C. T. (1962): Coesite from the Lake Bosumtwi crater, Ashanti, Ghana: Geological Society of America Special Paper. **68**, 218 p.

SHOEMAKER, E. M. (1977): Astronomically observable crater-forming projectiles. In: RODDY, D. J. and others, eds., Impact and explosion cratering. New York, Pergamon Press. 617–628.

Manuscript received 14 August, 1996.

Acta Mineralogica-Petrographica, Szeged, XXXVII, 51–74, 1996

ALTERATION PATTERNS IN THE UMM RUS GOLD MINE AREA, EASTERN DESERT, EGYPT

NADI A. SAAD; AHMED M. EL-BOUSEILY and KHALIL I. KHALIL*

Department of Geology, Faculty of Science, Alexandria University

ABSTRACT

Mineralogical studies reveal that the common alteration minerals in the Umm Rus gold mine are chlorite, epidote, sericite and carbonates. The carbonates are mainly calcite and ankerite. Sulphidization is a common process, while silicification is the most intensive alteration process in the study area. Four alteration zones are encountered; chlorite-epidote, sericite-chlorite, sericite-ankerite-chlorite-sulphides and quartz-carbonates-sulphides zones. The textural relationship between the alteration minerals indicate that chlorite and epidote were formed firstly, followed by sericite and then by ankerite and sulphides. All the studied mineral phases were affected by silicification. The distribution of the studied alteration phases indicates that the affecting hydrothermal solutions were enriched in H_2O and CO_2 in different proportions. Elements such as K, S, As, Zn, Pb, Cu and Au are added to the system during the alteration events.

On the basis of the combined geological, mineralogical and geochemical data, four alteration stages are envisaged:

a) The hydrothermal fluids invaded the rocks through N-S shear zones. At the beginning, these fluids were characterized by low CO_2/H_2O ratio which enhanced the alteration of the biotite to chlorite and epidote. The geothermometry of the studied chlorite proves a temperature of formation of about 225°C.

b) The fluids then, became enriched in K after the breakdown of biotite. These fluids reacted with feldspars to form sericite.

c) After the formation of chlorite, epidote and sericite, the CO_2/H_2O ratio in the fluids became high and consequently ankerite was originated during this stage. Also, sulphides were concomitant with conspicuous concentration of Fe, As, Cu and Au.

d) The last stage is characterized by a severe silicification of the previously formed minerals and the formation of quartz veins. All the preceeding stages were affected by this silicification. The SiO_2-rich solution most probably remobilized the gold from sulphides (pyrrhotite) in the gabbroic rocks adjacent the granodiorite and then redistributed this gold in some other sulphide phases e. g. pyrite and pyrrhotite forming during stage c.

INTRODUCTION

More than 95 gold localities (deposits and occurrences) are known in the Eastern Desert of Egypt (EL-RAMLY et al. 1970). The Umm Rus area, the subject of this paper, is one of the largest gold mines in Egypt. It lies in the central part of the Eastern Desert, at the intersection of latitude 25° 27' 56" N and longitude 34°34'47" E (*Fig. 1*).

Gold deposit in the Umm Rus area was mined since ancient time. At the begining of twentieth century, the deposit was mined by several companies and produced about 10.000 tons of the ore (HUME, 1937 and AMIN, 1955). In the 1937 and 1938, the deposit was inspected by the Egyptian Geological Survey and the ore reserves were estimated to be

* Alexandria, El-Shatby. 21526, Egypt

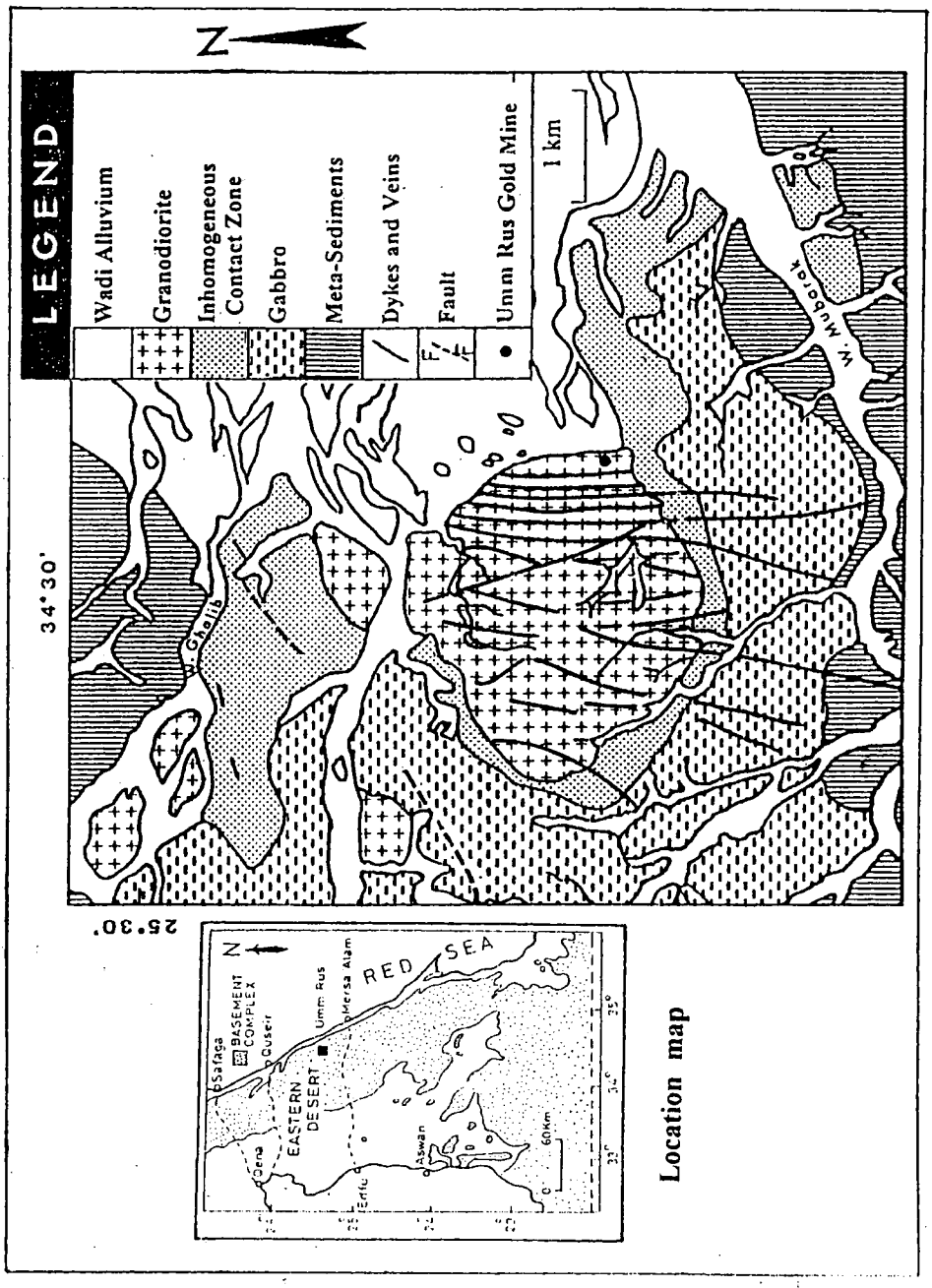

Fig. 1. Geology map of the Umm Rus area (after EL-MAHALLAWI 1984)

about 10.300 tons averaging 11,93 g/t Au (SABET, 1961). In 1940 another expedition defined additional 5800.00 tons of ore with an average of 10.85 g/t Au. During 1943–1946, the same expedition recorded 9370.00 tons of the ore. Some surface samples which were collected by the Egyptian Geological Survey during the 1968–1969 contain 27.2 g/t Au on the average. There is no information about mining activities carried out after 1969.

Field sampling for the present study (175 surface and 64 subsurface samples) was carried out to cover different rock types and quartz veins in the study area. Special attention was taken to the different alteration zones around the quartz veins. The surface sampling was carried out along profiles crossing mineralized and shear zones. Length of profiles and sampling intervals depended on ore localization and the thickness of the alteration zones. However, the subsurface samples were collected at two different depths.

A total of 115 thin and 68 polished sections were prepared for microscopic study, and results were confirmed by XRD particularly for the altered samples. Thirty polished-thin sections were microscopically selected and prepared for microprobe analysis of silicates and carbonates at the Geochemisches Institut (Göttingen University) using ARL-SEMQ-II electron microprobe equipped with six spectrometers and five different crystals (LiF, PET, ADP, TAP, PbSD). Matrix correction of the intensity measurements is made using the BENCE and ALBEE correction programme (1968). For the purpose of whole rock chemical analysis, a total of 30 samples were analyzed using a Philips PWI 408 XRF at the Geochemisches Institut, Göttingen University. The specific details of analytical precision and accuracy are given in HARTMANN and WEDEPOHL (1993).

Alteration zones in the Umm Rus area were examined by many authors as KAMEL et al. (1992) and HARRAZ and EL-DAHHAR (1994). The current study is carried out to fulfil the petrographical, mineralogical and geochemical characters of the different alteration zones, the nature of the mineralized fluids and to formulate the paragenetic sequence and the genetic model of the alteration processes.

GEOLOGIC SETTING

The Umm Rus area is covered by different rock types namely metasediments, serpentinites and related rocks, gabbros and granodiorites. The area is traversed by many quartz veins and dykes particularly in the central and southern parts of the area (*Fig. 1*).

The metasediments appear to be the oldest rock unit exposed in the area. They are regarded by KABESH et al. (1967) as typical geosynclinal sediments. The serpentinites and related rocks are presented by small exposures localized to the west and southwest of the Umm Rus area (out of the map of *Fig. 1*). The gabbro belongs to the younger ones of the Egyptian basement (TAKLA 1971) are represented by a wide exposure around the granodiorite pluton. They stratigraphically overlie the metasediments and cut across their foliation planes. The granodiorite pluton occurs as a semicircular body (ca. 7 km^2); occupiing the middle part of the area. Along the contact between the granodiorite and gabbro, a transitional heterogeneous zone mainly formed of metadiorite and metagabbro is recorded (*Fig. 1*). The granodiorite and the gabbro are traversed by several dykes and many quartz veins (*Fig. 1*). The dykes vary in composition from acidic, intermediate to basic types.

The Umm Rus gold mine area was affected by tectonism as manifested by the occurrence of numerous joints and subordinate faults particularly around the mine. The joints are of three main directions NE, NW and due E. The main fault in the investigated

area extends for more than 200 m in the NE along the contact between the gabbro and the metasediments.

More than twenty different quartz veins are occurred in the Umm Rus gold mine area. Two main trends are recognized, the dominant one has a N-S direction, while the second trend has a N-NE one. Generally, the veins dip to the W and SW with an average angle of about 30°. The main lode occurs at the southeastern corner of the Umm Rus granodiorite pluton extending for more than 200 m along the quartz vein strike and reaches more than 80 m down dip. The thickness of this vein does not exceed 40 cm.

PETROCHEMISTRY

The Umm Rus granodiorite is almost fresh, and it composed of plagioclase and potash-feldspars, hornblende and biotite. The microprobe analysis of these minerals are tabulated in Tables (1–4). Plagioclase composition ranges from albite to oligoclase. Some plagioclase crystals contain a minor amount of K (orthoclase molecule, Or) up to 2.84 mol% (Table 1). The K-feldspars normally contain a small amount of albite (Ab) and anorthite (An) in solid solution. They reach up to 3.13% and 3.29%, respectively (Table 2). Biotite is a common mineral in the present granodiorite. On the Al^{IV} versus $Fe^{+2}/(Fe^{+2}+Mg)$ binary diagram of *Figure 2*, all analyses fall in the biotite field. It can be seen from Table 3 that the sum of elements occuping the K-site is less than 1.00 mol%. The deficiency is commonly compensated by the introduction of H_2O. Biotite containing water of this nature may be classified as hydrobiotite, a term first introduced by STRUNZ (1966). The type of amphiboles present in the granodiorite of the Umm Rus area is generally ferrohornblende type, according to LEAKE's (1978) classification (*Fig. 3*). The amount of $(Fe^{+2}/Fe^{+2}+Mg)$ ranges from 0.513 to 0.608 mol% (Table 4).

ALTERATION PATTERNS IN THE MINE AREA

a) Alteration minerals

Chlorite is abundantly distributed in the altered zones of the Umm Rus gold mine area. It is mostly formed by replacement of biotite and sometimes hornblende and in relatively strong altered zones the chlorite occurs as a pseudomorphic mineral and may contain relicts of biotite and hornblende (Plate I, A). The chemical data of the analyzed chlorite (Table 5) proved the dominancy of brunsvigite in the studied altered granodiorite (Fig. 4). The use of chlorite as a geothermometer has been discussed by many authors as CATHELINEAU and NIEVA (1985) and CATHELINEAU et al. (1988). They concluded that the Al-content in the tetrahedral site of chlorite is a function of temperature of formation. Using the average mol% of Al in the tetrahedral site and appling their geothermometry, it can be concluded that the present chlorite indicates temperature of formation ranging from 180° to 285°C (*Fig. 5*) with an average 225°C.

In the slightly altered samples, epidote is a common alteration mineral and is closely associated with chlorite (Plate I, A). The current epidote is analyzed (Table 6) and the following ideal formula is deduced: $Ca_{1.991}\ Fe^{+3}{}_{1.052}\ Al_{1.793}$ (O, OH, SiO_4, $Si_{2.098}O_7$).

Sericite is a common alteration mineral in the study area; it is mostly formed by the alteration of feldspars (Plate I, B). The sericite-content increases towards the quartz vein. The chemistry of sericite (Table 7) reflects that its K-content is distinctly low and

TABLE 1

Selected microprobe analysis of plagioclase feldspars in the Umm Rus granodiorite*

Sample	Albite							Oligoclase				
No.	P1-1	P1-2	P1-3	P1-4	P1-5	P1-6	P1-7	P1-8	P1-9	P1-10	P1-11	P1-12
Na_2O	11.41	11.27	9.80	10.93	11.31	10.87	10.28	9.93	8.44	8.67	8.57	9.10
K_2O	b.d.	b.d.	0.46	b.d.	b.d.	b.d.	b.d.	b.d.	0.28	0.47	0.42	b.d.
CaO	b.d.	b.d.	0.82	b.d.	b.d.	b.d	0.72	2.61	5.19	4.73	4.42	4.49
FeO	b.d.	b.d.	0.12	b.d.	b.d.	b.d.	0.42	b.d.	b.d.	0.23	0.20	b.d.
Al_2O_3	19.93	19.87	20.10	19.50	19.84	19.57	19.69	21.32	23.76	22.55	23.01	22.07
MgO	b.d.	b.d	b.d.	b.d.	b.d.	b.d	b.d.	b.d.	b.d.	b.d.	b.d.	b.d.
SiO_2	68.78	69.21	69.36	69.60	69.29	69.30	68.78	66.35	62.14	63.60	63.01	64.15
Total	*100.12*	*100.35*	*100.66*	*100.03*	*100.44*	*99.74*	*99.89*	*100.21*	*99.81*	*100.25*	*99.63*	*99.81*
Na	0.960	0.944	0.816	0.916	0.947	0.913	0.864	0.842	0.726	0.744	0.737	0.783
K	–	–	0.025	–	–	–	–	–	0.016	0.027	0.024	–
Ca	–	–	0.038	–	–	–	0.033	0.123	0.247	0.224	0.21	0.213
Total	*0.960*	*0.944*	*0.879*	*0.916*	*0.947*	*0.913*	*0.897*	*0.965*	*0.989*	*0.995*	*0.971*	*0.996*
Fe^{+2}	–	–	0.004	–	–	–	0.014	–	–	0.008	0.0007	–
Al	1.018	1.011	1.017	0.993	1.009	0.999	1.006	1.099	1.243	1.177	1.202	1.154
Mg	–	–	–	–	–	–	–	–	–	–	–	–
Si	2.982	2.989	2.979	3.007	2.99	3.001	2.98	2.901	2.7	2.815	2.792	2.846
Total	*4.000*	*4.000*	*4.000*	*4.000*	*4.000*	*4.000*	*4.000*	*4.000*	*4.000*	*4.000*	*4.000*	*4.000*
Ab%	100.00	100.00	92.84	100.00	100.00	100.00	96.32	87.25	73.41	74.77	75.90	78.61
An%	–	–	4.32	–	–	–	3.68	12.75	24.97	22.51	21.63	21.39
Or%	–	–	2.84	–	–	–	–	–	1.62	2.72	2.47	–

* The structural formula of feldspars based on 4 numbers of cations excluding K, Na and Ca
b.d. = below detection

TABLE 2

Selected microprobe analyses of potash-feldspars in the Umm Rus granodiorite*

Sample No.	K-1	K-2	K-3	K-4
K_2O	13.52	15.85	16.71	15.97
Na_2O	0.26	0.34	0.25	0.29
CaO	b.d.	b.d.	0.59	0.66
FeO	0.39	b.d.	0.33	b.d.
Al_2O_3	18.33	19.16	18.69	18.26
SiO_2	67.31	64.64	64.55	65.01
Total	*99.81*	*99.99*	*101.12*	*100.19*
K	0.774	0.927	0.982	0.943
Na	0.023	0.030	0.022	0.026
Ca	–	–	0.029	0.033
Total	*0.797*	*0.957*	*1.033*	*1.002*
Fe^{+2}	0.013	–	0.011	–
Al	0.969	1.036	1.015	0.991
Si	3.018	2.964	2.974	3.009
Total	*4.000*	*4.000*	*4.000*	*4.000*
Or%	97.11	96.87	95.06	94.11
Ab%	2.89	3.13	2.13	2.60
An%	0.00	0.00	2.81	3.29

* The structural formula of feldspars based on 4 numbers of cations excluding K, Na and Ca

b. d. = below detection

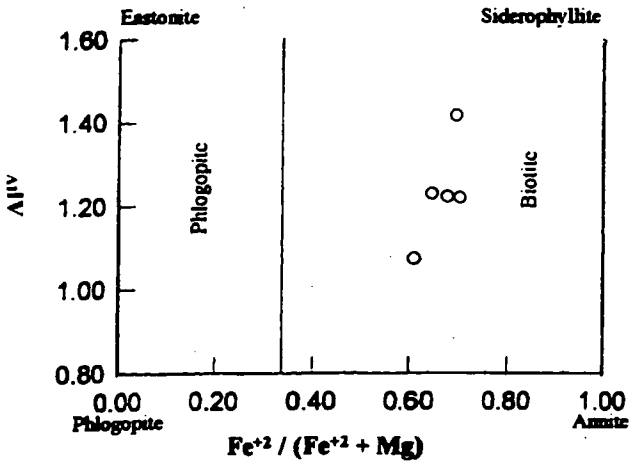

Fig. 2. Classification of biotite from the Umm Rus granodiorite (after DEER et al. 1985)

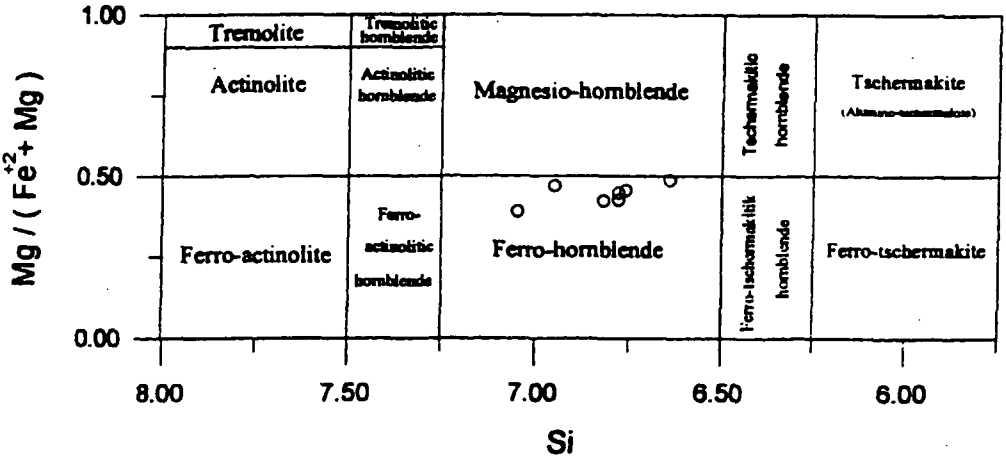

Fig. 3. Classification of amphiboles from the studied granodiorite, in which (Ca+Na)B ≥ 1.34 & NaB < 0.07 (after LEAKE 1978)

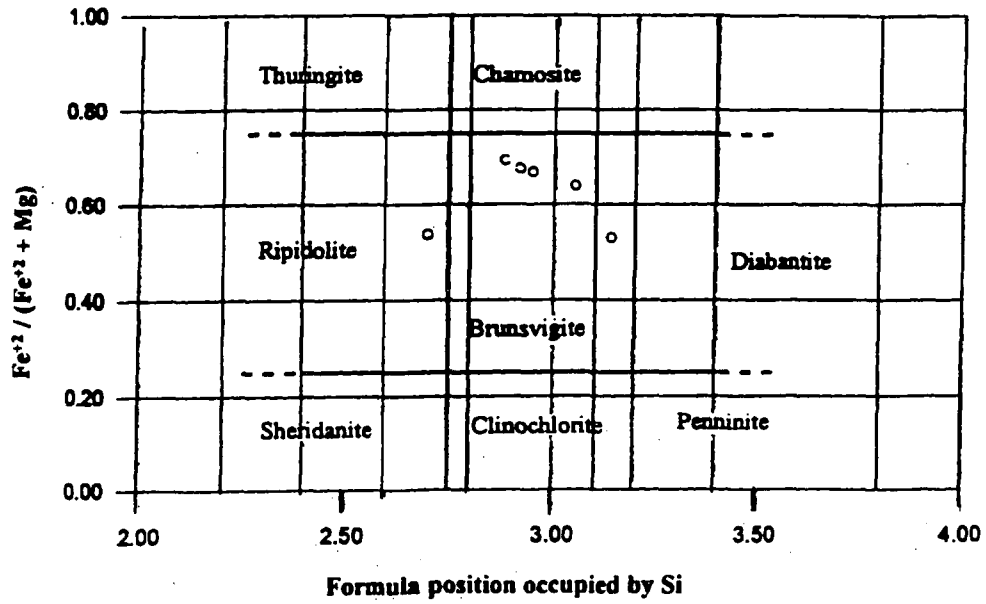

Fig. 4. Chemical classificaton of chlorite, altered from biotite, Umm Rus alteration zones (after FOSTER 1962)

TABLE 3

Selected microprobe analyses of biotite in the Umm Rus granodiorite*

Sample No.	B-1	B-2	B-3	B-4	B-5	B-6
FeO	22.11	23.19	26.05	27.60	27.71	25.42
Fe_2O_3	b.d.	b.d.	b.d.	2.19	b.d.	2.08
MnO	0.12	0.13	0.26	0.30	0.24	0.39
MgO	9.51	8.37	8.19	6.63	7.51	7.93
K_2O	9.03	8.95	7.85	7.07	7.54	7.74
Na_2O	b.d.	b.d.	b.d.	b.d.	b.d.	b.d.
CaO	0.25	0.17	b.d.	b.d.	0.11	b.d.
Al_2O_3	14.14	14.02	15.41	14.60	14.45	15.48
TiO_2	3.87	3.62	3.95	2.07	3.12	1.17
SiO_2	37.09	36.84	36.15	35.36	35.51	35.46
H_2O	3.83	3.77	3.91	3.81	3.83	3.83
Total	*100.22*	*99.06*	*101.77*	*99.63*	*100.02*	*99.50*
K	0.902	0.907	0.772	0.727	0.753	0.772
Na	–	–	–	–	–	–
Ca	0.021	0.014	–	–	0.009	–
H_2O	0.077	0.079	0.222	0.273	0.238	0.228
Total	*1.000*	*1.000*	*1.000*	*1.000*	*1.000*	*1.000*
Fe^{+2}	1.447	1.542	1.691	1.816	1.814	1.662
Fe^{+3}	–	–	–	0.130	–	0.122
Mg	1.109	0.992	0.947	0.777	0.876	0.924
Al	0.208	0.241	0.215	0.135	0.112	0.198
Ti	0.228	0.216	0.130	0.122	0.183	0.068
Mn	0.008	0.009	0.017	0.020	0.016	0.026
Total	*3.000*	*3.000*	*3.000*	*3.000*	*3.000*	*3.000*
Al	1.097	1.072	1.195	1.219	1.221	1.228
Si	2.903	2.928	2.805	2.781	2.778	2.772
Total	*4.000*	*4.000*	*4.000*	*4.000*	*4.000*	*4.000*
OH	1.489	1.464	1.997	1.870	1.972	1.878
O	0.511	0.536	0.003	0.130	0.028	0.122
Total	*2.000*	*2.000*	*2.000*	*2.000*	*2.000*	*2.000*
O	10.000	10.000	10.000	10.000	10.000	10.000
$Fe^{+2}/(Fe^{+2}+Mg)$	0.566	0.609	0.641	0.700	0.674	0.643

* the structural formula of biotite and amphiboles based on 7 and 13 number of cations respectively, excluding K, Na and Ca

b. d. = below detection

TABLE 4

Selected microprobe analyses of amphiboles in the Umm Rus granodiorite*

Sample No.	Am-1	Am-2	Am-3	Am-4	Am-5	Am-6	Am-7
CaO	10.40	10.79	10.63	10.60	10.23	11.23	11.90
Na_2O	1.38	1.54	1.59	1.43	1.48	1.01	0.90
K_2O	0.58	0.71	0.63	0.68	0.66	b.d.	b.d.
FeO	16.49	15.53	17.02	17.52	15.82	16.83	19.72
Fe_2O_3	5.66	8.53	7.27	7.55	8.85	9.01	5.36
MgO	8.25	8.26	7.79	7.24	7.47	6.95	7.12
MnO	0.61	0.66	0.78	0.81	0.93	0.52	0.41
TiO_2	1.51	1.59	1.54	1.57	1.50	b.d.	b.d.
Al_2O_3	6.53	6.90	6.49	6.53	6.70	7.61	6.46
SiO_2	45.62	43.46	44.49	44.38	44.29	44.85	46.29
H_2O	1.97	1.97	1.97	1.96	1.96	1.97	1.97
Total	*99.00*	*99.94*	*100.20*	*100.27*	*99.89*	*99.98*	*100.13*
Na	0.106	0.224	0.209	0.161	0.107	0.131	0.205
K	0.114	0.139	0.123	0.133	0.132	–	–
Total	*0.220*	*0.363*	*0.332*	*0.294*	*0.239*	*0.131*	*0.205*
Na	0.302	0.233	0.262	0.264	0.326	0.168	0.060
Ca	1.698	1.767	1.738	1.736	1.674	1.832	1.940
Total	2.000	2.000	2.000	2.000	2.000	2.000	2.000
Fe^{+2}	2.102	1.985	2.170	2.239	2.021	2.141	2.509
Fe^{+3}	0.649	0.866	0.784	0.827	0.985	1.031	0.613
Mg	1.872	1.881	1.770	1.648	1.703	1.576	1.618
Mn	0.079	0.085	0.100	0.105	0.122	0.066	0.057
Ti	0.173	0.183	0.176	0.181	0.169	–	–
Al	0.125	–	–	–	–	0.186	0.203
Total	*5.000*	*5.000*	*5.000*	*5.000*	*5.000*	*5.000*	*5.000*
Al	1.047	1.242	1.166	1.177	1.205	1.179	0.951
Si	6.953	6.642	6.784	6.781	6.763	6.821	7.049
Fe^{+3}	–	0.116	0.050	0.042	0.032	–	–
Total	*8.000*	*8.000*	*8.000*	*8.000*	*8.000*	*8.000*	*8.000*
OH	2.000	2.000	2.000	2.000	2.000	2.000	2.000
O	22.000	22.000	22.000	22.000	22.000	22.000	22.000
$Mg/Fe^{+2}+Mg$	0.471	0.487	0.449	0.424	0.457	0.424	0.392
$Fe^{+2}/Fe^{+2}+Mg$	0.529	0.513	0.551	0.576	0.543	0.576	0.608

TABLE 5

Selected microprobe analyses of chlorite in the Umm Rus alteration zones*

Sample No.	Ch-1	Ch-2	Ch-3	Ch-4	Ch-5	Ch-6
Fe_2O_3	b.d.	b.d.	1.00	b.d.	0.52	b.d.
FeO	25.03	27.78	32.85	34.19	34.76	28.51
MnO	b.d.	b.d.	0.52	0.54	0.51	0.23
MgO	12.46	8.8	9.4	8.45	9.47	13.79
CaO	0.24	0.19	n.d.	0.54	0.11	0.21
K_2O	0.14	0.34	1.13	0.32	0.62	b.d.
Na_2O	b.d.	0.11	b.d.	b.d.	b.d.	b.d.
Al_2O_3	21.44	23.5	16.35	17.86	17.02	19.79
TiO_2	b.d.	b.d.	0.27	1.81	0.21	1.07
SiO_2	29.82	28.46	26.58	26.32	26.8	25.52
H_2O	11.38	11.19	10.82	10.95	11.02	11.32
Total	*100.51*	*100.37*	*98.92*	*100.98*	*101.04*	*100.32*
Mg	1.203	0.985	1.552	1.379	1.536	1.723
Fe^{+3}	–	–	0.088	–	0.042	–
Fe^{+2}	–	–	0.208	0.238	0.26	–
Al	1.797	2.015	1.081	1.184	1.098	1.172
Mn	–	–	0.048	0.05	0.047	0.02
Ti	–	–	0.023	0.149	0.017	0.085
Total	*3.000*	*3.000*	*3.000*	*3.000*	*3.000*	*3.000*
Si	3.138	3.048	2.945	2.881	2.915	2.702
Al	0.862	0.952	1.055	1.119	1.085	1.298
Total	*4.000*	*4.000*	*4.000*	*4.000*	*4.000*	*4.000*
Mg	0.751	0.42	–	–	–	0.453
Fe^{+2}	2.203	2.489	2.841	2.892	2.902	2.524
Ca	0.027	0.021	–	0.063	0.012	0.023
K	0.019	0.047	0.159	0.045	0.086	–
Na	–	0.023	–	–	–	–
Total	*3.000*	*3.000*	*3.000*	*3.000*	*3.000*	*3.000*
OH	8.000	8.000	8.000	8.000	8.000	8.000
O	10.000	10.000	10.000	10.000	10.000	10.000
$Fe^{2+}/(Fe^{+2}+Mg)$	0.530	0.639	0.663	0.694	0.693	0.539

TABLE 6

Selected microprobe analyses of epidote in the Umm Rus alteration zones*

Sample No.	Ep-1	Ep-2	Ep-3
Fe_2O_3	17.10	16.78	17.30
MgO	0.24	0.23	0.23
CaO	22.75	22.99	22.25
SrO	0.20	0.10	0.13
Al_2O_3	18.51	18.97	18.21
TiO_2	0.53	0.41	0.49
SiO_2	37.83	37.53	38.01
H_2O	3.44	3.66	3.34
Total	*100.60*	*100.67*	*99.96*
Ca	1.995	2.014	1.964
Sr	0.010	0.005	0.006
Mg	0.029	0.028	0.028
Total	*2.034*	*2.047*	*1.998*
Al	1.784	1.828	1.768
Ti	0.034	0.025	0.030
Fe^{+3}	1.052	1.032	1.073
Total	*2.870*	*2.885*	*2.871*
Si	3.096	3.068	3.131
Al	–	–	–
Total	*3.096*	*3.068*	*3.131*
$Fe^{+2}/(Fe^{+2}+Al)$	0.371	0.361	0.378

* the structural formula of chlorite and epidote based on 10 and 8 number of cations respectively

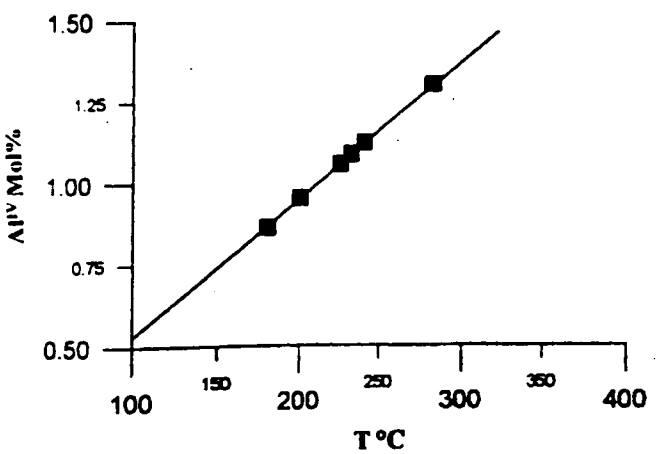

Fig. 5. Plot of Al^{IV} versus temperature for the chlorite available in the Umm Rus alteration zones (after CATHELINEA et al. 1988)

consequently the H_2O in the K-position is high. Accordingly, the sericite from the studied area can be classified as hydrosericite.

Two *carbonate* generations are distinguished in the altered zones of the Umm Rus granodiorite; less abundant calcite (generation I) and relatively abundant ankerite (generation II). Calcite occurs mostly as very fine-grained aggregates essentially replacing plagioclase, chlorite and hornblende. The chemical data presented in Table 8 show that the $CaCO_3$-content in calcite ranges from 94.42 to 98.60 mol%; the $MgCO_3$-component ranges from 1.40 to 2.03 mol%, while siderite and rhodochrosite are of minor significance. Ankerite is frequently present in altered sulphide-rich samples. It seems to replace chlorite (Plate I, C), plagioclase and sericite. The mineral chemistry reflects an ex-solution of dolomite-ankerite. The dolomite ranges from 36.52 to 59.84 mol%; and ankerite has a range of 35.42 to 62.60 mol% (Table 8). Thus the chemical formula of the minerals ranges from dolomitic-ankerite $[Ca_{.973}\ Mg_{.365}\ (Fe_{.648}Mn_{.014})_{.662}]_2\ (CO_3)_2$ to ankeritic-dolomite $[Ca_{.953}\ Mg_{.598}\ (Fe_{.426}\ Mn_{.023})_{.449}]_2\ (CO_3)_2$. A siderite component is also recorded on the ankerite as a solid solution up to 4.74 mol%.

Sulphidization is a common process in the Umm Rus gold mine. Most sulphides occur in the alteration zones and subordinately in the quartz vein. Pyrite, arsenopyrite and pyrrhotite are the common sulphide phases. Gold appears as specks in pyrite and aresenopyrite and sometimes it is filling fractures of the brecciated pyrite. *Silicification* is the most intensive alteration process due to hydrothermal acitivity in the study gold mine area. The dominant quartz veins have been most probably produced during this relatively young alteration process.

b) Alteration zones

The various alteration mineral assemblages characterizing distinct alteration zones (*Fig. 6*) in the granodiorite of the Umm Rus area can be divided into the following:

1. Chlorite-epidote zone (Zone R1)

This alteration zone is occured far away from the quartz vein (*Fig. 6*). This mineral assemblage is characterized by the predominance of chlorite and epidote formed as a result of biotite alteration (Plate I, A). Hornblende and K-feldspar in this zone are usually unaltered, whilst plagioclases are slightly sericitized.

2. Sericite-chlorite zone (Zone R2)

In this zone, many of the primary minerals are almost altered. Sericite and subordinate chlorite are the main alteration products. Calcite is the only distinguished carbonate, it is uncommon alteration product. Silicification is also present in this alteration zone, where silica occurs as a replacement mineral, filling cavities and/or formating quartz veinlets.

3. Sericite-ankerite-chlorite-sulphides zone (Zone R3)

This alteration zone is observed close to and in contact of the central quartz vein (Fig. 6). Minerals characterizing this zone are sericite, ankerite, chlorite and sulphides. Ankeritic carbonatization and sulphidization are the diagnostic feature in this zone. Ankerite seems to replace mainly chlorite (Plate I, C) and sometimes sericite. Most sulphide crystals as pyrite and arsenopyrite contain relics of wall rock material revealing a strong sulphidization of the pre-existing minerals.

4. Quartz-carbonates-sulphides-wall rock relicts zone (Zone R4)

SiO_2-rich fluids resulted in silicification of the previously formed minerals and deposition of the quartz vein. Many relicts of carbonates, wall rock material and sericite (Plate I, D) are recorded in this alteration zone. Some of these are arranged parallel to the foliation of the wall rocks (Plate I, E). On the other hand, sulphides prevailed in this zone

are more resistant against silicification than the other minerals and thus generally exhibit a relatively less degree of silicification (Plate I, F).

c) Geochemistry

Ion exchange between wall rock and ore-bearing fluids is the principal chemical process operative during the hydrothermal alteration. One approach to examine the chemical aspects of alterations is to determine the gain and loss of components in the entire rock mass during metasomatism and to refer these alterations to the observed mineral assemblages. The whole rock chemical composition of the Umm Rus gold mine lithologes of the different alteration zones and the unaltered granodiorite are presented in Table 9.

Mass balance calculations

The principles of mass balance are compatible to those described by MACLEAN and KRANIDIOTIS (1987). This method depends on the nature of the precursor rock. At the Umm Rus gold mine area, the fresh granodiorite is the only precursor which seems to be more or less chemically homogeneous (single precursor system). According to MACLEAN and KRANIDIOTIS (op. cit.) method, it is found that the most immobile element pair is Al_2O_3-Zr. The selection of such elements is based on: their proper linear regression relation, the high correlation coefficient and passing of the line relation through both the point of origin and the average bulk composition of the fresh granodiorite (*Fig. 7*). Al_2O_3 is preferred to be a monitor for the mass change calculation rather than Zr for its better correlation with the other elements. TiO_2 followed by Ba, Rb and Ga are relatively slight mobile. The gain and loss of chemical components were calculated by assuming a starting mass of 100 g of the fresh granodiorite according to the following formula:

Component "A"g = component A / Al_2O_3 wt% in altered rock x Al_2O_3 in fresh rock.

The results of mass gain and loss of the different alteration zones are given in Table 10 and illustrated in *Fig. 14*. The following is a brief discussion of the mass changes for each alteration zone:

1. Chlorite-epidote zone (R1)

The main chemical changes in this zone have involved the addition of SiO_2, Fe_2O_3, Na_2O and volatiles (L.O.I.), while losses took place in K_2O, CaO, and MgO (*Fig. 8a*). The gain of SiO_2 means that the silica added by silicification was more than that lost by the alteration of biotite to chlorite and epidote. The addition of iron and volatiles resulted in the formation of new iron-bearing hydrous phases, principally chlorite. The small loss of K indicates that the amount of sericite formed in this zone is not enough to consume all the K released from biotite during its alteration to chlorite and epidote. Thus, most of the remaining K was carried away in solution. The partial alteration of plagioclase to sericite led to the release of Ca which was partially used in the formation of epidote while the rest was lost from the system. The depletion in Mg in this zone may also be attributed to the chloritization of biotite. The main chemical changes among the trace elements is the gain of Sr. The mineral analysis indicate that epidote is the main Sr-bearing phase in this alteration zone.

2. Sericite-chlorite zone (R2)

Chemical changes in this zone seem to be mainly a result of two alteration processes: sericitization and chloritization. Sericitization of plagioclase feldspars yields a strong

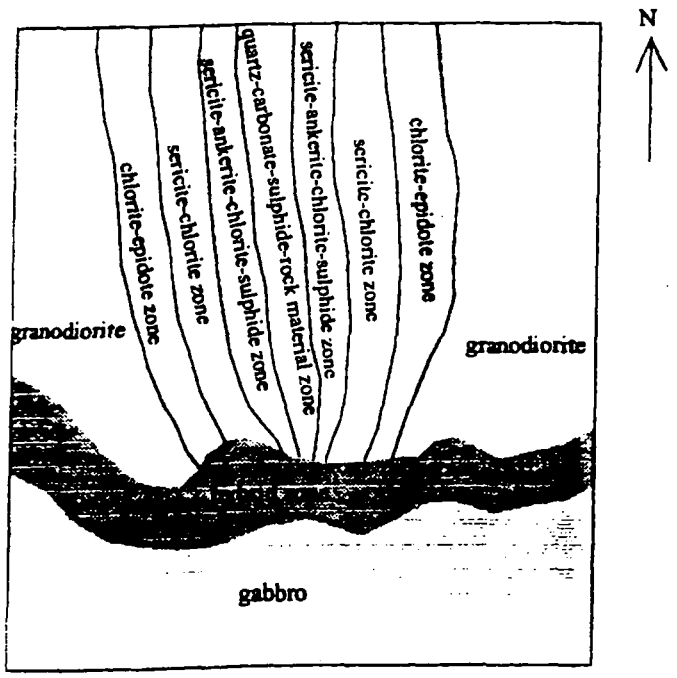

Fig. 6. Sketch illustrating the distribution of alteration zones and quartz vein in the Umm Rus gold mine

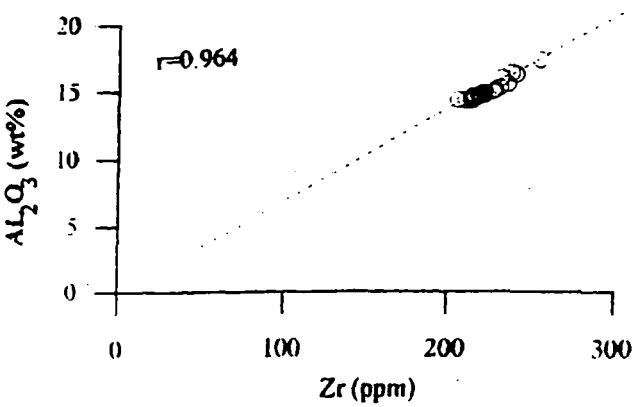

Fig. 7. Variation diagram illustrating the most two immobile elements (r = correlation coefficient).
● = average composition of fresh granodiorite ○ = altered samples

TABLE 7

Selected microprobe analyses of sericite in the Umm Rus alteration zones*

Sample No.	Sr-1	Sr-2	Sr-3	Sr-4	Sr-5	Sr-6	Sr-7
K_2O	6.33	6.71	4.89	9.25	5.63	6.28	5.25
Na_2O	0.33	0.15	0.11	0.19	0.16	0.29	0.27
CaO	b.d.	b.d.	0.53	0.48	b.d.	b.d.	b.d.
FeO	1.05	1.85	2.28	1.16	3.54	1.15	2.04
MgO	0.60	1.17	0.65	0.43	1.77	0.48	0.93
Al_2O_3	36.84	34.68	35.76	35.40	30.15	36.29	33.43
TiO_2	b.d.	0.30	b.d.	0.56	0.21	0.19	0.16
SiO_2	50.46	50.01	49.66	49.50	54.14	50.21	53.42
H_2O	4.77	4.72	4.73	4.64	4.75	4.74	4.79
Total	*100.38*	*99.59*	*98.61*	*101.32*	*100.36*	*99.63*	*100.29*
K	0.543	0.587	0.395	0.762	0.517	0.566	0.467
Na	0.043	0.020	0.013	0.024	0.022	0.040	0.037
Ca	–	–	0.036	0.033	–	–	–
(H_2O)	0.414	0.393	0.556	0.181	0.461	0.394	0.496
Total	*1.000*	*1.000*	*1.000*	*1.000*	*1.000*	*1.000*	*1.000*
Fe^{+2}	0.055	0.098	0.121	0.063	0.186	0.061	0.107
Mg	0.056	0.111	0.061	0.041	0.166	0.045	0.086
Al	1.889	1.777	1.818	1.869	1.637	1.885	1.799
Ti	–	0.014	–	0.027	0.010	0.009	0.008
Total	*2.000*	*2.000*	*2.000*	*2.000*	*2.000*	*2.000*	*2.000*
Al	0.835	0.821	0.853	0.803	0.597	0.822	0.663
Si	3.165	3.179	3.147	3.197	3.403	3.178	3.337
Total	*4.000*	*4.000*	*4.000*	*4.000*	*4.000*	*4.000*	*4.000*
OH	2.000	2.000	2.000	2.000	2.000	2.000	2.000
O	10.000	10.000	10.000	10.000	10.000	10.000	10.000
(H_2O)	2.000	2.000	2.000	2.000	2.000	2.000	2.000

* the structural formula of sericite based on 6 number of cations excluding K, Na and Ca
b.d. = below detection

TABLE 8

Selected microprobe analyses of carbonate generations in the Umm Rus alteration zones*

Sample	generation I			generation II							
No.	Car-1	Car-2	Car-3	Car-4	Car-5	Car-6	Car-7	Car-8	Car-9	Car-10	Car-11	Car-12
MgO	0.56	0.82	0.57	8.76	12.31	7.19	7.96	9.36	7.32	8.48	8.54	8.4
CaO	55.28	53.02	55.24	26.75	27.26	26.62	27.72	27.55	27.59	27.57	27.56	27.51
FeO	b.d.	2.05	b.d.	20.46	16.62	22.72	20.19	18.46	21.34	19.48	19.62	19.83
MnO	b.d.	0.5	b.d.	0.68	0.83	0.5	0.81	0.92	0.72	0.97	0.72	0.77
SrO	b.d.	b.d.	b.d.	b.d.	b.d.	b.d.	b.d.	b.d.	b.d.	b.d.	0.11	b.d.
CO_2	44.01	43.17	43.98	43.51	44.91	42.96	43.3	43.72	43.15	43.43	43.47	43.39
Total	*99.85*	*99.56*	*99.79*	*100.2*	*100.9*	*99.99*	*99.98*	*100*	*100.1*	*99.93*	*100*	*99.90*
Calcite	98.60	94.42	98.59	–	–	–	0.50	–	0.40	–	–	–
Magnesite	1.40	2.03	1.51	–	–	–	–	–	–	–	–	–
Dolomite	–	–	–	43.96	59.84	36.52	40.10	46.76	37.00	42.60	42.90	42.30
Siderite	–	2.85	–	3.50	4.74	2.74	–	1.10	–	0.30	0.40	0.50
Ankerite	–	–	–	52.54	35.42	60.74	59.40	52.14	62.60	57.10	56.60	57.20
Strontiarite	–	–	–	–	–	–	–	–	–	–	0.10	–
Rhodochrosite	–	0.70	–	–	–	–	–	–	–	–	–	–

The structural formulae of carbonates were calculated on the basis of 1 cation for minerals having calcite-structure and 2 cations for those having dolomite-structure CO_2 was added by calculation.
b.d. = below detection

depletion in Ca and Na, while chloritization of biotite produces high K concentration in the rock. Some of the released K was probably used during the potassic alteration of the plagioclase feldspars. These two hydrothermal processes may also lead to a loss in SiO_2 due to the expected leaching of silica, and gain in H_2O. The main chemical changes among the trace elements are a depletion in Sr and Zn, and a gain of Ba, Rb and Ni (Table 10 and *Fig. 8b*).

3. Sericite-ankerite-chlorite-sulphides zone (R3)

The average chemical compositon of this zone shows that there is a relatively strong depletion in Si and Na. The volatile constituents, K, Fe and little amounts of Ca and Mg were added to the system. The main chemical changes among the trace elements involved losses in Sr and Zn and gains in Rb and Ba. Slight gains in Ga, Ni and V are also recorded. The loss of SiO_2 from this zone could suggest either:

a) removal of silica during the breakdown of original silicate minerals. Microscopically, all the primary silicate minerals, except quartz, were altered, or
b) leaching of quartz. BÖHLKE (1989) showed that primary quartz was leached from the granodioritic wall rock during mineralization processes.

The loss of Na might have been resulted from the breakdown of plagioclase feldspars to sericite. The slight enrichment of Ca in this zone advocates that the Ca released from the breakdown of amphiboles and plagioclase feldspars was held up in the newly formed ankerite. The enrichment in K and volatiles in this zone reflects the intensity of sericitization. As ankerite is abundant in this zone, the expected composition of the volatile constituents should be mainly water and CO_2.

Most sulphide minerals in the Umm Rus gold mine area are found in this zone. Microscopically, sulphides are intergrown with and replace iron-bearing silicate and oxide

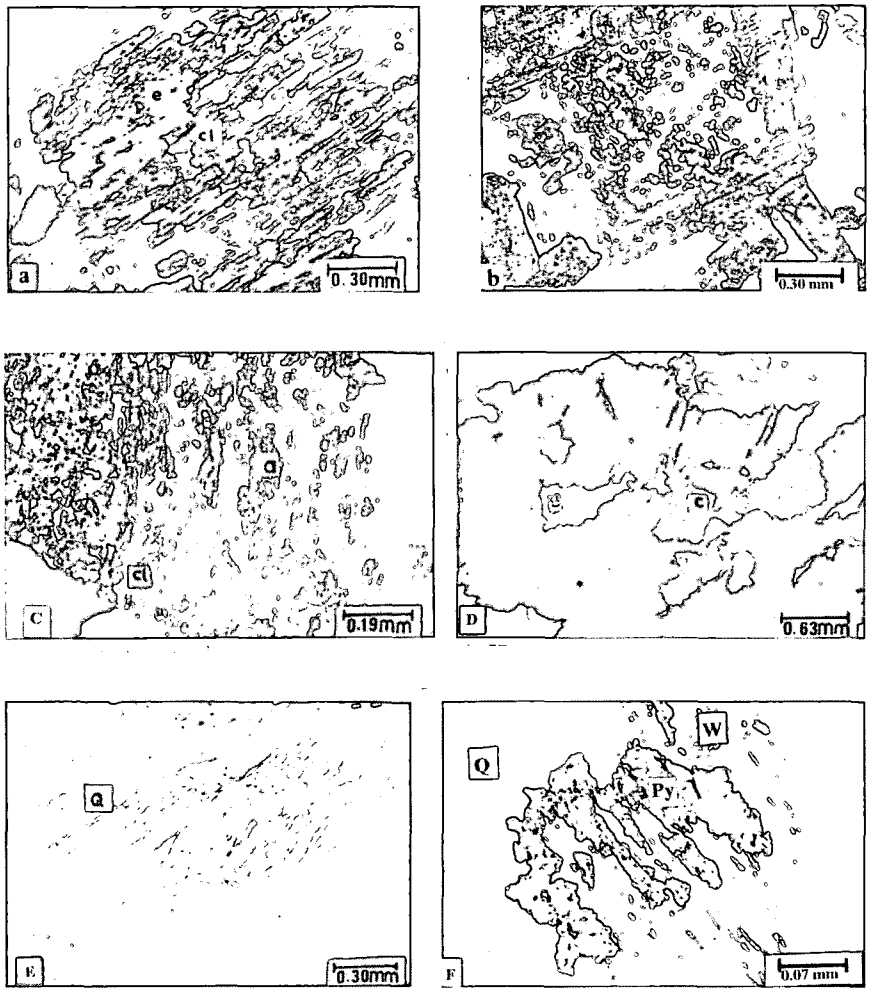

Plate I

A: Pseudomorphic chlorite (cl)-epidote (e) after biotite. Chlorite-epidote zone, R1 (C. N.)
B: Incomplete sericitization of coarse-grained plagioclase feldspar crystal (at the middle). Sericite-chlorite zone, R2 (C. N.)
C: Chlorite (cl) partially replaced by ankerite (a) "carbonate generation II.". Sericite-ankerite-chlorite-sulphide zone, R3 (C. N.)
D: Relics of fine-grained calcite (c) and sericite aggregates (s) are placed in coarse grained quartz. Quartz vein, R4 (C. N.)
E: Inclusions of mixed carbonate and sericite in coarse-grained quartz, note that these inclusions are arranged parallel to each other and to the foliation of the wall rock. Quartz vein, R4 (C. N.)
F: Replacement of pyrite (py) and wall rock material (w) by silica. Irregular contact between pyrite crystal and quartz is noticed. Quartz vein R4 (C. N.)

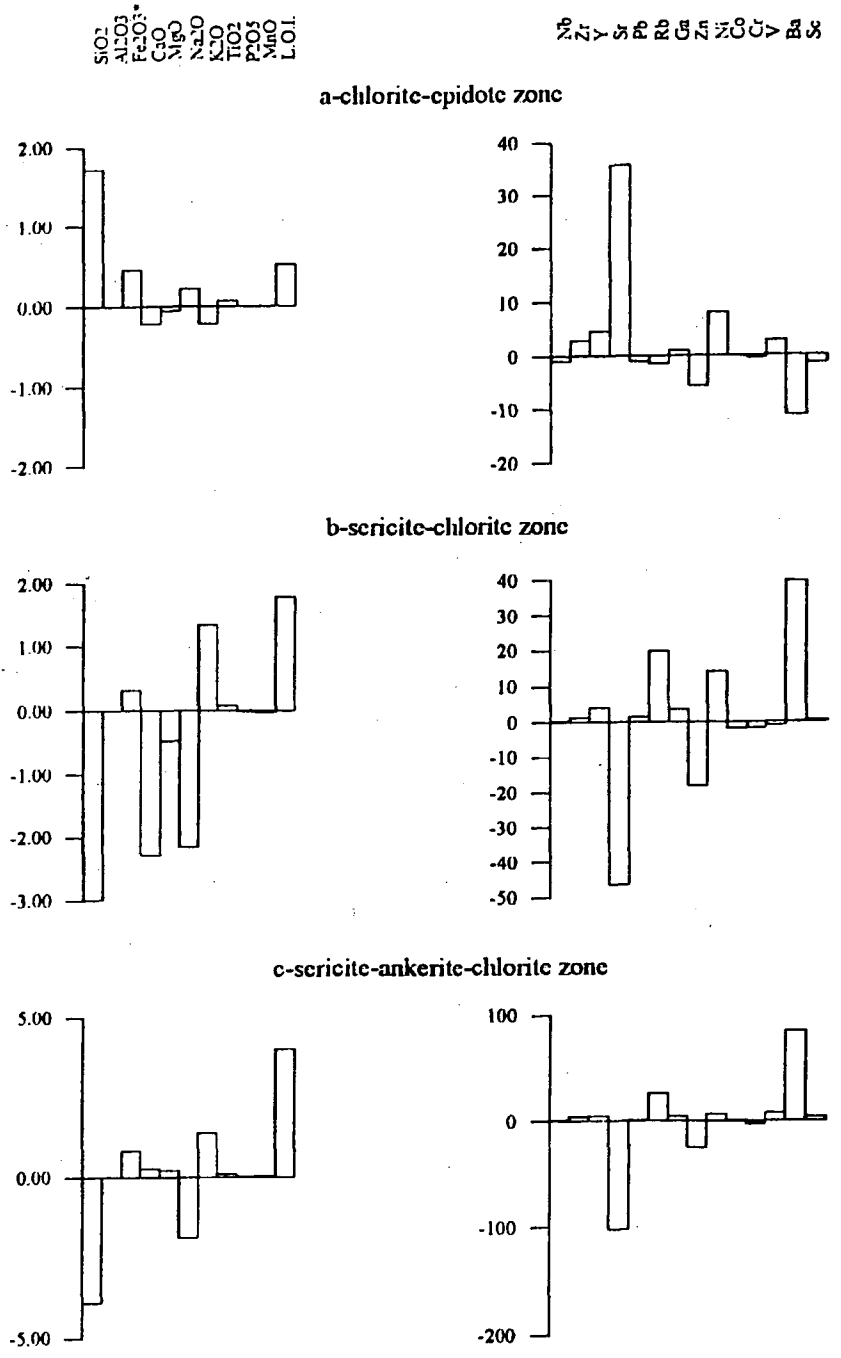

Fig. 8. Gains and losses in the alteration zones of the Umm Rus gold mine area. (major elements in wt%, trace elements in ppm).

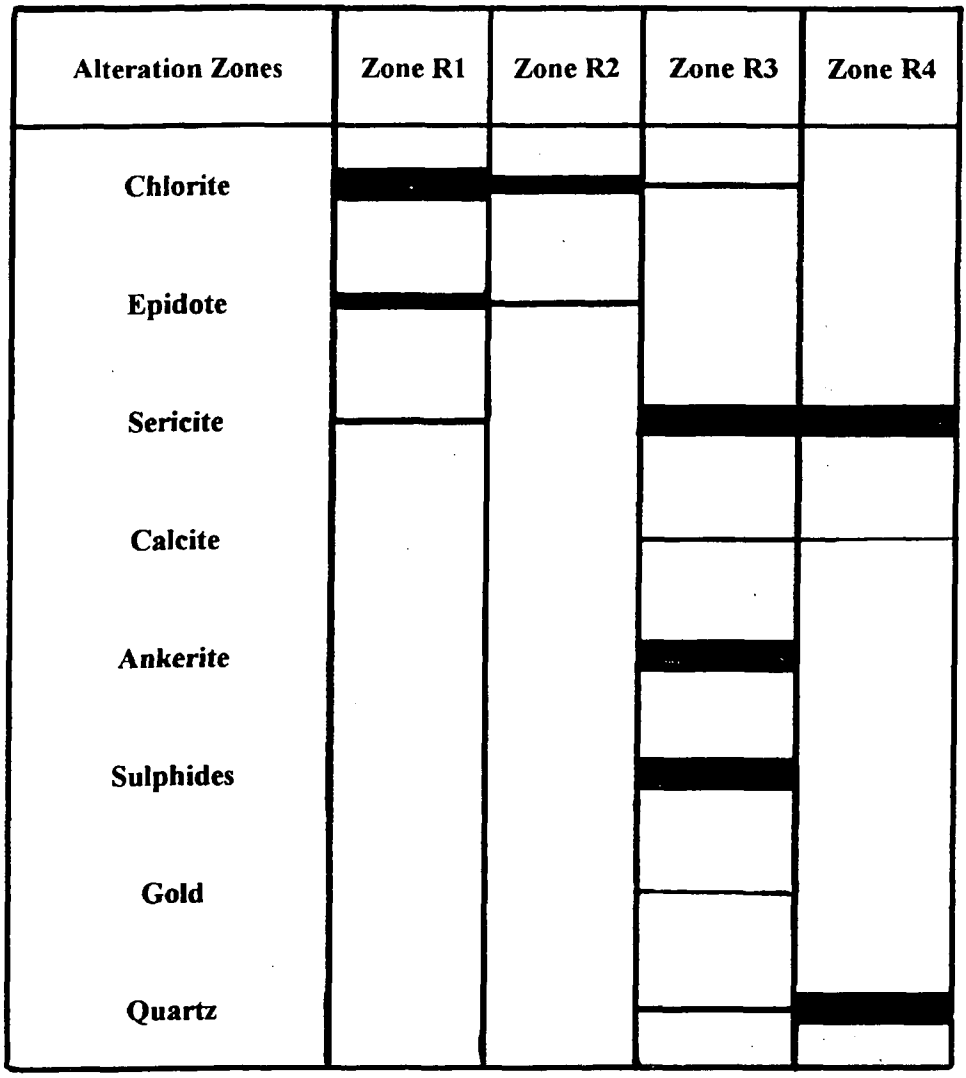

Fig. 9. Paragenetic sequence of the alteration minerals in the Umm Rus gold mine.
(Thickness of lines indicates the mineral abundance)

TABLE 9

Chemical composition of fresh granodiorite and its alteration zones in the Umm Rus gold mine area

Oxides	Fresh granodiorite		Chlorite-epidote		Sreicite-chlorite zone		Sericite-ankerite-chlorite-sulphides zone		Quartz vein	
wt%	Range	Mean(n=5)	Range	Mean(n=6)	Range	Mean(n=7)	Range	Mean(n=6)	Range	Mean(n=3)
SiO_2	67.20–68.40	67.6	66.40–67.90	67.47	65.30–70.90	67.49	61.50–63.80	62.85	> 99.5	> 99.50
Al_2O_3	14.60–15.80	15.02	14.30–15.00	14.62	14.40–17.40	15.69	14.30–15.30	14.83	< 0.1	< 0.10
Fe_2O_3	1.04–1.45	1.17	1.01–1.57	1.25	1.50–3.91	2.88	1.50–3.85	2.50	0.25–0.36	0.30
FeO	2.53–3.33	3.02	2.75–3.36	3.09	1.50–3.60	2.00	2.22–2.78	2.50	0.03–0.06	0.05
CaO	3.22–3.48	3.36	2.87–3.28	3.07	0.24–3.09	1.12	3.19–3.87	3.57	0.03–0.08	0.04
MgO	1.06–1.31	1.16	0.99–1.18	1.08	0.29–1.05	0.72	0.94–1.75	1.34	< 0.01	< 0.01
Na_2O	4.39–4.57	4.48	4.41–4.84	4.57	0.89–3.67	2.42	1.48–3.59	2.53	< 0.01	< 0.01
K_2O	2.10–2.26	2.19	1.48–2.07	1.93	2.50–5.03	3.69	2.59–4.54	3.52	< 0.01	< 0.01
TiO_2	0.50–0.55	0.52	0.55–0.57	0.57	0.54–0.70	0.63	0.09–0.40	0.59	0.02–0.04	0.03
P_2O_5	0.13–0.15	0.14	0.13–0.15	0.14	0.06–0.16	0.13	0.55–0.66	0.58	< 0.01	< 0.01
MnO	0.08–0.11	0.09	0.07–0.11	0.09	0.01–0.10	0.06	0.12–0.18	0.14	< 0.01	< 0.01
H_2O	0.12–0.16	0.14	0.11–0.22	0.17	0.21–0.38	0.22	0.09–0.15	0.11	< 0.01	< 0.01
L.O.N.	0.79–1.08	0.932	1.00–2.23	1.41	2.01–4.36	2.84	3.72–6.32	4.88	0.20–0.22	0.21
Total	*99.56–100.14*	*99.822*	*98.72–100.28*	*99.46*	*99.90–100.52*	*99.89*	*99.21–99.48*	*99.94*	*100.10–100.60*	*100.15*
Nb	6–7	6.6	4–8	5.50	6–10	7.14	5–11	7.33	b.d. – 1	0.83
Zr	206.9–244.7	220	210–226	217.00	206–255	231.14	215–230	221.17	9–10	9.67
Y	30–36	33.4	35–39	37.00	31–57	39.14	33–45	37.33	b.d. – 2	1.00
Sr	201–228	213.8	202–318	242.83	57–607	174.86	66–146	110.00	1–15	10.00
Pb	7–13	10.6	7–12	9.33	9–18	12.57	60–98	77.00	1–4	2.67
Rb	50–54	51.8	40–55	49.00	39–118	74.71	9–15	11.00	5–11	2.67
Ga	14–18	16.2	14–21	16.67	16–27	20.57	17–26	20.17	b.d.	b.d.
Zn	53–76	63.2	30–73	56.17	9–75	47.00	28–44	37.67	b.d.	b.d.
Ni	1–14	7.8	n.d. – 54	15.50	n.d. – 37	22.86	4–26	14.17	3–28	12.67
Co	10–11	10.4	8–11	10.00	5–12	8.86	5–13	10.83	2–4	2.67
Cr	12–17	13.6	11–15	12.83	9–16	12.43	7–13	10.83	66–73	69.00
V	44–50	47	49–51	48.50	26–69	48.00	46–60	53.83	4–8	5.67
Ba	450–491	467	358–493	443.67	335–738	529.14	443–708	544.83	b.d. – 17	7.33
Sc	9–13	10.8	6–12	9.17	7–20	11.71	9–22	14.17	b.d. – 1	0.30

Major oxides in wt% and trace elements in ppm
b.d. = below detection. Mean is calculated by excluding the values below detection limit.

TABLE 10

Mass exchange or the altered zones compared to fresh granodiorite in the Umm Rus gold mine area

Oxides and elements	Fresh granodiorite	Chlorite-epidote zone	Sericite-chlorite zone	Sericite-ankerite chlorite zone
SiO_2	67.60	1.72	–2.99	–3.94
Al_2O_3	15.02	0.00	0.00	0.00
Fe_2O_3*	4.53	0.46	0.32	0.82
CaO	3.36	–0.21	–2.29	0.26
MgO	1.16	–0.05	–0.47	0.20
Na_2O	4.48	0.22	–2.16	–1.92
K_2O	2.19	–0.21	1.34	1.38
TiO_2	0.52	0.07	0.08	0.08
P_2O_5	0.14	0.00	–0.02	0.01
MnO	0.09	0.00	–0.03	0.02
L.O.I.	0.93	0.52	1.79	4.01
Nb	6.60	–0.95	0.24	0.82
Zr	220.00	2.94	1.27	4.00
Y	33.40	4.61	4.07	4.41
Sr	213.80	35.67	–46.41	–102.39
Pb	10.60	–1.01	1.43	0.54
Rb	51.80	–1.46	19.72	26.19
Ga	16.20	0.93	3.49	4.23
Zn	63.20	–5.49	–18.21	–25.05
Ni	7.80	8.12	14.08	6.55
Co	10.40	–0.13	–1.92	0.57
Cr	13.60	–0.42	–1.70	–2.63
V	47.00	2.83	–1.05	7.52
Ba	467.00	–11.19	39.54	84.81
Sc	10.80	–1.38	0.41	3.55

* total iron as Fe_2O_3
Major oxides in wt%, trace elements in ppm

minerals. The presence of rutile, pseudorutile and leucoxene relicts which are a common feature in the sulphide grains, especially arsenopyrite and pyrite, supports the mentioned interpretation. It could suggest that sulphur and arsenic which originated from hydrothermal fluids reacted with iron in iron-bearing silicates and oxides (e.g. biotite, chlorite, magnetite and ilmenite) in the host rock to produce pyrite and arsenopyrite in the altered rock. Similar conclusions were reached by SAUNDERS and TUACH (1991) in the study of alteration processes in Rattling Brook Deposits, Canada. Sulphidation of primary Fe-bearing phases is a typical feature characterizes mesothermal gold deposits (COLVINE et al., 1984; GROVES and PHILLIPS, 1987 and BÖHLKE, 1989).

DISCUSSION AND CONCLUSION

In the light of the foregoing discussion, the following arguments can be concluded.

1. In the Umm Rus gold mine area, the main quartz veins cross-cut the granodiorite, the adjacent hybrid zones and gabbros. This indicates that the quartz veins are post-date than the magmatic event, i. e. the gold deposits show no close time relation to the granitic or the basic igneous bodies.
2. The gold mineralization in the studied mine area appears to be structurally controlled. The gold deposit is restricted to shear zones and fractures along which the mineralizing fluids penetrate the pre-existing wall rocks leaving behind different types of alteration zones.
3. The distribution of alteration zones around the main quartz vein has a more or less symmetrical patterns. Through these zones, the amounts of chlorite and epidote decrease whilst sericite, carbonates and sulphides increase towards the central quartz vein.
4. The textural relationship among the alteration minerals indicate that chlorite and epidote were formed firstly, followed by sericite and then by ankerite and sulphides (*Fig. 9*). All the studied mineral phases were affected by silicification.
5. The sulphides-gold specks-carbonates associations occur in both the quartz veins and the altered host rocks represent the last stable phases in the SiO_2-rich solutions. Therefore, they are relatively concentrated along shear zones through which SiO_2-rich solutions coming out causing silicification of the pre-existing rocks and forming the present quartz veins. The following aspects put the previous belief, that the quartz veins and the mineralization were cogenetic, in considerable doubt:

(i) the sulphides in the quartz veins are mostly associated with carbonates and relics from the wall rock materials. The so-called grey quartz appears to be richer in sulphides, carbonate relics and wall rock inclusions than in the milky one.

(ii) the presence of undigested wall rock material and xenoliths in sulphides is a dominant phenomenon.

(iii) the distribution of sulphides appear to be widely variable among gold mines in the Eastern Desert of Egypt, as well as within the same gold mine. In some gold deposits, the sulphides are more concentrated in the quartz veins (e. g. El-Sid mine), in others the sulphides are concentrated in the wall rock alteration zones (e. g. Umm Rus mine). If the sulphides and the quartz veins are cogenetic, such sulphides should be more or less regular in their distribution or even more concentrated in the quartz veins. Additionally, in other gold mines, many quartz veins are barren of any sulphides.

6. The patterns of alteration zones appear to be controlled by the wall rock--hydrothermal fluid interaction. The dominancy of the studied alteration phases indicates that the affecting hydrothermal solutions were enriched in H_2O and CO_2. As the amounts of sericite, ankerite and sulphides increase near the contact with the qurtz vein, this indicates a noticeable addition of K, S, H_2O and CO_2 by the progress of alteration from fresh granodiorite to quartz vein. Some other elements such as As, Zn, Pb, Cu and Au are also added to the system during the alteration events.
7. Most elements (trace and major ones) do not show strong mobilities in most of the alteration zones. Therefore, the mass balance (gains and losses) shows a limited range for element concentrations in these zones.

GENETIC MODEL

The interpretations of the combined geological, mineralogical and geochemical data in the present work aim at formulating a genetic model (*Fig. 9*) for the alteration zones which can be summarized in the following:

a) The hydrothermal fluids, were derived from below through N-S shear zones in the inspected mine area. At the begining of invasion, these fluids were characterized by low CO_2/H_2O ratio which easily altered the pre-existing biotite to some iron-bearing hydrous phases as chlorite and epidote. Some other ferromagnesian minerals e.g. hornblende are noticed to be unaffected by these fluids. The CO_2 content of fluids was not enough to permit the carbonates formation at this early stage of alteration. The geothermometry of the studied chlorite indicates its formation at about 225°C.

b) The fluids of the second stage became enriched in K after the biotite alteration in stage A. These fluids reacted with plagioclases to form sericite. The alteration of plagioclases to K-feldspars was accelerated by the K-enriched fluids. In this stage, the CO_2/H_2O ratio is still low, as indicated from the high H_2O content in the sericite (Table 7).

c) As the chlorite, epidote and sericite were formed, the proportion of H_2O decreased and then the CO_2/H_2O ratio became high in the fluids. Consequently, ankerite was originated in this stage. Sulphides characterizing zone R3 were concomitant with conspicuous concentration of Fe, As, Cu and Au. The presence of these sulphides suggests reducing environmental conditions. It is easily noticed that the given iron by the breakdown of the ferromagnesian minerals was completely consumed in the formation of the iron-bearing sulphide minerals.

d) The last stage is characterized by severe silicification that led to the formation of the quartz veins. All the previous stages were affected by this silicification. The intensity of silica replacement depends on the mineral compositions. Ankerite, chlorite, epidote, and sericite show strong and sometimes complete silicification, on the other hand, sulphides were weakly affected by SiO_2-rich solution. This solution is reworked and dissolved the pre-existing native gold in sulphides and then redistributed the gold in some sulphide phases e.g. pyrite and pyrrhotite. The enrichment of gold by this proposed process is advocated by MÜCKE and ADJIMAH (1994) on gold deposits of Prestea and Obuasi, Ashanti Belt, Ghana. However, the detailed work concerning the gold enrichment of the Umm Rus gold mine will be published elsewhere by the same authors.

ACKNOWLEDGEMENTS

The authors are grateful to Professor A. MÜCKE of Georg-August University, Göttingen, Germany for the facilities offered during the microprobe analysis. They are also indebted to Mr. ELLIS of the same university who helped in the analysis.

REFERENCES

AMIN, M. S. (1955): Geological features of some mineral deposits in Egypt. Bull. Inst. Desert, Egypt, S. 1, 208–239.

BENCE, A. E. and ALBEE, A. L. (1968): Empirical correction factors of electron microanalysis of silicates and oxides. J. Geol. **67**, 382–403.

BÖHLKE, J. K. (1989): Comparison of metasomatic reactions between a common CO_2-rich vein fluid and diverse wall rocks: Intensive variables, mass transfers, and Au mineralization at Alleghany, California. Econ. Geol., **84**, 291–327.

CATHELINEAU, M. and NIEVA, D. (1985): A chlorite solid solution geothermometer. The los Azufres geothermal system (Mexico). Contrib. Mineral. Ret. **91**, 235–244.

CATHELINEAU, M.; BOIRON, M. C.; HOLLIGER, P.; MARION, P. and DENIS, M. (1988): Gold in arsenopyrite: Crystal chemistry, location and state, pysical and chemical conditions of deposition. Econ. Geol. mono 6: The geology of gold deposits, 328–341.

COLVINE, A. C.; ANDREWS, A. J.; CHERRY, M. E.; DUROCHER, M. E.; FYON, A. J.; LAVINGNE, M. J.; MACDONALD, A. J.; MARMONT, S.; POULSEN, K. H.; SPRINGER, J. S.; and TROOP, D. G. (1984): An integrated model for the origin of Archean lode gold deposits. Ontario Geol. Survey open-file rept., 5524, 98pp.

DEER, T. G.; HOCKES, A. H. and ZUSSMAN, M. M. (1985): An introduction to mineralogy. London, Academic Press, 307pp.

EL-MAHALLAWI, M. (1984): Petrology and geochemistry of the intrusive rocks of Umm Rus area, Central Eastern Desert, Egypt. Ph. D. thesis, El-Minya Univ., Egypt.

EL-RAMLY, M.; IVANOV, S. S.; KOCHIN, G. G. and others (1970): The occurrence of gold in the Eastern Desert of Egypt. In: Studies on some mineral deposits of Egypt. (Ed. by Moharram O. et al.). Geol. Surv. Egypt, part 1, section A, Artical no. 4, 53–64.

FOSTER, M. D. (1962): Interpretation of the composition and a classification of the chlorites. U. S. Geol. Surv. Prof. Paper 414 A, 1–33.

GROVES, D. I. and PHILLIPS, G. N. (1987): The genesis and tectonic control on Arcean gold deposits of the Western Australian Shield – a metamorphic replacement model: Ore Geology Rev. 2, 287–322.

HARRAZ, H. Z. and EL-DAHHAR, M. A. (1994): Fluid-wall rock interaction and its implication on gold mineralization at Umm Rus gold mine area, Eastern Desert, Egypt. J. Geol., Egypt. 38, 2, 713–747.

HARTMAN, G. AND WEDEPOHL, K. H. (1993): The composition of peridotite tectonites from the Ivreacomplex (N Italy), residues from melt extraction. Geoch. Cosm. Acta. **57**, 1761–1782.

HUME, W. F. (1937): Geology of Egypt. The minerals of economic value associated with the intrusive Precambrian igneous rocks. Geol. Surv. Egypt. V. II, part III, 805 pp.

KABESH, M. L.; HILMY, M. E. and BISHADY, A. M. (1967): Geology of the basement rocks in the area around Umm Rus gold mine, Eastern Desert, Egypt. J. Geol. Egypt **11**, 59–85.

KAMEL, O. A., EL MAHALLAWI, M. and HILMY, H. M. (1992): Mineralogy of the Umm Rus gold-bearing quartz veins and the surrounding alteration zones, J. Min. Soc. Egypt **4**, 55–86.

LEAKE, B. E. (1978): Nomenclature of amphiboles. Can. Miner. **16**, 501–520.

MACLEAN, W. H. and KRANIDIOTIS, P. (1987): Immobile elements as monitors of mass transfer in hydrothermal alteration: Phels Dodge massive sulphide deposit, Matagami-Quebec. Econ. Geol. **82**, 951–962.

MÜCKE, A. and ADJIMAH, K. (1994): Ore texture and paragenesis of the gold deposits of Prestea and Obuasi, Ashanti Belt, Ghana. An ore microscopic study. Geol. Jb D100, Hannover 163–195.

SABET, A. H. (1961): Geology and mineral deposits of Gebel El-Sibai area, Red Sea Hills, Egypt, U.A.R. Ph.D. thesis, Lieden State Univ. Netherland, 189pp.

SAUNDERS, C. M. and TUACH, J. (1991): Potassic and Sodic alteration accompaning gold mineralization in the Ratting Brook deposit, Western White Bay, New Foundland Appalachians. Econ. Geol. 86, 555–569.

STRUNZ, H. (1966): Mineralogische tabellen. Berlin-Germany, Röder and Leipzig, 560 p.

TAKLA, M. A. (1971): Ore mineralogical and geochemical studies of some basic and associated ultrabasic igneous rocks, Eastern Desert, Egypt. Ph.D. Thesis, Cairo Univ. Egypt.

Manuscript received 3 January, 1996.

Acta Mineralogica-Petrographica, Szeged, XXXVII, 75-82, 1996

RARE-EARTH ELEMENTS OF GRANITOID ROCKS OF ST. KATHERINE AREA, SOUTH SINAI, EGYPT

HASSEN, I. and BUDA, Gy.

Department of Mineralogy, Eotvos L. University*

ABSTRACT

A group of granitic plutons and stocks outcrop in St. Katherine area, South Sinai (Egypt). They belong to the Late Precambrian Pan-African belt.

The granitoid rocks occupying St. Katherine area are composed of a comagmatic plutons and classified into three main phases according to their field relations and compositions: 1- quartz diorite, granodiorite and quartz monzonite (Gr_1), 2- monzogranite and biotite granite (Gr_2), 3- syenogranite, alkali feldspar granite and granophyre (Gr_3).

The distribution of REEs show variations in each phases as well as within one lithological unit which allow the interpretation of complex genesis of the massif.

The phase one (Gr_1) emplaced, as a basic magma in an intermediate magmatic chamber, containing a very low concentrations of REE. This has undergone a fractional crystallization, which resulted in an increase of the amount of ΣREE (average 102.16 ppm) with the moderately fractionated patterns (La/Sm = 6.07) and no significant negative Eu anomalies are found.

Phase two (Gr_2) has higher contents of ΣREE (average 116.86 ppm), and more fractionated LREE (La/Sm = 7.90) with a small negative Eu-anomalies.

Phase three (Gr_3) has a high contents of ΣREE (average 121.97 ppm) and fractionated LREE pattern with a relatively deep negative Eu-anomalies.

METHODS OF ANALYSIS

The REE and some other trace elements were analysed using INNA methods in Technical University, Budapest. The amount of samples used was of about 200 mg.

INTRODUCTION

St. Katherine area is located in the Arabo-Nubian belt of Central South Sinai (Fig. 1). The area covered about 1500 Km^2 of Precambrian crystalline basement complex. It mainly consists of Precambrian intrusive and extrusive rocks.

A detailed petrographic study of the Precambrian granitic rocks of St. Katherine Area was carried out by HASSEN (1987). More than ten varieties of granitoids and two varieties of syenite were recorded.

Granitoid rocks of St. Katherine area can be grouped into two major petrological, genetic and tectonic types (HASSEN and BUDA 1994);

* H-1088 Budapest, Múzeum krt. 4/A

1. Two feldspar granitoids:
   1a. Qz-diorite, Qz-monzonite, granodiorite and Hb. Bt. granite (Gr_1);
   1b. Coarse-grained monzogranite, pegmatitic Hb. Bt. monzogranite, porphyritic monzogranite and Bt. granite (Gr_2).
2. Alkali granitoids (Gr_3).
   2a. Alkali-feldspar granite.
   2b. Syenogranite.
   2c. Granophyre.

BENTOR (1985): subdivided the crustal history of the Arabo-Nubian Shield (South Sinai) into the following four Phases.

Phase I (>950 M.y.), is characterized by the emplacement of an oceanic mafic and ultramafic magmatic rock assemblage and volcanic equivalents. These ophiolite sequences which were tectonically transported.

Phase II (950-650 M.y.), is an "island arc" stage dominated by andesitic volcanism and intrusive equivalents. Most of these rocks are metamorphosed in the greenschist facies.

Phase III (650-590 M.y.), is characterized by magmas of calc-alkaline silica-rich compositions. Granitic plutons are spread haphazardly over the entire massif. This phase ended with a strong uplift, Arabo-Nubian joins the African craton (Gr_1 and Gr_2).

Phase IV (590-550 M.y.), was the "alkaline batholitic" event producing alkaline to peralkaline high-level granites and their extrusive equivalents. These rocks were emplaced during a non orogenic period where the rigid massif was subjected to tensional stresses, block faulting and differential uplift (Gr_3).

EYAL and HESKIYAHU (1980) described the Gr_3 of St. Katherine Plutons. It is composed of alkali syenogranite. Three distinctive petrographical zones can be distinguished: Zone A contains 30% quartz, 45% perthitic alkali feldspar, 20% plagioclase and 5% biotite, zone B is 300 to 500 meters thick and contains 30% quartz, 65% perthitic alkali feldspar and 5% biotite, zone C is a transition between A and B. It was concluded that the rocks of zone A represent the original rock type of the intrusion. Zone B is interpreted as a product of the reaction of alkaline solutions with the original rock in the highest part of the pluton.

ABUNDANCES AND VARIATION OF RARE EARTH ELEMENTS

Concentrations of REE in the rocks are greatly variable, reflecting the different degree of differentiation within, as well as between the granitoid types. Further variation can be excepted on account of irregular distribution of REE-bearing apatite, allanite, monazite and zircon.

The result of analyses carried out on the granitoid rocks of St. Katherine area are present in Table 1. REE abundance was normalized to a chondrite (ANDREWS, E. and EBIHARA, M. 1982).

All samples, show the typical granite pattern (CULLERS and GRAFT 1984). They are enriched in light rare earth elements (LREE) relative to heavy ones. Important differences between the three varieties occur in their $\sum$REE contents, their HREE fractionation and the size of their Eu-anomalies.

TABLE 1

Average of REE and some trace elements data for Katherine granitoid rocks

	Q_z-diorite, Q_z-monzonite and Granodiorite (Gr_1)			Monzogranite and Bt. Granites (Gr_2)			Syenogranite and alkali-feldspar granites (Gr_3)		
	Number of samples: 9			Number of samples: 24			Number of samples: 28		
ppm	mean	& std. dev		mean	& std. dev		mean	& std. dev	
Cr	87. 21 ±	54.19	70.50	49.71 ±	24.63	58.31	9.51 ±	2.87	6.94
Ni	14.22 ±	10.607	13.79	4.96 ±	1.89	4.47	6.88 ±	1.41	3.42
Co	21.70 ±	11.10	14.44	12.76 ±	4.70	11.12	1.99 ±	0.93	2.24
Sc	9.27 ±	5.94	7.72	4.37 ±	2.25	5.32	1.50 ±	0.69	1.78
V	46.78 ±	30.96	40.27	7.92 ±	4.32	10.22	6.29 ±	3.09	7.96
Cu	11.22 ±	12.76	16.61	5.29 ±	4.69	11.09	3.96 ±	2.10	5.41
Pb	10.22 ±	5.13	6.67	10.50 ±	3.86	9.20	19.07 ±	1.77	4.57
Zn	62.22 ±	17.37	22.60	38.04 ±	8.11	19.20	41.18 ±	13.19	34.01
Sb	0.46 ±	0.47	0.62	0.28 ±	0.20	0.39	0.16 ±	0.16	0.39
Rb	81.99 ±	15.59	20.28	102.08 ±	9.89	23.41	136.77 ±	13.08	33.72
Cs	2.55 ±	1.79	2.33	2.88 ±	1.56	3.70	1.00 ±	0.36	0.89
Ba	799.67 ±	148.82	193.61	702.29 ±	117.90	279.17	400.79 ±	93.25	240.47
Sr	628.11 ±	150.47	195.76	166.33 ±	75.32	178.34	128.14 ±	30.61	78.93
Ga	14.78 ±	3.95	5.13	7.58 ±	3.13	7.40	8.04 ±	3.33	8.06
Ta	0.75 ±	0.38	0.50	0.41 ±	0.13	0.25	0.75 ±	0.31	0.81
Nb	2.22 ±	1.38	1.80	3.63 ±	1.33	3.15	17.27 ±	3.45	8.90
Hf	4.59 ±	0.77	1.00	4.31 ±	0.58	1.37	4.44 ±	0.97	2.50
Zr	95.67 ±	53.40	69.47	83.75 ±	29.67	70.25	228.64 ±	65.23	158.02
Y	6.56 ±	3.71	4.83	5.29 ±	2.38	5.65	23.75 ±	4.02	10.38
Th	9.02 ±	3.20	4.17	12.10 ±	1.73	4.10	16.96 ±	2.21	5.69
U	4.52 ±	2.28	2.96	4.09 ±	1.66	3.93	4.40 ±	0.75	1.94
La	23.85 ±	2.36	3.07	30.27 ±	3.92	9.28	28.19 ±	4.25	10.95
Ce	47.62 ±	5.39	7.01	54.20 ±	9.25	21.90	53.00 ±	10.52	27.12
Nd	20.53 ±	4.78	6.22	22.43 ±	3.68	8.70	28.85 ±	4.87	12.55
Sm	3.93 ±	0.47	0.62	3.83 ±	0.62	1.46	4.62 ±	0.97	2.51
Eu	1.11 ±	0.17	0.23	0.84 ±	0.11	0.26	0.45 ±	0.12	0.30
Gd	3.48 ±	0.45	0.581	3.09 ±	0.31	0.74	3.17 ±	0.68	1.76
Tb	0.34 ±	0.09	0.11	0.40 ±	0.07	0.17	0.47 ±	0.15	0.39
Ho	0.26 ±	0.14	0.18	0.20 ±	0.09	0.21	0.48 ±	0.17	0.43
Tm	0.04 ±	0.03	0.04	0.00 ±	0.00	0.00	0.96 ±	0.13	0.33
Yb	0.81 ±	0.40	0.52	1.39 ±	0.24	0.58	1.39 ±	0.52	1.34
Lu	0.19 ±	0.03	0.04	0.21 ±	0.03	0.07	0.39 ±	0.05	0.14
ΣREE	102.16			116.86			121.97		
La/Sm	6.07			7.90			6.10		
La/Yb	29.44			21.77			20.28		
Ce/Yb	58.79			38.99			38.13		
Gd/Yb	1.12			2.22			2.28		

In order to facilitate the comparison of ΣREE pattern in different rock units, we plotted on diagram only the relatively homogenous granitoid groups of the Katherine complex (Fig. 1 a,b,c).

Gr_1; they display the lowest ΣREE abundances compared with the other two types. They have relatively low to moderate ΣREE contents and exhibit a limited range in composition (the range of 9 samples ΣREE = 133.24-85.45 ppm and average 102.16 ppm). They are characterized by low fractionated LREE (La/Sm_n ranges from 6.70 to 4.93

with average 6.07) and moderately fractionated HREE patterns (Gd/Yb_n ranges from 19.66 to 2.49 and the average 1.12}, and almost flat REE patterns with more or less absences of any significant negative Eu-anomalies. (Fig. 2a)

Gr_2; they have higher ΣREE content (186.19-53.53 and average 116.86), and have relatively stronger LREE and HREE fractionated patterns (La/Sm_n range from 12.83-6.07 with average 7.90 and Gd/Yb_n range from 6.07-1.25 and average 2.22}.

Samples which represent leuco-monzogranite show lower contents of ΣREE indicating a decrease in the REE content with increasing differentiation. Such a decrease in REE content could be attributed to the removal of some REE-bearing phases which reduce the REE content of the remaning liquid (Frey et al., 1978). This is agreement with the modal mineralogy, since the accessory minerals (apatite, sphene and zircon) are rich in the normal monzogranite, poor in the leuco-monzogranite, suggesting their removal by fractionation. (Fig. 2b)

Gr_3, they seem to be slightly different from the other granitoid types. ΣREE concentrations are greater than in the other types (307.93-67.65 with average 121.97 ppm), they are characterized by larger negative Eu-anomaly, flat HREE patterns (Gd/Yb_n=0.83-20.14 with average 2.28} and moderately fractionated LREE patterns {$(La/Sm)_n$=4.17-26.61 with average 6.10}. Larger negative Eu-anomalies in leucocratic rocks are common feature due to feldspar fractionation or fractionation of REE-rich accessory minerals (CULLERS and GRAF 1984).

The characteristic chondrite-normalized pattern of the Gr_3 (Fig.2c) shows a marked negative Eu anomaly, whereas that of the other types exhibit a significant flat Eu (Gr_1) or small negative anomaly (Gr_2).

The more or less flat HREE trend of the syenogranite is an important feature. This indicates that hornblende fractionation is less significant in the evolution of these granitoids; or that they are derived by partial melting of a source without residual amphibole and/or garnet.

DISCUSSION

The older granitoids (Gr_1) display moderately fractionated normalized REE patterns The $(La\backslash Sm)_n$ ratios of the older Sinai granitoids average 6.07. The younger granitoids are more evolved and have higher REE contents than the older granitoids. They display moderately to strong fractionated normalized REE patterns (La/Sm)n = 6.10 to 7.9) with moderate to strong negative Eu anomalies.

The three variety of granitoids are enriched in REE (Table 1). They exhibit LREE enrichment over HREE. The moderately fractionationated patterns of the LREE in older granite and a smaller one in the younger granite (Fig.1), are the only differences in the two units. Early fractionation of the feldspars may have caused depletion of Eu in the syenogranite. The patterns exhibited the older granite and the monzogranite are typical of those of calc-alkaline to subcalc-alkaline granites in the Arabo-Nubian Shield (MARZOUKI et al. 1982).

In case of Old granitoid (Fig 2a), there is no Eu anomaly. This can be regarded as a result of the fractional crystallization of the basic magma dominated by the plagioclase feldspar accumulation.

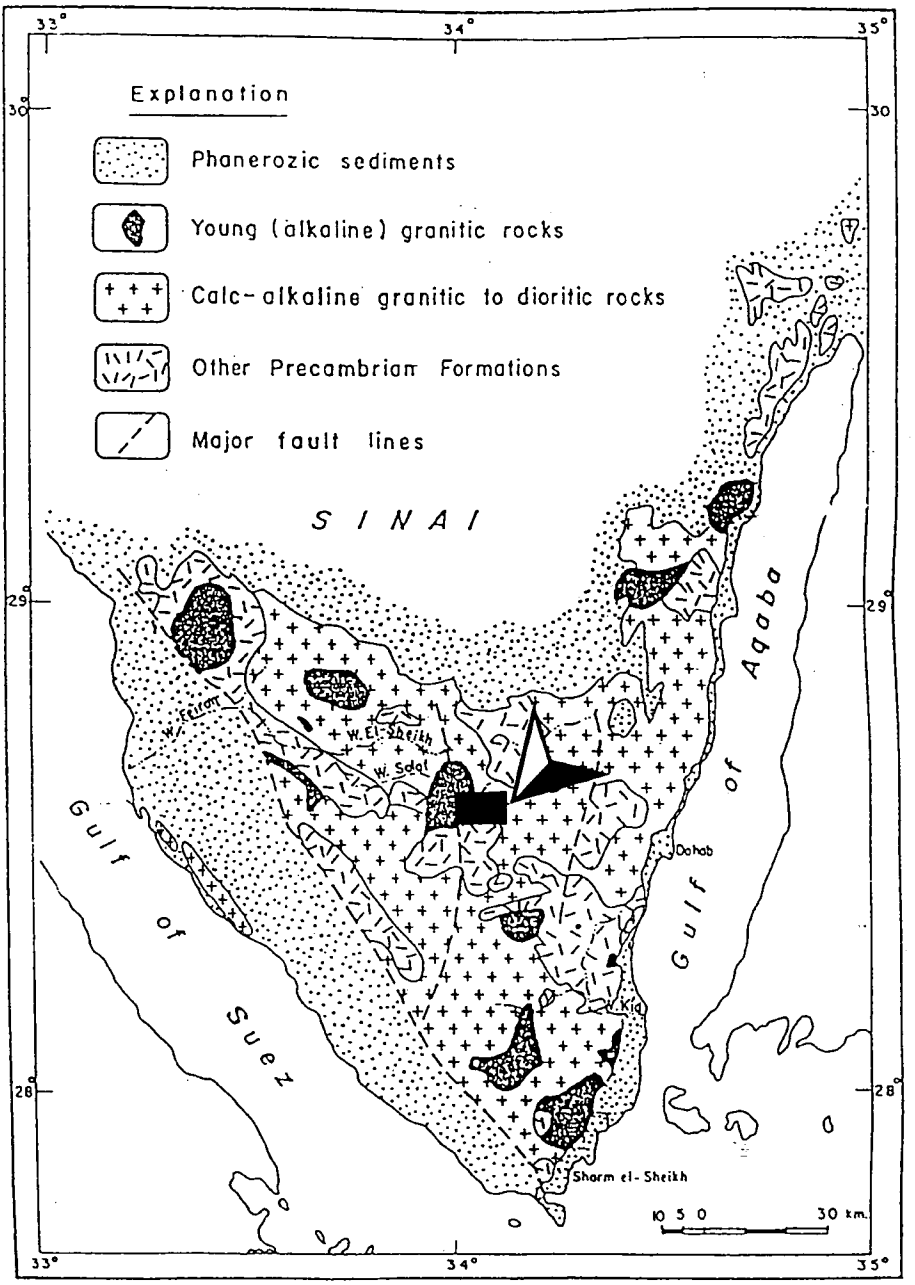

Fig. 1. Generalized geological map of the Precambrian of Sinai Peninsula after SHIMRON (1980).
➢ Studied area

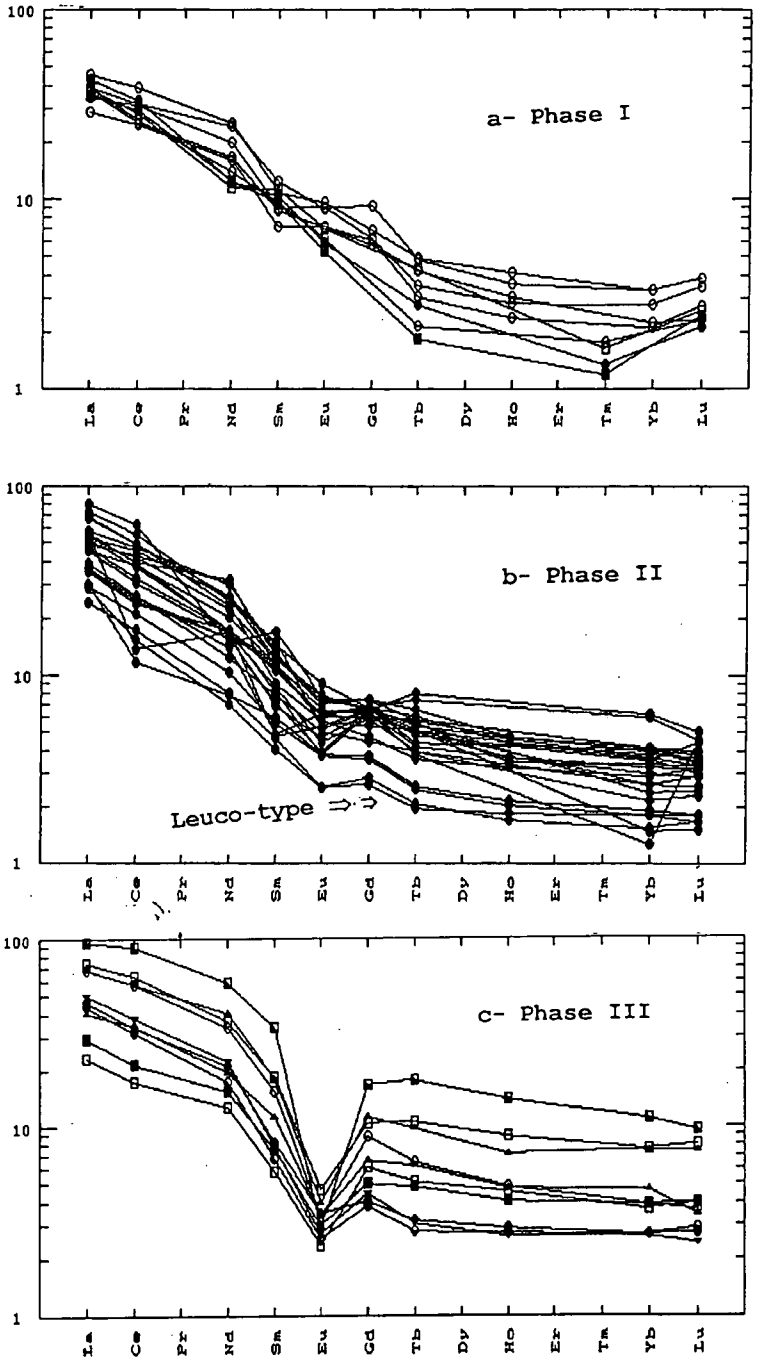

Fig. 2. Chondrite normalized REE distribution patterns of the three main phases of granitoids occurring in St. Katherine area.

Although there are certain discontinuities, the geochemical variations seem to show differentiation tendencies at least at the level of the old granite (Gr_1) and monzogranites (Gr_2) in one side and syenogranite in the another side.

The REE, distribution also indicates that the massif was generated by successive magma pluses and variations in each lithological unit as well as from one unit to another allow the interpretation of a complex genesis of the massif.

The first moment includes a basic magma (low values of REE) whose fractional crystallization in an intermediary magmatic chamber led to the appearance of Old granites.

A new magma plus, very likely richer in acidic materials, took over some of the previous crystals (resulting from the fractionation of the above mentioned rocks), and formed an intimate mixture, being emplaced at the actual level where a new magmatic differentiation took place.

Monzogranite of Gr_2, has typical subcalc-alkaline characters (HASSEN, 1987), behave less differentially from the Old granite. Therefore it is possible that the products of this phase might belong to modified old granitoids magma.

Potassic granites (Gr_3) probable generated in an ensialic tensional environment (HASSEN, 1987) having the high abundances of Y and Nb which, are typical of "within-plate" granites. Further, they have rather high contents of e.g. ΣREE, Zr, Th and U. Another important features is the flat HREE trend. This indicates that hornblende fractionation is less significant in the evolution of such granitoid; or that they are derived by partial melting of a source without residual amphibole and/or garnet.

Although the granites (Gr_3) may have been generated in a tensional setting, it is likely that a true continental rift was developed. Acid volcanics of the same age can be found where the Gr_3 are known in the investigated area (Katherine volcanics). In continental tensional environments, where degassing of the mantle occurs (BAILEY 1977). Continued heating by the gas flux may lead to melting of the upper mantle and lower crust. When the lower crust melted, the trace element characteristics were obtained by the mixing of the mantle volatiles, (rich in CO_2, alkalies and the trace elements characterstic of "within-plate" granites) with the crustal fusion products.

CONCLUSION

Three type of REE distribution can be distinguished:

Type 1: Quartz diorite and granodiorite (Gr_1) display moderately fractionated REE patterns, less fractionated HREE patterns and no significant Eu-anomalies.

Type 2: Monzogranite and normal (Gr_2) granite differ from the previous type in being more LREE fractionated and by the presence of small negative Eu-anomalies.

Type 3: The syenogranites and alkali feldspar granites (Gr_3) have fractionated LREE patterns and flat HREE patterns. With the exception of two samples, all the samples have relatively deep Eu-anomalies and high contents of REE compared to the other varieties.

REFERENCES

ANDREWS, E and EBIHARA, M. (1982): Solar-System abundances of the elements, Geochim. Cosmochim. Acta. **46**, 2363-2380.

BAILEY, J.C., (1977): Flourine in granitic rocks and melts: a review. Chem. Geol. **19**, 1-42.

BENTOR, Y.K. (1985): The crustal evolution of the Arabo-Nubian massif with special reference to the Sinai Peninsula. Precamb. Res., 1-74.

CULLERS, R.L. and GRAF, R.J. (1984): Rare earth elements in igneous rocks of the continental crust: Intermediate and silicic rocks-ore petrogenesis. In HENDERSON, P. (ed.): Rare earth element geochemistry. Elsevier, 501 pp.

EYAL, M and HESKIYAHU, T. (1980): "Katherina pluton; the outline of a petrologic framework". Israel J. of Earth Sci. **29**, 41-52.

FREY, F.A., CHAPPEL, B.W. and ROY, S.D. (1978): Fractionation of rare-earth elements in the Toulumne intrusive series, Sierra Nevada batholith, California: Geology. **6**, 239-242.

HASSAN, I.S. (1987): Geology and mineralization of Regata area, Central South Sinai, MSc. thesis, 1987. Suez Canal University, Egypt.

HASSAN, I. and BUDA, Gy. (1994): The Precambrian granitic rocks of St. Katherine area, south Sinai, Egypt "mode of emplacement and case history'. Acta Miner. Petr. Szeged, **XXXV**, 65-82.

MARZOUKI, F.M.H., JACKSON, N.J. and RAMSAY, C.R. (1982): Composition, age and origin of two Proterozoic diorite-tonalite complexes in the Arabian shield, Precambrian Res. **19**, 31-50.

SHIMRON. A.E., (1980): Proterozoic island arc volcanism and sedimentation in Sinai, Precamb. Res. **12**, 437-458.

Manuscript received 5 Aug. 1996.

Acta Mineralogica-Petrographica, Szeged, XXXVII, 83–87, 1996

GEOCHEMICAL INVESTIGATION OF PYROXENES FROM LOWER CRETACEOUS VOLCANICS FROM BOREHOLES OF THE GREAT HUNGARIAN PLAIN

S. MOLNÁR*

Department of Mineralogy, Geochemistry and Petrography
Attila József University

ABSTRACT

Originally the lower cretaceous volcanics known from boreholes of the Great Hungarian Plain proved to be feldspar-rich basaltic rocks. They are highly altered volcanics (Mg-metasomatism, spilitisation, weathering), and they contain as fresh component parts some grains of clinopyroxene. From electronmicroprobe analysis-data of the minerals is shown, that the pyroxenes are of diopside-salit-augite composition. It can be stated, that the analised grains refer to alcali magma, therefore the high alcalic content in the rocks is a result not only of metasomatism and contamination. The pyroxene analitical data supported the conception of rock-origin, that they are products of continental within-plate volcanism.

INTRODUCTION

The Lower cretaceous volcanics known from boreholes in the Great Hungarian Plain were originally felspar-rich basalts (SZEPESHÁZI 1960, 1977; MOLNÁR 1985). These rocks become highly altered (Mg-metasomatism, spilitization, weathering), thus only approximate conclusion could be drawn so far concerning the formation conditions the origin of magma.

In order to obtain more exact information, the chemical analyses of clinopyroxenes of these rocks were carried out. Measurements were made in microprobe of Satesa CAMEBAX type, under the following conditions: 15 kV accelerating voltage, 30 nA beam current and 10 s exposition time.

The standards below were used: diopside (Si, Mg, Ca, Al, Fe), albite (Na), and $MnTiO_3$ (Mn, Ti). The calculations of the ZAF correction was made by the computer of PDP 1123 type.

In the available 128 rock samples only three provided fresh pyroxenes. The grain diameters varied between 0,5 and 1 mm, this fact also limited the number of measurements.

* H-6701 Szeged P. O. Box 651.

INTERPRETATION OF MEASUREMENT DATA

In the minerals the Ca-quantities can be considered to be standard, the percentual ratio of CaO varied between 18 and 22 %.

The iron and magnesium contens showed less uninform values. This is coused by the fact that paralell with the prograding differentiation the ferro-iron enters the cristal lattice in ever greater amounts, instead of Mg. The lower iron content was measured in the cores of the mineral grains. This difference could not be identified under microscope, i.e. the minerals did not display sector zoning.

The composition of clinopyroxenes varied between $Ca_{45}Mg_{48}Fe_8$ and $Ca_{40}Mg_{39}Fe_{21}$ extreme values, i.e. are of diopside-augite-salite composition. In most cases these can be qualified as augites of relatively high Ca-contens (*Fig. 1*).

The TiO_2 contens were lower than expected. The average TiO_2 content proved to be 1,46 % in the mineral grains. This was rather asthonishing since in harmony with the chemical analyses of the rocks the average TiO_2 content is 3 %, sometimes values of about 5% also occurred. Consequently, titanium is enriched first of all in rutile and leukoxene that were identified under microscope, as well.

The sodium content is low, i.e. 0,4 %, some enrichment towards the rims of grains can be observed.

The studied grains contained 0,2 Mn, on the average.

The $\frac{Fe+Mn}{Fe+Mn+Mg}$ differentiation index varies between 0,1 and 0,3. This values were plotted as a function of the Ti and Al contents. It is known from the literature that parallel with prograding differentiation the Al and Ti contents that enter the crystal lattice increase and this fact is proved also by my measurements on pyroxenes of the samples studied.

It is more remarkable, hovewer, that the projection points are grouped within a narrow interval, this fact indicating a magma of low degree of differentiation (*Figs. 2* and *3*), or a phenomenon that only certain type was resistant to epigenesis or other effects.

Based on the data obtained during these investigation an attemt was made to determine the magma type and the tectonic position of the formation itself. First I used the method of LETTERIER (1982, see *Fig. 4.*). It seems, that most of the points fall to the alcali field. In the course of interpreting the main element analyses of the rocks it proved to be to be a serious problem to decide this question, moreower no exact answer could be given.

Nevertheless, these data serve as a reliable basis for the subsequent investigations based first of all on the inmobile trace elements.

To decide to the tectonic setting the discrimination method of NISBET-PEARCE (1977) was used. Trough this method has some veak points., i. e. separability is not always unambiguous and is based on the Na-, and Mn-values that fluctuate usually around the detection limit, it is remarkable, that practically without some exception the projection points fall to the within-plate alcali field, and this supports the statement based on the previous method.

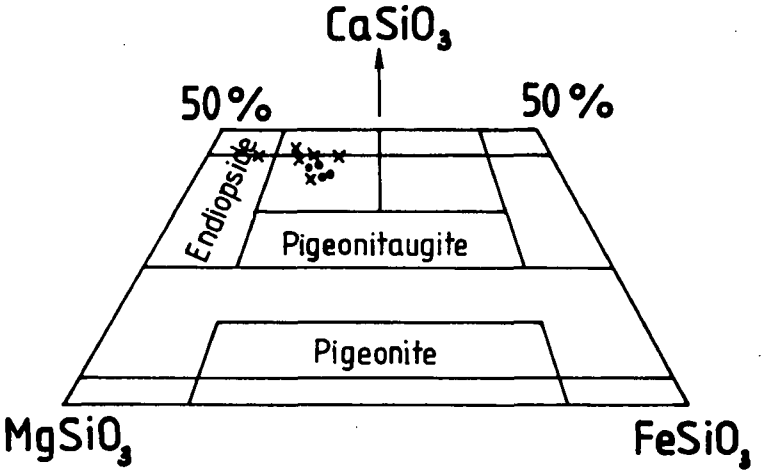

Fig. 1. Clinopyroxene compositions (after POLDERVAART and HESS, 1953).

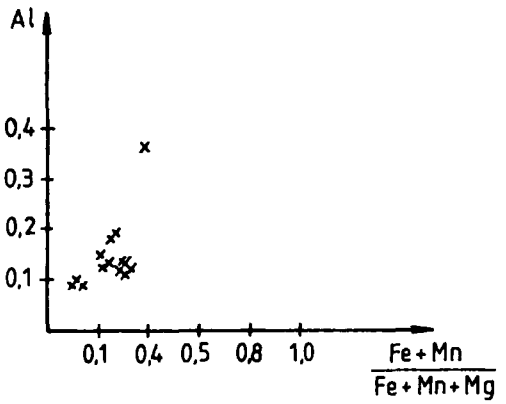

Fig. 2. The $\frac{Fe+Mn}{Fe+Mn+Mg}$ - Ti diagram

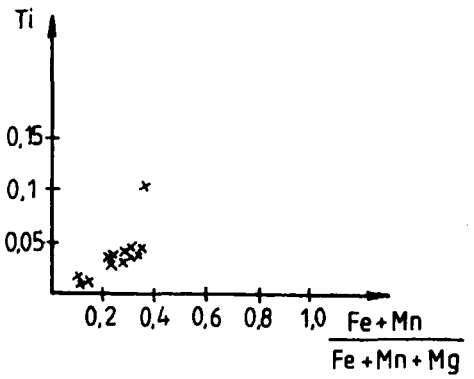

Fig. 3. The $\frac{Fe+Mn}{Fe+Mn+Mg}$ - Al diagram

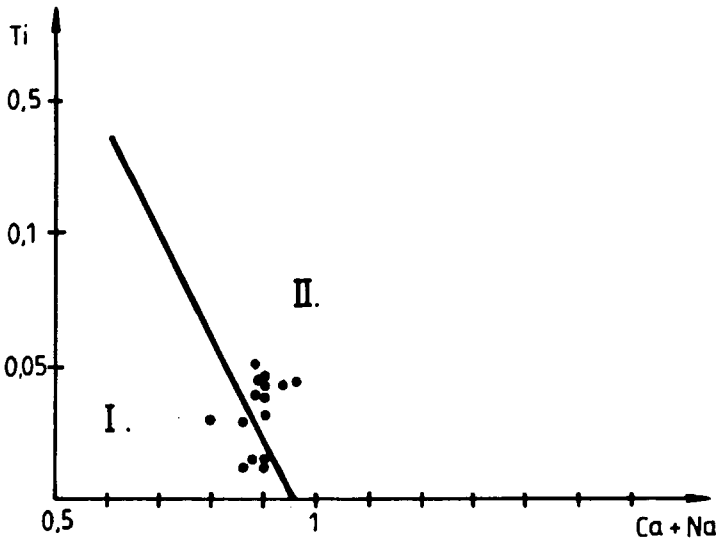

Fig. 4. The Ti-Na-Ca diagram (after LETTERIER et al. 1982).
I. Tholeiit field
II.Alcali field

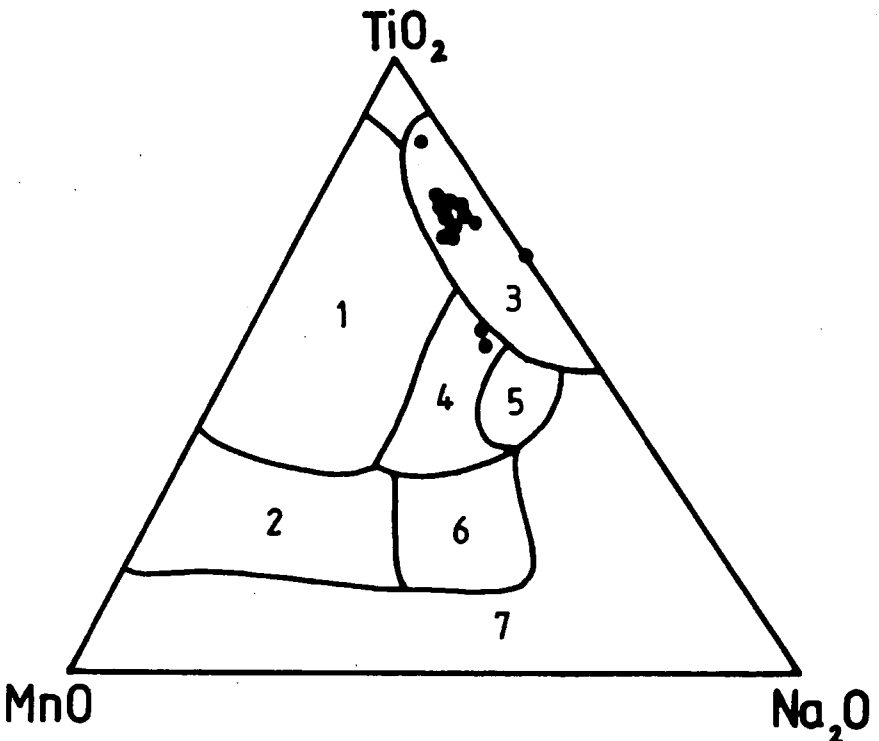

Fig. 5. The MnO-Na_2O-TiO_2 diagram (after NISBET and PEARCE, 1977).

CONCLUSIONS

1. The clinopyroxenes of the Lower Cretaceous volcanics of the Great Plain are of diopside-augite-salite composition.

2. The original magma was less differentiated, this is reflected by the Ti-contens, by the differentiation index and by former results.

3. Based on the chemical studies of pyroxene phenocrysts it can be stated that the mineral grains refer to alkali magma, that is proved by the discriminating method, too and this fact does not contradict to the statements based on main element analyses.

4. Consequently the high alkali content of the rocks is a result not only of Na-metasomatism and contamination.

5. Having interpreted the main element analyses (MOLNÁR, 1985) it was proved, that rock products of within-plate volcanism and this statement is supported by the pyroxene analytical data as well.

6. It is worthy of mention, that the pyroxene analytical data of Lower Cretaceous volcanics of the Great Plain display remarkable similarity to those Lower Cretaceous volcanics of the Mecsek Mountains (SW Hungary).

REFERENCES

DOBOSI, G. (1985): A mecseki alkáli bazaltok piroxén fenokristályainak geokémiai vizsgálata. (Geocemical investigation of pyroxene phenocrystals of mecsek alkali basalts. In hung.) Földt. Közl. **115**, 79-90.

LETTERIER, J. et al.(1982): Clinpyroxene composition as a method of identification of the magmatic affinites of paleovolcanic series. Eart Planet. Sci. Lett. **59**, 139-154.

LINDSLEY, H. D.(1982): Phase equilibria of pyroxenes at pressures > 1 atmosphere. in Pyroxenes ed. by PERWITT, C. T. Vol. **7**, 289-308.

MOLNÁR, S.(1985): Petrochemical character of the Lower Cretaceous volcanic rocks of the Great Hungarian Plain. Acta Miner. Petr. Szeged. XXVII, 33-38.

NISBET, E. G., PEARCE, J. A.(1977): Clinopyroxene composition in mafic lavas from different tectonic settings.Contr. Miner. Petr. **63**, 149-160.

POLDERVAART, A., HESS, H. H.(1953): Unit-cell dimensions of clinoenstatite and pigeonite in the relation the common pyroxenes. Amer. J. of Sci. **251**, 74.

SZEPESHÁZI, K.(1960): A Kecskemét–Szolnok közötti kréta időszaki vulkáni terület kőzetei. (The rocks of the cretaccous volcanic area between Kecskemét-Szolnok. in Hung.) MÁFI Évi Jel. 525- 535.

Manuscript received 18 Sep. 1996

Acta Mineralogica-Petrographica, Szeged, XXXVII, 89-98, 1996

THE DISTRIBUTION OF SULPHUR IN UPPER CRETACEOUS BROWN COALS FROM AJKA (CENTRAL TRANSDANUBIA, HUNGARY)

L. PÁPAY*

* Department of Mineralogy, Geochemistry and Petrography, Attila József University

ABSTRACT

In this study 25 brown coal samples have been examined from Ajka (Jókai mine). The total sulphur content of the studied Upper Cretaceous brown coals is highly variable abundances range from 2.1% to 9.7%, mean 5.1%. The dominant sulphur forms found in the samples were pyritic and organic sulphur. The sulphur content of the brown coals is generally less than 0.3%, the mean ~0.15%.

However, there is a difference between the distribution of sulpur in the lower and upper coal beds of the mine. The brown coal samples taken from the 1st bed can be characterized by extremely high total sulphur values (mean 7.5%!), where the pyritic sulphur is dominating giving 65% of the total sulphur content. In the 3rd, 4th, 5th and 6th coal beds of the lower coal series the prevalence of organic sulphur (≥70%), an average of ~20% pyritic sulphur and a minimal sulphate sulphur content can be traced. These latter distributions of the sulphur content are very similar to the values experienced during the earlier analyses of the average sulphur content of Transdanubian brown coals, the sequence is organic sulphur > pyritic sulphur > sulphate sulphur. The wide range of the total sulphur content within the individual coal beds – save the 6th one – refers to their heterogenous nature. The inorganic contents of the coal measures are also different, the average ash content of the samples taken from the coal beds showed an upward increase.

The high sulphur content of the coals of Jókai mine can be explained by the fact that they were deposited in a brackish or marine-influenced environment. The really high pyrite content of the 1st bed might be explained by the presence of interbedding clayish inorganic layers within the coal beds, while the high organic sulphur content of the lower coal series may reflect the influence of the carbonate rocks giving the bottom of seams and the low concentration of available reactive iron during peat formation and diaganesis.

INTRODUCTION

It is generally known that sulphur present in the coal is usually as inorganic and organic sulphur compounds. The inorganic sulphur content is originated mainly from iron sulphides (pyrite or marcasite; other sulphides are frequently found in very small quantities e. g. arsenic, copper, lead, zinc sulphides). The presence of sulphates (mainly of calcium and iron) is generally unimportant except in case of highly weathered or oxidized coal samples (weathering of pyrite may generate iron sulphates). Although elemental sulphur sometimes occurs in some coals. The sulphur content is conventionally given in total sulphur values and the so-called forms of sulphur that are pyritic, sulphate and organic sulphur, with the assumption that pyritic sulphur embodies all the metallic sulphides as well.

The first step in the overall process of sedimentary pyrite formation is the bacterial reduction of sulphate, under anoxic conditions. The amount of pyrite formed in a sediment

* H-6701 Szeged, P. O. Box 651, Hungary

depends on three factors: sufficient dissolved sulphate, concentration of organic matter and reactive iron minerals. Pyrite forms during shallow burial, via the reaction of detrital iron minerals with H_2S. The H_2S is produced by the reduction of interstitial dissolved sulphate by bacteria using sedimentary organic matter as reducing agent and energy source. The initial product of this reaction is not pyrite but rather a series of metastable iron monosulphides which during early diagenesis transform to pyrite by reaction with polysulphide ions (BERNER 1972, 1981, 1984). However, the last reaction step is very complicated process. According to a part of the study pyrite single crystals could be formed rapidly and directly by the reaction of iron monosulphide with polysulphide ions (RICKARD 1975), but direct pyrite formation was not observed in case of reactions of Fe(II) and Fe(III) solutions with polysulphide (LUTHER III 1991). On the other hand a number of laboratory studies have demonstrated that pyrite can be synthesized rapidly from inorganic solution under suitable conditions (HOWARTH 1979) or DROBNER et al. (1990) reported the formation of pyrite under fastidiously anaerobic conditions in the aqueous system of FeS and H_2S.

In the fresh-water amount of sulphate less than in sea-water, during burial sulphate supply become difficult too, therefore in these circumstances pyrite forms not only via reduction of sulphate. According to ALTSCHULTER et al. (1983) the pyrite formation in organic-rich sediment is commonly linked to H_2S formed within the organic tissues and suggests that the sulphid may derive largely from organic sulphur.

In the sediments, H_2S formed from microbial reduction of sulphate initially reacts with available iron to form iron sulphid minerals and more gradually with organic matter to form organosulphur compounds (TUTTLE and GOLDHABER 1993). The organic sulphur compounds found in coals have been categorized according to functionality: thiols, sulphides, thiophenes, thiopyrones (GIVEN and WYSS 1961; ATTAR 1979). In their experiments CASAGRANDE et al. (1979) demonstrated that not only $H_2{}^{35}S$ is incorporated in peat as organic sulphur, but elemental sulphur as well (CASAGRANDE and NG 1979). Hydrogen sulphide is an important intermediate for pyrite and organic sulphur formation in peats (CASAGRANDE 1987).

The H_2S produced by bacterial sulphate reduction exhausts not only in reactions mentioned above, but a part of the H_2S escapes from the sulphate reduction zone as well. In a study on recent bioturbated sediments BERNER and WESTRICH (1985) found that only <10–75% of the reduced sulphur remains in the sediments. They have concluded that the main mechanism of loss of reduced sulphur are oxidation "by O_2 mixed into the sediments by the benthos and, to a lesser extent, via enhanced H_2S transport resulting from benthic irrigation". Therefore we may support that the mechanisms enumerated by BERNER and WESTRICH (1985) did not operate in sediments were bioturbation is absent. Thus these sediments have lost no more than 25% (and probably much less) of the reduced sulphur produced in them (VETŐ and HETÉNYI 1991).

There is an almost universal tendency for the sulphur content of seams in close proximity to marine bands to be abnormally high (WANDLESS 1955; WILLIAMS and KEITH, 1963; REIDENOUER et al. 1967 and others). The high sulphur content is due to the increased availability of sulphate ions in sea-water and by the activity of anaerobic bacteria. Coals, which were deposited in calcium-rich swamps, show similar properties to marine-influenced coals. Calcareous basements, or influx of calcium-rich waters from surrounding swamp areas, reduce the acidity of the peat to a much greater degree than does sea-water (SZÁDECZKY-KARDOSS 1952; STACH et al. 1982).

CECIL et al. (1979) concluded that low ash and low sulphur coals were deposited as fresh-water peats which were underlain and overlain by fresh-water clastic sediments in which limestones were absent. Where limestones are present in fresh-water sedimentary sequences the coals are of intermediate ash yield and sulphur content. High ash and high sulphur coals are associated with brackish or marine sediments.

GEOLOGICAL SETTING

The Upper Cretaceous brown coal mine (Jókai) in the Transdanubian Central Range is situated at the NW edge of the S Bakony Mountains, SE from the town of Ajka in the middle of the Ajka Basin (*Fig. 1.*).

In the NW foreland of the S Bakony Mountains the Senonian coal-bearing series can be found along a 20–25 kilometres long line. The Upper Triassic Norian dolomite complex ("Hauptdolomit") forms the bottom of this coal-bearing series. Besides these the Kössen beds (Rhaetian) are represented by distinctive forms of limestones, dolomites, marls and clay marls and respectively the rocks of another Upper Triassic Rhaetian deposit the Dachstein Limestone ("Dachsteinkalk") (KOZMA 1991). The classical term of Ajka Coal Formation covers a unit which consists of an alternation of coal-bearing argillaceous and calcareous rocks deposited in lacustrine and, later, salt water swamps which developed parallel with the marine transgression in the Senonian (HAAS et al. 1977). The series of the Ajka Coal Formation is composed of a multiple cyclical succession of coal, grey clay marl, marl, sandstone and limestone layers. In the lower strata of the formation the presence of an abundant molluscs indicate freshwater facies while in the upper strata it shows an increasing tendency in salinity with cyclical changes (HAAS and EDELÉNYI 1979).

The Ajka brown coal measures approximately 120 m thick vertically with a 130 coal benches, with the help of the well identifiable unproductive interbeddings can be divided into a lower and upper coal series.

The lower coal series has a 14–25 m vertical thickness and contains most of the coal beds. The 2^{nd}, 3^{rd}, 4^{th}, 5^{th} and 6^{th} coal beds are divided by slightly different interbeddings in the mine. These unproductive interbeddings are 0.3–2.0 metres thick vertically. Between the coal beds and in the beds themselves the appearance of light brown calcareous marls, carbonaceous marls can be observed.

The upper coal series is divided from the lower one by one a 1–20 metres thick ligh grey clay marl interbedding. In the coal series only one workable seam can be found which is called the 1^{st} or Amber Coal Bed. It was named after the fossilized resins of Cretaceous pine forests, though as it turned out later on practically amber might be found in any of the seams. The amber was given the name of Ajkait after the town of Ajka. Above the 1^{st} bed the previously mentioned light grey clay marl layers occur again in 5 to 20 metres thickness. The geological literature give the name 0 (zero) bed to the 4–5 metres thick carbonaceous clay, argillaceous coal and marl mollusc bearing layers above the 1^{st} coal bed thus indicating that the discovery of this seam took place after the accepted numbering of the coal beds of the series (KOZMA 1991).

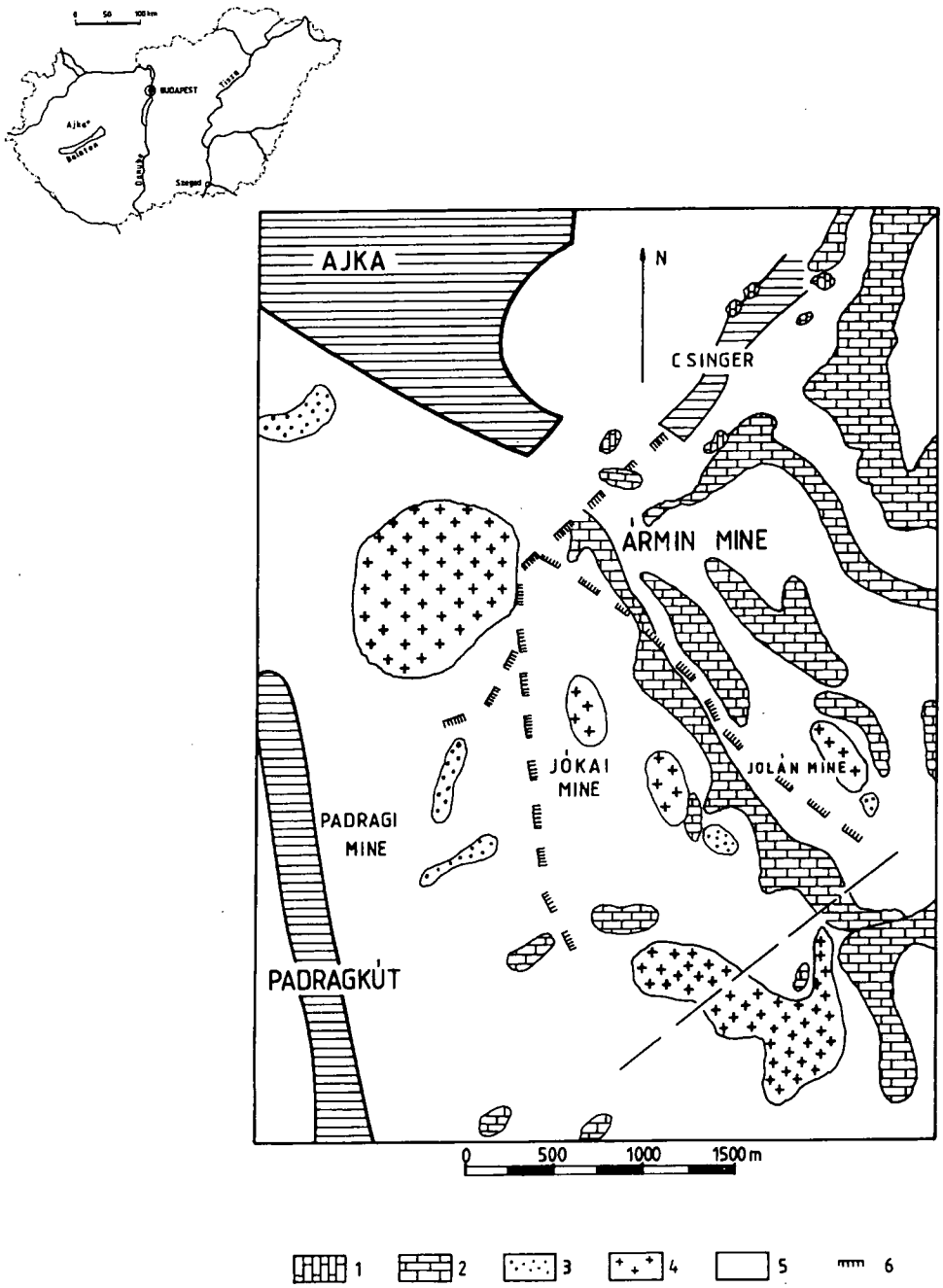

Fig. 1. Geological sketch map of the Ajka Basin (after KLESPITZ, 1971)
Legend: 1 = Upper Cretaceous limestone, 2 = Eocene limestone, 3 = Miocene pebbles, 4 = Pliocene basalt, 5 = Pleistocene, holocene deposits, 6 = Fault, 7 = The boundary of the erosion coal bed.

SAMPLES AND ANALYTICAL METHODS

25 brown coal samples have been examined from Ajka (Jókai Mine) (Table 1). First the samples were ground to grain size d≤0.2 mm.

The total carbon content was measured at 1000 °C under intense oxygen flow by combusting in a Carmhograph-8 (Wösthoff) equipment.

The determination of calcite and dolomite by gasometry is based on the fact that calcite dissolves rapidly and perfectly in 1:1 HCl at room temperature, but dolomite dissolved after some time and very slowly. At the same time both calcite and dolomite dissolves after 5 minutes boiling (HETÉNYI and VARSÁNYI 1975). 1 cm^3 CO_2 = 0.1976 g CO_2; C_{carb} = 0.2729 x CO_2.

The determination of the total sulphur was carried out with Eschka procedure. The Eschka method consist of thoroughly mixing the powered coal sample with Eschka mixture (two parts calcined MgO and one part anhydrous Na_2CO_3) and then ashing the mixture in muffle furnace at 800 °C. The ashed coal is leached with hot water and filtered, and sulphate precipitated with $BaCl_2$ was determined by gravimetric analysis as barium sulphate. This method is most accurate for coal samples containing no more than 6 or 7% sulphur (TSAI 1982).

The sulphur content of disulphide in coal samples was reduced by nascent hydrogen to hydrogen sulphide in the presence of Cr(II)-ions. The hydrogen sulphide originated from reduction was buddled through a cadmium acetate solution and the sulphur content of disulphide was determined by iodometry.

The sulphate sulphur was determined by extraction of the powered coal samples with hydrochloric acid followed by precipitation with barium chloride and weighing as barium sulphate.

In every case the organic sulphur was determined by the difference between the total sulphur and inorganic sulphur.

RESULT AND DISCUSSION

Examining the data published in Hungarian geological reports concerning the Ajka mine (Table 2) it can be concluded that primarily we have to deal with records of the total sulphur content of the Hungarian coals. It can be plainly seen mainly in case of the more data found in the reports (FEJÉR et al. 1989) as well that there are extreme variations in the quantities of the total sulphur content in the brown coal samples of the Jókai mine. Our measurements proved these extreme variations too. The results of experiments are summarized in Table 3.

The total sulphur content of Upper Cretaceous brown coals from Ajka is highly variable abundances range from 2.1% to 9.7%, mean 5.1%. Pyritic and organic sulphur are dominant sulphur forms in them. The sulphur content of brown coals is generally less than 0.3%, with a mean of ~0.15%. Besides the general features of the coal measures we have to take in to consideration the fact that the development of the individual coal beds might be different within the whole system along with the distribution of sulphur content; thus the data concerning the individual coal beds give us more accurate information about the mine. The distribution of sulphur is different in the 1^{st} bed and the 3^{rd}, 4^{th}, 5^{th} and 6^{th} beds of the lower coal series. The brown coal samples taken from the 1^{st} bed can be characterized by extremely high total sulphur values (mean 7.5%!), where the pyritic

TABLE I

Markings connected with the brown coal samples from Ajka (Jókai Mine)

Sample No.	Symbol	Sampling	Features of the coal samples
1	J/I/1	1st coal bed; coal drawing (37/1)	Slightly stratified durain coal
2	J/I/2	1st coal bed; coal drawing (37/1)	Durain coal with vitrain lenticles
3	J/I/3	1st coal bed; coal drawing (37/1)	Durain coal with vitrain lenticles; similar to J/I/2
4	J/III/4	3rd coal bed; coal drawing (52/6)	Unstratified durain coal with vitrain lenticles
5	J/III/5	3rd coal bed; coal drawing (52/6)	Unstratified vitrain lenticles coal with brown precipitated resin
6	J/III/6	3rd coal bed; coal drawing (52/6)	Slightly stratified coal with vitrain streaks and fragments of gastropods
7	J/III/7	3rd coal bed; air way of coal preparation (38/IV)	Unstratified durain coal
8	J/III/8	3rd coal bed; haulage drift of coal preparation (38/IV)	Durain coal with fragments of molluscs
9	J/III/9	3rd coal bed; air way of coal preparation (38/IV)	Unstratified durain coal
10	J/IV/10	4th coal bed; coal drawing (52/6)	Unstratified durain coal
11	J/IV/11	4th coal bed; coal drawing (52/6)	Unstratified durain coal
12	J/IV/12	4th coal bed; coal drawing (52/6)	Unstratified vitrain coal with millimetre sized gypsum
13	J/IV/13	4th coal bed; haulage drift of coal preparation (38/IV)	Vitrain coal with fragments of molluscs
14	J/IV/14	4th coal bed; haulage drift of coal preparation (38/IV)	Durain coal
15	J/IV/15	4th coal bed; haulage drift of coal preparation (38/IV)	Vitrain coal with fragments of molluscs
16	J/IV/16	4th coal bed; air way of coal preparation (38/IV)	Vitrain coal
17	J/IV/17	4th coal bed; air way of coal preparation (38/IV)	Vitrain coal with fragments of molluscs
18	J/V/18	5th coal bed; coal drawing (52/6)	Slightly stratified durain coal
19	J/V/19	5th coal bed; coal drawing (52/6)	Slightly stratified vitrain lenticles coal
20	J/V/20	5th coal bed; coal drawing (52/6)	Unstratified durain coal with vitrain lenticles
21	J/V/21	5th coal bed; 38/IV air way of coal preparation	Durain coal
22	J/V/22	5th coal bed; air way of coal preparation (38/IV)	Vitrain lenticles coal with fragments of molluscs
23	J/VI/23	6th coal bed; coal drawing (52/6)	Hard, vitrain and durain streaks coal
24	J/VI/24	6th coal bed; coal drawing (52/6)	Crumbly, clarain earth coal
25	J/VI/25	6th coal bed; coal drawing (52/6)	Moderately hard, durain coal with fragments of molluscs

TABLE 2

The total sulphur content and distribution of sulphur in brown coal from Ajka on the basis of published data

Station of sampling	Number of samples	S_t^a wt% (mean)	S_p^a wt% (mean)	S_{sz}^a wt% (mean)	S_{org}^a wt% (mean)
Ajka[1]	6	4.30–5.58[1a] (4.98)			
	–	6.9[1b]			
Ajka[2]	3	2.88–3.98 (3.52)			
Ajka[3]	8	3.4–4.5 (4.0)	0.7–1.3 (1.0)	0.2–0.5 (0.3)	1.6–3.3 (2.7)
Jókai mine[4]	37	1.57–9.34 (3.39)			

S_t^a, S_p^a, S_{sz}^a, S_{org}^a: total, pyritic (+sulphide), sulphate, organic (by difference) sulphur content in air dried sample.

[1] VITÁLIS I. (1939): Occurrence of coals in Hungary; [1a] after GRITTNER, 1906; [1b] after VARGA J. and NYÚL Gy., 1937.

[2] SZÁDECZKY–KARDOSS E. (1952): Coal Petrology.

[3] MR. KOVATSITS M., WOLF GY. (1980): Sulphur survey of the Hungarian commerical coals.

[4] FEJÉR L., OSWALD GY., SZÉLES L. (1989): The method and results of the sulphur content survey of the Hungarian coals.

sulphur is dominating giving 65% of the total sulphur content. In the 3rd, 4th, 5th and 6th coal beds of the lower coal series the prevalene of organic sulphur (≥70%), an average of ~20% pyritic sulphur and a minimal sulphate sulphur content can be traced. These latter distributions of the sulphur content are very similar to the values experienced during the earlier analyses of the average sulphur content of Transdanubian brown coals, the sequence is organic sulphur > pyritic sulphur > sulphate sulphur (PÁPAY 1993). The wide range of the total sulphur content within the individual coal beds – save the 6th one – refers to their heterogenous nature. The inorganic contents of the coal measures are also different, the average ash content of the samples taken from the coal beds showed an upward increase. The high sulphur content of the coals of Jókai mine can be explained by their deposition in a brackish or marine-influenced environment. The really high pyrite content of the 1st bed might be explained by the presence of interbedding clayish inorganic layers within the coal beds. As it is known, in the argillaceous rocks the amount of reactive iron is plenty 6.5% (Fe_2O_3+FeO), but at the same time in carbonates the iron content is only 0.5% or lower (WOYTKEVITSH et al. 1977). The quantity of available ferrous ion is an important factor for pyrite formation. At the same time the high organic sulphur content of the lower coal series may reflect the influence of the carbonate rocks giving the bottom of seams and the low concentration of available reactive iron during peat formation and diagenesis.

ACKNOWLEDGEMENT

This work has been supported by the Hungarian Scientific Research Fund (OTKA) grant No. T 007445.

TABLE 3

Distribution of sulphur in brown coal samples at Ajka (Jókai Mine) in addition to data of the moisture, ash, total, inorganic, organic carbon content

Symbol	W^a %	A^d %	C_t %	C_{carb} %	C_{org} %	S_t^a %	S_p^a %	S_{sz}^a %	S_{org}^a % (diff.)	S_t^{daf} %	S_p^{daf} %	S_{sz}^{daf} %	S_{org}^{daf} % (diff.)
J/I/1	7.6	32.7	41.3	0.2	41.1	4.5	1.9	0.1	2.5	7.5	3.2	0.1	4.2
J/I/2	7.0	26.2	44.5	0.2	44.3	8.4	5.8	0.2	2.8	13.2	8.7	0.3	4.2
J/I/3	6.2	40.1	31.3	0.2	31.2	9.7	7.0	0.7	2.3	18.6	13.0	1.3	4.3
J/III/4	9.1	10.4	60.6	0.1	60.5	7.9	2.3	0.1	5.5	9.8	2.9	0.1	6.8
J/III/5	9.0	12.6	64.8	0.6	64.2	5.3	0.3	< 0.1	~ 4.9	6.8	0.4	~ 0.1	~ 6.3
J/III/6	8.6	13.9	60.6	0.6	60.0	4.8	0.3	< 0.1	~ 4.4	6.2	0.4	~ 0.1	~ 5.7
J/III/7	7.6	15.8	56.0	0.1	55.9	6.3	1.6	0.1	4.6	8.2	2.1	0.1	6.0
J/III/8	6.1	32.9	43.1	3.9	39.2	3.9	0.7	< 0.1	~ 3.1	6.4	1.2	~ 0.1	~ 5.1
J/III/9	7.8	20.4	53.5	0.1	53.4	5.7	2.4	0.1	3.2	7.9	3.3.	0.1	4.5
J/IV/10	7.8	14.3	58.9	0.2	58.7	5.5	1.1	0.1	4.3	7.0	1.4	0.1	5.5
J/IV/11	8.2	11.1	63.7	0.1	63.6	5.5	0.8	0.2	4.5	6.8	1.0	0.2	5.6
J/IV/12	8.0	13.0	59.6	0.6	59.0	6.3	0.5	0.3	5.5	8.0	0.6	0.4	7.0
J/IV/13	5.1	38.8	34.1	4.0	30.1	3.2	0.4	< 0.1	~ 2.7	5.7	0.7	~ 0.2	~ 4.8
J/IV/14	8.5	13.1	53.8	0.2	53.6	6.3	1.3	0.2	4.8	8.0	1.7	0.3	6.1
J/IV/15	4.3	41.4	32.2	5.5	26.7	2.1	0.4	< 0.1	~ 1.6	3.9	0.7	~ 0.2	~ 3.0
J/IV/16	6.0	48.6	28.5	0.1	28.4	4.8	2.9	0.2	1.7	10.6	6.4	0.4	3.7
J/IV/17	5.3	38.1	40.3	4.2	36.1	3.2	0.6	< 0.1	~ 2.5	5.7	1.1	~ 0.2	~ 4.4
J/V/18	8.0	11.7	63.7	0.2	63.5	3.6	0.7	0.1	2.8	4.5	0.9	0.1	3.5
J/V/19	8.2	23.8	54.0	0.7	53.3	3.7	1.0	0.1	2.6	5.4	1.5	0.1	3.8
J/V/20	8.2	13.9	58.9	0.2	58.7	5.2	1.2	0.1	3.9	6.6	1.5	0.1	5.0
J/V/21	7.7	25.3	46.7	0.1	46.6	6.3	3.2	0.3	2.8	9.4	4.8	0.4	4.2
J/V/22	6.7	25.7	50.0	2.4	47.6	4.6	0.8	< 0.1	~ 3.7	6.8	1.2	~ 0.1	~ 5.5
J/V/23	9.5	11.5	58.1	0.2	57.9	4.0	1.1	0.1	2.8	5.1	1.4	0.1	3.6
J/VI/24	9.3	8.9	63.7	0.2	63.5	3.1	0.3	0.1	2.7	3.8	0.4	0.1	3.3
J/VI/25	9.7	13.3	58.5	0.4	58.1	3.6	0.2	0.2	3.2	4.7	0.3	0.3	4.1

W^a: analitical moisture wt %; A^d: ash (air dried sample) wt %; C_t, C_{carb} C_{org}: total, carbonate (inorganic), organic carbon contect wt %;
S_t^a, S_p^a, S_{sz}^a, S_{org}^a: total, pyritic (+sulphide), sulphate, organic (by difference) sulphur content in air dried sample
S_t^{daf}, S_p^{daf}, S_{sz}^{daf}, S_{org}^{daf}: total, pyrite (+sulphide), sulphate, organic (by difference) sulphur content; dry, ash-free basis

REFERENCES

ATTAR A. (1979): Sulfur groups in coal and their determination. In: Analytical Methods for Coal and Coal Products, Vol. III, 353–357. Academic Press, New York.

ALTSCHULER Z. S., SCHNEPFE M. M., SILBER C. C. and SIMON F. O. (1983): Sulfur diagenesis in Everglades peat and origin of pyrite in coal. – Science **221**, 221–227.

BERNER R. A. (1972): Sulfate reduction, pyrite formation, and the oceanic sulfur budget. – in: The Changing Chemistry of the Oceans, Eds. Dyrssen D. and Jagner D., Almqvist and Wiksell, Stockholm, 347–361.

BERNER R. A. (1981): Authigenic mineral formation resulting from organic matter decomposition in modern sediments. – Fortschr. Miner. **59**, 117–135.

BERNER R. A. (1984): Sedimentary pyrite formation: An update. – Geochim. Cosmochim. Acta, **48**, 605–615.

BERNER R. A. and WESTRICH J. T. (1985): Bioturbation and the early diagenesis of carbon and sulfur. – Am. J. Sci. **285**, 193–206.

CASAGRANDE D. J., IDOWU G., FRIEDMAN A., RICKERT P., SIEFERT K. & SCHLENZ D. (1979): H_2S incorporation in coal precursors: origins of organic sulphur in coal. – Nature **282**, 599–600.

CASAGRANDE D. J. & NG L. (1979): Incorporation of elemental sulphur in coal as organic sulphur. – Nature **282**, 598–599.

CASAGRANDE D. J. (1987): Sulphur in peat and coal. – In: Scott A. C. (ed): Coal and coal-bearing strata: Recent Adv. Geol. Soc. Spec. Publ. **32**, 87–105.

CECIL C. B., RENTON J. J., STANTON R. W. & FINKELMAN R. B. (1979): Mineral matter in coals of the central Appalachian Basin. – 9th Internat. Congr. Carbonif. Strat. Geol. Abstr. p. 33, Urbana Ill.

DROBNER E., HUBER H., WACHTERSHAUSER G., ROSE D. & STETTER K. O. (1990): Pyrite formation with hydrogen evolution under anaerobic conditions. – Nature **346**, 742–744.

FEJÉR L., OSWALD GY., SZÉLES L. (1989): A magyarországi kőszenek kéntartalom-felmérésének módszere és eredménye (The method and results of the sulphur content survey of the Hungarian coals) (in Hungarian). – Központi Földtani Hivatal kiadványa, Budapest.

GRITTNER A. (1906): Szénelemzések (Coal analyses). Budapest. In: Vitális I. (1939): Magyarország szénelőfordulásai (Occurence of coals in Hungary) (in Hungarian). Sopron.

GIVEN P. H. & WYSS W. F. (1961): The chemistry of sulfur in coal. – British Coal Utilization Research Association Monthly Bulletin, **25**, 165–179.

HAAS J., J. EDELÉNYI E., CSÁSZÁR G. (1977): Mezozoós formációk vizsgálata a Dunántúli-középhegységben (Study of mesozoic formations of the Transdanubian Central Mountains in Hungary) (in Hungarian with English abstract). – Annual Report of the Hungarian Geological Institute of 1975, 259–269.

HAAS J., J. EDELÉNYI E. (1979): A dunántúli-középhegységi felsőkréta üledékciklus ősföldrajzi elemzése (Paleogeographic analysis of the late Cretaceous sedimentary cycle in the Transdanubian Central Mountains, W Hungary) (in Hungarian with English abstract). – Annual Report of the Hungarian Geological Institute of 1977, 217–224.

HETÉNYI M., VARSÁNYI I. (1975): Rapid determination of calcite and dolomite for routine analysis by gasometry. – Acta Miner. Petr., Szeged **XXII/1**, 165–170.

HOWARTH R. W. (1979): Pyrite: its rapid formation in a salt marsh and its importance in ecosystem metabolism. – Science **203**, 49–51.

KLESPITZ J. (1971): Az ajkai barnakőszén medence Jókai Bánya területének bányaföldtani viszonyai (Geology of the Jókai brown coal mine in the Ajka Basin (in Hungarian with German abstract). – Föld. Kut. **XIV/1–2**, 6–14.

KOVATSITS M.-NÉ, WOLF GY. (1980): A hazai kereskedelmi széntermékek minőségi katasztere (Sulphur survey of the Hungarian commercial coals) (in Hungarian). Budapest–Tatabánya, KBFI, Magyar Szénbányászati Tröszt.

KOZMA K. (1991): Az ajkai szénbányászat története. (The history of the coal mining at Ajka) – Veszprémi Szénbányák, Veszprém, 29–38.

LUTHER III G. W. (1991): Pyrite synthesis via polysulfide compounds. – Geochim. Cosmochim. Acta, **55**, 2839–2849.

PÁPAY L. (1993): Distribution of sulphur in Transdanubian (Hungary) and Middle European brown coals. – Acta Geologica Hungarica, **36/2**, 241–249.

REIDENOUER D., WILLIAMS E. G. & DUTCHER R. R. (1967): The relationship between paleotopography and sulfur distribution in some coals of western Pennsylvania. – Economic Geology, **63**, 632–649.

RICKARD D. T. (1975): Kinetics and mechanisms of pyrite formation at low temperature. – Amer. J. Sci. **275**, 636–652.

STACH, E., MACKOWSKY M.-TH., TEICHMÜLLER M., TAYLOR G. H., CHANDRA D., TEICHMÜLLER R. (1982): *Stach's textbook of coal petrology*. – Gebrüder Borntraeger, Berlin, Stuttgart.

SZÁDECZKY-KARDOSS, E. (1952): Szénkőzettan (Coal petrology) (in Hungarian). Akadémiai Kiadó, Budapest.
TSAI S. C. (1982): Fundamentals of coal benefication and utilization. Elsevier Scientific Publishing Company, Amsterdam–Oxford–New York, 227.
TUTTLE M. L. and GOLDHABER M. B. (1993): Sedimentary sulfur geochemistry of the Paleogene Green River Formation, western USA: Implications for interpreting depositional and diagenetic process in saline alkaline lakes. – Geochim. Cosmochim. Acta, **57**, 3023–3039.
VARGA J. and NYÚL GY. (1937): A magyar tüzelőszeripar (The Hungarian fuel industry). Technika. Budapest, 1 sz. – In: Vitális I. (1939): Magyarország szénelőfordulásai (Occurrence of coals in Hungary) (in Hungarian). Sopron.
VETŐ I. & HETÉNYI M. (1991): Fate of organic carbon and reduced sulphur in dysoxic-anoxic Oligocene facies of the Central Paratethys (Carpathian Mountains and Hungary). In: Tyson R. V. and Pearson T. H. (eds.): Modern and Ancient Continental Shelf Anoxia. Geological Society Special Publication No. 58, 449–460.
VITÁLIS I. (1939): Magyarország szénelőfordulásai (Occurrence of coals in Hungary) (in Hungarian). Sopron.
VOYTKEVITSH, G. V., A. E. MIRSHNIKOV, A. S. POVARENNIKH, V. G. PROHOROV (1977): Краткий справочник по геохимии (Brief guide to geochemistry). – Nedra, Moszkva 80–83.
WANDLESS A. M. (1955): The occurrence of sulphur in British coals. – J. Inst. Fuel. **28**, 54–62.
WILLIAMS E. G. & KEITH M. L. (1963): Relationship between sulfur in coals and occurrence of marine roof beds. – Economic Geology, **58**, 720–729.

Manuscript received 17 May, 1996

Acta Mineralogica-Petrographica, Szeged, XXXVII, 99–128, 1996

ALPINE POLYPHASE METAMORPHISM OF THE OPHIOLITIC SZARVASKŐ COMPLEX, BÜKK MOUNTAINS, HUNGARY

SADEK GHABRIAL, D.*, ÁRKAI, P.*, NAGY, G.*

Laboratory for Geochemical Research, Hungarian Academy of Sciences,
H-1112 Budapest, Budaörsi út 45, Hungary

Corresponding author: DR. PÉTER ÁRKAI

ABSTRACT

The Szarvaskő ophiolite-like Jurassic complex (southwestern Bükk Mountains, NE Hungary) shows Alpine metamorphic crystallizations related to two distinct events. The younger (Cretaceous) regional event was formerly evidenced by ÁRKAI (1983). The new result presented here prove an earlier hydrothermal (ocean-floor) metamorphic event resulted from the interaction of seawater-derived fluids with the still hot oceanic crust. Metamorphic grade increases downwards from the prehnite-pumpellyite or zeolite facies (metabasalts), through the greenschist facies (metadiabases), to the greenschist/amphibolite transitional and amphibolite facies (metagabbros). In metagabbros, the scarcity of secondary (metamorphic) clinopyroxene and Mg-Fe amphibole, and the compositional changes of the green metamorphic amphibole from hornblende to actinolitic hornblende suggest that the metamorphic crystallization occurred at temperatures decreasing from about 700 to 400°C. The metamorphic clinopyroxene is always poor in its Al content reflecting subsolidus re-equilibration of magmatic clinopyroxene during ocean-floor hydrothermal metamorphism. However, the metamorphic clinopyroxene reported from other ophiolitic gabbro occurrences is much lower in Al and Ti contents (MÉVEL et al., 1978; GIRARDEAU and MÉVEL, 1982; MÉVEL, 1988; GILLIS, 1995) than that of the Szarvaskő complex. The metamorphic amphibole formed in metadiabases is rather actinolitic in composition, and coexists with albite, chlorite and titanite, indicating temperature below 400°C. The phases formed in metabasalts during hydrothermal metamorphism were modified by subsequent Alpine regional prehnite-pumpellyite facies metamorphism. The younger, low temperature regional (dynamothermal) metamorphism produced prehnite-pumpellyite facies assemblages in meta-igneous rocks, and late diagenetic to low temperature anchizonal alteration in the surrounding sedimentary rocks, as stated earlier by ÁRKAI (1983). The compositional variation of Ca-Al silicate minerals (i.e. prehnite, pumpellyite and epidote) could not be taken as indicative of metamorphic conditions because of their high variance occurrences. However, a large variation in Fe content of these minerals was commonly recorded, and appears to be depend largely on the fluid composition, mode of occurrence and/or on the extent of rock alteration, but is weakly related to bulk rock chemistry. In the low variance assemblages, the average $X_{Fe}3+$ values of coexisting prehnite, pumpellyite and epidote are 0.003, 0.137 and 0.008, respectively. This contrasts with the results of CHO et al. (1986), who found that the $X_{Fe}3+$ values most probable increase in order of prehnite, through pumpellyite to epidote.

INTRODUCTION

The oceanic lithosphere is generally subjected to ocean-floor, hydrothermal metamorphism beneath mid-oceanic ridges. Considering a typical vertical profile of an ophiolitic suite, zeolite facies assemblages commonly occur in the pillow lava followed

* H-1112 Budapest, Budaörsi út 45.

downwards by greenschist facies within the sheeted dike complex. The amphibolite facies is restricted to the upper part of the gabbroic horizon (COLEMAN 1977). As an uncommon exception, granulite facies assemblages were also reported from gabbroic rocks (ISHIZUKA, 1985).

The Mesozoic dismembered ophiolite-like magmatic sequence of the Szarvaskő complex in the Bükk Mountains belongs to the innermost tectonic unit of Western Carpathians, forming the southern part of Gemer-Bükk unit (*Fig. 1*). This unit derived from the Inner Dinarides, and their present position has been related to Tertiary large-scale horizontal displacements (KOVÁCS 1982). The most important geological, tectonic and metamorphic features of the Bükk Mountains and the Jurassic Szarvaskő complex and its surroundings are shown in *Figs. 2* and *3*, respectively.

Previous works have shown that the Szarvaskő complex consists mostly of a series of ultrabasic and basic rocks that had been intruded locally (in the Tóbérc quarry) by cross-cutting acidic dikes and veins, showing sharp contact with the enclosing gabbro (SZENTPÉTERY, 1953; BALLA et al. 1983; DOWNES et al. 1990; SADEK GHABRIAL et al. 1994). The sedimentary environment of the ophiolite complex is represented mainly by terrigenous deep-water clastics. The geochemical data obtained by BALLA et al. (1983), DOBOSI (1986) and DOWNES et al. (1990) indicate oceanic tholeiitic nature of the complex. As regarded by DOWNES et al. (1990), the basic magma of Szarvaskő was contaminated by terrigenous sediments during its evolution in a shallow magma chamber. Mineralogically, the gabbros and related intrusive rocks are very similar, but they differ mainly in the proportions of rock forming minerals (SZENTPÉTERY 1938, 1940, 1953). Ilmenite, titanomagnetite and olivine formed first. These were followed by pyroxenes and plagioclase, including diallage, hypersthene, bronzite and basic to intermediate plagioclase with minor amounts of augite and diopside. In some samples olivine also occur. The appearance of hydrous minerals (brown hornblende and biotite), forming large crystals in the latest stage of magmatic crystallization, suggests that the crystallization of the magma within the intrusive bodies occurred at fairly high P_{H2O} which strongly increased with advancing crystallization (BALLA et al. 1983). Plagiogranite consists chiefly of plagioclase, biotite and quartz with garnet and accessories including apatite, zircon and sphene (EMBEY-ISZTIN et al. 1985; DOWNES et al. 1990). Biotite is totally replaced by chlorite, epidote and prehnite (SADEK GHABRIAL et al. 1994). Diabase is the dominant igneous rock type in the Szarvaskő area. Two main kinds of diabases were recognized, namely holocrystalline-grained and aphanitic-glassy ones (SZENTPÉTERY, 1953). Phenocrysts are rare, represented by intermediate plagioclase. Augite is the common mafic silicate, while hornblende and biotite are usually missing. As to DOWNES et al. (1990), the common minerals in basic rocks of the Szarvaskő complex are plagioclase and clinopyroxene with ilmenite, magnetite and pyrite being present as accessories.

As to ÁRKAI (1983), the Szarvaskő metabasites show prehnite-pumpellyite facies alteration. The adjoining sedimentary formations were subjected to regional (dynamothermal) alteration ranging in grade from late diagenesis up to the low-temperature part of the anchizone. Based on the fairly good coincidence of metamorphic grades established in the metabasic rocks and in their sedimentary environment, the prehnite-pumpellyite facies alteration of metabasic rocks was rendered to the regional metamorphic event, which should have obliterated the products of an eventual (but not proved) earlier metamorphic episode (ÁRKAI 1983).

This paper presents the results of a detailed metamorphic petrological study carried out on the whole profile of the ophiolite-like pile of the Szarvaskő complex, paying special

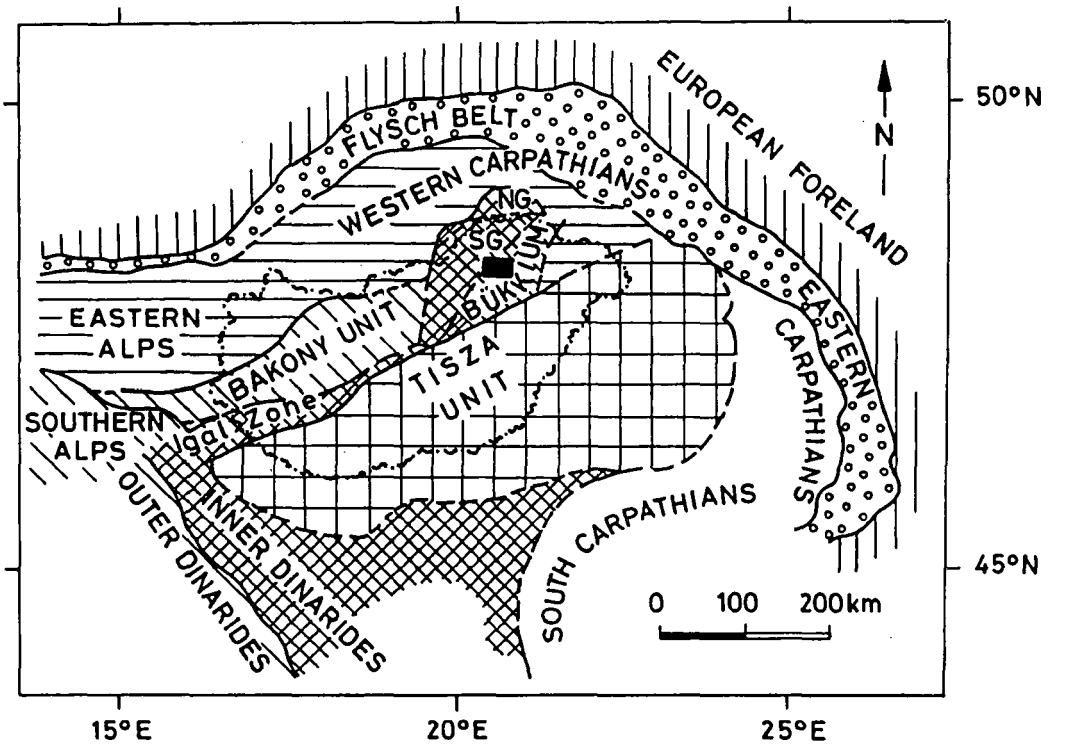

Fig. 1. Position of the Bükkium within the Alp-Carpathian-Dinaric frame.

attention to the distinction between the products of the regional (dynamothermal) and the eventually preceding hydrothermal (ocean-floor) metamorphic events.

MATERIALS AND METHODS

In the Szarvaskő area (*Fig. 3*), samples studied were collected from the Tóbérc quarry (metagranites and metagabbros), the Tardos quarry (metagabbros) and from a series of road cuts, small quarries and valley exposures along a profile, crossing in N-S direction the Szarvaskő complex (metagabbros, metadiabases, metabasalts). Macroscopic and microscopic investigations were done to define rock types, the primary and secondary mineral assemblages, and microstructural features.

For X-ray diffractometric study, the samples were crushed using a jaw crusher, and ground in a mortar mill (Type Pulversette 2, Fritsch) for 3 min. The modal compositions and the illite and chlorite crystallinity indices were evaluated on unoriented powder mounts of the whole rock samples, and on highly oriented (sedimented) <2μm grain size fractions. The latters were separated by differential settling of the rock powder in distilled

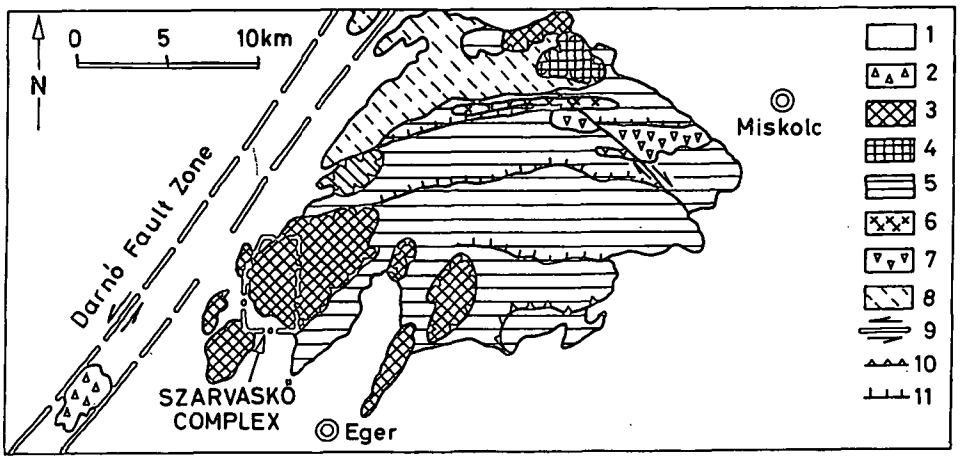

Fig. 2. Simplified geological and metamorphic map of the Bükk Mountains after CSONTOS (1988), KOVÁCS (1989) and ÁRKAI (1983, 1991). Legend: 1=Tertiary and Quaternary (diagenetic zone), 2=Upper Permian-Mesozoic South Gemer unit (diagenetic zone), 3=Jurassic Szarvaskő-Mónosbél (Little Plateau) Nappe (diagenetic, low-T anchizonal), 4=Triassic Kisfennsík Nape (diagenetic zone), 5-8=Fennsík (Bükk Plateau) Parautochthon, 5=Triassic and Jurassic sedimentary Fms. (anchi-epizonal), 6=Carnic metabasalts (pumpellyite-actinolite facies), 7=Ladinian metaandesites (greenschist facies), 8=Middle Carboniferous-Permian sedimentary Fms. (anchi-epizonal), 9=strike-slip fault, 10=nappe boundary, 11=major imbrications within the nappes.

water, pipetting the suspension onto glass slides and drying at room temperature following the procedure suggested by KÜBLER (1968). In order to determine the expandable clay minerals/components, some of the <2μm mounts were solvated by exposing the samples to ethylene glycol vapour in an oven at 80°C for 4 h. The XRD measurements were carried out using a Philips PW-1730 X-ray diffractometer with CuK_{α} radiation, graphite monochromator, proportional counter, divergence and receiving slits of 1°, at 45 kV, 35 mA, goniometer speeds of 2°/min and "°/min, and time constant of 2 s. The illite and chlorite crystallinity indices, i.e., the full width values measured at half maximum (FWHM) of the 10Å basal reflection of illite-muscovite and the 14 and 7Ĺ basal reflections of chlorite abbreviated as IC(002), ChC(001) and ChC(002) were calibrated against KÜBLER's illite crystallinity scale. The ranges of KÜBLER's anchizone (KÜBLER, 1968, 1990) as measured in the present work are 0.284-0.435 $\Delta^{\circ}2\Theta$ for IC(002), 0.310-0.427 for ChC(001) and 0.262-0.331 for ChC(002), using <2μm grain-size fraction, sedimented, air-dried mounts with a material amount of ca. $2mgcm^{-1}$ (for details see ÁRKAI, 1991 and ÁRKAI et al. 1995).

The chemical compositions of minerals were determined by a JEOL JCXA-733 electron microprobe at 15 kV and 30 nA, with an electron beam diameter of approximately 5-10 μm. The wave-dispersive spectrometric quantitative analyses were made using the correction methods of BENCE and ALBEE (1968). The standards used for most minerals were orthoclase (Si, Al and K), artificial glass (Fe, Mg and Ca), albite (Na), spessartite (Mn) and rutile (Ti), while those used for garnet were spessartite (Si, Al and Mn), olivine (Mg), hematite (Fe) and Wollastonite (Ca). Relative to the measured values, the standard deviation of the measurements of the given elements or oxides was approximately 2.5%.

The major element chemical analyses were done by a Perkin Elmer 5000 atomic absorption spectrophotometer, using lithium metaborate digestion. Other methods such as gravimetric for SiO_2 and H_2O, permanganometric for FeO and volumetric for CO_2, were also applied.

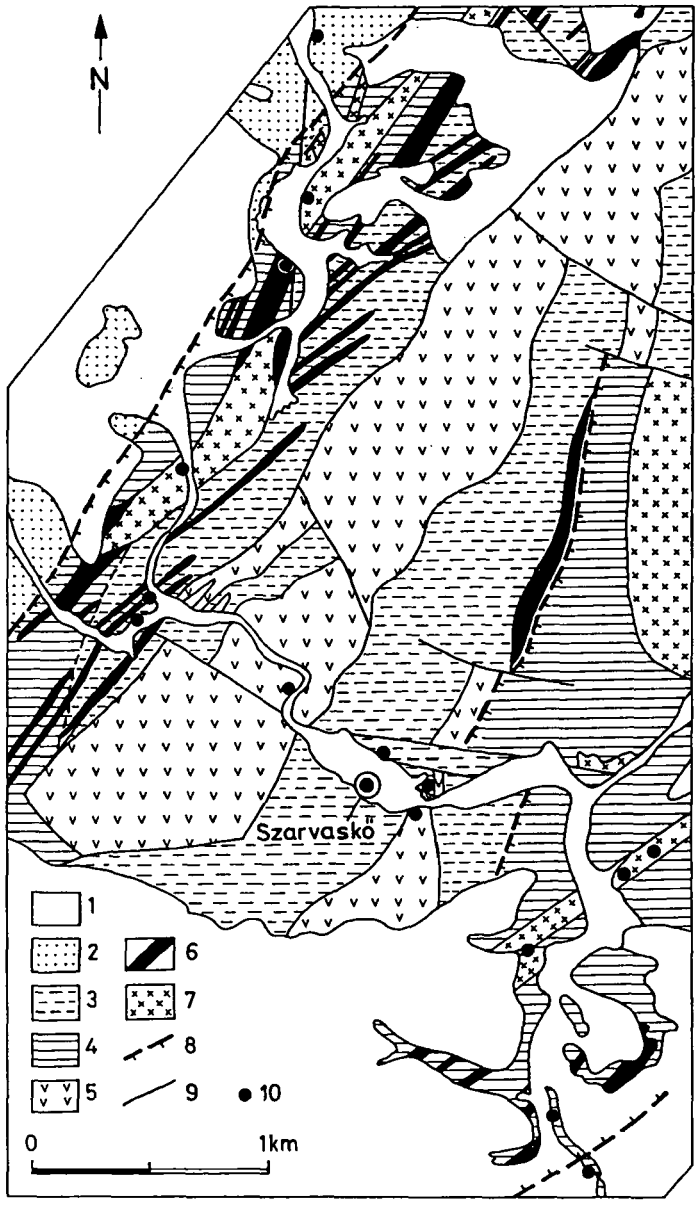

Fig. 3. Geological map of the Jurassic Szarvaskő complex of the Bükk Mountains after BALLA (1982), strongly simplified. Legend: 1=Cenozoic and recent sediments, 2-4=Jurassic sedimentary Fms., 2=Mónosbél Fm.: slate with metachert and sandstone intercalations and limestone olistoliths (Lias-Dogger?), 3=Szarvaskő Fm.: upper, cherty slate (Lias), 4=Szarvaskő Fm.: lower, flysch-like slate (pelitic-silty) with sandstone (Lias), 5-7=igneous rocks, 5=basalt, locally with pillow structure, 6=diabase dykes and sills, 7=cumulate gabbroic intrusives with subordinate ultramafic and acidic differentiates, 8=overthrusting (nappe boundary), 9=fault (within nappe), 10=localities of the investigated sample groups.

PETROGRAPHY

The *clastic rocks* associated with the ophiolite complex are characterized by common development of rough fracture cleavage, pencil cleavage, an expression of incipient slaty cleavage and by rare appearance of crenulation cleavage. In the pelitic matrix of some samples, cryptocrystalline elliptic granules possible representing altered microfossils are commonly found. The clastic rocks are characterized by mineral assemblages containing considerable amounts of quartz, plagioclase, white mica and chlorite besides rare amounts of calcite, pyrite, rutile, hematite, chlorite/smectite mixed-layer mineral, smectite and vermiculite. Illite-muscovite (white mica) and chlorite are the dominant phyllosilicates. The quantities of the others phyllosilicates are subordinate. While mixed-layer chlorite/smectite often occurs, smectite and vermiculite were found only sporadically. Cracks are widespread, mostly filled with quartz, calcite and hematite.

The *pillow lavas* are made essentially of fine-grained crystals of plagioclase and clinopyroxene with few sporadic phenocrysts. In some specimens, the matrix shows a notable variation in texture, being glassy in nature. Plagioclase is the dominant mineral occurring usually as acicular or lath-shaped crystals. It is completely albitized: An <5%. The clinopyroxene is of augitic composition, occurring mostly as fine, unaltered crystals. Besides the fine-grained clinopyroxene, few coarse crystals were also recorded. Sometimes, chlorite with traces of titanite replaced partially the clinopyroxene. Ilmenite, hematite, pyrite and calcopyrite are also present as accessories. Other secondary products such as white mica, pumpellyite, Mg-epidote (epidote with MgO content between 0.2 and 1.2%, see CHO and LIOU 1987), chlorite and rarely chlorite/smectite mixed-layer mineral appear mostly along the fractures cutting across the matrix and the plagioclase crystals, particularly the coarser ones. Veins consist commonly of quartz, albite, calcite, prehnite, pumpellyite, epidote, Mg-epidote and chlorite.

The original porphyritic texture of the fine to medium-grained *metadiabases* is still preserved. The phenocrysts are commonly represented by plagioclase with subordinate clinopyroxene. The groundmass is composed of the same minerals. The plagioclase phenocrysts occur as corroded, fractured crystals. The plagioclase of the groundmass is mostly found as euhedral lath-shaped crystals. The plagioclase is totally recrystallized to albite, showing average anorthite content ranging from 1 to 5%. Traces of pumpellyite are also present as alteration products of plagioclase. The chemistry of clinopyroxene phenocrysts is similar to that of the groundmass clinopyroxene, being represented by augitic composition. Few augite crystals having relatively higher Mg content are enclosed in large, poikilitic plagioclase crystal. The clinopyroxene phenocrysts altered partly or completely to chlorite and actinolite (Plate II/3). Titanite and quartz were occasionally observed in association with chlorite, they may be formed when Ti and Si was released during alteration of clinopyroxene. The clinopyroxene of the groundmass is represented by rounded crystals, that are generally fresh, or rarely, are slightly altered to chlorite. The accessory minerals commonly include apatite, ilmenite, rutile, hematite and zircon. The fissure fillings of these rocks are made of chlorite, quartz, albite, calcite prehnite, pumpellyite and Mg-epidote. Laumontite was found only in one sample. In addition to chlorite, chlorite/smectite mixed-layer mineral was also determined in subordinate quantities in several samples.

The plutonic series comprises mainly *gabbroic rocks* within which nests of leucocratic rocks form a small portion, being regarded as the end products of the crystallization differentiation of the mafic magma. Gabbros exhibit a coarse-grained texture and consist

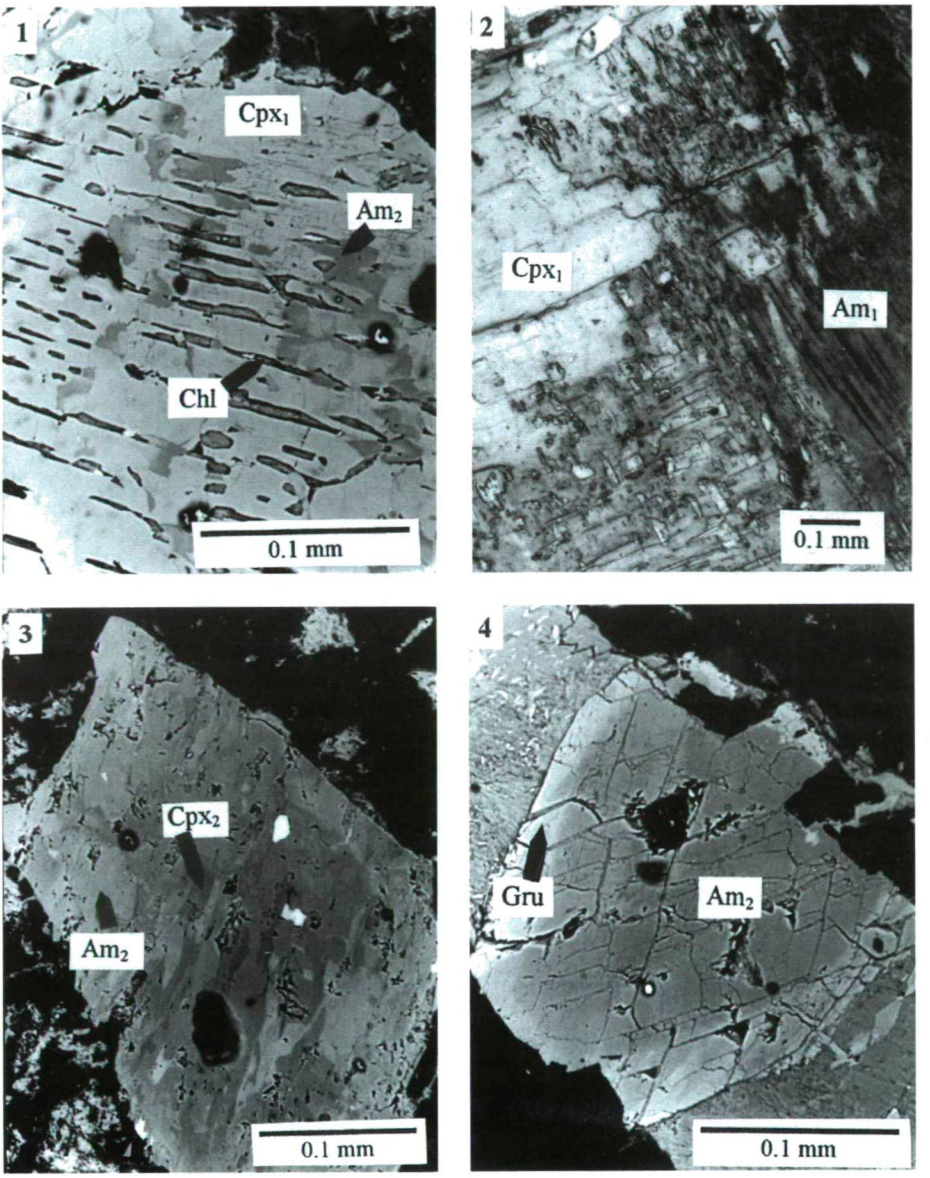

Plate I.

I/1. Alteration stages of clinopyroxene (Cpx_1) from metagabbro, showing patches of green amphibole (Am_2) and chlorite (Chl) along the cleavage planes of Cpx_1. Sample No. DG-6. Back scattered electron (BSE) image.
I/2. Magmatic clinopyroxene (Cpx_1) rimmed by magmatic brown amphibole (Am_1) from the metagabbro sample No. DG-22. Blebs of relic clinopyroxene (Cpx_1) are found in the amphibole rim. Plane polarized light.
I/3. Secondary (metamorphic) clinopyroxene (Cpx_2) forms intergrowths with secondary (metamorphic) amphibole (Am_2) in the metagabbro sample No. DG-27. BSE image.
I/4. Zoned metamorphic amphibole within a chlorite vein with actinolitic hornblende (Am_2) core and grunerite (Gru) rim from the metagabbro sample No. DG-22. BSE image.

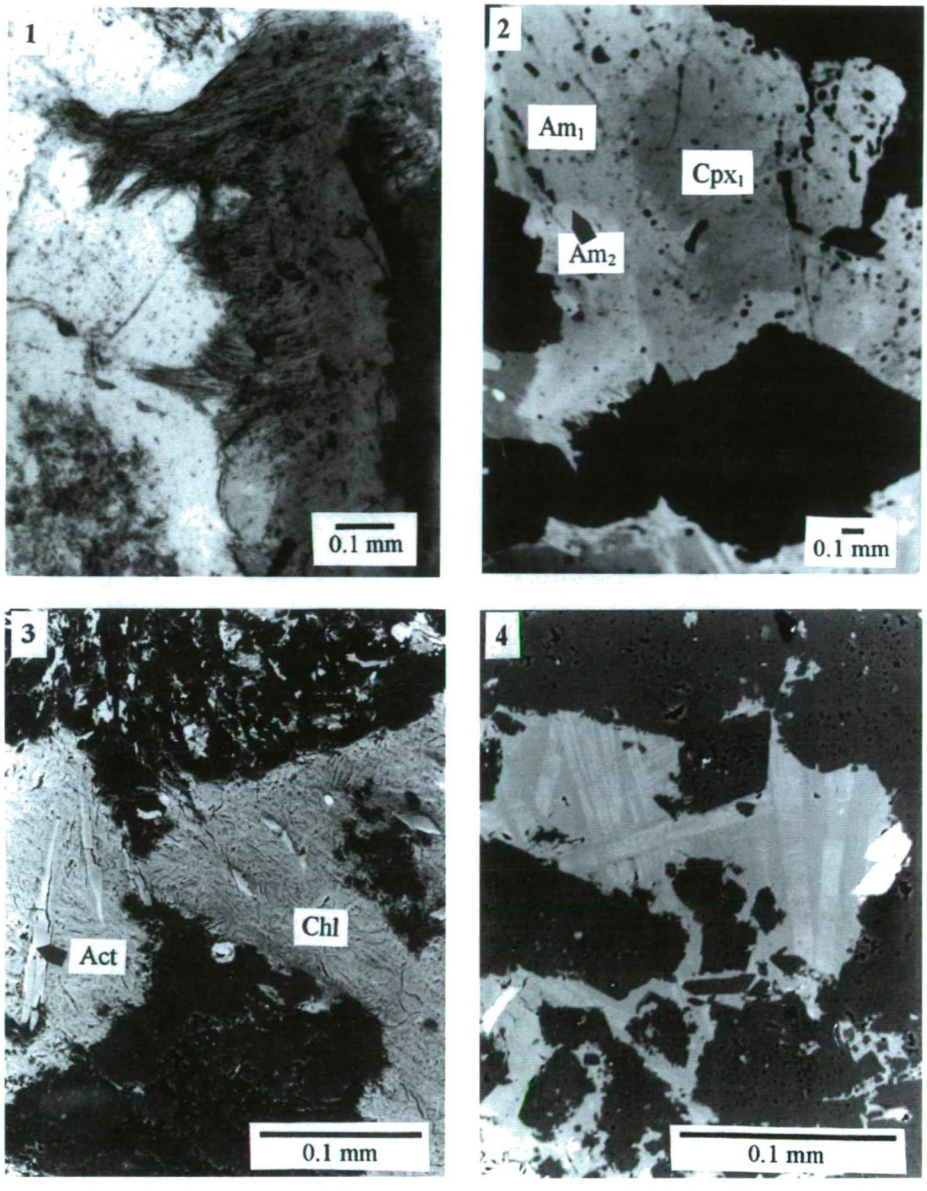

Plate II.

II/1. Fibres of green, metamorphic amphibole in association with chlorite at the edge of a green amphibole grain from the metagabbro sample No. DG-6. Plane polarized light.
II/2. Brown amphibole (Am_1), forming rim around magmatic clinopyroxene (Cpx_1), grades into green amphibole (Am_2) and actinolite and chlorite fibres in metagabbro sample No. DG-6. BSE image
II/3. Clinopyroxene crystals altered to chlorite (Chl) and actinolite (Act) in metadiabase sample No. DG-13. BSE image.
II/4. Exsolution of Fe-rich prehnite in host Fe-poor prehnite in metagranite sample No. DG-5b. BSE image.

principally of plagioclase, clinopyroxene and amphibole. Chlorite pseudomorphs after olivine (but without relics) were scarcely recognized. Plagioclase occurs mostly as euhedral prismatic crystals, being commonly of albitic composition (An_1 to An_6) with traces of oligoclase (An_{19} to An_{29}). The alteration products of plagioclase include pumpellyite, prehnite, Mg-epidote and calcite. Clinopyroxene is the dominant ferromagnesian mineral that frequently occurs as subhedral or anhedral crystals. The clinopyroxene is augite and salite, sometimes showing simple zoning that displays an enrichment in Fe content and depletion in Mg and Ca contents towards the edges. Clinopyroxene was partially or wholly replaced by amphibole and chlorite. In the early stages of alteration, amphibole forms patches in the mineral, while chlorite is found along the cleavage planes of clinopyroxene (Plate I/1). Metamorphic clinopyroxene occurs scarcely as minute grains at the edge of primary clinopyroxene or forms intergrowth with metamorphic amphibole (Plate I/3). This metamorphic clinopyroxene was distinguished by its higher Si and Ca and lower Al, Ti and Na contents from the magmatic one. Such chemical differences between the two generations of clinopyroxenes are consistent with previous observations in other ophiolitic gabbros (MÉVEL 1987, 1988). The brown primary amphiboles formed in the late (hydrous) stage of magmatic crystallization as large crystals or as rims around clinopyroxene. Like other magmatic amphiboles from oceanic gabbros, they usually exhibit hornblende composition and are enriched in Ti, Al and Na, as compared to the metamorphic amphibole. In the brown rimmed amphibole, blebs of relic clinopyroxene were recognized (Plate I/2). The chemical composition of the rimmed brown amphibole is identical with that of the large individual crystals of brown amphibole. Its origin is, therefore, preferably considered as magmatic or high-temperature deuteric as reported by GIRARDEAU and MÉVEL (1982). This brown amphibole is frequently surrounded by green secondary amphibole that sometimes shows fibrous texture and is characterized by hornblende and actinolitic hornblende composition (Plates II/1 and II/2). This structural relationship was commonly described also in other ophiolitic rocks (MÉVEL 1987, 1988; BORTOLOTTI et al. 1990). In rare cases, zoned amphibole with actinolitic hornblende core and grunerite or cummingtonite rim was observed (Plate I/4). The boundary between the two amphiboles is sharp reflecting a miscibility gap between them during their metamorphic crystallization (see SHIDO 1958). Opaque minerals and apatite are the main accessory minerals, while zircon was rarely recorded. The opaque minerals are represented mainly by homogeneous ilmenite or ilmenite-rutile intergrowth. They are usually mantled by intimately mixed fine grains rich in iron and silica. In few samples, titanomagnetite was also recognized.

The fissure fillings of metagabbros contain prehnite, pumpellyite, chlorite, quartz and calcite. The Fe content of the veined prehnite varies widely from 0.012 to 0.726, and sometimes Fe-rich prehnite forms rim around Fe-poor one. Talc and smectite are rarely found, representing metamorphic and weathering products, respectively.

The petrography of *metagranites* is fully described by SADEK GHABRIAL et al. (1994). Generally, they composed mainly of quartz and plagioclase with minor amounts of biotite that is completely altered to chlorite, prehnite, epidote and titanite. K-feldspar could not be distinguished in these rocks like other oceanic plagiogranites (COLEMAN 1977). Plagioclase crystals are totally albitized (An_1-An_7) and sometimes contain prehnite and white mica along their cracks and cleavage planes. On the basis of the proportion of garnet, these rocks were classified into garnet-poor or -free and garnet-rich granites. The garnet was formed produced by local assimilation of the country rocks (BALLA et al., 1983; SADEK GHABRIAL et al. 1994). The metasediment xenoliths are commonly

associated with garnet-rich rocks, and are composed chiefly of plagioclase with average An_{23} and chlorite that seems to be formed after biotite. No preferred orientation could be observed in these xenoliths. The fissure fillings in metagranites consist of fine aggregates of chlorite, calcite, prehnite, quartz, albite and titanite. Prehnite located near to the fractures usually contains an appreciable amount of iron. In few cases, Fe-rich prehnite forms exsolution laths in host Fe-poor prehnite (Plate II/4).

MINERAL CHEMISTRY

Plagioclase

The magmatic plagioclase, presumably with basic-intermediate composition has been extensively altered. Thus, the plagioclase from the studied meta-igneous rocks is represented mainly by albite (Table 1). In metagabbros, oligoclase (An_{19-29}) was rarely observed in association with albite. There are two possible models for explaining the presence of oligoclase, namely: (i) incomplete albitization of plagioclase and (ii) the oligoclase formed during ocean-floor metamorphism (see ISHIZUKA 1985) and persisted as instable phase during the regional (dynamothermal) metamorphism. Significant amounts of K averaging 0.025 per formula unit (cation number on the basis of 8 oxygen) is found in the oligoclase structure, while the K content in the associated albite is very low, averaging only 0.005. Oligoclase was also recorded from the metasedimentary rocks that form enclaves in the metagranites with an average of An_{23}.

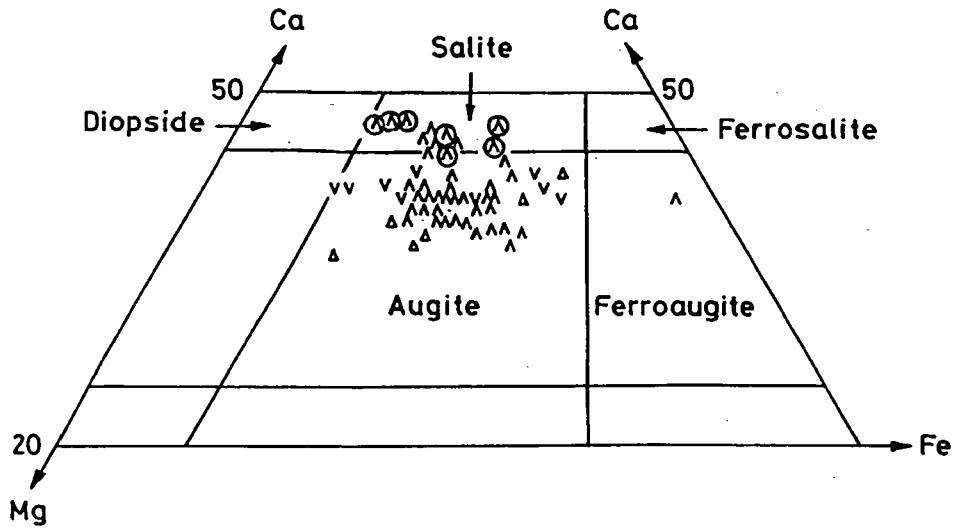

Fig. 4. Compositions of the studied clinopyroxene plotted on the pyroxene quadrilateral. Symbols: ^ = metabasalt; = metadiabase; metagabbro. The symbols of secondary (metamorphic) clinopyroxene are circled.

Clinopyroxene

Most of the analysed clinopyroxenes are augite (*Fig. 4*). Their Mg/Fe ratios depend strongly on the bulk rock chemistry. As to MÉVEL (1987, 1988), the most significant differences between the magmatic and metamorphic clinopyroxenes are related to the abundances of Ti, Al, Si, Ca and Na. The metamorphic clinopyroxene is always richer in

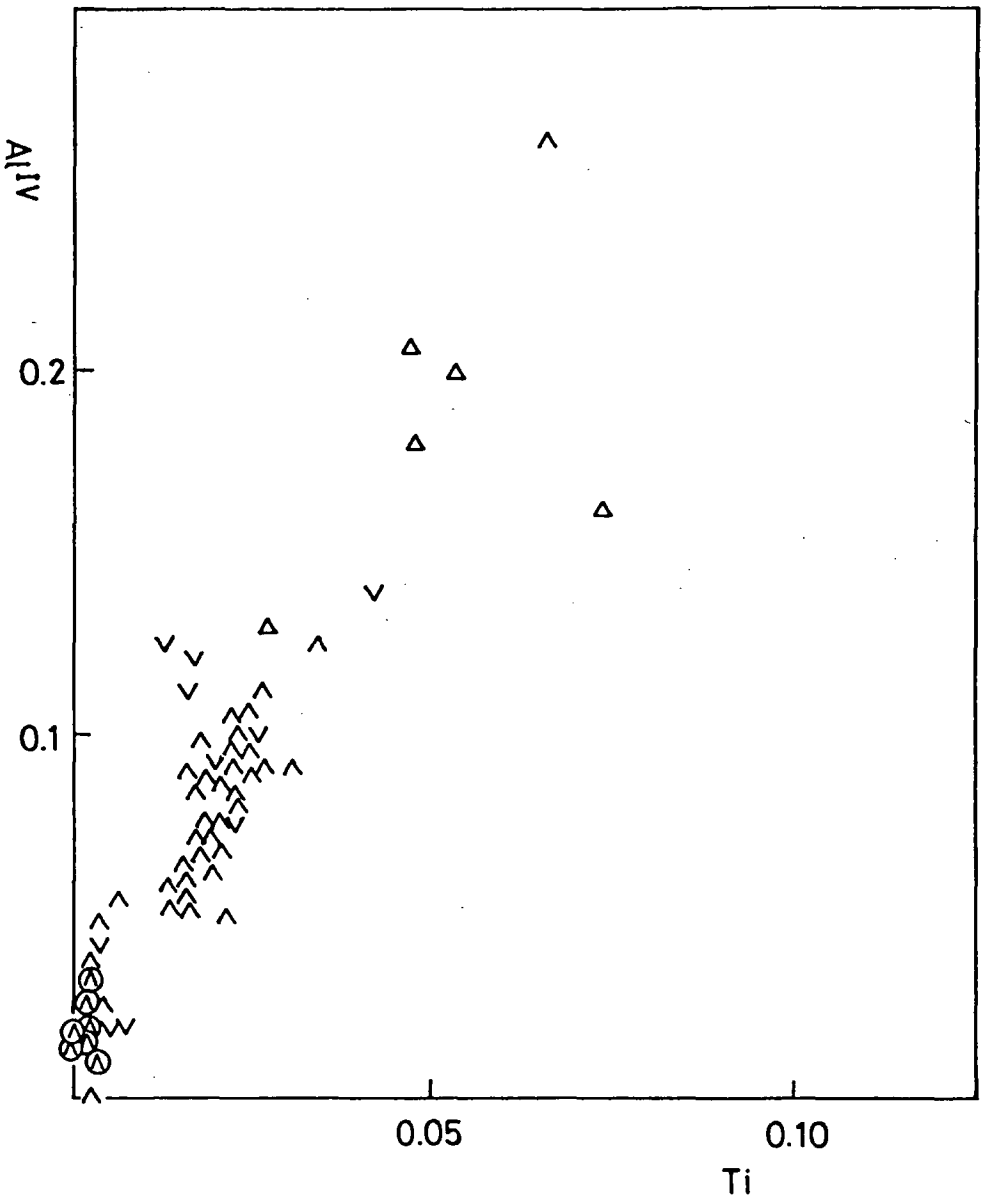

Fig. 5. The plot of Ti against Al^{IV} of clinopyroxene from the Szarvaskő complex. Symbols: = metabasalt; = metadiabase; = metagabbro. The symbols of secondary (metamorphic) clinopyroxene are circled.

Si and Ca, and poorer in Al, Ti and Na than the magmatic one (see also GILLIS 1995). The present data show that the clinopyroxene of metabasalts contains more Al and Ti than that of the intrusive rocks (Table 2). This may be attributed to subsolidus re-equilibration of clinopyroxene during ocean-floor metamorphism which might also cause the appearance

of metamorphic clinopyroxene in metagabbros. The continuous transition between the formation of magmatic and metamorphic clinopyroxenes may be related to the initial high temperature phase of hydrothermal metamorphism which might cause incomplete recrystallization of primary magmatic clinopyroxene resulting in quasy continuous changes in clinopyroxene chemistry (*Fig. 5*). Thus, the continuous transition between primary and secondary clinopyroxenes may be the result of non-equilibrium character of hydrothermal metamorphism that is common in such metamorphic settings. The notable depletion of Al and Ti in some clinopyroxenes from metadiabases and metagabbros seems also to depend on the concentration of iron: the Fe-rich clinopyroxene is always characterized by low values of Al and Ti (DEER et al. 1964).

Amphibole

Magmatic brown amphibole is widespread in metagabbros as large, individual crystals or as rims around clinopyroxene grains. This type of amphibole is of hornblende and tschermakitic hornblende composition (*Fig. 6*), being enriched in Ti, Al and Na and depleted in Si as compared to metamorphic amphiboles (Table 3). Nonetheless, the TiO_2 and K_2O contents of these magmatic amphiboles (reaching maximum of 2.84 and 0.33 weight-%, respectively) are not comparable to those reported by MÉVEL (1988) from oceanic gabbros (4% TiO_2 and 0.6-0.8% K_2O), but they resemble to those given by GIRARDEAU and MÉVEL (1982); EVARTS and SCHIFFMAN (1983).

The metamorphic amphiboles are widespread in metagabbros, forming rims around magmatic amphibole and clinopyroxene. They are almost characterized by actinolitic hornblende and hornblende compositions (*Fig. 6*), and vary in colour from pale brown to green with decreasing Ti content. The pale brown amphibole is a relatively Ti-rich hornblende that is followed by green actinolitic hornblende, reflecting variations of Si, Al^{IV} and Ti with decreasing crystallization temperature of amphiboles. The dark green amphibole relates to the increase in Fe content. In rare cases, sharply zoned amphibole with actinolitic hornblende core and Mg-Fe amphibole (grunerite and cummingtonite) rim was recognized, suggesting a miscibility gap between the two amphiboles during their metamorphic crystallization. In metadiabases, metamorphic amphiboles are uncommonly developed at the expense of magmatic clinopyroxene. The former ones are rather actinolitic in composition, and are plotted in the actinolite field or at the limit between the actinolite and actinolitic hornblende fields *(Fig. 6)*. The Fe/Mg ratios of amphiboles seem to be largely controlled by bulk rock composition.

Chlorite

In FOSTER's (1962) diagram used for classification, the chlorites of the studied rocks fall mostly in the brunsvigite field (Table 4). Not only the Fe/Mg ratios, but also the Al^{IV} contents of chlorite are strongly governed by bulk rock compositions, although the Al^{IV} content of chlorite has been used as an empiric geothermometer by several authors (CATHELINEAU 1988; JOWETT 1991 and others). For example, there is a significant difference in Al^{IV} contents between the chlorites of metagranite and metagabbro (Table 4), although the temperature of metamorphism should have been the same for both rock types. The petrogenetic evaluation of chemistry and structural characteristics of chlorites and their precursor phases from the Szarvaskő complex is outlined by ÁRKAI and SADEK GHABRIAL (1996).

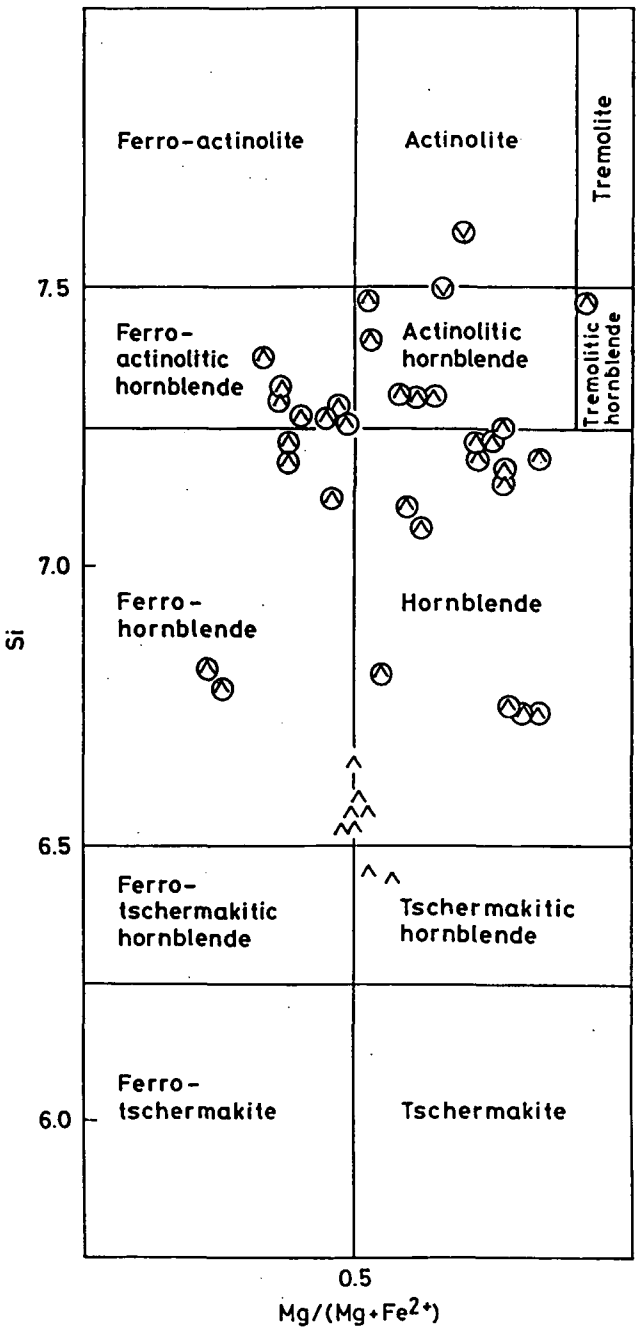

Fig. 6. A plot of Si versus $Mg/(Mg+Fe^{2+})$ of amphiboles from the Szarvaskő complex (after LEAKE 1978). Symbols: = metadiabase; = metagabbro. The symbols of secondary (metamorphic) amphibole are circled.

Epidote

Epidote is widespread in metagranites as replacing magmatic biotite, and as filling vugs, in which it is usually associated with prehnite, chlorite, calcite, albite and quartz. The $X_{Fe}3+$ values (where $X_{Fe}3+ = Fe^{3+}/[Fe^{3+}+Al]$) of both textural types of epidote are apparently identical, ranging from 0.234 to 0.248. Epidote of metabasites mostly shows high Mg contents approaching pumpellyite composition (Table 5). Similar epidotes were named Mg-epidote by CHO and LIOU (1987), who mentioned that this mineral is predominant in somewhat higher grade rocks (transitional zone between the prehnite-pumpellyite and greenschist facies, and greenschist facies) than the Mg-poor epidote, the latter being common in prehnite-pumpellyite facies rocks. In the Szarvaskő ophiolite complex, Mg-epidote was more commonly observed in the prehnite-pumpellyite facies metabasic rocks than in prehnite-actinolite facies metagranites.

In metabasalts, epidote from low variance assemblages contains very low Fe content with $X_{Fe}3+$ values averaging 0.008. The Fe contents of epidote don't show a trend towards lower values with increasing metamorphic grade, as suggested by NYSTRÖM (1983).

Prehnite

Prehnite was observed in all types of the investigated meta-igneous rocks, being more common in the plutonic than in the extrusive ones. It usually occurs as vein fillings (or vugs) in association with other minerals, and as replacing pre-existing minerals such as plagioclase and biotite.

The compositional variation of prehnite in term of $X_{Fe}3+$ (where $X_{Fe}3+ = Fe^{3+}/[Fe^{3+}+Al]$) largely depends on its mode of occurrence (Table 6). The lowest Fe contents, with $X_{Fe}3+$ values averaging 0.025, are found in prehnite formed within plagioclase. Prehnite formed after ferromagnesian silicate minerals is characterized by intermediate $X_{Fe}3+$ values ranging from 0.057 to 0.129. The Fe contents of prehnite found in veins and vugs are highly varying even in two neighbouring prehnite crystals, with $X_{Fe}3+$ values attaining a maximum of 0.358. Prehnites formed at the expense of magmatic minerals constitute high variance assemblages, whereas the veined prehnites constitute variable, sometimes low variance assemblages. The veined prehnite characteristic of high variance assemblages coexisting only with chlorite and quartz ± calcite ± sphene, forms aggregates in which the Fe contents of the individual prehnite crystals strongly vary: the Fe-richer prehnite lies always close to the border. Sometimes, Fe-poor prehnite is rimmed by Fe-rich prehnite, or encloses exsolution laths of Fe-rich prehnite. Further research is needed to explain the possible reasons of these phenomena which may be related to non-equilibrium crystallization of prehnite as well as to temperature dependent chemistry of prehnite, including Fe^{3+} immiscibility at low temperatures. Zoned prehnite with Fe-rich core and Fe-poor rim was also recognized. In contrast, prehnite associated with other Ca-Al silicate minerals + chlorite + quartz from low variance assemblages shows consistently very low $X_{Fe}3+$ values in metabasalts ranging from 0.002 to 0.004, and higher $X_{Fe}3+$ values in metagranites ranging from 0.036 to 0.292.

As a whole, the chemistry of prehnite cannot be assumed as a reliable indicator of metamorphic temperature, confirming the earlier statements of CHO et al. (1986), BEVINS and MERRIMAN (1988). More likely, the chemistry of the fluid phase and the mode of occurrence may control the composition of prehnite.

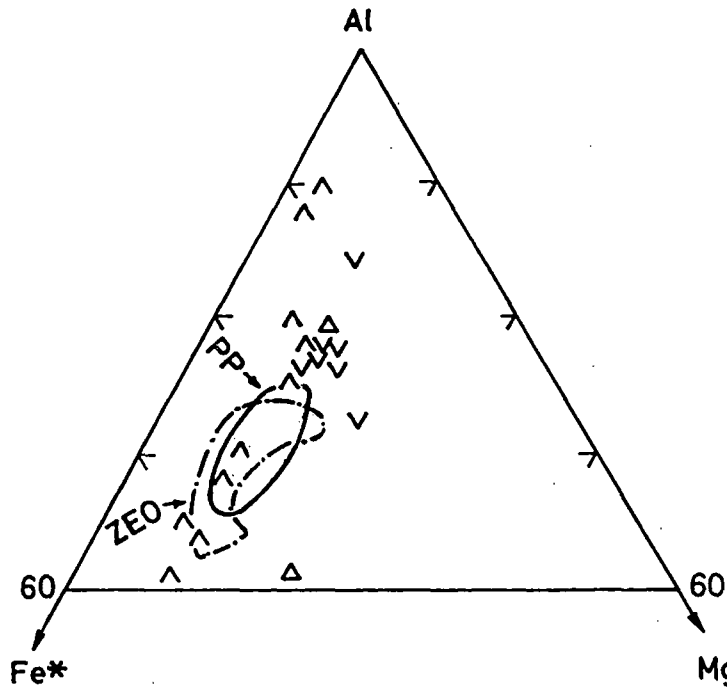

Fig. 7. Al-Fe*-Mg diagram displaying pumpellyite compositions of the studied rocks. Solid and dash-dotted lines border the compositional fields of low-variance pumpellyite from prehnite-pumpellyite and zeolite facies, respectively, given by CHO et al. (1986). Symbols: = metabasalt; = metadiabase; = metagabbro.

Pumpellyite

Pumpellyite has been recorded in all types of metabasic rocks, but is lacking in metagranites. It forms granular aggregates in veins with other minerals, and replaces plagioclase and clinopyroxene in the matrix. Pumpellyite is abundant in high variance assemblages, where it is characterized by extensive Fe-Al substitution (Table 7). Therefore, the pumpellyite should not be used as an indicator of metamorphic grade as regarded by CHO et al. (1986). The $X_{Fe}3+$ values of pumpellyite from low variance assemblages are relatively lower than those from high variance assemblages. Due to the smaller number of data obtained from pumpellyite of low variance assemblages, these $X_{Fe}3+$ values cannot be applied for determining the metamorphic grade. Displaying high Al contents, the analysed low variance pumpellyites from the Szarvaskő area are plotted outside the compositional fields of low variance pumpellyites given by CHO et al. (1986) for zeolite and prehnite-pumpellyite facies (*Fig. 7* and Table 7). It seems to be very likely that compositional variations in pumpellyite are governed mostly by the extent of host rock alteration (see also NYSTRÖM 1983) and by the effective fluid chemistry, while the bulk composition shows little control on pumpellyite chemistry.

The average $X_{Fe}3+$ values of coexisting prehnite, pumpellyite and epidote are 0.003, 0.137 and 0.008, respectively. These values contrast with the results of CHO et al. (1986), who found that the $X_{Fe}3+$ values most probably increase in order of prehnite, through pumpellyite to epidote.

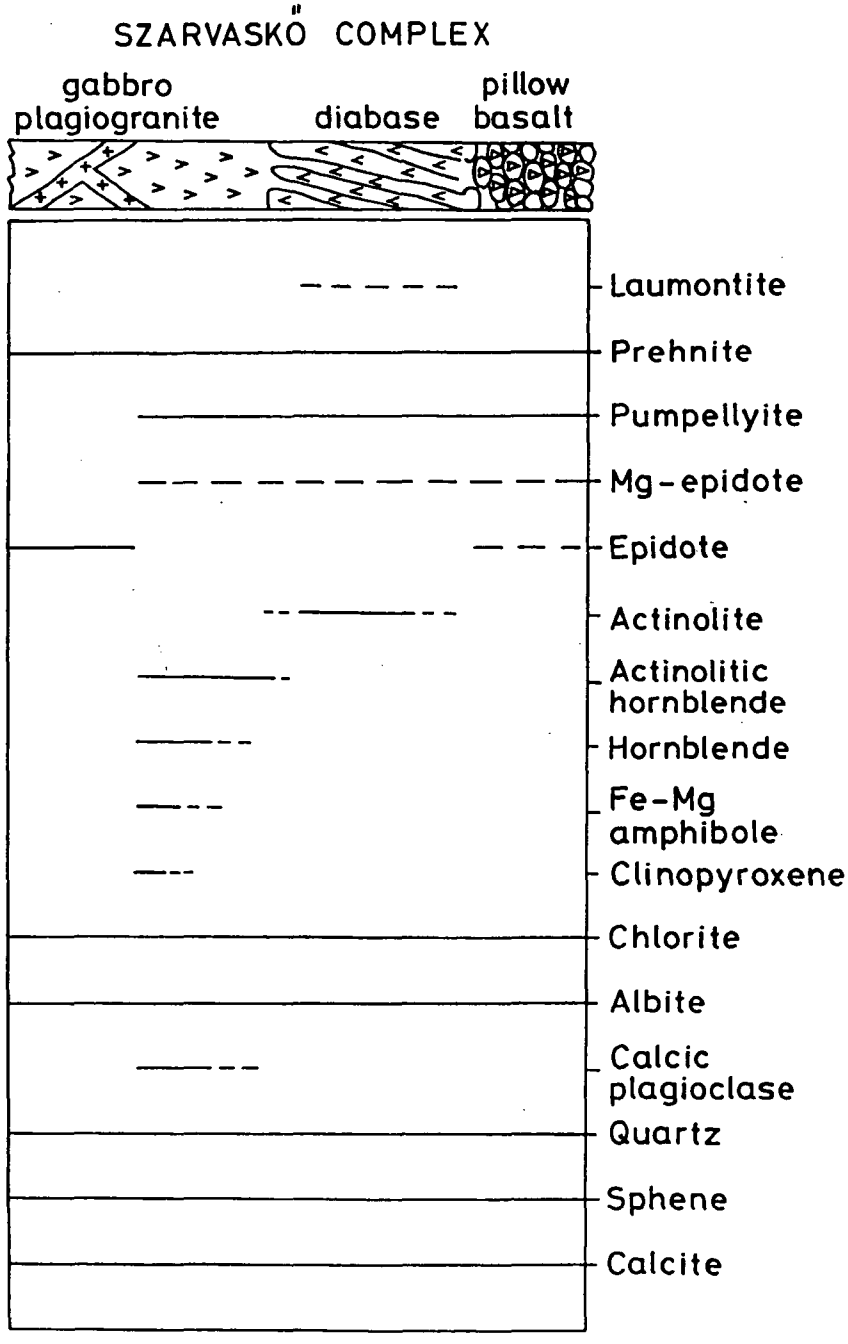

Fig. 8. Distribution of metamorphic minerals in the simplified vertical profile of the Szarvaskő ophiolite complex.

Other minerals

Laumontite is the only zeolite mineral that occurs only in one metadiabase sample. Its composition is generally homogeneous, having an ideal formula. Laumontite might form at lower temperatures than the other metamorphic minerals, perhaps in a late stage of cooling (uplift). Garnets from garnet-rich and garnet-poor metagranites are characterized by similar composition, being almandine-rich (Alm_{75-76}, Pyr_{7-11}, $Spess_{9-14}$, $Gross_{4-5}$). The chemistry of garnet has been fully described and interpreted by SADEK GHABRIAL et al. (1994).

METAMORPHISM

The ophiolitic rocks of the Szarvaskő complex display significant change in their mineral parageneses, reflecting the effects of different metamorphic events, including also local metasomatic processes. The combined effect and superposition of these different metamorphic processes which may be attributed to ocean-floor hydrothermal, burial and regional metamorphic events, are likely to produce various secondary minerals, almost showing a wide variation in their composition. Therefore, the evolution path of these rocks is rather difficult to reconstruct.

Hydrothermal (ocean-floor) metamorphism

Hydrothermal metamorphism occurring at the oceanic ridge axes, has been commonly resulted in formation of disequilibrium mineral assemblages, while the original igneous fabrics have been preserved. The distribution of secondary minerals in the Szarvaskő complex is depicted in *Fig. 8.* In metagabbros, albite and traces of oligoclase coexist replacing the more calcic, magmatic plagioclase. Magmatic clinopyroxene and brown amphibole have been uralitized producing heterogeneous crystals of green amphibole that are frequently zoned from hornblende to actinolitic hornblende showing decrease in their Al^{IV} and Ti contents towards the rims. This compositional trend can be related to the decrease of temperature during the crystallization of amphiboles. In rare cases, clinopyroxene has probably also recrystallized, forming minute grains of metamorphic clinopyroxene. In addition, Fe-Mg amphibole also appears as rims around metamorphic green amphibole grains. Thus, metagabbros show crystallization in amphibolite and greenschist/amphibolite transitional facies (700-400°C; see also LIOU et al. 1974 and MOODY et al. 1983), displaying a gradual cooling from upper amphibolite facies condition that is responsible for the development of secondary clinopyroxene, hornblende to actinolitic hornblende, Fe-Mg amphibole and calcic plagioclase, to lower amphibolite or greenschist/amphibolite transitional facies that is characterized by actinolitic hornblende + oligoclase + albite ± sphene ± chlorite assemblage. The gradual cooling of gabbro and the reacting fluid phase might be a consequence of changing tectonic position, namely, the spreading away from the ridge axis.

Most of the primary minerals of metagranites have also been altered. The plagioclase is of albitic composition. Other main constituents are chlorite, epidote, prehnite and titanite representing pseudomorphs after pre-existing biotite. The metagranites are characterized by albite + chlorite + prehnite + epidote + titanite assemblage. As suggested by EVARTS and SCHIFFMAN (1983), the presence of epidote-bearing and actinolite-free assemblage indicates greenschist facies metamorphism and is characteristic of low pressure conditions, while prehnite is paragentically late. Moreover, this assemblage may

also be equivalent to the low pressure prehnite-actinolite facies of LIOU et al. (1985,1987), forming between ca. 200 and 350°C.

The secondary minerals of metadiabases include albite, chlorite and amphibole that belongs to the actinolitic group. The two latter minerals were formed after primary clinopyroxene, indicating that the metadiabases were subjected to greenschist facies metamorphism (<400°C; LIOU et al. 1974 and MOODY et al. 1983).

No evidence is available on the eventual ocean-floor hydrothermal metamorphism of the pillow basalt. The basaltic layers might have been partially recrystallized into either zeolite or prehnite-pumpellyite facies associations during hydrothermal alteration as have been recorded from other ophiolitic pillow lavas (COLEMAN 1977; ÁRKAI 1983; DI GIROLAMO et al. 1992). The younger regional (dynamothermal) metamorphic event, corresponding to prehnite-pumpellyite facies, should has overprinted and obliterated the lower temperature associations formed eventually during the ocean-floor alteration.

Regional (dynamothermal) metamorphism

As it was demonstrated in the previous part, there are considerable uncertainties in the genetic interpretation of low-temperature mineral assemblages. These assemblages may be attributed to (i) the late, cooling stages of hydrothermal metamorphism; (ii) the somewhat younger, Cretaceous regional (dynamothermal) metamorphism as proved earlier by ÁRKAI (1983); or (iii) the combined, superimposed effects of the formers two events, both producing mainly prehnite-pumpellyite facies assemblages.

Out of these, the explanation (iii) seems to be the most probable, because it is not possible to distinguish between the alteration products of both metamorphic processes indicated by (i) and (ii), and the compositions of secondary minerals are not homogeneous, referring to non-equilibrium conditions.

During the Alpine regional metamorphic event, the adjoining sedimentary rocks of the Szarvaskő complex suffered late diagenetic – low-temperature anchizonal orogenic transformations, the estimated temperature of which agrees fairly well with that of the prehnite-pumpellyite facies determined in the metadiabase and metagabbro varieties (ÁRKAI 1983).

The secondary mineral assemblages of the metasedimentary rocks (quartz + albite + white mica + chlorite + calcite ± smectite ± vermiculite ± chlorite/smectite mixed-layer mineral ± pyrite ± rutile ± hematite) are not diagnostic for determining exactly the metamorphic grade. The averages of IC(002), ChC(001) and ChC(002) of the <2μm grain-size fraction samples of the metaclastic rocks are 0.388, 0.452 and 0.398, respectively, using a goniometer speed of 2°/min (Table 8). The IC(002) average indicates anchizonal conditions. Based on the relatively high chlorite crystallinity values, these rocks fall in the diagenetic range, using the chlorite crystallinity boundaries of the anchizone proposed by ÁRKAI (1991). This may be due to the broadening of the 7Å and 14Å chlorite peaks in the presence of other minerals having similar spacing such as vermiculite, smectite and chlorite/smectite mixed-layers. As a whole, most of metamorphic indicators show that the sedimentary environment of Szarvaskő complex underwent transitional late diagenetic- – low-temperature anchizonal regional transformations.

The matabasic rocks of the Szarvaskő complex exhibit prehnite-pumpellyite facies assemblages which include quartz, chlorite, prehnite, pumpellyite, epidote and calcite. Excluding pumpellyite, similar assemblages were found in the metagranites (SADEK GHABRIAL et al. 1994). The lack of pumpellyite in metagranites can be properly explained by inappropriate bulk composition. Actinolitic amphibole was also recorded from the

metadiabases, and its origin relates to ocean-floor (hydrothermal) metamorphism (see the preceding part). The refined petrogenetic grid of FREY et al. (1991) showed that the bulk rock composition plays an important role in determining the mineral assemblages in metabasites transitional between sub-greenschist and greenschist facies, because the P-T fields of the four sub-greenschist facies (i.e. ZEO, PrP, PrA and PA) partially to completely overlap. This might explain the juxtaposition of assemblages having different low-grade metamorphic facies and being developed at the same P-T conditions. Two spatially related assemblages (Prh-Pmp-Ep-Chl-Qtz and Prh-Act-Ep-Chl-Qtz) were recognized by POWELL et al. (1993) in a hyaloclastic metabasalt sample, whereas the compositions of both epidote and prehnite are considerably different reflecting the presence of two distinct univariant assemblages rather than one invariant assemblage. BEVINS and ROBINSON (1993) described prehnite-pumpellyite and prehnite-actinolite facies assemblages in metabasites associated with epizonal pelites. Prehnite-pumpellyite facies assemblages occur in metabasites with $MgO/(MgO+FeO)_{chlorite}$ ratios of <0.54, while prehnite-actinolite facies assemblages are present in metabasites with $MgO/(MgO+FeO)_{chlorite}$ ratios of >0.54. These authors also recognized actinolite-bearing prehnite-pumpellyite facies assemblage in metabasites with $MgO/(MgO+FeO)_{chlorite}$ ratio of 0.50 in epizonal circumstances. On the other hand, metabasites with the prehnite-pumpellyite facies assemblages were found in association with diagenetic and anchizonal pelites. In these metabasites, the range of $MgO/(MgO+FeO)_{chlorite}$ ratios is rather broad (0.31-0.65). The analysed chlorite from the Szarvaskő metadiabases, which are associated with diagenetic – low-temperature anchizonal pelitic rocks, has relatively low MgO/(MgO+FeO) ratios ranging from 0.29 to 0.51. Therefore, the actinolite is considered to be of hydrothermal (ocean-floor) metamorphic origin. The IC(002) averages of the <2μm fraction samples measured at 2°/min goniometer speed are 0.369 Δ°2θ for the metagranites and 0.282 Δ°2θ for the metagabbros, indicating anchizonal alterations for both rock types. These conditions based on illite crystallinity data may be considered as roughly equivalent to those of the prehnite-pumpellyite facies. Based on the chlorite crystallinity boundaries of the anchizone given by ÁRKAI (1991) for metasediments, the metagranites show high temperature anchizonal metamorphism, while the metabasic rocks fall mostly in the diagenetic range or near to the diagenesis/anchizone boundary that corresponds to transitional conditions between zeolite and prehnite-pumpellyite facies. The larger chlorite crystallinity values of the metabasic rocks can be explained by the presence of interstratified smectitic and/or vermiculitic components in chlorite. As also given in Table 7, the chlorite crystallinity averages decrease downwards in the ophiolite-like pile from the pillow lava through the diabase down to the cumulate gabbro. This trend may be interpreted as a remnant of the late, cooling stage of ocean-floor metamorphism characterized by steep thermal gradient. In this case, the younger orogenic (dynamothermal) event could not totally obliterate these differences. Furthermore, the differences between the chlorite crystallinity values obtained from metagranites and from metabasic rocks relate most probably to the effects of bulk chemistries on chlorite chemistry (ÁRKAI and SADEK GHABRIAL 1996). The temperatures (metabasalt: 236°C; metadiabase: 224-252°C; metagabbro: 230-280°C; metagranite: 276-350°C) estimated by the chlorite-Al^{IV} geothermometer of CATHELINEAU (1988) support this difference between metagranites and metabasic rocks.

TABLE I

Averages of chemical compositions (weight-%) and cation numbers of plagioclase

Rock type	metabasalt	metadiabase		metagabbro			metagranite					enclave metasediment
Sample No.	DG-33	DG-13	DG-16	DG-2a	DG-21b	DG-22	DG-1	DG-5b	DG-5d	DG-34b	DG-34d	DG-34e
n	1	4	4	3	4	6	4	4	4	4	4	3
SiO_2	66.66	68.12	67.03	63.09	66.71	67.76	67.61	67.21	69.16	66.66	68.23	62.31
Al_2O_3	19.59	20.48	20.28	22.56	20.52	19.89	20.46	20.25	19.16	20.57	20.10	24.05
CaO	1.02	0.17	0.92	4.57	0.64	0.83	0.60	0.32	0.15	1.10	0.11	4.77
Na_2O	10.95	11.99	10.70	8.51	11.81	11.04	11.38	11.03	11.33	10.58	12.20	8.79
K_2O	0.08	0.04	0.04	0.43	0.07	0.11	0.11	0.56	0.09	0.23	0.06	0.16
Total	98.30	100.80	98.97	99.16	99.75	99.63	99.68	99.36	100.15	99.13	100.70	100.08
					number of the cations on the basis of 8 (O)							
Si	2.959	2.954	2.954	2.810	2.928	2.967	2.948	2.959	3.008	2.196	2.965	2.753
Al	1.025	1.047	1.054	1.186	1.062	1.026	1.05	1.051	0.996	1.069	1.029	1.257
Ca	0.049	0.008	0.043	0.219	0.030	0.039	0.029	0.015	0.007	0.052	0.005	0.226
Na	0.943	1.008	0.914	0.675	1.005	0.937	0.962	0.942	0.956	0.905	1.028	0.752
K	0.005	0.002	0.002	0.025	0.004	0.006	0.006	0.031	0.005	0.013	0.003	0.009
Total	4.981	5.019	4.967	4.915	5.029	4.975	4.996	4.999	4.971	4.939	5.031	4.992
An%	5	1	5	24	3	4	3	2	1	5	1	23

n = number of analyses

TABLE 2

Averages of chemical compositions (weight-%) and cation numbers of clinopyroxene

Rock type	metabasalt	metadiabase		metagabbro							
Sample No.	DG-33	DG-13	DG-16	DG-6	DG-21b	DG-22		DG-27		DG-37c	DG-34dd
n	5	2	8	4	7	6	1**	6	6**	9	7
SiO_2	48.32	51.52	50.51	50.85	50.65	51.16	53.03	50.85	52.66	50.76	49.97
TiO_2	1.80	0.53	0.62	0.70	0.71	0.56	0.00	0.75	0.04	0.50	0.93
Al_2O_3	4.13	3.69	1.97	2.74	2.05	1.38	0.31	1.72	0.45	1.70	3.07
*FeO	11.28	6.33	11.88	9.99	13.62	11.96	10.65	11.67	9.33	11.58	10.11
MnO	0.25	0.17	0.26	0.30	0.42	0.55	0.35	0.36	0.36	0.39	0.38
MgO	14.92	17.33	13.33	14.33	13.41	11.64	13.55	14.32	13.71	14.18	13.38
CaO	18.59	20.90	20.34	19.92	19.35	19.85	22.88	19.50	23.27	19.81	21.38
Na_2O	0.29	0.26	0.30	0.38	0.24	0.30	0.07	0.31	0.14	0.34	0.34
K_2O	0.01	0.00	0.00	0.03	0.00	0.00	0.00	0.02	0.00	0.02	0.02
Total	99.59	100.64	99.21	99.23	100.45	100.39	100.85	99.51	99.96	99.28	98.61
number of the cations on the basis of 6 (O)											
Si	1.826	1.882	1.924	1.915	1.915	1.949	1.981	1.925	1.977	1.928	1.890
Al^{IV}	0.171	0.118	0.076	0.085	0.085	0.050	0.014	0.075	0.020	0.070	0.110
Al^{VI}	0.013	0.041	0.013	0.037	0.007	0.012	0.000	0.002	0.000	0.006	0.026
Ti	0.051	0.015	0.018	0.020	0.020	0.016	0.000	0.021	0.001	0.014	0.026
$*Fe^{2+}$	0.358	0.193	0.380	0.315	0.431	0.478	0.333	0.370	0.294	0.368	0.320
Mn	0.008	0.006	0.008	0.010	0.013	0.018	0.011	0.012	0.012	0.013	0.012
Mg	0.838	0.944	0.755	0.805	0.755	0.660	0.755	0.808	0.767	0.803	0.753
Ca	0.754	0.819	0.830	0.804	0.784	0.811	0.916	0.791	0.937	0.807	0.866
Na	0.021	0.018	0.022	0.027	0.018	0.022	0.005	0.023	0.010	0.025	0.025
K	0.001	0.000	0.000	0.002	0.000	0.000	0.000	0.001	0.000	0.001	0.001
Total	4.042	4.036	4.026	4.019	4.029	4.015	4.015	4.029	4.018	4.035	4.030
Ca%	38.5	41.8	42.0	41.6	39.5	41.2	45.4	39.9	46.6	40.6	44.4
Fe+Mn%	18.7	10.2	19.7	16.8	22.4	25.2	17.1	19.3	15.2	19.1	17.0
Mg%	42.8	48.0	38.3	41.6	38.1	33.6	37.5	40.8	38.2	40.3	38.6

* Total iron calculated as FeO and Fe^{2+}
** secondary clinopyroxene
n = number of analyses

TABLE 3

Averages of chemical compositions (weight-%) and cation numbers of amphibole. The calculations of cation numbers follow the scheme of ROBINSON et al. (1982)

Rock type		metadiabase	metagabbro						
Sample No.		DG-13	DG-2a		DG-6		DG-22	DG-27		DG-37c
n		2**	4***	1**	7***	4**	9**	3***	3**	8**
SiO_2		52.28	43.25	48.07	43.61	49.02	48.27	46.77	49.63	49.48
TiO_2		0.16	2.75	0.61	1.85	1.52	0.74	1.62	0.72	0.54
Al_2O_3		1.73	9.26	5.72	8.82	4.37	3.01	8.19	4.26	2.48
*FeO		19.66	20.12	21.03	21.54	19.80	27.14	11.87	17.12	22.74
MnO		0.22	0.30	0.43	0.29	0.26	0.36	0.17	0.32	0.39
MgO		12.78	8.40	10.13	7.83	10.47	7.42	15.05	13.07	10.98
CaO		11.22	10.10	9.97	10.67	11.12	8.98	11.70	11.28	8.60
Na_2O		0.20	2.32	1.04	1.94	0.91	1.49	1.67	1.19	1.59
K_2O		0.06	0.29	0.22	0.36	0.20	0.36	0.17	0.17	0.27
Total		98.31	96.79	97.22	96.91	96.67	97.77	97.21	97.76	97.07
number of the cations on the basis of 23 (O)										
Si		7.543	6.551	7.075	6.647	7.326	7.259	6.745	7.229	7.267
Al	T	0.294	1.449	0.925	1.353	0.642	0.534	1.255	0.731	0.429
Fe^{3+}		0.163	–	–	–	0.032	0.207	–	0.040	0.304
Al		–	0.205	0.067	0.230	0.135	–	0.137	–	–
Ti		0.017	0.313	0.068	0.210	0.058	0.084	0.175	0.078	0.060
Fe^{3+}	M_1	0.888	0.604	1.238	0.575	0.557	1.173	0.654	0.719	1.402
Mg	M_3	2.747	1.896	2.223	1.770	2.303	1.663	3.235	2.838	2.405
Fe^{2+}		1.321	1.946	1.350	2.178	1.913	2.033	0.778	1.326	1.087
Mn		0.027	0.037	0.054	0.037	0.034	0.046	0.020	0.039	0.046
Fe^{2+}		–	–	–	–	–	–	–	–	–
Mn	M_4	–	0.001	–	–	–	0.001	–	–	–
Ca		1.735	1.639	1.573	1.743	1.782	1.448	1.808	1.764	1.355
Na		0.056	0.361	0.297	0.257	0.208	0.401	0.192	0.211	0.433
Na	A	–	0.320	–	0.313	0.056	0.032	0.255	0.124	0.018
K		0.010	0.057	0.041	0.071	0.038	0.070	0.031	0.032	0.051
Total		14.801	15.37	14.911	15.384	15.084	14.951	15.285	15.131	14.857
Al		0.294	1.653	0.992	1.582	0.777	0.534	1.392	0.731	0.429
Na		0.056	0.681	0.297	0.570	0.264	0.434	0.466	0.335	0.452
A		0.010	0.377	0.041	0.384	0.094	0.102	0.285	0.156	0.069
$(Al+Fe^{3+})^{IV}$		0.458	1.449	0.925	1.353	0.674	0.741	1.255	0.771	0.733

* total iron calculated as FeO
** green amphibole
*** brown amphibole
n = number of analyses

TABLE 4

Averages of chemical compositions (weight-%) and cation numbers of chlorite

Rock type	metabasalt	metadiabase			metagabbro				metagranite					enclave metased.
Sample	DG-33	DG-13	DG-16	DG-6	DG-21b	DG-22	DG-37c	DG-34dd	DG-1	DG-5b	DG-5d	DG-34b	DG-34d	DG-34e
n	5	10	5	4	8	8	7	7	9	7	4	4	4	2
SiO_2	28.18	29.28	28.82	26.78	26.96	27.27	27.11	27.37	27.21	24.45	26.33	26.20	25.69	26.94
TiO_2	0.00	0.08	0.06	0.07	0.11	0.56	0.67	1.02	1.54	0.27	1.02	0.95	0.49	1.59
Al_2O_3	16.35	18.19	15.67	17.45	15.35	14.60	14.05	16.79	17.64	19.83	17.60	17.91	18.79	17.89
*FeO	30.95	25.88	27.75	27.80	39.04	37.34	37.42	29.09	31.54	36.18	31.51	36.06	34.94	33.13
MnO	0.40	0.39	0.39	0.22	0.30	0.34	0.42	0.36	0.69	0.38	0.55	0.50	0.42	0.49
MgO	10.73	14.74	13.42	12.63	6.41	6.88	7.47	11.20	8.94	7.02	8.56	6.73	6.72	6.48
CaO	0.67	0.65	0.56	0.70	0.49	0.40	0.52	1.01	0.75	0.24	0.67	0.52	0.94	0.72
Na_2O	0.03	0.02	0.02	0.06	0.02	0.02	0.02	0.01	0.04	0.03	0.04	0.05	0.05	0.04
K_2O	0.02	0.01	0.02	0.03	0.03	0.04	0.04	0.08	0.16	0.04	0.12	0.14	0.07	0.88
Total	87.33	89.24	86.71	85.75	88.71	87.45	87.72	86.94	88.52	88.45	86.41	89.05	88.11	88.16
number of the cations on the basis of 28 (O)														
Si	6.153	6.051	6.227	5.874	6.075	6.186	6.149	5.964	5.898	5.445	5.864	5.786	5.704	5.938
Al^{IV}	1.847	1.949	1.773	2.126	1.925	1.814	1.851	2.036	2.102	2.555	2.136	2.2148	2.296	2.062
Al^{VI}	2.358	2.481	2.218	2.391	2.151	2.090	1.905	2.280	2.406	2.651	2.481	2.448	2.626	2.586
Ti	0.000	0.013	0.009	0.012	0.019	0.095	0.113	0.167	0.251	0.046	0.171	0.156	0.082	0.264
$*Fe^{2+}$	5.654	4.484	5.014	5.104	7.365	7.082	7.100	5.312	5.722	6.740	5.869	6.667	6.498	6.106
Mn	0.075	0.068	0.072	0.041	0.058	0.066	0.080	0.067	0.127	0.073	0.103	0.094	0.080	0.090
Mg	3.491	4.528	4.321	4.127	2.149	2.325	2.525	3.633	2.887	2.330	2.844	2.211	2.226	2.129
Ca	0.158	0.144	0.130	0.164	0.118	0.098	0.127	0.235	0.137	0.056	0.161	0.121	0.221	0.170
Na	0.012	0.008	0.009	0.026	0.009	0.010	0.009	0.006	0.018	0.014	0.019	0.021	0.023	0.018
K	0.007	0.003	0.001	0.009	0.008	0.013	0.011	0.023	0.045	0.011	0.035	0.040	0.021	0.247
Total	19.755	19.729	19.774	19.873	19.877	19.779	19.870	19.724	19.621	19.920	19.684	19.758	19.776	19.608

* Total iron calculated as FeO and Fe^{2+} n = number of analyses

TABLE 5

Averages of chemical compositions (weight-%) and cation numbers of epidote

Rock type	metabasalt		metadiabase	metagabbro	metagranite		
Sample No.	DG-33	DG-33**	DG-13**	DG-37c**	DG-1	DG-34b	DG-34d
n	2	10	2	1	2	2	2
SiO_2	37.59	36.58	38.13	37.38	37.41	38.36	38.14
TiO_2	0.00	0.00	0.01	0.00	0.21	0.30	0.92
Al_2O_3	28.74	22.57	27.34	26.46	24.50	24.58	23.89
$*Fe_2O_3$	0.33	9.58	5.44	3.29	11.72	12.19	12.15
MnO	0.33	0.12	0.24	0.03	0.10	0.31	0.22
MgO	0.00	0.63	0.76	0.73	0.05	0.03	0.10
CaO	24.12	22.65	21.89	23.28	23.31	23.47	23.09
Na_2O	0.05	0.13	0.02	0.04	0.04	0.06	0.01
K_2O	0.01	0.00	0.00	0.00	0.00	0.03	0.00
Total	91.17	92.26	93.83	91.21	97.34	99.33	98.52
	number of the cations on the basis of 25 (O)						
Si	6.160	6.123	6.129	6.157	5.962	5.997	6.008
Al^{IV}	–	–	–	–	0.038	0.016	0.012
ΣZ	6.160	6.123	6.129	6.157	6.000	6.013	6.020
Al^{VI}	5.551	4.443	5.180	5.137	4.564	4.513	4.425
$*Fe^{3+}$	0.041	1.219	0.658	0.453	1.408	1.436	1.442
Ti	0.000	0.000	0.001	0.000	0.025	0.035	0.109
ΣY	5.592	5.662	5.839	5.590	5.997	5.984	5.976
Mn	0.046	0.017	0.033	0.004	0.013	0.041	0.029
Mg	0.000	0.157	0.181	0.179	0.012	0.007	0.022
Ca	4.238	4.067	3.769	4.110	3.982	3.933	3.899
Na	0.016	0.040	0.005	0.013	0.012	0.017	0.002
K	0.001	0.001	0.000	0.000	0.000	0.006	0.000
ΣW	4.301	4.282	3.988	4.306	4.019	4.004	3.952
$X_{Fe^{3+}}$	0.007	0.215	0.113	0.081	0.236	0.241	0.246

* total iron calculated as Fe_2O_3 and Fe^{3+}

** Mg-epidote

n = number of analyses

TABLE 6

Averages of chemical compositions (weight-%) and cation numbers of prehnite

Rock type	metabasalt		metagabbro			metagranite				
Sample	DG-33	DG-2a	DG-21b	DG-22	DG-34dd	DG-1	DG-5b	DG-5d	DG-34b	DG-34d
n	3	4	6	11	4	4	8	4	3	7
SiO_2	42.47	44.50	43.33	43.86	42.54	43.91	43.08	43.47	44.49	42.91
TiO_2	0.00	0.02	0.08	0.06	0.03	0.05	0.05	0.07	0.02	0.02
Al_2O_3	23.46	22.83	22.11	21.13	22.94	23.39	22.68	24.15	23.64	22.33
$*Fe_2O_3$	0.06	0.38	3.42	3.01	2.37	0.94	2.58	0.51	0.25	2.08
MnO	0.03	0.04	0.01	0.06	0.03	0.03	0.01	0.02	0.02	0.03
MgO	0.01	0.01	0.04	0.29	0.13	0.04	0.01	0.01	0.00	0.01
CaO	26.89	26.44	26.62	26.14	26.73	26.97	27.36	27.61	26.85	27.14
Na_2O	0.05	0.11	0.00	0.02	0.06	0.13	0.04	0.04	0.35	0.05
K_2O	0.04	0.04	0.03	0.04	0.02	0.02	0.01	0.01	0.04	0.02
Total	93.01	94.37	95.64	94.61	94.85	95.49	95.82	95.89	95.66	94.58
	number of the cations on the basis of 22 (O)									
Si	6.011	6.183	6.019	6.141	5.951	6.059	5.974	5.947	6.107	6.018
Al^{IV}	1.989	1.817	1.981	1.859	2.049	1.941	2.026	2.053	1.893	1.982
ΣZ	8.000	8.000	8.000	8.000	8.000	8.000	8.000	8.000	8.000	8.000
Al^{VI}	1.920	1.922	1.633	1.627	1.730	1.862	1.679	1.808	1.933	1.707
$*Fe^{3+}$	0.006	0.040	0.366	0.320	0.250	0.098	0.271	0.150	0.026	0.221
Ti	0.000	0.002	0.009	0.006	0.003	0.006	0.005	0.005	0.002	0.002
ΣY	1.926	1.964	2.008	1.953	1.983	1.966	1.955	1.963	1.961	1.930
Mn	0.004	0.005	0.001	0.008	0.004	0.004	0.001	0.001	0.002	0.004
Mg	0.001	0.002	0.009	0.060	0.026	0.009	0.002	0.021	0.000	0.002
Ca	4.083	3.938	3.963	3.923	4.009	3.989	4.067	4.051	3.951	4.080
Na	0.013	0.029	0.000	0.004	0.016	0.035	0.009	0.006	0.092	0.013
K	0.008	0.008	0.005	0.006	0.005	0.004	0.003	0.006	0.006	0.005
ΣX	4.109	3.982	3.978	4.001	4.060	4.041	4.082	4.085	4.051	4.104
$X_{Fe^{3+}}$	0.003	0.020	0.183	0.164	0.126	0.050	0.139	0.077	0.013	0.115

* total iron calculated as Fe_2O_3 and Fe^{3+}

n = number of analyses

TABLE 7

Averages of chemical compositions (weight-%) and cation numbers of pumpellyite

Rock type	metabasalt	metadiabase		metagabbro		
Sample No.	DG-33	DG-13	DG-16	DG-21b	DG-22	DG-37c
n	2	1	6	3	3	4
SiO_2	36.12	37.25	36.64	36.20	37.44	36.75
TiO_2	0.00	0.00	0.03	0.19	0.56	0.00
Al_2O_3	23.58	26.93	23.88	20.76	21.57	25.17
$*Fe_2O_3$	10.23	4.38	7.02	15.89	10.60	3.59
MnO	0.15	0.22	0.10	0.06	0.07	0.07
MgO	3.07	1.81	2.33	1.56	1.61	1.75
CaO	19.81	23.35	22.16	19.68	21.36	23.00
Na_2O	0.02	0.02	0.02	0.05	0.00	0.06
K_2O	0.02	0.00	0.01	0.03	0.25	0.00
Total	93.01	93.96	92.19	94.42	93.46	90.39
	number of the cations on the basis of 16 (O)					
Si	5.918	5.944	6.012	6.002	6.174	6.072
Al^{IV}	0.124	0.056	0.012	0.016	–	–
ΣZ	6.042	6.000	6.024	6.018	6.174	6.072
Al^{Y}	4.000	4.000	3.996	3.977	3.931	4.000
$*Fe^{Y}$	–	–	–	–	–	–
Ti	0.000	0.000	0.004	0.023	0.069	0.000
ΣY	4.000	4.000	4.000	4.000	4.000	4.000
Al^{X}	0.430	1.009	0.610	0.064	0.261	0.898
$*Fe^{X}$	1.270	0.531	0.875	2.002	1.330	0.500
Mg	0.748	0.431	0.568	0.386	0.396	0.429
ΣX	1.448	1.971	2.053	2.452	1.987	1.827
Mn	0.021	0.030	0.014	0.008	0.010	0.010
Ca	3.482	3.994	3.899	3.499	3.775	4.072
Na	0.006	0.006	0.007	0.016	0.000	0.019
K	0.003	0.000	0.002	0.006	0.053	0.001
ΣW	3.512	4.030	3.922	3.529	3.838	4.102
X_{Fe*}	0.223	0.096	0.160	0.331	0.241	0.093

* total iron calculated as Fe_2O_3 and Fe^{3+}

n = number of analyses

TABLE 8

Mean values and standard errors (in parentheses) of phyllosilicate crystallinity indices ($\Delta°2\theta$)

XRD parameters	Rock type	Whole rock, AD		<2µm fractions, AD		<2µm fractions, EG	
		2°/min	½°/min	2°/min	½°/min	2°/min	½°/min
ChC(001)	**meta-pelite**	0.348 (0.020)	0.323 –	0.452 (0.023)	– –	0.394 –	– –
	meta-basalt	– –	– –	0.449 (0.008)	0.399 (0.013)	0.536 –	0.454 –
	meta-diabase	0.404 (0.020)	0.364 –	0.388 (0.014)	0.332 (0.014)	0.482 (0.028)	0.424 (0.022)
	meta-gabbro	0.353 –	– –	0.421 (0.026)	0.372 (0.015)	0.343 (0.007)	0.301 (0.014)
	meta-granite	0.271 (0.016)	– –	0.332 (0.017)	0.226 (0.008)	0.324 (0.017)	0.250 –
ChC(002)	**meta-pelite**	0.358 (0.011)	0.290 (0.022)	0.398 (0.012)	0.306 (0.022)	0.313 –	0.275 –
	meta-basalt	0.410 (0.012)	0.370 (0.013)	0.372 (0.010)	0.342 (0.009)	0.392 (0.008)	0.357 –
	meta-diabase	0.337 (0.006)	0.287 (0.011)	0.359 (0.011)	0.321 (0.010)	0.380 (0.014)	0.346 (0.012)
	meta-gabbro	0.314 (0.011)	0.256 (0.010)	0.337 (0.009)	0.306 (0.010)	0.310 (0.009)	0.296 (0.014)
	meta-granite	0.276 (0.006)	0.229 (0.003)	0.282 (0.008)	0.246 (0.007)	0.283 (0.001)	0.245 (0.005)
IC(002)	**meta-pelite**	0.364 (0.014)	0.234 (0.023)	0.388 (0.023)	0.262 (0.053)	0.288 (0.047)	0.253 (0.046)
	meta-basalt	– –	– –	– –	– –	– –	– –
	meta-diabase	– –	– –	0.352 –	– –	– –	– –
	meta-gabbro	– –	– –	0.285 (0.024)	0.245 (0.016)	0.318 –	0.244 –
	meta-granite	0.220 –	– –	0.369 (0.027)	0.300 (0.022)	0.353 (0.010)	0.296 –

AD = Air-dried preparations of the <2µm fractions.
EG = Ethylene glycol-solvated preparations of the <2µm fractions.

CONCLUSION

In the Mesozoic dismembered ophiolite complex of the Szarvaskő area (Bükk Mountains, NE Hungary), imprints of two metamorphic events were distinguished. In the initial stage of hydrothermal (ocean-floor) metamorphism, metamorphic minerals characteristic of high temperature and low pressure (e.g. new generation of clinopyroxene, calcic amphibole and a Fe-Mg amphibole) were formed. The grade of hydrothermal metamorphism increases downwards from the prehnite-pumpellyite or zeolite facies (metabasalt), through the greenschist facies (metadiabase), to the greenschist/amphibolite transitional and amphibolite facies (metagabbro). The existence of second generation of clinopyroxene, namely an Al-poor clinopyroxene in metagabbros indicates re-equilibration of magmatic clinopyroxene during hydrothermal metamorphism that has been rarely recorded so far in the literature. The changes in amphibole chemistry and in mineral associations refer to continuous cooling (retrogression) in the course of hydrothermal metamorphism. The composition of the metamorphic amphibole formed during hydrothermal metamorphism in the metagabbros grades from hornblende to actinolitic hornblende while that of metadiabase is actinolitic in composition, reflecting variations in its Si, Al^{IV} and Ti contents with decreasing grade upwards in the ophiolite profile. The younger (Alpine, Cretaceous) orogenic (dynamothermal) metamorphism - as it was shown by ÁRKAI (1983) - produced mainly prehnite-pumpellyite facies assemblages in matabasic rocks and late diagenetic to low-temperature anchizonal alterations in the associated metaclastic rocks. This younger, regional metamorphic event could not perfectly obliterate and re-equilibrate the earlier products of hydrothermal metamorphism. As a consequence, typical non- equilibrium, mixed assemblages have persisted.

The large variations in the compositions of Ca-Al silicate minerals suggest that the fluid chemistry, mode of occurrence and the extent of rock alteration rather than temperature are the main controls of their compositions. In the low variance assemblages, the average $X_{Fe}3+$ values of coexisting prehnite, pumpellyite and epidote are 0.003, 0.137 and 0.008, respectively. This contrasts with the suggestion of CHO et al. (1986) who mentioned that the $X_{Fe}3+$ values most probable increase in order of prehnite, through pumpellyite to epidote.

ACKNOWLEDGEMENTS

The authors are grateful to Mr Z. WIESZT for major element bulk chemical analyses and to Mrs O. KOMORÓCZY for the technical assistance in XRD work carried out in the Laboratory for Geochemical Researches, Hungarian Academy of Sciences.

The present work forms a part of one of the authors (P.Á.) metamorphic petrological research programme No. T 007211/1993-1996 supported by the Hungarian National Science Found (OTKA), Budapest.

REFERENCES

ÁRKAI, P. (1983): Very low- and low-grade Alpine regional metamorphism of the Paleozoic and Mesozoic formations of the Bükkium, NE-Hungary. Acta Geol. Hung. **26**, 83-101.

ÁRKAI, P. (1991): Chlorite crystallinity: an empirical approach and correlation with illite crystallinity, coal rank and mineral facies as exemplified by Palaeozoic and Mesozoic rocks of northeast Hungary. J. Metamorphic Geol. **9**, 723-734.

ÁRKAI, P. and SADEK GHABRIAL, D. (1996): Chlorite crystallinity as an indicator of metamorphic grades of low-temperature meta-igneous rocks: a case study from the Bükk Mountains, northeast Hungary. Clay Minerals (in press).

ÁRKAI, P., SASSI, F. P. and SASSI, R. (1995): Simultaneous measurements of chlorite and illite crystallinity: a more reliable tool for monitoring low- to very low-grade metamorphisms in metapelites. A case study from the Southern Alps (NE Italy). Eur. J. Mineral. **7**, 1115-1128.

BALLA, Z. (1982): Geological map of vicinity of Szarvaskő. Published by the Hung. Geol. Institute, Budapest.

BALLA, Z., HOVORKA, D., KUZMIN, M. and VINOGRADOV, V.I. (1983): Mesozoic ophiolites of the Bükk Mountains (North Hungary). Ofioliti. **8**, 5-46.

BENCE, A.E. and ALBEE, A. (1968): Empirical correlation factors for electron microanalysis of silicates and oxides. J. Geol. **76**, 382-403.

BEVINS, R.E. and MERRIMAN, R.J. (1988): Compositional controls on coexisting prehnite-actinolite and prehnite-pumpellyite facies assemblages in the Tal y Fan metabasite intrusion, North Wales: implications for Caledonian metamorphic field gradients. J. Metamorphic Geol. **6**, 17-39.

BEVINS, R.E. and ROBINSON, D. (1993): Parageneses of Ordovician sub-greenschist facies metabasites from Wales, U.K. Eur. J. Mineral. **5**, 925-935.

BORTOLOTTI, V., CELLAI, G., VAGGELLI, G. and VILLA, I.M. (1990): $^{40}Ar/^{39}Ar$ *dating of Apenninic ophiolites:* 1. Ferrodiorites from La Bartolina Quarry, southern Tuscany, Italy. Ofioliti. **15**, 1-16.

CATHELINEAU, M. (1988): Cation site occupancy in chlorites and illites as a function of temperature. Clay Minerals. **23**, 471-485.

CHO, M. and LIOU, J.G. (1987): Prehnite-pumpellyite to greenschist facies transition in the Karmutsen metabasites, Vancouver Island, B.C. J. Petrol. **28**, 417-443.

CHO, M., LIOU, J.G. and MARUYAMA, S. (1986): Transition from the zeolite to prehnite-pumpellyite facies in the Karmutsen metabasites, Vancouver Island, British Columbia. J. Petrol. **27**, 467-494.

COLEMAN, R.G. (1977): *Ophiolites. Springer*, Berlin, 229 pp.

CSONTOS, L. (1988): Étude géologique d'une portion des Carpathes internes: la masif du Bükk (NE de la Hongrie) (Stratigraphie, structures, métamorphisme et géodznamique). Thése Doctorat Univ. Sci. Tech. Lille Flandres-Artois, Lille, 327 pp.

DEER, W.A., HOWIE, R.A. and ZUSSMAN, J. (1964): Rock-forming minerals. Vol. 2. Longmans, London, 379pp.

DI GIROLAMO, P., MORRA, V. and PERRONE, V. (1992): Ophiolitic olistroliths in Middle Miocene turbidites (Cilento Group) at Mt. Centaurino (Southern Apennines, Italy). Ofioliti. **17**, 199-217.

DOBOSI, G. (1986): Clinopyroxene composition of some Mesozoic igneous rocks of Hungary: the possibility of identification of their magma type and tectonic setting. Ofioliti. **11/1**, 19-34.

DOWNES, H., PANTÓ, GY., ÁRKAI, P. and THIRLWALL, M.F. (1990): Petrology and geochemistry of Mesozoic igneous rocks, Bükk Mountains, Hungary. Lithos. **24**, 201-215.

EMBEY-ISZTIN, A., NOSKE-FAZEKAS, G., KURAT, G. and BRANDSTATTER, F. (1985): Genesis of garnets in some magmatic rocks from Hungary. Tschermaks Mineral. Petrogr. Mitt. **34**, 49-66.

EVARTS, R.C. and SCHIFFMAN, P. (1983): Submarine hydrothermal metamorphism of the Del Puerto ophiolite, California. Amer. J. Sci. **283**, 289-340.

FREY, M., DE CAPITANI, C. and LIOU, J.G. (1991): A new petrogenetic grid for low-grade metabasites. J. Metamorphic Geol. **9**, 497-509.

FOSTER, M.D. (1962): Interpretation of the composition and a classification of the chlorites. U.S. Geol. Surv. Prof. Pap. **414-A**, 1-33.

GILLIS, K.M. (1995): Controls on hydrothermal alteration in a section of fast-spreading oceanic crust. Earth Planet. Sci. Lett. **134**, 473-489.

GIRARDEAU, J. and MÉVEL, C. (1982): Amphibolitized sheared gabbros from ophiolites as indicators of the evolution of the oceanic crust: Bay-of-Islands, Newfoundlands. Earth Planet. Sci. Lett. **61**, 151-165.

ISHIZUKA, H. (1985): Prograde metamorphism of the Horokanai ophiolite in the Kamuikotan Zone, Hokkaido, Japan. J. Petrol. **26**, 391-417.

JOWETT, E.C. (1991): Fitting iron and magnesium into the hydrothermal chlorite geothermometer: GAC/MAC/SEG Joint Annual Meeting (Toronto, May 27-29, 1991), Program with Abstracts. **16**, A62.

KOVÁCS, S. (1982): Problems of the "Pannonian Median Massif" and the plate tectonic concept. Contributions based on the distribution of the Late Paleozoic-Early Mesozoic isotopic zones. Geol. Rundsch. **71**, 617-640.

KOVÁCS, S. (1989): Major events of the tectono-sedimentary evolution of the North Hungarian Paleo-Mesozoic Tethys. In: Tectonic Evolution of the Tethyan Region, (SENGÖR, A.M.C. ed.), pp. 93-108. Kluwer Academic Publishers, Dordrecht.

KÜBLER, B. (1968): Evaluation quantitative de métamorphisme par la cristallinité de l'illite. Bull. Centr. Rech. Pau S.N.P.A. **2**, 385-397.

KÜBLER, B. (1990): "cristallinité" de l'illite et mixed-layers: breve révision. Schweiz. Miner. Petr. Mitt. **70**, 89-93.

LEAKE, B.E. (1978): Nomenclature of amphiboles. Amer. Mineralogist. **63**, 1023-1052.

LIOU, J.G., KUNIYOSHI, S. and ITO, K. (1974): Experimental studies of the phase relations between greenschist and amphibole in a basaltic system. Amer. J. Sci. **274**, 613-632.

LIOU, J.G., MARUYAMA, S. and CHO, M. (1985): Phase equilibria and mixed parageneses of metabasites in low-grade metamorphism. Mineral. Mag. **49**, 321-335.

LIOU, J.G., MARUYAMA, S. and CHO, M. (1987): Very low-grade metamorphism of volcanic and volcanoclastic rocks - mineral assemblages and mineral facies. In: Low Temperature Metamorphism, (FREY, M. ed.), pp. 59-113. Blackie & Son, Glasgow.

MÉVEL, C. (1987): Evolution of oceanic gabbros from DSDP Leg 82: influence of the fluid phase on metamorphic crystallizations. Earth Planet. Sci. Lett. **83**, 67-79.

MÉVEL, C. (1988): Metamorphism in oceanic layer 3, Gorringe Bank, Eastern Atlantic. Contrib. Mineral. Petrol. **100**, 496-509.

MOODY, J.B., MEYER, D. and JENKINS, J.E. (1983): Experimental characterization of the greenschist/amphibole boundary in mafic systems. Amer. J. Sci. **283**, 48-92.

NYSTRÖM, J.O. (1983): Pumpellyite-bearing rocks in Central Sweden and extent of host rock alteration as a control of pumpellyite composition. Contrib. Mineral. Petrol. **83**, 159-168.

POWELL, W.G., CARMICHAEL, D.M. and HODGSON, C.J. (1993): Thermobarometry in a subgreenschist to greenschist transition in metabasites of the Abitibi greenstone belt, Superior Province, Canada. J. Metamorphic Geol. **11**, 165-178.

ROBINSON, P., SPEAR, F.S., SCHUMACHER, J.C., LAIRD, J., KLEIN, C., EVANS, B.W. and DOOLAN, B.L. (1982): Phase relations of metamorphic amphiboles: natural occurrence and theory. In: Amphiboles: Petrology and Experimental Phase relations, Reviews in Mineralogy, Vol. 9B, (VEBLEN, D.R & RIBBE, P.H. eds.), pp. 1-227. Mineralogical Society of America.

SADEK GHABRIAL, D., ÁRKAI, P. and NAGY, G. (1994): Magmatic features and metamorphism of plagiogranite associated with a Jurassic MORB-like basic-ultrabasic complex, Bükk Mountains, Hungary. Acta Miner. Petr. Szeged. **35**, 41-69.

SHIDO, F. (1958): Plutonic and metamorphic rocks of the Nakoso and Iritono districts in the central Abukuma Plateau. J. Fac. Sci. Univ. Tokyo. **11**, p.131.

SZENTPÉTERY, S. (1938): Szarvaskőer hornblendite mit ausführlicher physiographie. Acta Litt. Sci. Univ. Szeged, Acta Chem. Min. Phys. **6**, 175-250.

SZENTPÉTERY, S. (1940): Über den pyroxenit von Szarvaskő (Bükkgebirge, Ungarn). Acta Univ. Szegediensis, Acta Chem. Min. Phys. **7**, 165-191.

SZENTPÉTERY, Zs (S.) (1953): Le massif de diabase et de gabbro de la partie méridionale de la montagne Bükk. MÁFI Évk. **41**, 1-92 (in Hungarian with French abstract).

Manuscript received 6 Sep. 1996.

Acta Mineralogica-Petrographica, Szeged, XXXVII, 129–141, 1996

THE OPHIOLITE MELANGE OF WADI DUNQASH AND ARAYIS, EASTERN DESERT OF EGYPT: PETROGENESIS AND TECTONIC EVOLUTION

A. M. ABDEL-KARIM[1], M. M. EL-MAHALLAWY[2] and F. FINGER[3]

Geology Department, Faculty of Science, Zagazig University[1] ;
Geology Department, Faculty of Science, El-Minia University[2] ;
Egypt and Institute of Mineralogy, Salzburg University[3]

ABSTRACT

Wadi Dunqash and Wadi Arayis in the central and southern Eastern Desert of Egypt are characterized by the presence of metamorphosed dismembered ophiolite sequence. This sequence consists of harzburgite-serpentinite, pyroxenite-chlorite schist; normal and sheared metagabbros; metabasalt and meta-andesite and their schists.

Major and trace element studies indicate that the present sequence can be comparable with the ophiolitic ultramafic-mafic cumulates. The metagabbros and metavolcanics pertain to a high-Ti ophiolite, exhibit tholeiitic and minor calc-alkaline nature, derived from ocean floor-island arc transitional basalts, suggest their probable back-arc environment.

INTRODUCTION

The ultramafic-mafic rocks constitute one of the distinctive rock group in the late Precambrian of Egypt. Recently, many authors have attempted to identify the mafic-ultramafic assemblage in the Eastern Desert of Egypt as ophiolite complexes and hence as fragment of oceanic crust. Ophiolites in the Eastern Desert always occur as allochthonous and commonly dismembered ultrabasic to basic bodies frequently interlayered with highly foliated peilitc layers (SHACKLETON et al. 1980, RIES et al. 1983, BASTA et al. 1983, ABU EL ELA 1985). More or less complete ophiolite sections are described from Wadi Ghadir (EL SHARKAWI and EL BAYOUMI 1979), Qift-Quesir road near Fawakhir (NASSEEF et al. 1980), Wadi Mubarak (HASSANEIN 1984) and Wadi Esel (ABU EL ELA and ALY 1990).

Only very few previous studies carried out on the ophiolite melange of Wadi Dunquash (ABU EL ELA 1985) and Wadi Arayis (ABDEL-KHALEK et al. 1992). The studies concentrated on the regional geology, geodynamic evolution and tectonic specularities.

This study presents the mode of occurrences and new whole-rock chemical data for the mafic-ultramafic assemblage of Wadi Dunquash and Arayis in the central and southern Eastern Desert of Egypt, in an attempt to clarify the magmatic history and the past tectonic environment.

---

[1] Zagazig, Egypt
[2] El-Minia, Egypt
[3] A-5020 Salzburg, Akademiestrasse 26, Austria

GEOLOGIC SETTING

The ophiolite melange of Wadi Dunqash and Arayis occupy the extremely westernmost parts of the Precambrian rocks of the Eastern Desert of Egypt (*Fig. 1*). The geology of the present ophiolite melange distributed in the two areas were treated elsewhere (ABU EL ELA 1985 and ABDEL-KHALEK et al. 1992). The following is a synopsis of the geology of the areas in question starting with the oldest rock unit (*Fig. 1*).

I) *Gneisses* represent the oldest rock unit in Wadi Arayis area. They include muscovite biotite granodiorite gneisses and biotite granodiorite gneisses. Both types are foliated, lineated and folded. They are sometimes graded to hornblende-biotite- and garnet-biotite gneisses. The present gneisses are overthrusted by the ophiolite melange.

II) *Ophiolite melange* forms hanging wall of the major thrust in Wadi Arayis. The trends of the major thursts run, more or less, in NW-SE in Wadi Arayis. In Wadi Dunqash the trend of the major thrust is NEN-SWS and EN-SW direction. The ophiolite melange includes allochthonous dismembered blocks and fragments of ultramafics, metagabbros and metavolcanics with a matrix of low grade metamorphosed metasediments and metapyroclastics.

a) *The ultramafic rocks* are the most widespread being represented by serpentinite and chlorite schist with relics of harzburgites in Wadi Arayis and harzburgites and pyroxenites in Wadi Dunqash. They crop out in variable size and range from small blocks and lenses of low relief to huge steeply inclined sheets forming mountains of moderately high relief (814 m a.s.l. in G. Dunqash and 630 m a.s.l. in Arayis) thrusted over the melange matrix. The present serpentinite and its derivatives have not sign of thermal contact on the enveloping rocks, emphasizing that these rock bodies are allochthonous (ASHMAWY 1987). The contact is mostly marked by veins of asbestos and magnesite and black-walls of talc and chlorite schists. The present ultramafics are charged with lenses mostly of chromite and minor talc and magnesite. The serpentinite sheets of Dunqash are structrally either overlain by or overthrusted on the metasediments. The thrust zones are regular and dip 50°–60°N. The present rocks are mostly intruded by syntectonic older granites in Wadi Dunqash and late tectonic younger granites in Wadi Arayis.

b) *The metagabbros*, in the two area under study, occur as variable size masses of low to moderate to relief. They show tectonic contact against the metasediment matrix as well as other melange blocks. The present metagabbros are strongly sheared, being foliated and display minor folds. They range from fine grained to pegmatitic and from normal gabbros to leucogabbros. The pegmatitic gabbros occurs as pockets and irregular masses and veins within the normal gabbros, possess tectonic contacts with them.

c) *The metavolcanics* form small elongated blocks and fragments inside the melange matrix of Wadi Dunqash and Wadi Arayis. They are frequently medium to fine grained, massive or sheared and displaying well developed lineation. These rocks are represented by metabasalts and meta-andesites or their equivalent schists. In Dunqash area, the metavolcanics are mostly exhibited pillow structure. The pillows are aphanitic, ovoidal to elongate shapes and range in size from 10–65 cm. Pillow breccias are also common. They are highly sheared particularly along fault contact with the serpentinites. In Arayis area, the pillow structure is not observed probably due to the strong deformation and metamorphism of the metavolcanics which converted mostly into amphibolite schists.

d) *The volcanoclastic metasediments* are widely distributed rock unit in both studied areas, mostly form the matrix enclosing the ophiolite fragments. They are slightly to strongly sheared, folded and lineated. Wide development of albitization, chloritization,

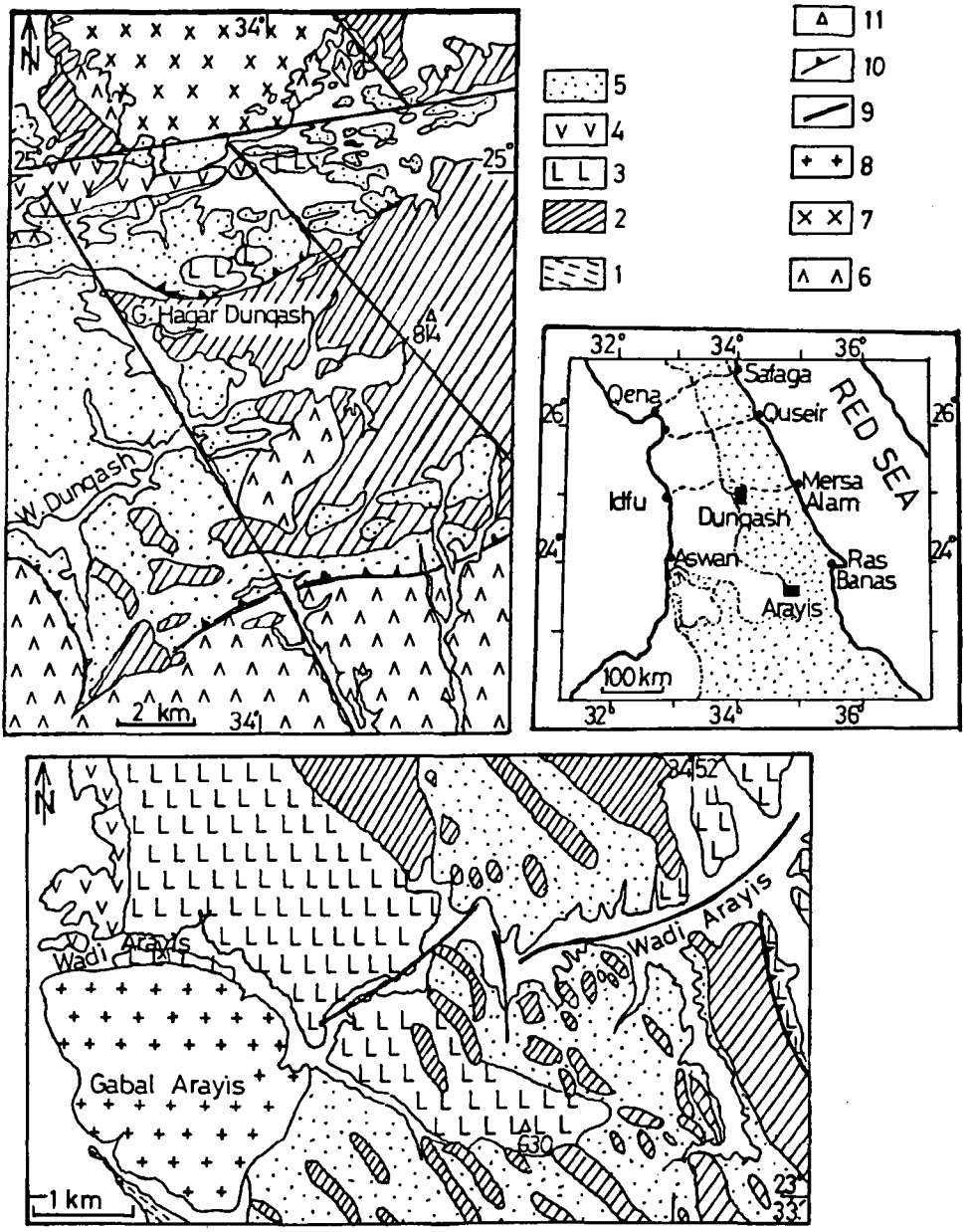

Fig. 1. Geologic map of the studied ophiolite melange of Wadi Dunqash (after ABU EL ELA 1985) and Wadi Arayis (After ABDEL-KHALEK et al. 1992) with some modifications.
1 = Pre-Pan African gneisses, Ophiolite melange, 2 = peridotite and its derivatives, 3 = metagabbros, 4 = metavolcanics, 5 = volcanoclastic metasediments (matrix), 6 = island arc metavolcanics, granitoid rocks, 7 = syntectonic granites, 8 = late tectonic granites, 9 = major tectonic lines, 10 = thurst with direction of dip, 11 = triangulation point.

sericitization and sometimes epidotization are common alteration products of the present rocks. They are represented by metagreywackes, metasiltstones, phyllites and schists, all are within the zone of greenschist regional metamorphism. The different beds usually grade into each other without sharp boundaries. The metagreywackes include feldspathic and volcanic varieties, the latter contain andesitic rock fragments beside quartz and feldspar crystal fragments. Tuffaceous meta-andesite and metadacite intercalated with metamudstones are common in Dunqash area.

III) *Island arc metavolcanics* are recorded only in Dungash area as elongated belt overthrusted on the metasediments and intruded by the syntectonic older granites. The thrust zone dips 50°–60° N. These rocks include basic and intermediate composition are volcanics with subordinate metapyroclastics.

IV) *Granitoid rocks* comprise syntectonic granites (Wadi Dunqash), and late tectonic granites (Wadi Arayis). The contact of these rocks with the enveloping ophiolite melange are sharp and distinct. The Dunqash granites are represented by calc alkaline foliated quartz diorite to granodiorite rocks, meanwhile the Arayis granites are perthitic leucocratic granites.

PETROGRAPHY OF THE OPHIOLITE MELANGE

The petrographic description of the ultramafics and their derivatives, metagabbros, and metavolcanics of Wadi Dunqash and Arayis are briefly discussed in the followings:

I) **Ultramafic rocks**

Peridotites and their derivatives include primary rocks such as peridotites and pyroxenites as well as their alteration products, namely serpentinites which comprise antigoritite, lizardite-antigorite serpentinite and magnesite-antigorite serpentinite. Meanwhile, the derivatives include chlorite schists, talc schists and talc-quartz carbonate rocks.

Harzburgite-serpentinite is recorded in Wadi Dunqash and Arayis area. It consists of primary olivine and minor pyroxene variably altered to serpentine minerals. Talc and carbonate are accessory minerals. Olivine forms fine granules mostly altered to antigorite. Pyroxene relics are represented by enstatite. They are subjected to different degree of serpentinization. Lizardite occurs as interpenetrating blades and is slightly replaced by talc and carbonates.

Pyroxenite-serpentinite is recorded in Wadi Dunqash area. It consists of primary enstatite and augite variably altered to serpentine or chlorite. Tremolite and magnetite are accessory minerals. Orthopyroxene commonly is in exsolution lamellae within the clinopyroxene.

Serpentinites are recorded in Wadi Dunqash and Arayis areas. They are made up mainly of antigorite or lizardite admixed with chrysotile. In this rocks, the primary minerals are completely obliterated. Carbonate, talc, chlorite, chromite and iron oxide are accessories. Antigorite forms xenoblastic blades resulting in interlocking texture. Lizardite occurs as extremely fine grained flakes and scales showing hourglass texture and scarce mesh texture. Chrysotile forms cross-fibrous veinlets within the shear zone. Iron oxide is concentrated along the mesh rim-core boundaries. Chromite occurs as dissiminated grains, lenses and veins.

The ultramafic schists comprise the chlorite, and talc schists. In the *clorite schist*, chlorite (clinochlore) mostly occurs as the main mineral constituent. Chlorite occurs in the

form of pseudospherulitic blades. In the *talc schist*, radial, fibrous and granular aggregates of talc is the dominant mineral.

In *talc, and quartz carbonate rocks*, carbonates constitute the varieties. Magnesite is the most predominant carbonate minerals, calcite, talc and quartz are less common.

II) **Metagabbros**

The metagabbros display rapid grain-size variations from fine to pegmatoid varieties, with either normal or sheared structure. In normal metagabbros, the primary minerals (pyroxene) and textures (ophitic and subophitic) are still partly preserved, while the original textures are obliterated and tectonized and mylonitized ones are common in the sheared metagabbros. The normal and sheared metagabbros are recognized in the studied two areas.

The *normal metagabbros* range from mesocratic to leucrocratic, quartz injected metagabbros and from pyroxene-hornblende to and hornblende metagabbros. They are composed of pyroxene and/or hornblende and plagioclase. Tremolite-actinolite, zoisite and titanite are the accessory minerals. Pyroxene relic is represented by enstatite and augite. Enstatite is mostly altered to antigorite or chlorite while augite is either rimmed by uralite indicating the oceanic metamorphism or transformed into tremolite-actinolite ± chlorite. Plagioclase (An_{35-40}) is partly altered to saussurite, albite and kaolinite ± calcite.

The *sheared metagabbros* are composed mainly of strongly deformed clinopyroxene, amphibole and plagioclase ± quartz with minor epidote and apatite. The clinopyroxene exhibits kink-bands and is either altered to tremolite-actinolite aggregates or recrystallized to fine grained ones of the same mineral. The plagioclase (An_{32-37}) is intensively altered to albite, epidote and carbonate.

III) **Metavolcanics**

The metavolcanics consist mostly of metabasalts and meta-andesites and their alteration products (e. g. chorite-tremolite-actinolite and tremolite-actinolite schists). The primary minerals and even the primary textures are still partly preserved in metabasalts and meta-andesites, while they are completely obliterated in the schists.

Metabasalts consist of pyroxene relic, plagioclase and hornblende together with secondary tremolite-actinolite. Quartz, epidote, apatite and iron oxide are the main accessory minerals. They display ophitic and subophitic textures. Variolitic, intersertal and porphyritic textures are sometimes observed. Augite occurs as anhedral prismatic crystals, slightly altered to tremolite-actinolite aggregates or replaced by hornblende. Plagioclase (An_{8-12}) forms fine laths, variolites and rarely phenocrysts altered to kaolinite and sericite. The meta-andesites consist of plagioclase, hornblende and chlorite with subodinate amounts of calcite, quartz, titanite, apatite and iron oxide. They exhibit porphyritic and fluidal textures.

The schists consist mainly of tremolite-actinolite, strongly altered plagioclase ± chlorite, epidote and carbonate. The accessory minerals include apatite and iron oxide. Albite forms fine grained metablasts and rarely porphyroblasts containing acicular grains of actinolite. Relic augite and saussuritized plagioclase are sometimes seen. Iron oxide (Ti-rich) is mostly transformed into titanite ± rutile.

On the basis of the mineral assemblage and textures, as well as the alteration products, the present serpentinites, metagabbros and metavolcanics have been metamorphosed up to the greenschist facies.

GEOCHEMISTRY OF THE OPHIOLITE MELANGE

Chemical analyses were carried out on 27 rock samples (Table 1) representing the ophiolite suite of Wadi Dunqash and Wadi Arayis areas (nine from the ultramafics, eleven from the metagabbros and seven from the metavolcanics). Major and trace element analyses were carried out by computerized XRF Spectrometer system "Philips PW 1400" using pressed pellets in Institute of Mineralogy, Salzburg University, Austria. The major elements of the ultramafics are recalculated on a water-free basis.

Petrochemical classification:

I) *Ultramafic rocks*

On the normative Opx-Ol-Cpx diagram of STRECKEISEN (1976); *Fig. 2a*, the present ultramafic from Wadi Dunqash fall within the fields of orthopyroxenite and harzburgite, while those from Wadi Arayis fall within the harzburgite field.

II) *Metagabbros*

On the normative Px-Pl-Ol diagram of STRECKEISEN (1976); *Fig. 2b*, Wadi Dunqash metagabbros fall with in the fields of olivine gabbro-norite and gabbro-norite, while Wadi Arayis metagabbros fall within the fields of olivine gabbro-norite, gabbro-norite and leucogabbro. COLOMBI (1988) proposed the use of SiO_2 variations with increasing $FeO_t/(FeO_t+MgO)$ to classify the ophiolitic gabbros. The present metagabbros from Wadi Dunqash fall within the clinopyroxene (cpx) gabbro, while those from Wadi Arayis fall within or around the fields of cpx-gabbro and ferro-gabbro (*Fig. 2c*).

III) *Metavolcanics*

WINCHESTER and FLOYD (1977) inferred the discrimination of altered and metamorphosed volcanic suites of different magma series and their differentiation products in terms of SiO_2 content and Zr/TiO_2 ratio (*Fig. 2d*). All the analyses of the present rocks have Zr/TiO_2 ratios < 0.03, suggesting that these metavolcanics are indeed basaltic composition with minor andesite.

Magma Type:

Identification of the magma type helps to elucidate past tectonic setting of the unknown magmatic belts (MIYASHIRO 1974, 1975; WINCHESTER and FLOYD 1977).

MIYASHIRO's diagrams (*Fig. 3a, b* and *c*) and the AFM diagram (*Fig. 4a*) show a diverse in magma type of the present rocks which range from tholeiitic (TH) to calc alkaline (CA) series. The chemical data on MIYASHIRO's diagrams indicate that the majority of the metavolcanics and metagabbros are TH with a few CA type and fall within or around the field of basalts from the Alp ophiolite (DAL PIAZ et al., 1981; BECCULUVA et al. 1984; ABDEL-KARIM 1992) (*Fig. 3a* and *b*). On the AFM diagram, the analyses of metavolcanics are TH, while the metagabbros are mainly TH with a few samples showing CA affinity.

Ophiolitic Affinity and Tectonic Setting

STRONG and MALPAS (1975) and COLEMAN (1977) drew the composition fields of ultramafic and mafic cumulates (ophiolitic cumulates) using AFM diagram (*Fig. 4a*) and $CaO-Al_2O_3-MgO$ diagram (*Fig. 4b*). In these figures, the ultramafic rocks from Wadi Dunqash fall within ultramafic-mafic cumulate field except a few samples of the metapyroxenites which enriched in FeO_t and Al_2O_3 and depleted in CaO probably due to the enrichment of these samples in Fe-rich chlorite. Wadi Arayis ultramafics fall within the field of metamorphic peridotite and ultramafic-mafic cumulate.

The metagabbros from both areas fall within the field of oceanic gabbros from Mid Cayman Ridge (CAYTROUGH 1979) and Egyptian metagabbros (GHONEIM et al. 1992),

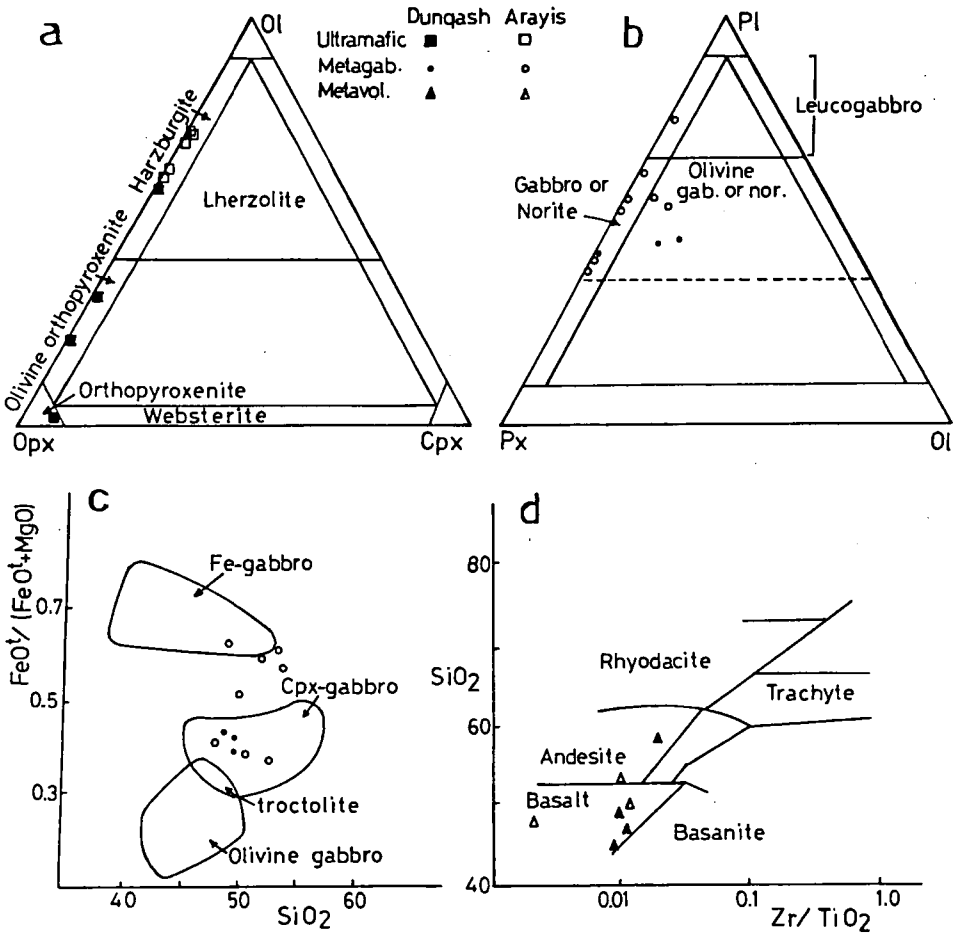

Fig. 2. Plots show the chemical classifications of the studied ophiolites:
a) normative Opx-Ol-Cpx diagram for the ultramafics and after STRECKEISEN (1976),
b) normative Px-Pl-Ol diagram for the metagabbros after STRECKEISEN (1976),
c) FeOt/(FeOt+MgO) versus SiO_2 diagram for the metagabbros after COLOMBI (1988),
d) SiO_2 versus Zr/TiO_2 diagram for the metavolcanics after WINCHESTER and FLOYD (1977).

Fig. 4a. Moreover, the present metagabbros together with the metavolcanics fall mostly within the mafic cumulate field of COLEMAN (1977), *Fig. 4b.*

The ophiolites are generally classified into high-Ti, low-Ti and very low-Ti (BECCALUVE et al. 1983). SERRI (1981) and DECCALUVA et al. (1983) used the variation diagram of TiO_2 versus $FeO_t/(FeO_t+MgO)$ ratio in gabbroic complex and basaltic rocks to discriminate between high- and low-Ti ophiolites. *Fig. 5a* reveals that the present metagabbros and metavolcanics from the both areas under studied belong to a high-Ti ophiolites.

The present ophiolite suite can be comparable with the high-Ti ophiolite of transitional MOR for the following:

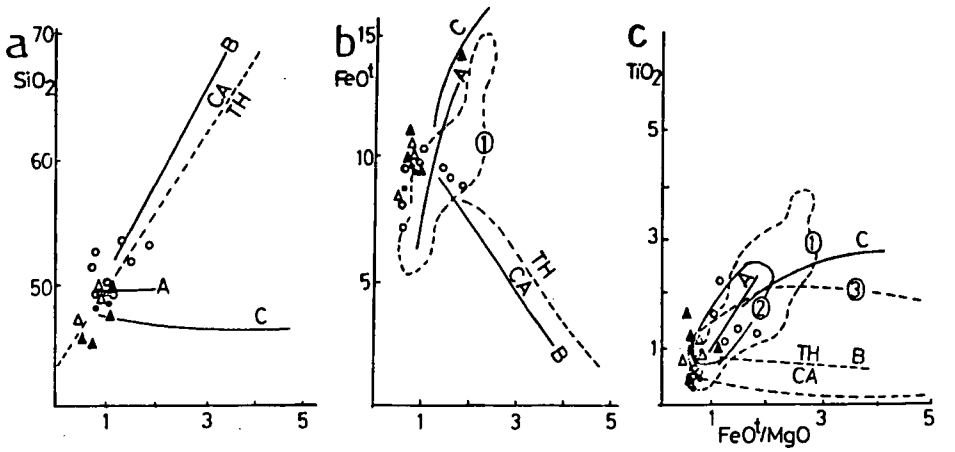

Fig. 3. SiO_2-, FeO_t- and TiO_2 versus $FeO_t/(FeOt+MgO)$ variation diagrams for the studied metagabbros and metavolcanics. The dashed line separating the tholeiitic (TH) and calc-alkaline (CA) series, and the solid trend lines for abyssal tholeiites (A), the Asama calc-alkaline volcano (B) and Skaergaard intrusions (C) are after MIYASHIRO (1975a). Fields: 1 = Basalts from Western Alps ophiolite after DEL PIAZ et al. (1981), BECCALUVA et al. (1984), ABDEL KARIM (1991); 2 = Abyssal tholeiites and 3 = Island arc volcanics after MIYASHIRO (1975b).

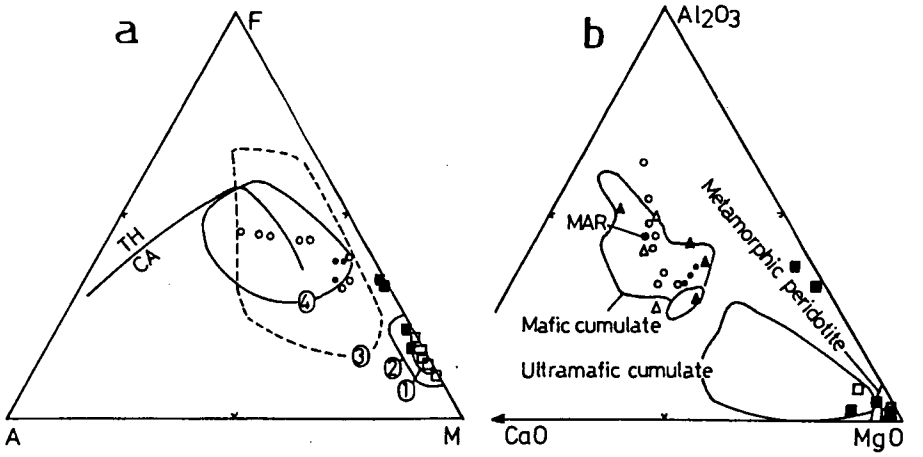

Fig. 4. Plots show the ophiolitic affinities and magma type of the studied rocks. a) AFM diagram after IRVINE and BARAGAR (1971), Fields: 1 = metamorphic peridotites and 2 = mafic-ultrmafic cumulates after STRONG and MAPLAS (1975), 3 = oceanic gabbros (CAYTROUGH, 1979), 4 = Egyptian metagabbros (GHONEIM et al., 1992) b) CaO-Al_2O_3-MgO diagram after COLEMAN (1977).

Plots of metagabbros and metavolcanics on TiO_2-FeO_t/MgO diagram (*Fig. 5a*) after MIYASHIRO (1975) indicate their abyssal tholeiite with a few samples showing island arc affinity.

Plots of the present metagabbros and metavolcanics on Ti-Cr diagram (*Fig. 5b*) after PEARCE et al. (1975) reveal their ocean floor and island arc setting.

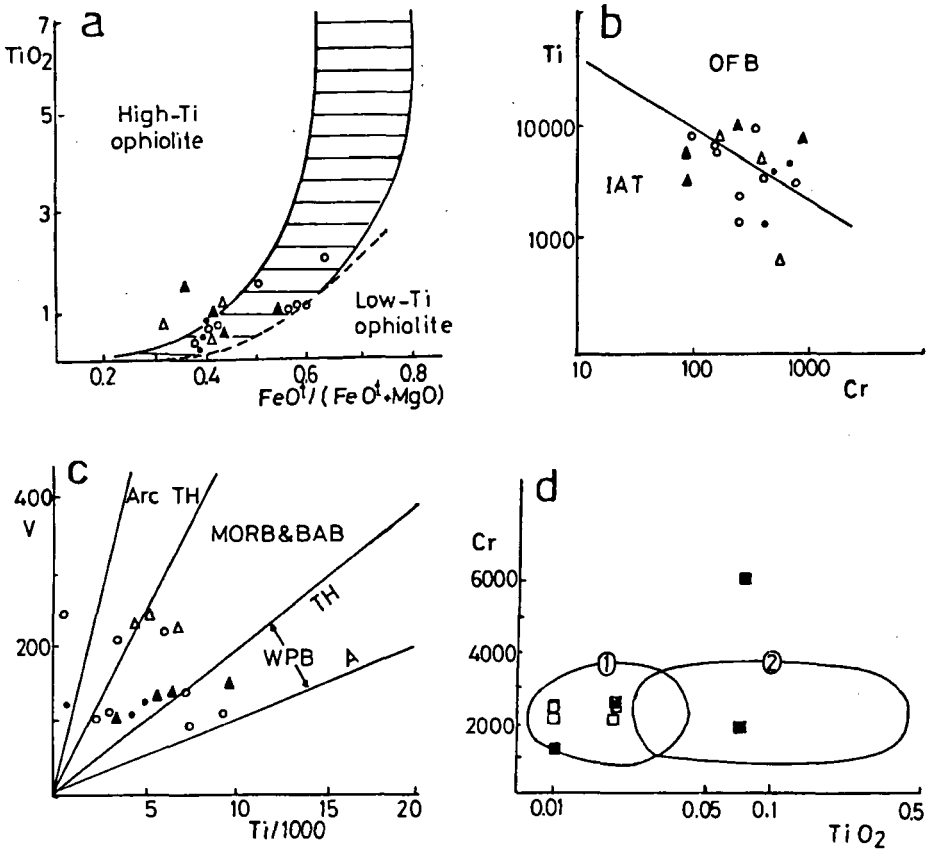

Fig. 5. Plots show the magma type and tectonic setting of the studied metagabbros and metavolcanics.
a) TiO_2-FeO_t/(FeO_t+MgO) diagram after SERRI (1981). Shaded field denotes gabbroic rocks from Atlantic and Indian oceans.
b) Ti-Cr diagram after PEARCE (1975). OFB = Ocean floor basalts, IAT = Island arc tholeiites.
c) V-Ti/1000 diagram after SHARVAIS (1982). BAB = Back-arc basin, WPB = Within plate basalts, TH = Tholeiite, A = Alkaline.
d) Cr-TiO_2 diagram after PEARCE et al. (1984). Fields: 1 = Supra-subduction zone ophiolite, 2 = MORB ophiolite.

Plots of the metagabbros and metavolcanics on V-Ti diagram (*Fig. 5c*) after SHERVAIS (1982) indicate that the present rocks fall mostly within or around the field of mid-ocean ridge and back-arc basin basalt with a few samples showing TH of arc and within plate.

Plots of the ultramafic rocks on the simple discrimination diagram of Cr-TiO_2 (*Fig. 5d*) of PEARCE et al. (1984) which differentiate between the ophiolites of the supra-subduction zone (SSZ) and mid-ocean ridge (MOR) show that most of the present ultramafics fall within the field of supra-subduction zone ophiolite (SSZ).

TABLE 1

Results of chemical composition of the ophiolite of Wadi Dunqash and Wadi Arayis, Eastern Desert, Egypt

	Metaultramafics Wadi Dunqash				*Wadi Arayis*					*Metagabbros Wadi Dunqash*			*Wadi Arayis*							*Metavolcanics Wadi Dunqash*				*Wadi Arayis*		
	109	*109/1*	*109/2*	*102/3*	*96/3*	*96/3*	*99/1*	*101/3*	*96/1*	*111*	*112'*	*112*	*111/2*	*95*	*97*	*97/1*	*94/2*	*93*	*101/1*	*101/2*	*105/1*	*105/5*	*107/1*	*106/1*	*99/4*	*99/5*	*98*
SiO_2	40.10	32.07	33.55	64.14	42.36	44.12	43.23	41.22	31.38	49.63	48.50	49.57	48.84	51.10	52.24	52.53	53.12	53.34	48.74	50.09	45.21	47.46	45.07	58.02	47.05	49.40	52.53
TiO_2	0.02	2.86	0.07	0.01	0.01	0.02	0.01	0.02	0.08	0.73	0.52	0.21	0.56	0.38	1.26	0.51	1.17	1.09	2.22	1.54	1.17	1.06	1.63	0.54	0.75	1.16	0.77
Al_2O_3	4.25	15.36	14.48	1.22	1.14	1.12	1.03	4.11	14.50	11.96	12.50	12.25	11.68	13.34	16.42	12.22	18.74	14.06	13.84	16.05	13.10	12.92	10.21	14.60	9.64	18.77	13.62
Fe_2O_3	8.50	15.23	13.79	5.09	8.78	7.18	8.10	9.53	4.58	1.58	1.32	1.42	1.59	1.31	1.62	1.20	1.39	1.55	1.70	1.62	1.80	2.39	1.62	1.25	1.29	1.80	1.77
FeO	1.81	3.05	2.76	1.02	1.76	1.44	1.02	1.91	0.92	7.88	8.11	7.12	7.94	6.55	7.58	6.01	6.94	7.76	8.50	8.07	8.98	44.93	8.06	8.26	6.93	9.28	8.83
MnO	0.15	0.15	0.21	0.06	0.16	0.10	0.14	0.15	0.05	0.15	0.16	0.15	0.14	0.14	0.14	0.13	0.12	0.17	0.12	0.14	0.16	0.16	0.22	0.17	0.16	0.18	0.17
MgO	41.33	24.55	28.39	24.35	44.21	45.77	44.21	39.49	34.24	13.49	13.70	14.17	14.11	12.84	6.27	12.49	4.57	7.10	9.17	9.38	15.55	11.61	17.16	6.53	18.08	9.49	10.45
CaO	0.88	0.70	0.10	2.68	0.87	0.12	0.34	2.61	0.07	8.60	8.88	9.83	9.53	11.08	8.03	11.18	7.11	8.61	10.78	10.19	7.90	7.99	12.27	6.83	13.57	6.48	10.03
Na_2O	–	0.06	–	–	–	0.05	–	–	–	1.61	1.91	2.42	0.48	1.28	3.29	1.99	4.56	3.23	2.81	2.50	0.41	1.78	1.30	2.46	0.69	1.74	1.36
K_2O	–	0.04	–	–	–	–	–	–	–	0.24	0.20	0.05	0.87	0.41	1.21	0.20	0.75	1.03	0.22	0.13	1.54	0.82	1.05	0.83	0.14	0.64	0.14
P_2O_5	0.04	0.55	0.05	0.02	0.02	0.03	0.02	–	0.02	0.15	0.10	0.02	0.13	0.09	0.38	0.10	0.53	0.28	0.07	0.11	0.26	0.27	0.17	0.17	0.02	0.23	0.11
LOI	2.90	5.37	6.50	1.32	0.63	–	1.80	1.92	13.50	2.95	3.60	2.97	4.11	2.32	2.51	2.43	0.95	1.74	1.73	0.17	2.52	2.05	1.30	0.27	2.10	0.80	0.12
Total	99.98	99.99	99.90	99.91	99.93	99.93	99.87	98.98	98.98	99.50	99.98	99.06	99.98	99.84	99.85	99.99	99.95	99.96	99.80	99.99	99.80	99.14	99.07	99.96	99.98	99.97	99.90
Ba	125	11	40	41	39	32	48	31	22	150	120	47	190	133	266	67	361	300	71	66	242	431	111	281	66	746	68
Zn	–	4	4	–	–	–	–	–	4	95	85	23	69	97	140	102	333	149	86	76	103	85	104	118	49	102	43
Y	–	–	–	–	–	–	–	–	–	3	2	–	2	–	6	–	8	14	–	–	14	10	11	12	10	17	12
Sr	2	36	4	43	3	3	2	6	1	262	188	150	160	517	504	427	537	350	444	414	159	570	120	321	100	137	145
Rb	–	–	–	–	–	–	–	–	–	2	2	–	6	–	14	–	3	10	–	–	11	22	–	10	–	83	–
Th	3	4	3	5	2	7	–	4	–	–	–	–	1	–	3	6	–	2	–	5	1	–	2	2	5	–	–
Pb	4	–	4	6	3	4	7	10	–	–	10	–	2	–	6	4	11	11	–	19	–	–	–	1	9	–	7
Ga	10	18	25	10	11	10	9	10	16	16	12	13	16	17	20	17	24	19	17	18	16	18	16	19	13	19	15
Zn	35	115	109	59	36	39	27	35	102	55	43	38	6	63	76	54	111	90	50	76	64	84	97	81	38	58	62
Hf	–	–	–	–	–	–	–	–	–	2	2	1	2	2	2	2	6	3	1	1	3	3	2	2	–	3	1
Co	150	83	77	79	151	142	149	145	63	40	35	36	50	41	31	43	18	30	35	36	53	22	33	7	53	42	33
Cr	2350	2050	2031	1615	2565	2460	2219	2258	9987	705	520	421	883	258	103	398	118	159	250	331	969	194	246	102	577	187	395
V	105	50	56	17	47	148	40	107	725	101	105	120	216	102	91	107	133	95	239	114	114	115	135	95	232	216	248
Ce	–	–	–	–	1	–	–	–	–	47	32	28	26	2	18	9	56	34	–	50	17	55	14	32	–	92	–
La	–	15	–	12	–	–	48	–	–	–	10	17	–	–	16	–	9	–	–	–	33	20	11	–	13	–	–
Cl	150	137	122	94	213	448	105	131	66	109	93	78	125	55	138	163	25	172	104	175	54	108	159	138	160	47	130
S	118	327	60	117	296	195	67	291	29	890	88	161	276	44	658	1070	227	297	75	71	528	84	197	132	47	507	68
Ni	2350	1256	1190	1666	2414	2408	2588	1413	1350	109	102	95	140	104	45	208	33	29	79	78	346	19	84	22	113	188	96
Nb	8	19	–	11	11	13	10	–	–	5	–	–	7	–	–	3	11	–	–	–	7	8	–	–	–	–	–

DISCUSSION AND CONCLUSION

The field investigation of the mafic-ultramafic assemblage of Wadi Dunqash and Wadi Arayis, Eastern Desert of Egypt, reveal that the occurrence of harzburgite serpentinite and pyroxenite-chlorite schists followed by metagabbros (normal and sheared) and metavolcanics (metabasalts and meta-andesites and their alteration products). The present assemblage were emplaced into volcanoclastic metasediments with no sign of thermal contact. This sequence may be classified as a dismembered ophiolite suite in the sense of the GSA Penrose Conference (1972). The general extention trends of the present ophiolite melange are NW-SE direction in Wadi Arayis and ENE-WSW in Wadi Dungash. The presence of volcanoclastic materials in the metasediments (as well as the island arc calc-alkaline metavolcanics in Dungash) probably indicate the presence of nearby island arc. The major elements geochemistry confirms this conclusion.

The high-Ti ophiolite are generated in a number of transitional tectonic settings, related to an incipient or more mature stage of MORB and marginal basin magmatism (BECCALUVA et al. 1983). The present mafic-ultramafic sequence show a similarity with high-Ti ophiolite of transitional-MORB. This features reveal from discrimination diagrams (*Fig. 5*) which show ocean floor- or abyssal tholeiite-island arc trends for the metagabbros and metavolcanics and supra-subduction zone (SSZ) for the ultramafic rocks.

The present-day SSZ ophiolites lie in fore-arc and parts of some back-arc basins; whereas MORB ophiolites lie in incipient oceans, major oceans, "leacky" transform faults and most back-arc basins. Moreover, compositional fields for some marginal basins fall into two groups. Those from back-arc basins which fall entirely within the MORB field, and from back-arc and fore-arc basins plot within or to the left of the island arc tholeiite. Subsequently, the present mafic-ultramafic sequence probably represent the best analogues for transitional MORB, attribute to their transitional setting between ocean floor basalt and island arc.

The following facts probably suggest a similarity of the present mafic-ultramafic assemblage with the ophiolite suite:

1. The metagabbros and metavolcanics are derived from tholeiitic with minor calc-alkaline magma.
2. Both the metagabbros and metavolcanics are transitional between ocean floor and island arc.
3. Both the metagabbros and metavolcanics exhibit a back-arc basin-MORB affinity.
4. The ultramafics are similar to that associated with the SSZ ophiolite, support that they are not typical MORB (i. e., transitional).

Therefore, the variation of both magma type and tectonic setting of the present rocks can be interpreted if the present ophiolites are implicated in back-arc system. Similar results are given by KRONER et al. (1987), ABU EL-ELA and ALY (1990) and others. The view is consistent with the presence of studied ophiolite assemblage within the volcanoclastic metasediments.

REFERENCES

ABDEL-KARIM, A. M. (1991): Comparative petrological and geochemical study of some ophiolite occurrences in the Alps-Carpathian system, Ph. D. Thesis, Eötvös Lorand Univ., Budapest, 223p.

ABDEL-KHALEK, M. L., TAKLA, M. A., SEHIM, A., HAMIMI, Z. and EL MANAWI, A. W. (1992): Geology and tectonic evolution of Wadi Beitan area, Southeastern Desert, Egypt. Geology of the Arab World. Cairo Univ., 369–394.

ABU EL ELA, A. M. and ALY, S. M. (1990): The ophiolite suite of Wadi Esel, Eastern Desert, Egypt. Proc. Egypt. Acad. Sci. **40**, 27–39.

ABU EL ELA, F. F. (1985): Ophiolitic melange of the Abu Mireiwa district, central Eastern Desert, Egypt. Ph. D. Thesis, Assiut Univ.

ASHAWY, M. H. (1987): The ophiolitic melange of the south Eastern Desert of Egypt; remote sensing field work and petrographic investigation. Ph. D. Thesis, Berliner Geowiss. Abh., Berlin, (A), **84**, 134 p.

BASTA, E. Z., CHURCH, W. R., HAFEZ, A. M. A. and BASTA, F. F. (1983): Proterozoic ophiolitic melange and associated rocks of Gabal Ghadirarea, Eastern Desert, Egypt. 5th Intern. Conf. on Basement Tectonics, Cairo Univ. Abstract vol.

BECCALUVA, L., GIROLAMO, P., MACCIOTTA, G. and MORRA, V. (1983): Magma affinities and fractionation trends in ophiolites. Ophioliti. 8, 3, 307–324.

BECCALUVA, L., DAL PIAZ, G. V. and MACCIOTA, G. (1984): Transtonial to norma MORB affinities in ophiolitic metabasites from the Zermatt-Saas, Combin and Antrona units, Western Alps: Implication for the paleogeographic evolution of the Western Tethyan basin. Geol. Mijnbouw. **63**, 165–177.

CAYTROUGH, P. (1979): Geological and geophysical investigation of the Mid-Cayman Ridge spreading center. In Talwani, M., Harrison, G. E. and Hayes, D. E. (eds.): Maurice Ewig Series, 2, Am. Geophys. Union, 66–95.

COLEMAN, R. G. (1977): Ophiolites. Springer Verlag, New York, 299p.

COLOMBI, O. A. (1988): Metamorphisme et geochimie des roches mafiques des Alpes. Duest-centrales (geoprofil Viege-Domodossala-Locarno). Ph. D. thesis, Lausanne Univ., 195p.

DAL PIAZ, G. V., VENTURELLI, G., SPEDEA, P. and DI BASTTISTILNI G. (1981): Geochemical features of metabasalts and metagabbros from the Piedmont ophiolite nappe. Italian Western Alps. N. Jb. Min. Abh, **142**, 248–269.

EL SHARKAWI M. A. and R. M. EL BAYOUMI (1979): The ophiolites of Wadi Ghadir area, Eastern Desert, Egypt. Ann. Geol. Surv. Egypt. **9**, 125–135.

GHONEIM, M. F., TAKLA, M. A. and LEBDA, E. M. (1992): The gabbroic rocks of the Central Eastern Desert, Egypt: A geochemical approach. Annals Geol. Surv. Egypt. **XVIII**, 1–21.

HASSANEIN, S. M. (1984): Ophiolite-melange complex of Wadi Mubarak area, Eastern Desert, Egypt. Ph. D. Thesis, Cairo Univ.

IRVINE, T. N. and BARAGAR, W. R. (1971): A guide to the chemical classification of the common volcanic rocks. Can. J. Earth Sci. **8**, 523–548.

KRONER, A., GREILING, R., REISCHMANN, T. HUSSEIN, I. M., STERN, R. J., DURR, S., KRUGER, J. and ZIMMER, M. (1987): The Pan-African crustal evolution in the Nubian segment of northeast Africa. In KRONER, A. (ed.): Proterozoic Lithospheric Evolution. Geodyn. Ser., Am. Geophys. Union. **17**, 235–257.

LE MAITRE, R. W., BATERMAN, P., DUDEK, A., KELLER, J., LAMEYRE, M. J., SABINE, P. A., SCHMID, R., SØRENSEN, H., STRECKEISEN, A., WOOLEY, A. R. and ZANETTIN, B. (1989): A classificiation of igneous rocks and glossary of terms. Blackwell, Oxford.

MIYASHIRO, A. (1974): Volcanic rock series in island arc and active continental margins. Am. J. Sci. **274**, 331–355.

MIYASHIRO, A. (1975a): Classification, characteristic and origin of ophiolites. J. Geol. **83**, 249–281.

MIYASHIRO, A. (1975b): Volcanic rock series and tectonic setting. Annual Rev. Earth Planet. Sci. **3**, 251–269.

NASSEEF A. O., BAKOR, A. R. and A. H. HASHAD (1980): Petrography of possible ophiolitic rocks along the Qift-Quesir road, E. D., Egypt. Bull. Inst. Applied Geol., King Abdul-Aziz Univ. Jaddah **3**, (4), 157–168.

PEARCE, J. A. (1975): Basalt geochemistry used to investigate post-tectonic environments on Cyprus. Tectonphysics. **25**, 41–67.

PEARCE, J. A., LIPPARD, S. J. and S. ROBERTS (1984): Characteristics and tectonic significance of supra-subduction zone (ssz) ophiolites. In B. P. KOKELAAR and M. F. HOWELLS (eds.). Spec. Publ. Geol. Soc. **16**, 77–94.

Penrose Conference (1972): Ophiolite. Geotimes. **17**, No. 12, 24–25.

RIES, A. C., SHACKLETON, R. M., GRAHAM, R. H. and W. R. FITCHES (1983): Pan-African structures, ophiolites and melange in the Eastern Desert of Egypt: a traverse at 26° N. J. Geol. Soc. London. **140**, 75–95.

SERRI, G. (1981): The petrochemistry of ophiolitic gabbroic complexes: a key for the classificaton of ophiolities into low-Ti and high-Ti types. Earth Planet. Sci. Lett. **52**, 203–212.

SHACKLETON, R. M., RIES, A. C., GRAHAM, R. H. and W. R. FITCHES (1980): Late Precambrian ophiolite melange in the Eastern Desert of Egypt. Nature **285**, 472–474.

SHAERVAIS, J. W. (1982): Ti-V plots and the petrogenesis of modern and ophiolitic lavas. Earth Planet. Sci. Lett. **58**, 101–118.

STRONG, D. and MALPAS, J. G. (1975): The sheeted dykes layer of the Betts Core Ophiolite Complex does not represent spreading – Further discussion. Can. J. Earth Sci. **12**, 844–896.

WINCHESTER, J. A. and FLOYD, P. A. (1977): Geochemical discrimination of the different magma series and their differentiation products using immobile elements. Chem. Geol. **20**, 325–343.

Manuscript received 5 August, 1996.

Acta Mineralogica-Petrographica, Szeged, XXXVII, 143–160, 1996

Project No. 276
Paleozoic geodynamic domains and their alpidic evolution in the Tethys

METAMORPHIC FORMATIONS AND THEIR CORRELATION IN THE HUNGARIAN PART OF TISIA MEGAUNIT (TISIA COMPOSITE TERRANE)

T. SZEDERKÉNYI

University of Szeged
Dept. of Mineralogy, Geochemistry and Petrology*

ABSTRACT

Theory of Tisia as an isolated and rigid median-mass located into the inner region of Pannonian Basin originated from PRINZ (1914). After 65 years rise this idea partly defeated partly transformed. Nowadays the Tisia Megaunit is regarded as lihosphere fragment broken off the southern margin of Variscan Europe during the Jurassic (Bath) and after a compilated drifting and rotation it occupied the present tectonic position in the Miocene giving the basement complex – of East Slavonia (Croatia) – South Hungary–North Vojvodina (Yugoslavia) and West Transylvania (Romania). Crystallines and covering Late Paleozoic and Mesozoic overstep sequences show a rarely uniform lithology, lithostratigraphy and geological evolution. On the basis of these features both Pre-Mesozoic as well as Mesozoic sequences are ranged into numerous terranes and subterranes. Each one has tectonically determined boundaries and characteristic lithological-lithostratigraphic content and evolution.

The crystalline mass of Hungarian section of Tisia Megaunit is subdivided into three terranes and eight subterranes. All are represented by the same amount of lithostratigraphic units. This lithostratigraphic classification can be regarded as an experimental model which is reasonably suitable for correlation within the Megaunit and in all probablity it fulfils our expectations in the correlation with Variscan Europe.

INTRODUCTION

The first ideas of so-called "median mass" of the Carpathian system arose at the beginning of this century in the Hungarian (Austro-Hungarian) geology. Common feature of these hypotheses is assumption of an old /Paleozoic or older/ and rigid crystalline mass with "boot-stretcher" role; i.e. after an ancient mountain period and following breaking up and sinking, this mass is served as a core for uplifting of the Carpathians which practically surrounds and adheres it (PRINZ 1914, 1926; LÓCZY sen. 1918; KOBER 1921). This idea had obliged to suffer hard criticism from the birth until prevailing of up-to-date plate tectonic interpretations (SZEDERKÉNYI 1984), but it has not extincted perfectly until today. Its re-interpreted and refreshed variety incorporated the present evolutional picture of Alpine-Carpathian system.

What is the Tisia Megaunit today? A fragment which broke off the southern margin of Variscan Europe during the Jurassic and after a complicated drifting and rotation it occupied the present tectonic position in the Miocene, giving the basement formations of East Slavonia (Croatia), South Transdanubia (Hungary) and southern part of Great Plain

* H-6701 Szeged, P. O. Box 651. Hungary

(Hungary and Vojvodina) as well as West Transylvania /SZEDERKÉNYI 1974, 1984; KOVÁCS 1982, FÜLÖP 1994; KOVÁCS et al. 1996/.

TISIA MEGAUNIT AS A COMPOSITE TERRANE

Terrane is a crust-fragment (block) bordered by considerable fractures, lineaments or accretional complexes or (krypto) sutures. It is characterised by diverse evolution which differs from that of adjacent block(s) and based upon non-horizontal lithofacial changes, as well as stratigrapic-, paleontolological-, structural-, deformational-, e.t.c. inner continuity (after KEPPIE and DALLMEYER 1990 with a little modification). This principle offered basis for the Pre-Tertiary basement of Hungary to range into a terrane system (KOVÁCS et al. 1996) which was realised upon the following evoloutional background (FÜLÖP et al. 1987).

– Pre-Alpine (Pre-Variscan and Variscan) tectono-cycle
– Alpine (Tethyan) "geosynclinal" cycle
– Paleo-Alpine (Cretaceous) nappe movements
– Meso-Alpine (Paleogene-Early Miocene) strike-slip faulting
– Neo-Alpine (from Middle Miocene up to recent time) cycle with the formation of Pannonian Basin.

It is evident that the crystalline mass as a part of Variscan Europe formed during Carboniferous by accretion of earlier lithosphere-fragments (terranes and composite terranes) and broke up by Penninic rifting (Bath stage) and after a complicated drifting and rotation it joined to the Alpine Europe (BALLA 1986). Hence "Tisia Composite Terrane" designation terminologically refers to the Pre-Late Carboniferous (crystalline) mass only, while the " Tisia Terrane" name belongs to the Alpine stage of the Megaunit. The latter is bordered by Mid-Hungarian lineament (Zagreb-Kulcs line, WEIN 1969) as well as Save Moslavina -Sombor-Becej-Lipova lineament and Somes fracture zone.

Pre-Alpine terranes and sub-terranes of Tisia Composite Terrane (Tisia Megaunit) are as follows: *(Fig.1.)*

Drava Terrane
- Babócsa Sub-terrane
- Baksa Sub-terrane

"Para-Autochton" Terrane
- Mecsek-North Plain Sub-terrane
- Middle Plain Sub-Terrane

Szeged-Békés-(Codru) Terrane
- Kelebia Sub-Terrane
- Tisza Sub-terrane
- Battonya Sub-terrane
- Sarkadkeresztúr Sub-terrane

"Outliers" (wedges, nappe-vrecks and remnants)
- Horváthertelend Unit (terrane)
- Szalatnak-Unit (terrane)
- Ófalu - Unit (terrane)
- Tázlár- Unit (terrane)
- Álmosd Unit (terrane)

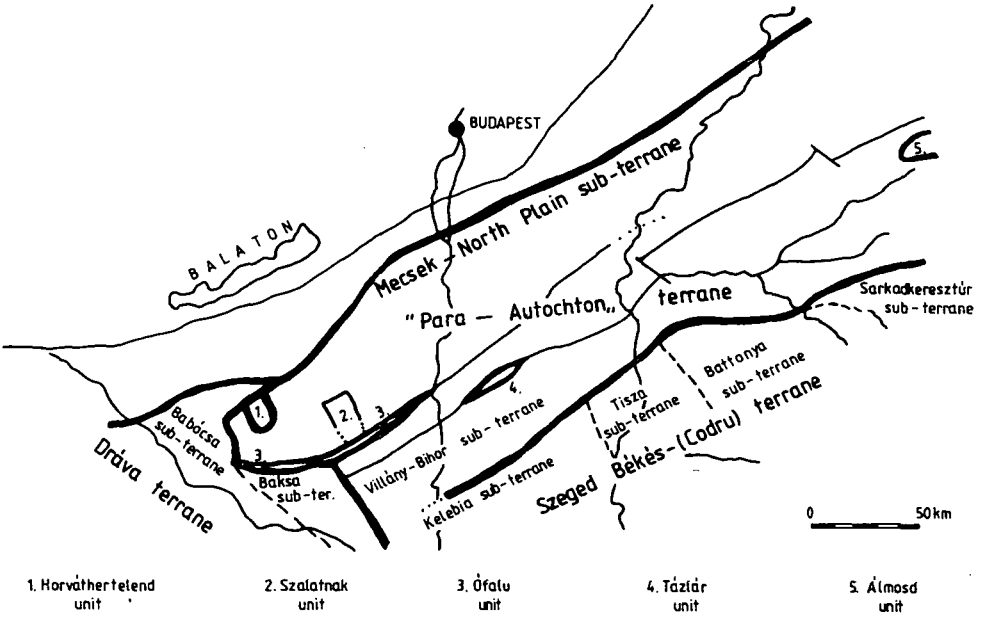

Fig. 1. Areal extension of units of Tisia Composite Terrane in Hungary.

As it appears from this list, besides terranes and sub-terranes several small units (nappe remnants, wedged bodies of larger tectonic zones) are also found in the Tisia Composite Terrane which show perfectly else lithological and metamorphic features. Really, they can also be regarded as terranes.

All terranes and sub-terranes have tectonically well-determined extensions and boundaries as well as characteristic lithostratigraphic columns and evolution. An acceptable lithostratigraphic classification of metamorphic bodies can be realised only if data with sufficient quality and quantity are available for the fulfilment of the following four requirements: (1) data for proving of pre-metamorphic rock-quality and facial characters, (2) data for determination of types and intensity of the metamorphic events, (3) data for the giving of succession of deformational events and their timing, (4) data for marking out of terranes and their subdivisions.

PROTOLITHS OF CRYSTALLINES OF TISIA COMPOSITE TERRANE

Protolith analysis was carried mainly out by geochemical methods using elements which retained their concentrations and ratios during the metamorphic process and metamorphic reactions had taken place more or less on isochemical way.

Prevailing rock association of Tisia crystallines is gneiss and mica-schist as well as related anatectic granitoids which derived mostly from greywacke-pelitic type sedimentary sequences (SZEDERKÉNYI 1984. *Fig 2)* with several m.-s thick mafic lava and/or tuff intercalations. These latter show tholeiitic basalt and tuff character in general (SZEDERKÉNYI 1983). Based on new geochemical data and up-to-date discriminating

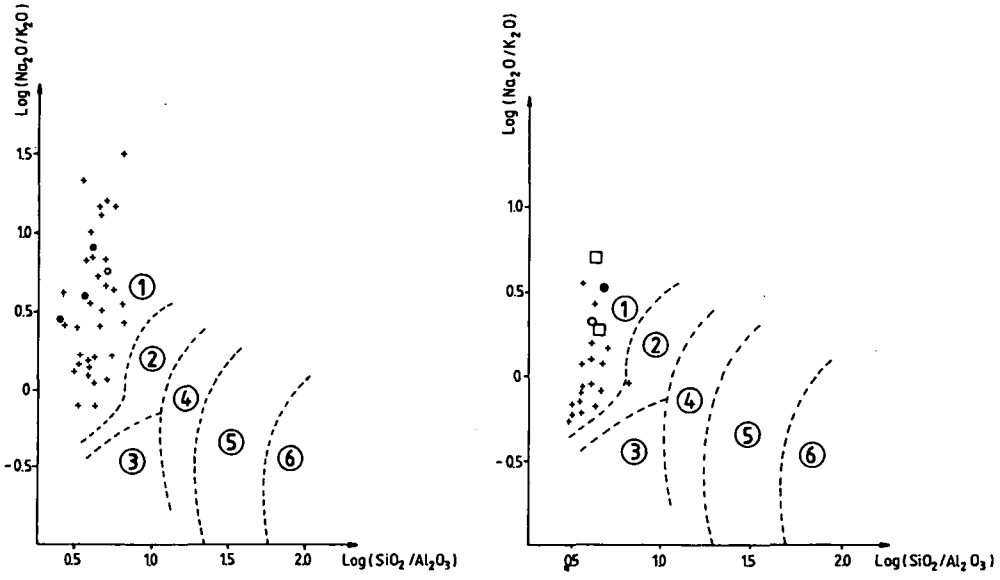

Fig.2. PETTIJOHN-POTTER-SIEVER (1972) diagram from the gneisses and micashists of Great Plain. Legend: 1. greywacke, 2. sub-greywacke, 3. arcose, 4. sub-arcose, 5. aleurolite, 6. Shale
Symbols represents different occurrence from every part of Great Plain.

methods these volcanics represent bac-arc basin tholeiite (T-MORB) origin (M. TÓTH 1995). In the rock-columns of South Transdanube and southern part of Great Plain some acidic tuff intercalations also occur showing a presumptive continental margin volcanic effect, too. Baksa-, as well as Tisza Sub-terranes also contain several m.-s thick carbonatic (marl, limestone, dolomite marl, dolomite) layers interbedding the psammitic-pelitic sediment column. No signs in any other terranes or sub-terranes are available of the existence of carbonatic layers or lenses.

METAMORPHISM

Apart from several "outliers" (nappe-vrecks and tectonic wedges) the metamorphic process comprised one or more progressive and several retrograde phases developed on the backgroud of single or sometimes two tectono-metamorphic characters of Tisia metamorphics plotted by *Fig.3*. Three characteristic fields are separated on the Miyashiro diagram: (1) High- pressure, approximately low-temperature metamorphism having P= 9,5-12 Kb. pressures and 12 °C/km thermal gradients. It settled in a few smaller covered occurrences extending along half-way line of "Para-autochton" Terrane (RAVASZ-BARANYAI 1969; M.TÓTH 1995). (2) Metamorphism characterised by medium-pressure and temperature (Barrow-type) deformation showing P= 4-6,5 Kb pressures and 24-27°C/km thermal gradients. This type is predominant in the "Para-autochton" Terrane but it can be detected on the whole area of Tisia Composite Terrane. (3) Low-pressure and high-temperature metamorphism characterised by P=2-3 Kb pressures and 70°C/km

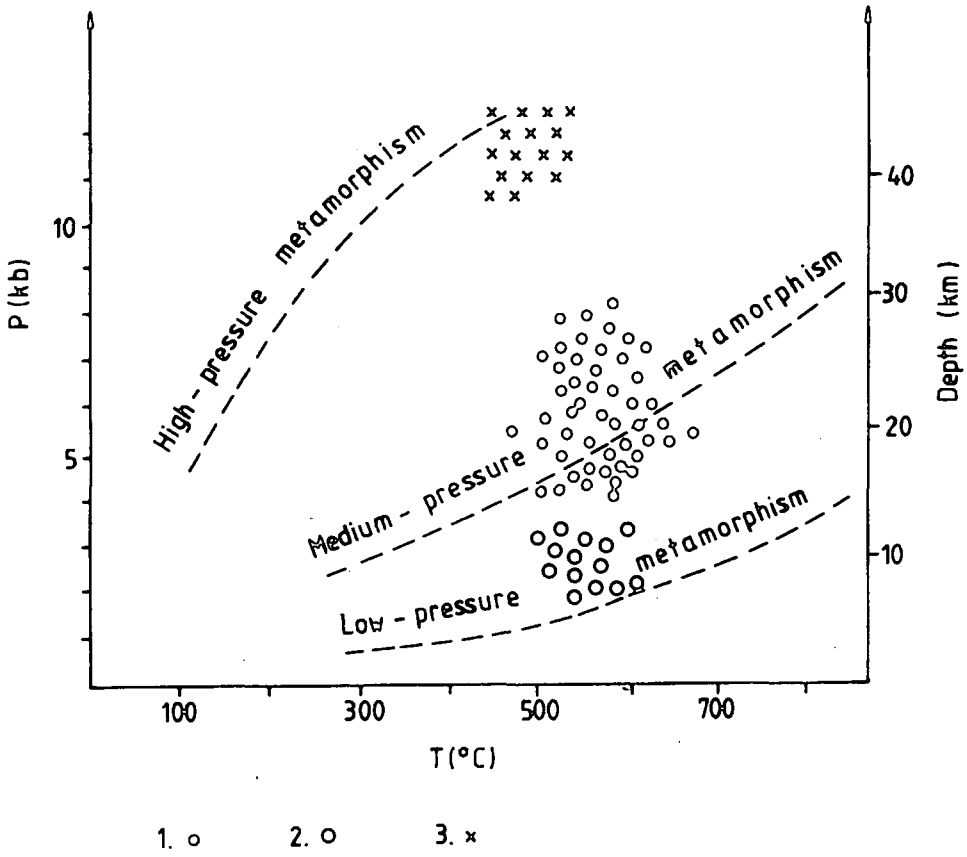

Fig.3. Pressure and temperature character of crystalline mass of Tisia Composite Terrane. Legend: /1/ Barrow-type crystalline schists, /2/. andalusite-bearing crystalline schists. /3/ high-pressure-low temperature eclogites.

thermal gradients overprinting the Barow-type metamorphic mass in the southern section of Tisia Composite Terrane {Drava Terrane and Szeged-Békés-(Codru) Terrane}.

A complete sequence of polymetamorphic deformations is shown by *Fig.4.* together with its every phasis, as follows:

1. This phasis of the polymetamorphism is corresponding to the previously-mentioned deformation No.1. on the Fig.3. which is detected about in a 10 Km-s wide zone located into the axial part of "Para-autochton" Terrane running near Szeghalom-Szarvas-Szank-Ófalu-Gyód traverse. It is represented by obduced ultramafic small bodies (SZEDERKÉNYI 1974; GHONEIM and SZEDERKÉNYI 1979; BALLA 1983) and low-temperature eclogites, amphibolites (RAVASZ-BARANYAI 1969; M.TÓTH 1995). This zone is assumed as a Pre-Variscan suture representing 400-440 Ma Rb/Sr ages (KOVÁCS et al. 1985).

2. Medium-pressure and temperature Barrow-type progressive metamorphic event corresponding to deformation No.2. in the Miyashiro diagram *(Fig. 3.)* as the very-first

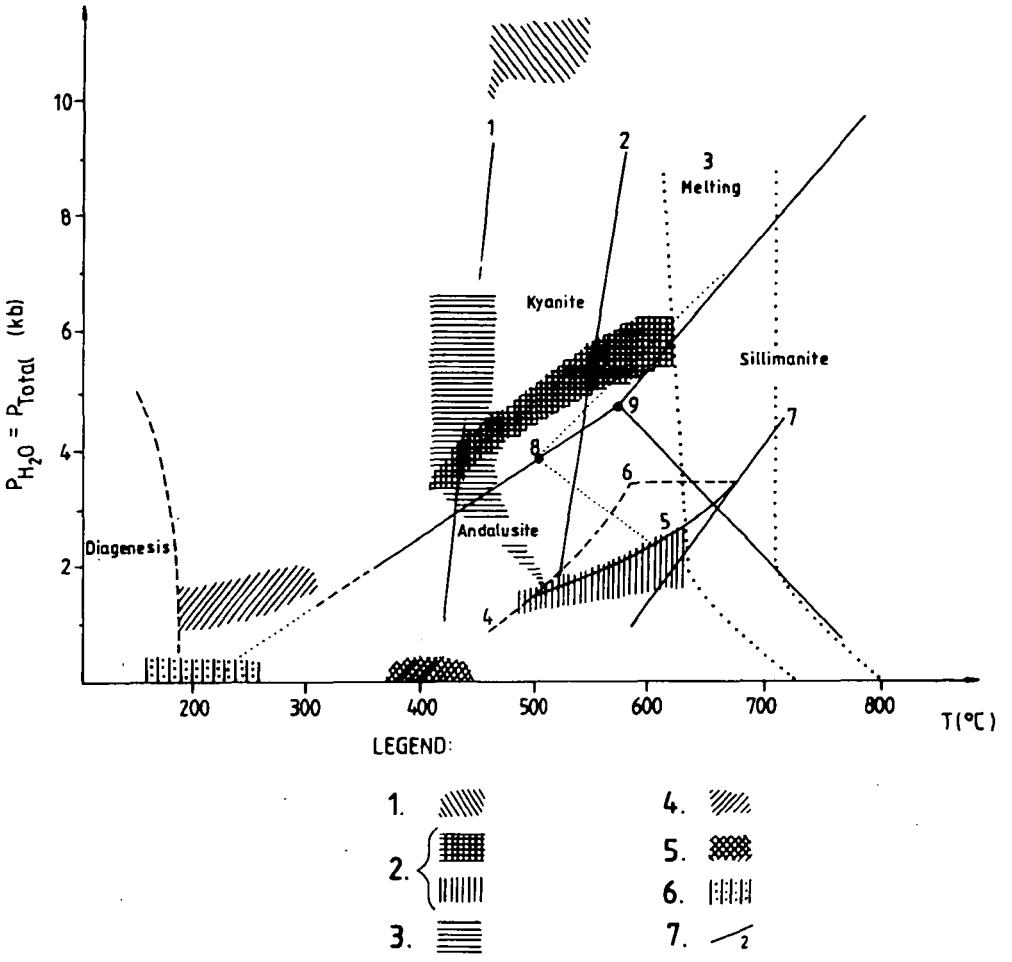

Fig.4. P-T diagram of metamorphic events of Tisia Composite Terrane. Legend: /1/ Pre-Variscan(?) high P.-metamorphism /2/ Variscan Barrow-type and high-T metamorphism, /3/ Variscan blastomylonitization, /4/ Alpine regional retrogression, /5/ Upper-Cretaceous contact metamorphism (Banatite), /6/ Lower Permian hydrothermal metasomatism (rhyolite) , /7/ phasis boundaries of important mineral reactions, as follows: 1. stilpmomelane+muscovite out, biotite+muscovite in, 2. staurolite in, 3. melting, 4. chloritoide+quartz=Fe-cordierite+sillimanite +H_2O, 7. muscovite+quartz= Orthoclase+Al_2SiO_5+H_2O, 8. Al_2SiO_5 triple-point by Holdaway, 9. Al_2SiO_5 triple-point by Greenwood.

manifestation of Variscan metamorphism and at the same time it is the most powerful deformation in the metamorphic history of Tisia Composite Terrane characterised by 350-330 Ma Rb/Sr and K/Ar ages (KOVÁCH et al. 1985; SVINGOR and KOVÁCH 1981; BALOGH KAD. and ÁRVA-SÓS 1983).

3. Blastomylonitization and following low-pressure and high temperature event occurred in the metamorphics of southern part of Tisia Megaunit with 330-270 Ma Sr/Rb and K/Ar ages (SVINGOR and KOVÁCH 1981; KOVÁCH et al. 1985; BALOGH KAD. and ÁRVA-SÓS 1983/. It corresponds to deformation No. 3. in the Miyashiro diagram (*Fig.3.*).

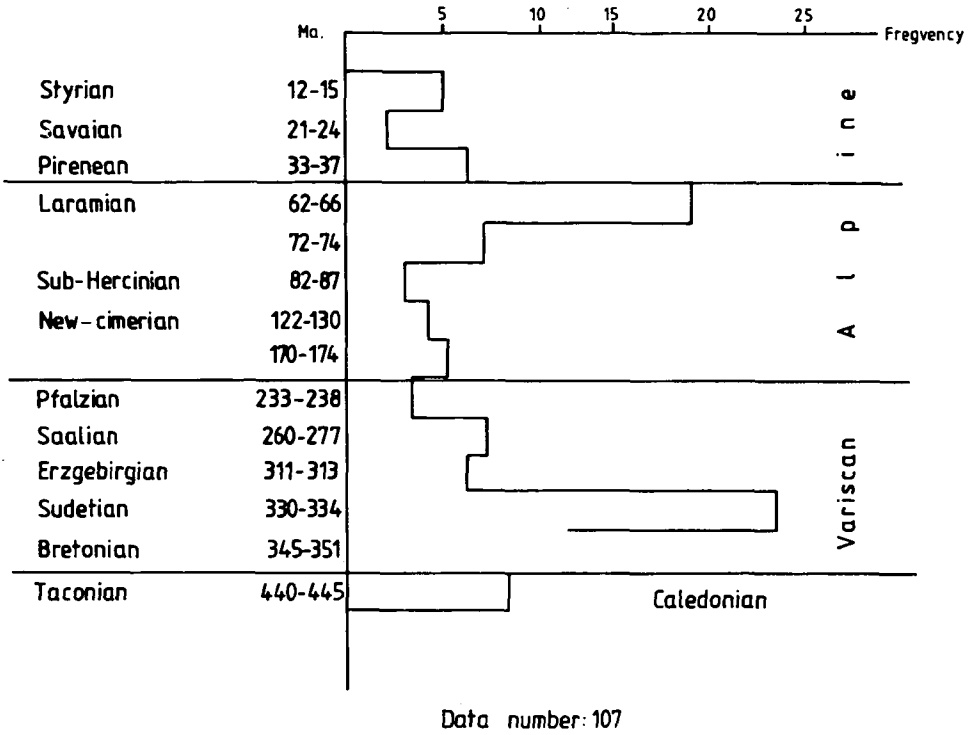

Fig.5. Frequency of isotopic ages of crystallines of Tisia Composite Terrane (SZEDERKÉNYI et al. 1991)

4. Pre-Upper Cretaceous retrogression succeed to Mesozoic in general due to the tensional tectonism.

5. Thermal /contact/ metamorphism concerning Late Cretaceous banatite intrusions found in the Szeged-Békés-(Codru)Terrane and characterised by 75-64 Ma (SZEDERKÉNYI 1984), (BALOGH KAD. and ÁRVA-SÓS 1983).

6. Hydrothermal metasomatism belonging to Lower Permian-Lower Pannonian subvolcanic-volcanic events found in the whole area of Tisia Composite Terrane.

This succession of metamorphic phases is also proved by the frequency diagram of absolute ages *(Fig. 5)*.

ROCK-TYPES AND ASSOCIATIONS

Due to the above-mentioned deformation system, rocks of the pre-metamorphic idealised rock-column /reviewed in a previous chapter/ transformed into crystalline schists and in some places into granitoids. The *Fig. 6.* shows an idealised crystalline rock-association of Tisia Composite Terrane by two characteristic rock-columns. One of them (A) represents the "Para-autochton" and Drava Terranes, the other (B) does the Szeged-Békés-(Codru) Terrane and Baksa Sub-terrane. A common lithological feature of both

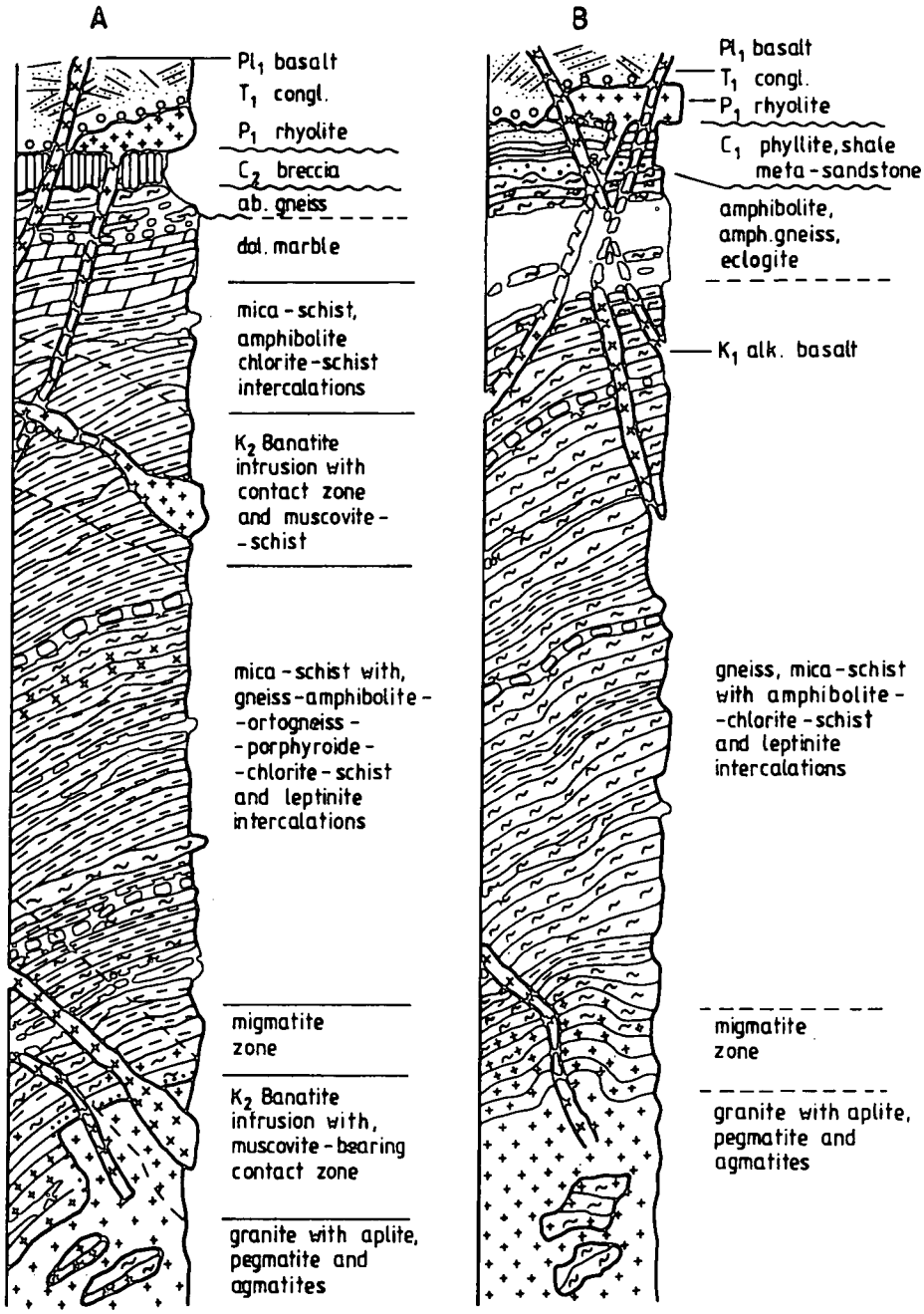

Fig. 6. Idealized rock-column of crystallines of Tisia Composite Terrane. "A" = Szeged-Békés-/Codru/ Terrane, "B"= Para-autochton" and Dráva Terranes

rock-columns can be seen namely existence of palingenetic granite in the lowermost parts of them containing crystalline schist xenolites and aplites and/or pregmatites. Without sharp boundaries 500-1600 m. thick folded migmatite zone covers the granitic bodies which goes into a folded and frequently sheared and /or mylonitized, sometimes fractured very-thick (several thousand m.) gneiss - mica-schist complex. Ratio between alternating gneiss - mica-schist rock-types shows a detectable lateral and vertical variety. So, smaller or larger lithostratigraphically separative gneiss or mica-schist-rich bodies (formation, maybe members) have been designated. Corresponding to the protolith character and metamorphic grade the gneiss - mica-schist complexes is interrupted by from several cm to a few m. thick amphibolite, chlorite-schist, leptinite, marble, dolomite-marble, calc-silicate gneiss intercalations which here and there can be groupped into larger lithostratigraphic units /members or rarely formations/, too.

All rock-units have detectable mineral parageneses with critical minerals and mineral associations as well as observable and determinable isograds and isoreaction-grads (SZEDERKÉNYI 1976, 1984). Difference between two idealised rock-columns is manifested by the existence or the lack of carbonatic rocks and in the frequency of amphibolite bands and finally, in the quality of younger volcanic dykes and subvolcanic intrustions.

TECTOGENESIS

Based on ages, succession of metamorphic events and related deformation characters as well as P-T conditions and existence of special "indicator rocks" (eclogites, blue-schists, ultramafics) the following global tectonic Paleozoic history may be determined in the crystallines of Hungarian part of Tisia Megaunit:

1. 440-400 Ma old (SVINGOR and KOVÁCH 1981) Caledonian event. Its signs are retained in a narrow (5-10 Km. broad) and weakly recovered belt only , located into the geometric axis of "Para-autochton" and Drava Terranes streching from Szeghalom (East Hungary) up to Görgeteg-Babócsa (South Transdanube) traverse. High-pressure low-temperature eclogites at Kőrösvidék (Szeghalom, M.TÓTH 1985) and SE Transdanube (GÖRCSÖNY, RAVASZ-BARANYAI 1969) or several obduced serpentinized ultramafic bodies (SZEDERKÉNYI 1974; GHONEIM and SZEDERKÉNYI 1979; BALLA 1983/ as well as several characteristic amphibolite xenolites enclaved into the northern margin of granite mass of Mórágy Hill (SE Transdanube) postulated a Caledonian suture.

2. 350-330 Ma old (SVINGOR and KOVÁCH 1981, KOVÁCH et al. 1985, BALOGH KAD. et al. 1983) Variscan collisional event can be regarded as culmination of Variscan orogenesis. During this period the accretion of Variscan Europe including the development of crystalline rock-types, associations and lithostratigraphic units were accompanied by mega-, macro- and micro-folding, shearing and blastomylonitization. Forming of palingenetic granite belts at the axial zones of synclinoria happened during the same period; although , the Late Variscan low-pressure and high-temperature effect (late orogenic heating up during 330-270 Ma. period) undoubtedly helped the granitization.

3. Fractures from the main orogenic event are unknown. However, after the granite genesis and before Upper Carboniferous sinking some important fracturing events had taken place, as follows:

– Nappes having unknown vergency. Their remnants are found as Horváthertelend and Szalatnak nappe-vrecks or outliers.

– NW-SE striking trancurrent fault bordering the Drava Terrane eastward,

– Stike-slip faults having ENE-WSW strike (oldest manifestation of so-called Mecsek-alja Belt" as well as Baja-Tázlár-Túrkeve-Nyírábrány fracture) which close into itself Ófalu and Tázlár units as wedges.

Period taking from late Carboniferous up to Lower-Triassic is characterised mostly by epirogenetic movements controlled the evolution of Late Carboniferous and Permian sedimentation. Formations of this process exist as non-metamorphic "overstep" sequences settled mainly on the erosional surface of crystallines.

LITHOSTRATIGRAPHIC CLASSIFICATION AND CORRELATION

It is well-known that conventional stratigraphic methods are unusable in the metamorphic masses because the original signs are considerably or totally destroied and borders of metamorphic units generally cut the pre -metamorphic lihostratigraphic units and alloied them into a single metamorphic one. Acceptably defined smallest metamorphic lihostratigraphic unit which can be marked out with certainity is the formation. Its boundaries coincide to that of pre-metamorphic ones in the very-low and partly in the low-grade metamorphic mass so, criteria referring to the sedimentary lihostratigraphic system can be utilized here. Unfortunately, insignificant minority of rock- units of Tisia Composite Terrane can be classified by this method, only.

In the overwhelming majority of cases – as it was mentioned previously – (mainly medium-high-grade metamorphics) amalgamate a fairly big portion of earlier units. In this situation a new litholigical content develops with new borders and new age which corresponds to the age of last heating. Therefore smallest and acceptable lithostratigraphic unit may be the complex. Idealized rock-columns presented by *Fig. 6.* give an appropriate example of metamorphic complexes. Based on an attempt (being at an advanced stage) the following lithostratigraphic units are realised by the Metamorphic Branch of Hungarian Stratigraphic Committee:

1. Ófalu Phyllite Formation

Meta-greywacke- phyllite- crystalline limestone and interbedded meta-basalt, actinolite-schist, prophyrite and prophyroide form a low-grade metamorphic sequence which is embedded as a wedge into the "Mecsekalja" Tectonic Belt with 40 km length and more than 2 km width. The weakly folded and tilted (sometimes perpedicular) rock-bands are strongly sheared in general, except a few siliceous shale and crystalline limestone intercalations. Silification these latter are attributed a marine volcanic activity running synchronously with the sedimentation. They preserved some uncertain plant-remnants and fossils (Conodont fragments). Carbonised plant-remnants are supporting tissue relics derived from botanically fairly well-developed plants (KEDVES and SZEDERKÉNYI 1996) so, age of the protoliths can be ranged about into Upper Silurian (not older) epoch. Strongest shearing took place at the northern margin of the formation and due to a considerable friction-heat and related potassium metasomatism a weak melting developed in it.

2. Ófalu Serpentinite Formation

Within the Ófalu Phyllite Formation near Ófalu a small (12 m wide and about 100 m long) nearly perpendicular serpentinite body is wedged into the meta-greywacke along fracture zones. It is interpreted as an obduced lower lithosphere remnant (BALLA 1983)

and this grey-coloured rock-association shows a lherzolite origin (GHONEIM and SZEDERKÉNYI 1979).

3. Gyód Serpentinite Formation

It consists of two of same size occurrences which are regarded as two separated 5-6 km long and 600-700 m wide lithostratigraphic members: (1) Helesfa serpentinite and talc-schist association forms a nearly perpendicular lens-like body wedged into the Variscan granite along broad shearing zones filled by talc-rich metamorphics penetrated by numerous metasomatized aplite dikes not only in the shearing zones but in the serpentinite body, too. This latter consists of sheared and perfectly serpentinized harzburgite showing diapiric structure (SZEDERKÉNYI 1974, 1977). (2) The Gyód member occupies a perpendicular position at the northern margin of the Baksa Sub-terrane but whitin it. Its country-rocks are medium-grade crystalline schist belonging to the Baksa Complex. No traces of shearing are observable, thus the process of serpentinization is not so perfect as it is in the Helesfa serpentinites. In a central narrow plane a less serpentinized harzburgite zone is retained. According to BALLA (1983) both members of the Gyód Serpentinite Formation can be regarded as obduction wedges.

4. Görcsöny Eclogite Formation

A weakly investigated formation located into the Baksa Sub-terrane near its northern margin . It consists of retrograde "symplectite". Its size and extensions are unknown (RAVASZ-BARANYAI 1969). Based on analogies, it looks like to belong to high-pressure low-temperature eclogites written by M.TÓTH (1995) near Szeghalom (East Hungary).

5. Szalatnak Shale Formation

It is comprised by strongly and complicatedly folded two dark-grey shale occurrences separated from each-other: Szalatnak body can be found in the Eastern Mecsek Mts. and the Horváthertelend one is in Western Mecsek. (1) At the Szalatnak the rock-column is subdivided into three lithostratigraphic members, two shale ones and a 80 m thick basalt agglomerate member between them. More than 1500 m thick sequence is underlain by Mórágy Granite Formation. Thin siliceous shale stripes are characteristic in the shale members and several anthracite-like intercalations also occur mainly in the lower member containing characteristic Llandoverian Conodont fauna (KOZUR 1984) and Garptolite fragments (ORAVECZ 1964). Whole rock-mass suffered a very-low grade metamorphism (prehnite-quartz facies, SZEDERKÉNYI 1974) which turns into a low-grade one (ÁRKAI et al. 1996) in the lower part of the rock-column. This formation extends about on 200 km^2 area covered by Permian and/or Lower Triassic sandstones and it tectonically is regarded as a Late Variscan nappe-vreck having unknown vergency. During the Carboniferous (before the nappe movements) a small (about 1 km large) syenite-porphyry intrusion (Szalatnak Syenite-porphyry Formation) invaded into the lower member causing a fractured and hardly examined thin contact aureole in it. (2) Exactly the same shale and similar nappe-outlier can be found at the western frame of Mecsek Mts. covered by Badenian sediments near Horváthertelend, but it is not studied yet in detail..

6. Szalatnak Syenite-porphyry Formation

A small (about 1 km^2 large) hypabissal (nearly subvolcanic) intrusion of a grey, coarse-grained holocrystalline syenite-granodiorite body which caused a few m thick fractured contact aureole. Its Rb/Sr ages (SVINGOR and KOVÁCH 1981) show a Variscan late

kinematic origin (328-310 Ma.). The geochemical character differs from that of Mórágy granite postulating an intrusion preceeded the Carboniferous nappe movements.

7. Babócsa Complex

It is bordered by Middle Hungarian Lineament NW-ward and NW-SE striking transcurrent fault located between "Para-autochton" and Drava Terranes as well as the fracture bordering the Villány Mts. westward. Southward this complex extends over Croatian area. Areal extension in the Hungarian side is larger than 1000 Km^2. It consists mostly of medium-grade gneiss with subordinate mica-schist and amphibolite intercalations, which latter is generally mylonitized. Its idealized rock-column is the same as *Fig. 6B*. Apart from an uncertain Caledonian datum (JANTSKY 1979) double Variscan metamorphic phases are recognised. The first one is represented by a Barrow-type deformation having P=6-9 Kb pressure and 17-27 °C/km thermal gradients, the second one is an andalusitic higher temperature {34°C/km thermal gradients} phasis (ÁRKAI 1984; TÖRÖK 1989). Overstep sequence above the crystallines is a Late Carboniferous molasse.

8. Baksa Complex

It gives the crystalline floor of Villány Mts. and its northern foreground up to the Mecsek Mts.. Its SW border is manifested in the fracturing zone which coincides with transcurrent fault located between "Para-autochton" and Drava (KASSAI 1977). Petrographically this complex consists of a weakly-folded migmatite - gneiss - mica-shist - marble - dolomite marble-calc-silicate gneiss association characterised by a remarkable isograde system showing zones and isograds from sillimanite up to chlorite with a south-west progressivity trend (SZEDERKÉNYI 1976). Its idealized rock-column is the same that of *Fig.6A*. (without banatites)

Thickness of this complex exceeds 10 km. Two 250 m and 25 m thick marble and dolomite marble members are characteristic in the sillimanite zone accompanied by fairly thick (23-30 m) amphibolite beds. Near Gyód locality an obduced (BALLA 1983) and partly serpentinized ultramafic body is wedged into this complex (Gyód Serpentinite Formation). North of this body a formerly mentioned single eclogite (now symplecite) occurrence (RAVASZ-BARANYAI 1969) as well as a characteristic high temperature overprinting with andalusite in the northern margin of the complex are found (LELKES-FELVÁRI and SASSI 1983) showing at least three phases of the polymetamorphism altogether. Upper Carboniferous (Vestphalian) coal-bearing molasse covers the Baksa Complex as overstep sequence.

9. Mórágy Complex

It consists of Mórágy -Kecskemét granite range and accompanied migmatite - gneiss - mica-schist flanks on its both sides. Its idealized rock-column is perfectly same that of *Fig. 6B*. Most characteristic part of the complex is the granite range itself. Forming a not-too broad axial stripe of an ENE-WSW striking synclinorium zone, the granite body forms an about 200 km long and 25-30 km broad continuons belt beginning at Szigetvár (South Trandanubia) and near Szolnok which disappears below the Upper Cretaceous-Paleogene flysch complex (JANTSKY 1979). It is composed petrographically by porphyroblastic granite-granodiorite mass with biotite and/or amphibole-rich xenolites. The latter show 440-400 Ma Rb/Sr ages (SVINGOR and KOVÁCH 1981; KOVÁCH et al. 1985) suggesting a Pre-Variscan (Caledonian?) deformation but it requires further confirmation. These

granites are S-type mixed meta and peraluminous syn-collisional rocks (BUDA 1981, 1985, 1995). Forming wings of the synclinorium it is accompanied by crystalline schists showing typical polimetamorphism. In the first phase of Variscan deformation a Barrow-type event had taken place with P= 6-8 Kb pressure and 14-26 °C/km thermal gradients extending over whole area of Tisia Composite Terrane (SZEDERKÉNYI et al. 1991). In the second phase a low-pressure high-temperature retrogression was characteristic along the Mecsekalja Tectonic Belt and the eastern continuation of Mecsek Mts. (Vajta, LELKES-FELVÁRI et al. 1989) with late kinematic (322 Ma old) andalusites. Overstep sequences are Permian and/or Lower Triassic sandstones.

10. Tázlár Phyllite Formation

About 15 km long and 300 m wide double bodies are wedged into the gneisses of Mecsek -North Plain Sub-terrane by a NE-SW striking fault zone in the central area of the Danube-Tisza interfluve. Not more than 300 m thick greenish-grey coloured carbonate-phyllite with black graphitic phyllite stripes gives the rock-content of these bodies. Their age is uncertain; according to FÜLÖP (1994) it may be Early Palaeozoic or Early Carboniferous.

11. Kőrös Complex

It is comprised by crystallines of Middle Plain Sub-terrane and bordered by Baja-Túrkeve-Nyírábrány fracture zone northward, South-Hungarian Nappe Belt southward. Its eastern border is found somewhere at the Transylvanian Apuseni Mts. Its rock-column is perfectly same that of *Fig. 6B.* Similarly to the Mórágy Complex a more than 250 km long and narrow not continuous granite range (embedded into 15-20 km wide migmatite belt) forms axial zone of the complex. Within the range five 5-10 km wide and 15-25 km long granite bodies settled along the Jánoshalma-Jászszentlászló-Endrőd-Füzesgyarmat-Kőrösszegapáti traverse represented by S- and I-types porphyroblastic biotite granite-granodiorite rocks (BUDA 1985, 1995) which form at once synclinorium axis, too. Similarly to that of Mórágy Complex this granite-migmatite range is accompanied by medium-grade gneiss – mica-schists – amphibolite associations in both sides as flanks of an ENE-WSW striking synclinorium. Apart from the previously mentioned complexes, these crystallines show double-facial progressive metamorphism, only. The first is the Caledonian(?) phasis appearing along Szeghalom-Szarvas-Szank-Ófalu-Helesfa traverse in 5-10 km broad zone as a presumed suture. The second one is the Variscan Barrow-type deformation (medium-pressure and temperature P-T circumstances and 350-330 Ma isotope age). Phasis marked by andalusite is perfectly missing from the metamorphic history of Kőrös Complex.

12. Álmosd Formation

Low-grade chlorite schist-two mica-schist and graphite-bearing biotite schist association forms an Upper Cretaceous nappe outlier (on about 20 km^2 area) thrusting over the metamorphics of Kőrös Complex at the Romanian-Hungarian border. It has N-W vergency and it genetically is same as low-grade metamorphics of Szeged-Békés-(Codru)-Terrane i.e. South Hungarian Nappe Belt.

13. Kelebia Complex

It is the westernmost sub-unit of Szeged-Békés-(Codru) Terrane which is bordered by the nappe boundary west- and northward, Ásotthalom-Bordány sinking eastward. It extends over Yugoslavian area southward. Covered by Lower Permian rhyolitic and/or

Lower Triassic red-beds low-and medium-grade strongly-folded two-mica-schists sometimes chlorite schists form the metamorphic rock-mass in unknown thickness. The mentioned Barrow-type Variscan metamorphic phasis and contact zones of several small banatite intrusions and dykes near Kunbaja and Kelebia characterize the metamorphism. Its idealized rock-column is the same as *Fig. 5A.* without marble and variscan granitoids.

15. Tisza Complex

It is bordered by nappe boundary northward and the Ásotthalom-Bordány sinking westward and so-called "Makó trough" eastward. Southern border is found somewhere in the Yugoslavian Bačka area. Its idealised rock-column is presented on the *Fig. 6A.* A characteristic peculiarity is a 200 m thick marble-dolomite marble member near Kiskundorozsma (Szeged) as the single carbonatic rock-association in the crystalline basement of Great Plain. Besides these marbles a small deep- plutonic granite occurrence and related migmatites (near Deszk) as well as medium-grade slightly folded gneiss - mica-schist alternation are also typical in the whole South Hungarian Nappe Belt {Szeged-Békés-(Codru) Terrane}. 350-330 Ma old first Variscan (Barrow-type) phasis with P= 6-8 Kb pressure and 500-570°C temperature as well as 330-320 Ma old second Variscan phasis with blastomylonitization and third, late kinematic 320-315 Ma old high-temperature and low-pressure retrogression (P= 3-4 kb pressure and T= 580-600°C temperature) and finally Upper Cretaceous banatite magmatism and related contact metamorphism as main metamorphic events are characteristic. The latter is comprised by small elongated intrusions and relatively broad (400-600 m) accompained tourmaline-rich muscovite schist aureoles near Ferencszállás and Kiszombor with ENE-WSW strike (SZEDERKÉNYI 1984; SZEDERKÉNYI et al.1991). Overstep sequences are Lower Triassic red-beds.

16. Battonya Complex

In the Hungarian section it consists of 15–25 km long and 10–15 km wide body (stretching over Romania and Yugoslavia) represented mainly of by granite and a few associated migmatite and crystalline schists. Boundaries are Makó "Trough" westward, Békés Basin eastward and the nappe boundary nortward. Porphyroblastic orthoclase-biotite granite and associated enclaves give the predominant portion of deep-plutonic body. Beginning from Yugoslavian Bačka and finishing in the Transylvania Apuseni Mts. this granite similarly to the Mórágy Complex also form a more than 150 km long and not too broad continual range. Contrary the Mórágy mass the magma of this deep-plutonic granite body at Battonya-Mezőhegyes after an in situ melting moved a little upward as an intrusion during the phasis of Variscan late kinematic movement period (SZEPESHÁZY 1969; SZEDERKÉNYI 1984; KOVÁCH et al. 1985). All deformational and age data are the same that of Tisza Complex. Overstep sequence is the Lower Permian molasse.

17. Sarkadkeresztúr Complex

It is an isolated 15 km long and 5 km wide crystalline basement – high uplifting on the eastern side of Békés Basin having a W-E elongation it consists of light-grey diatexite and subordinately porphyroblastic orthoclase-biotite granite. In both side of the high they are accompanied by medium-grade gneiss - mica-shist - amphibolite association showing the same deformational and time characters that of Tisza Complex (SZEDERKÉNYI 1984).

18. and 19. Vilyvitány mica-schist and Füzérkajata Porphyroide Formations

Being apparently isolated from the main mass of the Tisia Composite Terrane (no boreholes in the basement of Upper Cretaceous-paleogene flysch-trough are available), so, the character of their deformation and isotopic ages as well as tectonic considerations and overstep sequences can show that these units may belong to the Tisia, but based on newer petrological and tectonic interpretations carried out by VOZÁROVÁ and VOZÁR (1987) they are ranged now into the Tatra-Vepor Unit of Western Carpathians.

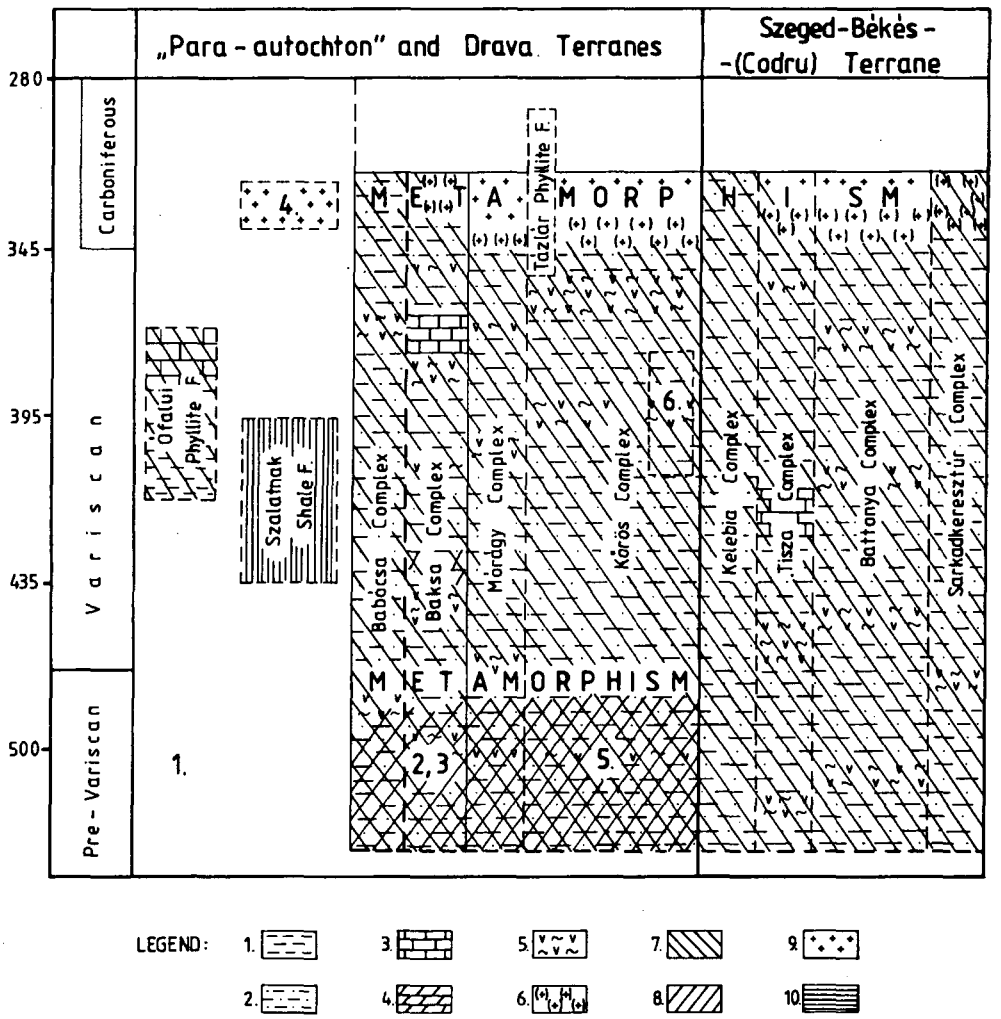

Fig. 7. Lithostratigraphic table of crystallines of Hungarian part of Tisia Composite Terrane. Legend: /1/= pelite, /2/ =greywacke, /3/= limestone, /4/= dolomite, /5/ basic lava, tuff, /6/= migmatite, /7/= Variscan deformation , /8/ Pre-Variscan deformation, /8/ granitoide intrusion, /10/ slate.

Lithostratigraphic table of complexes and formations are presented by *Fig.7* shows perpendicular and lateral relationships among the units of Tisia Composite Terrane. This table differs strongly from those ones which are compiled for sedimentary formations. Difference appears mainly in the block-like construction. Due to considerable burial, recovered, kown unit-borders are rather rare in our metamorphics and it causes serious difficulties in the recognition and delineation of heteropic units. Thus, the characters of lateral relationships can not be presented, moreover, inside a rock-column an authentic presentation of a succession is also not easy.

The lithostratigraphic table *(Fig.7)* tries to display together the quality of metamorphics and the tectono-metamorphic cycles in the time in continual rock-columns which are beginning at the age of protolith and finishing at the time of last progressive metamorphic event. It seems to be expedient to record the time scale of Earth history, too. The lithological content is presented by conventional signs and the metamorphism by shade-lines. The shade-lines can extended to the whole rock-column which means in this case that each rock of the rock-column suffered metamorphism. Age of metamorphic event can be red from the position of the "metamorphism" notice. The outliers (nappe remnants and tectonic wedges) are sitting in "empty space" in the lithostratigraphic table (because their parent-complexes are unknown), or in the rock column of receptor unit.

One sub-terrane in the lithostratigraphic table corresponds to one complex. Units of Drava- and "Para-autochton" Terranes occupy a relatively autochton situation compared to that of Szeged-Békés-(Codru) Terrane, i.e. they are "Para-autochtonous" and contrary the latter they collect themselves into an independent group isolated from the "nappe complexes and formations".

Lateral relationships of metamorphic lithostratigraphic units are clearly expressed in the global identity of protholits and metamorphic character as well as culminating time of metamorphic phases together with migmatization and palingenesis. Apart from the outliers some essential differences are existing between two main groups of lihostratigraphic table which are manifested in the follows:

– Pre-Variscan deformation can be detected in the para-autochtonous terranes, exclusively.

– Variscan late kinematic heating (andalusite mineralization) occurs first of all in the nappe units.

– Upper Cretaceous contact metamorphism in Hungarian area of Tisia Megaunit (belonging to the banatitic intrusions) occured in the nappe units, only.

ACKNOWLEDGEMENT

Many thanks to the National Scientific Fund (OTKA) for the financial support of this research-work.

REFERENCES

ÁRKAI, P. (1978): A Tázlára terület metamorfitjainak leírása. (Description of metamorphics of Tázlár Area.) Manuscript in Hungarian. Kézirat. MOL Adattár, Szolnok.

ÁRKAI, P., LANTAI, CS., LELKES-FELVÁRI, GY., NAGY, G. (1996): Biotite in a Paleozoic metagreywacke complex, Mecsek Mts, Hungary: conditions of Low-T metamorphism deduced from illite and chlorite crystallinity, coal rank, white mica geobarometric and microstructural data. Acta Geol. Hung. Budapest (in press).

BALLA, Z. (1982): Development of the Pannonian Basin basement trough the Cretaceous-Cenozoic collision: a new synthesis. Tectonophysics. **88**, 61-102.

BALLA, Z. (1983): A Dél-dunántúli ultrabázitok lemeztektonikai értelmezése. (Tectonic interpretation of South-Transdanubian ultramafics). In Hungarian . Földt. Közl. **113**, 39-56.

BALOGH, KAD., ÁRVA-SÓS , E., BUDA, GY. (1983): Chronology of granitoid and metamorphic rocks of Transdanubia (Hungary). Ann. Inst. Geol. Geofiz. **61**, 359-364. Bukarest.

CSONTOS, L. , NAGYMAROSI, A., HORVÁTH , F. KOVÁC M. (1992): Tertiary evolution of the intracarpathian area: a model. Tectonophysis **208**, 221-241.

FÜLÖP, J., DANK, V. et. al (1987): Magyarország földtani térképe a kainozoikum elhagyásával. M: 1:500.000. (Geological map of Hungary without Cenozoic. M:1:500.000) Hung. Geol. Survey. Budapest.

FÜLÖP, J. (1994): Magyarország Geológiája: Paleozoikum II. (Geology of Hungary: Palaeozoic II). Academia Kiadó, Budapest.

GHANEM, M.A.E., RAVASZ-BARANYAI, L. (1969): Petrographic study of the crystalline basement rocks, Mecsek Mts., Hungary. Acta Geol. Ac.Sci. Hung. **13**, 191-219.

JANTSKY, B. (1979): A mecseki gránitosodott alaphegység földtana. (Geology of granitized crystalline basement of Mecsek Mts.) Annales of Hung .Geol. Survey. **60**, 1-3 1-385.

KEPPIE, J.D., DALLMEYER, R.D. (1990): Introduction to terrane analysis and the tectonic map of Pre-Mesozoic terranes in Circum-Atlantic Phanerozoic orogens. Abst. Vol. IGCP Project 233 Meeting. 24-27. Göttingen

KOBER L. (1921): Bau der Erde. Wien.

KOVÁCH, Á., SVINGOR. É., SZEDERKÉNYI, T. (1985): Rb-Sr dating of basement rocks from the southern foreland of the Mecsek Mountains, Southern Transdanubia, Hungary. Acta Miner. Petr. Szeged. **XXVII**, 51-56.

KOVÁCS, S. (1982): Problems of the "Pannonian Median Massif" and the plate-tectonic concept. Geol. Rundschau. **71**, 617-638.

KOVÁCS, S., SZEDERKÉNYI T., ÁRKAI P., LELKES-FELVÁRI, GY., BUDA GY., NAGYMAROSI, A. (1996): Explanation to the terrane map of Hungary. Final Vol. of. Rep. of IGCP Project No. 276. Athens-Padova (In press)

KOZUR, H. (1994): Muellerisphaeria eine neue Ordung von Mikrofossilien umbekanuter systematischer stellung aus dem Silur und Unterdevon von Ungarn. Geol. Pal. Mitt. Innsbruck, **13**/16, 125-148.

LÓCZY, L. sen. (1918): Magyarország földtani szerkezete (A Magyar Szent Korona Országainak leírása) (Geological structure of Hungary. Description of Countries of Hungarian St. Crone). In Hungarian. Budapest.

M. TÓTH, T.: (1995): Retrograde eclogite in the crystalline basement of the Kőrös Unit, Hungary. Acta Miner. Petr. Szeged. **XXXVI**, 117-129.

ORAVECZ, J. (1964): Szilur képződmények Magyarországon (Silurian formations in Hungary) In Hungarian. Földt. Közlöny. **94**, 3-9.

PRINZ, GY. (1914): Magyarország Földrajza. A magyar föld és életjelenségeinek leírása.(Geography of Hungary Description of Hungarian and its life) In Hungarian, Budapest.

RAVASZ-BARANYAI, L. (1969): Eclogite from the Mecsek Mountains, Hungary. Acta Geol. Ac.Sci, Hung., **13**, 315-322.

SZEDERKÉNYI, T. (1974 a): Paleozoic magmatism and tectogenesis in Southeast Transdanubia, Hungary. Acta Geol. Ac Sci. Hung. **18**, 305-313.

SZEDERKÉNYI, T. (1974 b): A DK-dunántúli paleozoós képződmények ritkaelem kutatása. (Rare-element investigation of Paleozoic complexes of southeast Transdanubia) In Hungarian. PhD Theses. MTA Library. Budapest.

SZEDERKÉNYI, T. (1976): Barrow-type metamorphism in the crystalline basement of southern Transdanubia. Acta Geol. Hung. **13**, 27-34.

SZEDERKÉNYI, T.: (1977): Geological evolution of South Transdanubia (Hungary) in Paleozoic time. Acta Miner. Petr. Szeged, **XXIII**, 3-14.

SZEDERKÉNYI, T. (1983): Origin of amphibolites and metavolcanics of crystalline complexes of South Transdanubia, Hungary. Acta Geol. Hung. **26**, 103-136.

SZEDERKÉNYI, T. (1984): Az Alföld kristályos aljzata és földtani kapcsolatai. (Crystalline basement of the Great Plain and its geological connections). In Hungarian. Dr. Sc. Diss. MTA Library, Budapest.

SZEDERKÉNYI, T., ÁRKAI, P. , LELKES-FELVÁRI, GY. (1991): Crystalline groundfloor of the Great Hungarian Plain and South Transdanubia, Hungary. (In Geodynamic Evolution of the Pannonian Basin). Serb. Ac. of Sci. Arts.Ac.. Conferences **LXII**. Dept. of Nat. and Mat. Sci. **4**, 261-273. Belgrade.

SZEPESHÁZY, K. (1969): Kőzettani adatok a battonyai gránit ismeretéhez. (Petrographic data for the Battonya granite). In Hungarian. Ann. Rep. of Hungarian Geol. Survey from 1967, 227-266.

TÖRÖK, K. (1983): Fluid inclusion study of the gneiss from the borehole Nagyatád K-11, SW Transdanubia , Hungary. Acta Miner. Petr. Szeged. **XXX**, 115-126.

VOZÁROVÁ, A., VOZÁR, J. (1987): West Carpathian Late Paleozoic and its paleotectonic development. In: FLÜGEL, H.W. SASSI, F. P., GRECULA, P.: Pre-Variscan and Variscan Events in the Alpine Mediterranean Mountain Belts. 469-487. Bratislava.

Manuscript received 17 Aug. 1996

Acta Mineralogica-Petrographica, Szeged, XXXVII, 161–164, 1996

THE AGE OF THE SO-CALLED "BOSTONITE" ROCKS OF MÓRÁGY HILL, S-HUNGARY

CS. SZABADOS[1]

Department of Mineralogy, Geochemistry and Petrography
Attila József University

E. ÁRVA-SÓS[2]

Institute of Nuclear Research of the Hungarian Academy of Sciences

ABSTRACT

MAURTTZ and CSAJÁGHY (1952) could not define exactly the data of consolidation and the genetic origins of the rocks found in the Mórágy granite and which was named "bostonite" by them. These questions have not been answered since that. K/Ar isotopic age of these rocks may reflects that the consolidation happened parallely to that of the rocks of the Early Cretaceous alkaline volcanism.

INTRODUCTION

The greenish coloured dyke rocks of Kismórágy quarries were mentioned firstly by RÓTH (1876) and he named them as "diabas-diorite". They were perhaps "bostonites". This reddish-coloured dyke rocks which were characterized petrographically by MAURITZ and CSAJÁGHY (1952) on the basis of their mineral composition and major element content were already regarded bostonites and the products of granitoid magmatism or the Early Cretaceous volcanism. The rocks which resemble the feldspar rich rocks described by MAURITZ (1952), and which are called "bostonites" are rendered by researches into three lithostratigraphic units, as follows:

1. The Mórágy Complex (Early Carboniferous)
2. The Gyűrűfű Rhyolite Formation (Early Permian)
3. The Mecsekjános Basalte Formation (Early Cretaceous)

1. Post-orogenetic rocks which are joint up to aplitic rocks:

– On the basis of the rock-material of boreholes of the Mecsek Mts. and the petrographic characters of the dyke rocks of Mórágy Hill (GHANEM and RAVASZ-BARANYAI, 1969; JÁRÁNYI, 1970; HETÉNYI and RAVASZ-BARANYAI, 1973).

– On the basis of REE content of these rock types (PANTÓ, 1980).

[1] H-6701 Szeged, P. O. Box 651, Hungary
[2] H-4001 Debrecen, P. O. Box 51, Hungary

2. These rock types have a Paleosoic age:

BARABÁS and IMREH (1956) found "bostonite" like pebbles in the Upper Permian and Upper Triassic sandstones. They raised the idea of two different genesis of bostonitic rock. VADÁSZ (1960) admitted it.

3. These rocks of Mórágy Hill are products of the Early Cretaceous alkaline volcanism.

– On the basis of petrographical-petrological researches (JANTKSY 1950, 1979; CSALAGOVITS 1964; FORGÓ et al. 1966; SZEDERKÉNYI 1974; BILIK 1979; HARANGI 1990, 1993; HUEMER 1993).

– On the basis of Rb/Sr ages (142-143±20 Ma by SVINGOR and KOVACH 1978).

– On the basis of K/Ar ages (108-110±5 Ma by ÁRVA-SÓS et al. 1979, 1987, 1992).

RESULTS

The investigated rocks occur as dykes in the granite. Therefore, determination of their lithostratigraphic age is impossible.

The K/Ar isotopic age determination is the prepared and carried method in the ATOMKI, Debrecen, which is well aplicable in the igneous and methamorphic rocks. However, we usually get more exact K/Ar ages from the separated minerals of the fresh rock (e. g.: amphibole and micas) which keep the Ar well. The K/Ar isotopic ages of feldspathoid rocks reflect on the data of their consolidation or, since the feldspars have a low retaining capacity of the Ar, it reflects the date of the latest tectonic or thermal event which "rejuvenated" the rock.

Three new K/Ar data of the whole rock and also on the separated feldspar minerals together with the three previous data clearly yield that the age of the reddish-coloured trachyte dyke rocks is between 106–118 million years. This may mean that the consolidation of these rocks happened parallely to that of the rocks of the Early Cretaceous alkaline volcanism. Since those rocks which were little altered only and had relatively high retaining capacity, they could not lose much Ar, therefore these ages are acceptable (Table 1.).

Our research includes the first K/Ar data of the trachyandesites of Kismórágy. Both yielded a younger age than that of the trachytes. The average age (95 Ma) coincides with the Austrian orogen activity. It is possible that the K/Ar isotopic age shows the last tectonic effect. In this case the K/Ar isotopic data of the every rock type of this area should shows this the average (95 Ma). However, the K/Ar datum of the reddish-coloured trachyte dyke is 118 Ma in Kismórágy quarry No. 3. It is nearest to that of the trachyandesite rocks of Kismórágy quarry No. 5. Because we don't believe that different secondary effects happened in this territory, therefore the younger K/Ar data of trachyandesites as compared to trachytes may have been formed in two possible ways:

– the trachyandesite rocks are product of a younger volcanic event, or

– these younger data are the result of a strong decomposition and Ar-loss of the rock, therefore, the age of these rocks so to say grown younger again.

Petrographical characteristics of trachyandesite rocks shows strongly altered features. Therefore this second hypothesis is acceptable.

The K/Ar data of the trachytic and trachyandesitic rocks (so-called bostonitic rocks) are shown by Table 1.

TABLE 1

LOCALITY, ROCK TYPE	FRACTION	K-CONT %	$^{40}Ar_{rad/g}$ (ncm^3/g)	$^{40}Ar_{rad}$ %	AGE (Ma)
Mórágy trachyte	w. r.	4.83	$2.1944x10^{-5}$	93.3	113.3±4.3
Kismórágy q. No. 3. trachyte	w. r.	4.151	$1.9655x10^{-5}$	65.9	118.0±4.7
Ófalu-Aranyos-v. trachyite	K-feldspar M < 0.16 mm	4.62	$2.0322x10^{-5}$	78.1	109.9±4.2
Kismórágy q. No. 5. trachyandesite	w. r. acetous	5.07	$1.8891x10^{-5}$	73.6	93.5±3.6
Kismórágy q. No. 6. trachyandesite	w. r. acetous	7.179	$2.7904x10^{-5}$	75.5	97.4±3.8

Previous measurement of K/Ar

Ófalu "bostonite"	w. r.	4.21	1.821	82.0	106+7
	w. r.	4.21	$1.950x10^{-5}$	95.0	113+7
Mórágy "bostonite"	w. r.	4.67	$2.074x10^{-5}$	90.0	108+6

REFERENCES

ÁRVA-SÓS E. (1979): K-Ar módszeres kormeghatározások a Mecsek hegységből. Egyetemi doktori értekezés. Manuscript, Debrecen.

ÁRVA-SÓS E., BALOGH K., RAVASZ-BARANYAI L., RAVASZ CS. (1987): Mezozóos magmás kőzetek K/Ar kora Magyarország egyes területein. MÁFI Évi Jel. az 1985. évről, 295–307.

ÁRVA-SÓS E., RAVASZ-BARANYAI L. (1992): A Mecsek és Villányi hegység között feltárt kréta telérkőzetek K/Ar kora. MÁFI Évi Jel. az 1990. évről, 229–240.

BARABÁS A. (1956): A mecseki perm időszaki képződmények. Kandidátusi értekezés. Manuscript, Budapest.

BILIK I. (1979): A Mecsek hegység alsókréta tengeralatti vulkáni képződményei. Egyetemi doktori értekezés. Manuscript, Budapest.

CSALAGOVIS J. I. (1964): De la palingenése calédonienne et des rapports de grande tectonique du Massif de socle cristallin du Sud du Bassin Pannonien (Cisdanubie). Ann. Hist. Nat. Mus. Nat. Hung., Min.-Pal., **56**, 31–54.

FORGÓ L., MOLDVAY L., STEFANOVITS P., WEIN GY. (1966): Magyarázó Magyarország 200000-es földtani térképsorozatához. L-34-XIII. Pécs. MÁFI

GHANEM M. A. E. A., RAVASZ-BARANYAI L. (1969): Petrographic study of the crystalline basement rocks, Mecsek Mountains, Hungary. Acta Geol. Acad. Sci. Hung. **13**, 191–219.

HUEMER H. (1993): Geochemie und Petrogenese der kretazischen Vulkanite im östlichen Mecsek-Gebirge (Süd-Ungarn). PhD. thesis. Manuscript, Bécs.

HARANGI Sz. (1990): A kelet-mecseki alsókréta vulkáni kőzetek geokémiai jellegei (Sokváltozós matematikai módszerek alkalmazása magmás geokémiai vizsgálatokban). Egyetemi doktori értekezés. Manuscript, Budapest.

HARANGI Sz. (1993): A Mecsek hegység alsókréta vulkáni kőzetei. Kandidátusi Értekezés. Manuscript, Budapest.

HETÉNYI R., RAVASZ-BARANYAI L. (1973): A baranyai antracittelepes felsőkarbon összlet a Siklósbodony 1. és a Bogádmindszent 1. sz. fúrás tükrében. MÁFI Évi Jel. 1973. évről. 323–361.

IMREH L. (1956): A mecseki felsőtriász homokkőösszlet felső részének kőzettani vizsgálata. MÁFI Évkönyve **45**, 53–72.

JANTSKY B. (1950): A mecseki kristályos alaphegység földtani viszonyai. MÁFI Évi Jel. az 1950. Évről, 65–77.

JANTSKY B. (1979): A mecseki gránitosodott kristályos alaphegység földtana. MÁFI Évkönyv **LX**. 30, 147, 150.

JÁRÁNYI K. (1970): A Mórágy környéki gránitoid kőzetek vizsgálata, különös tekintettel a gránitosodás folyamatára. Szakdolgozat. Manuscript, ELTE, Budapest.
KISS J. (1962): A hydrothermal environment of Pb-Zn-Cu in the Erdősmecske granite. Annales U.S.B.d.R.E. Tomus V.
MAURITZ B., CSAJÁGHY G. (1952): Alkáli telérkőzetek Mórágy környékéről. Földt. Közl. **82**, 137–142.
PANTÓ Gy. (1980): Rikaföldfémek geokémiája és néhány alkalmazási területe. Doktori értekezés. Manuscript,, MTA Könyvtár, Budapest 101–121.
RÓTH S. (1876): Fazekasbodai-mórágyi hegylánc (Baranymegye) eruptív kőzetei. Magyar Kir. Földt. Int. Évkönyve **IV/3**.
SZABADOS Cs. (1996): Bostonit-e a mórágyi bostonit. Földtani Közlöny, in press.
SZABADOS Cs. (1996): Petrological characteristics of the so-called "bostonite" rocks of Mórágy Hill, Mecsek Mts., S-Hungary. Workshop "Magmatic Events in Rifted Basins" under the aegis IGCP Project No. 369., Budapest. In abstract.
SZABADOS Cs. (1996): Petrological characteristics of the so-called "bostonite" rocks of Mórágy Hill, Mecsek Mts., S-Hungary. Acta Geologica Hungarica. In press.
SZAKMÁNY Gy., JÓZSA S. (1994): Rare pebbles from the miocene conglomerate of Mecsek Mountains, Hungary. Acta Miner. Petr. Szeged **XXXV**, Supplementum, 53–64.
SVINGOR É., KOVÁCH Á. (1978): A Mecsek hegységi bosztonit kora Rb/Sr kormeghatározások alapján. Földt. Közl. **108**, 94–96.
SZEDERKÉNYI T. (1974): A délkelet-dunántúli ópaleozóos képződmények ritkaelem kutatása. Kandidátusi értekezés. Manuscript, MTA Könyvtár.
VADÁSZ E. (1960): Magyarország földtana. Akadémiai Kiadó (2. kiadás) Budapest.

Manuscript received 6. Sept. 1996.

Acta Mineralogica-Petrographica, Szeged, XXXVII, 165–180, 1996

PETROGRAPHIC STUDY ON JURASSIC PROFILE NEAR MÁRIAKÉMÉND VILLAGE, SOUTHERN BARANYA HILLY COUNTRY, S HUNGARY

BÉLA RAUCSIK

University of Attila József, Department of Mineralogy, Geochemistry and Petrology*

ABSTRACT

On the basis of the study on profile of the quarry near Szederkény village between the Mecsek and the Villány Mountains, it can be stated that it is mostly built up by slope facies formations. Presumably, there was a near subaerial, shallow marine facies that supplied the bioclast material (mostly crinoid calcarenite) getting the slope. Pelitic sediments with siliceous sponge and pelagic planktons were formed during the periods of rest between the given sediment transports.

By the characters of the sedimentation this sequence can be divided into three parts, and, within these, two zones formed by intensive gravitational transport can be interpreted. These zones are characterised by crinoid allodapic limestone, lithoclastic limestone and calcareous marl. Other parts of the sequence are also dominated by slope facies. However, the open marine pelitic sediment is also important as a consequence of the more moderated intensity of the transportation.

Three facies of the Upper Liassic-Lower Dogger sequence in the Mecsek Mountains (the plateau facies Pusztakisfalu Limestone, the basin facies Komló Calcareous Marl, and the intermediate slope facies) probably coexisted for long time: interdigitation and closed connection of their formations are characteristic for this period.

INTRODUCTION

Between the Villány and the Mecsek Mountains – in the area of the Southern Baranya Hilly Country – formations of the basement crop out in some places. First works about the area – PETERS (1862), SZABÓ (1867), LENZ (1872) – were only outlined description of rocks exposed in the quarries that were intensively mined at that time. By some fossils SZABÓ (1867) and LENZ (1872) regarded the beds to be Liassic and Upper Jurassic, respectively. The first more detailed description can be found in the report of LÓCZY Jr. (1912). Summarising the tectonic arguments, he brought the outcrops covered by loess and included by the E-W hill range into connection with the SE end of the Mecsek Mountains. According to him, strike of the beds is NNE, their inclination is 312/15°, and their age is Middle Liassic. On the basis of the former published fossils and analogy of rocks near Ófalu village, VADÁSZ (1913) dated the outcrops as Lower Dogger. According to him in Máriakéménd village grey and yellowish cherty-sandy layers "with crinoid-like forms" are exposed. In his classic monograph of ammonites in Villány Mountains, LÓCZY Jr. (1915) mentioned petrified tree-trunk remains in this area. He supposed the original environment to be alongshore facies, and he concluded that rock material of the "blocks" deposited in an enclave of the Liassic-Dogger sea of the Mecsek Mountains. In his monograph entitled

* H-6701 Szeged, P. O. Box 651, Hungary

"A Mecsekhegység" (The Mecsek Mountains), VADÁSZ (1932) completed the fauna that had been known; he dated the exact origin of the rocks in the Aalenian Stage by the analogy of the Crinoid-bearing limestone near Ófalu and Pusztafalu villages, and by emphasising their difference from the marly formation of the Mecsek Mountains that he regarded as a heteropic one. VADÁSZ also mentioned this beds in his lecture book entitled "Magyarország földtana" (Geology of Hungary) published in 1960. He supposed the original environment as a calm, shallow sea that was not deeper as a subneritic one, and he identified the pelitic material of the sediment to be terrigenous. Using results of geophysical and geological studies BARANYAI and JÁMBOR (1962) attempted to compile the map of basement of the SE Transdanubia. This map shows Middle Jurassic formations in a narrow zone of E-W strike in line of Monyoród-Bár villages. The most detailed description of the surface outcrops has been given by KASZAP (1963). He completed the fauna with foraminifer forms, which supported its stratigraphic position in the Aalenian stage determined by belemnites and brachiopods. In his description of the quarry near Szederkény village, he divided the profile into two parts. Crinoid limestone with pale red or grey chert lens is characteristic for the lower part, while the upper part is characterised by thin-bedded, highly weathered, frequently friable cherty limestone and chert. He mentions clay, quartz grains, sponge skeletal components, and remains of siliceous foraminifers, ostracodes, gastropods and radiolarians in the insoluble residue. Beds with purer lime content contain brachiopods, belemnites and ammonites. In the higher "member", there are crinoid parts in the chert. According to KASZAP it can be interpreted as a result of syngenetic silicification. He described sponge skeleton elements in the elutration and insoluble residue of the green, micaceous, sandy as well as calcareous clay layers. According to him, inclination of the beds is 360/8°, 345/16°, 45/20°. The neighbouring profile near Máriakéménd village, and outcrops near Versend and Székelyszabar villages are sketchy characterised in his paper, too. Barabás et al. (1964) call attention to the feature that Aalenian crinoid, cherty limestone in the Máriakéménd-Bár range petrographically and faunustically has a Mecsek type facies, although, tectonically it should be Villány type. WEIN et al. (1966) and WEIN (1967) regard the formations of this zone as nearshore facies. In his diploma work, SCHLEMMER (1984) made a detailed analysis of Jurassic columns of boreholes Somberek 1 and Máriakéménd 3, and divided the formations into 13 microfacies types. This study was completed by sedimentological and mineralogical analysis of the samples. In his opinion, these formations do not show a transition to formations of similar age in Villány Mountains, but, together with Middle Jurassic beds of the Mecsek Mountains, they were formed in a complete basin system. He supposes that in this interval there was topographically accentuated basin area in which the slope facies sedimentation occupied the greatest area. The Pusztakisfalu Limestone formed on plateaus, near crinoid communities. Sedimentation in the deeper, inner parts of the basin is characterised by pelitic, aleuritic, carbonate deposit (Komló Calcareous Marl). He stated that these three facies coexisted for a long time during the Upper Lias - Lower Dogger, their formations are characterised by interdigitation and closed connection, and gave example for postponement of spreading area of the facies.

This work presents a petrographic and microfacies study of profile in the old, abandoned quarry lying 2 km to the south of Máriakéménd village and belonging administratively to Szederkény village (*Fig. 1*).

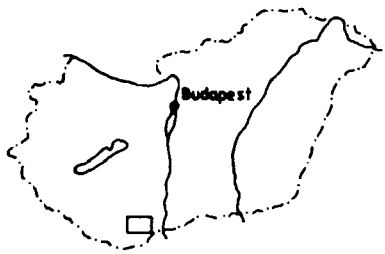

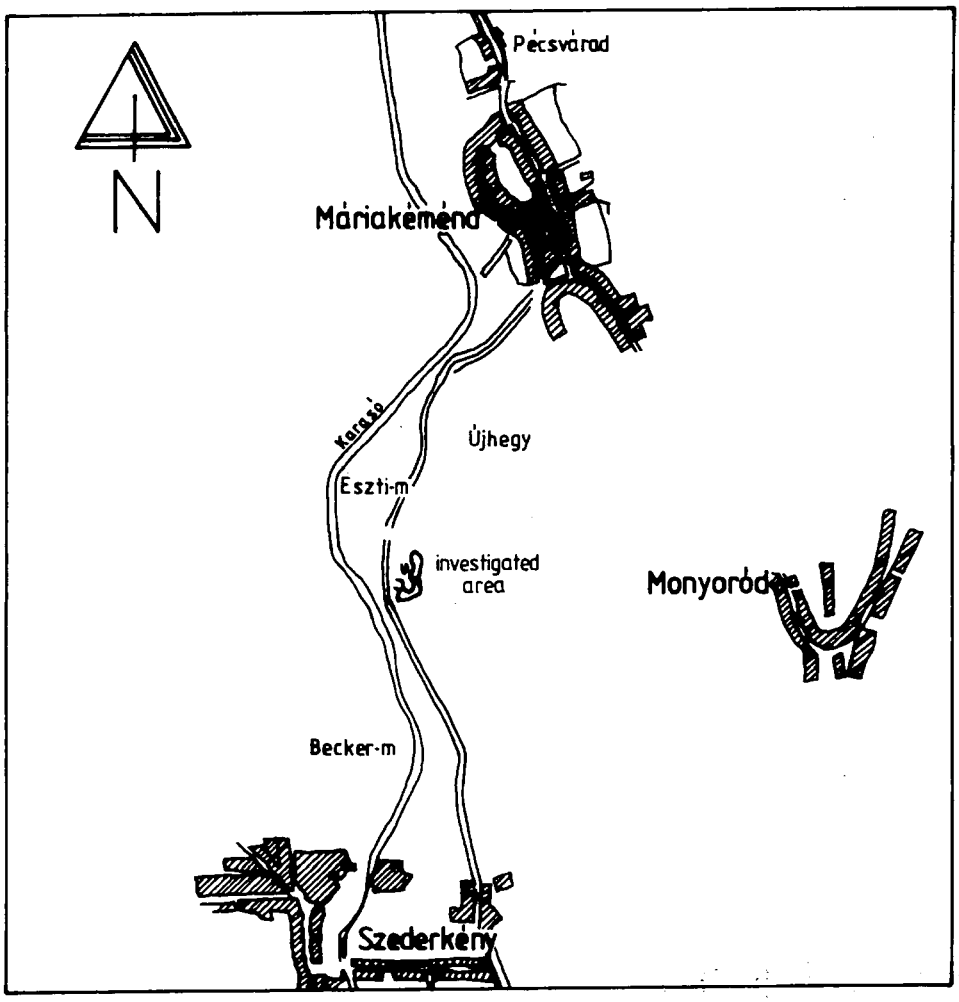

Fig. 1. Location map of the studied outcrop

GEOLOGICAL SETTING

The Mecsek and the Villány Mountains are two classic and well-exposed Mesozoic areas of the Tisza Unit. In the basin between these areas, there are Triassic and Jurassic beds outcropping from below younger formations, and form a part of the emerged Mesozoic Máriakéménd-Báta Range. This tectonic unit belongs to the Villány zone, possibly to its northernmost reverse fault (nappe?) of NNW vergence (*Fig. 2*), however, it is questionable how the stratigraphic features of the Villány Mountains are valid for the whole zone (BARABÁS et al. 1964; KÖRÖSSY 1982; SCHLEMMER 1984). This uncertainty is particularly sharp in our case because formations as old as our profile of Aalenian age (VADÁSZ 1935; KASZAP 1963) has not been pointed out in the Villány Mountains. However, Jurassic beds in the Mecsek zone near Pusztakisfalu and Ófalu villages contain layers of the same age and similar facies (PETERS 1862; VADÁSZ 1935; HETÉNYI et al. 1972; PATAKY et al. 1982). According to the issue of "Magyarország mélyfúrási alapadatai" (Drilling basic data of Hungary), in the drillings of the Máriakéménd-Báta range there is an erosion interface between the Jurassic formations and the Middle Triassic Csukma Dolomite. Traversed thickness of the Jurassic formations in the boreholes Máriakéménd No. 3 and Somberek No. 1 is 70 and 542 m, respectively.

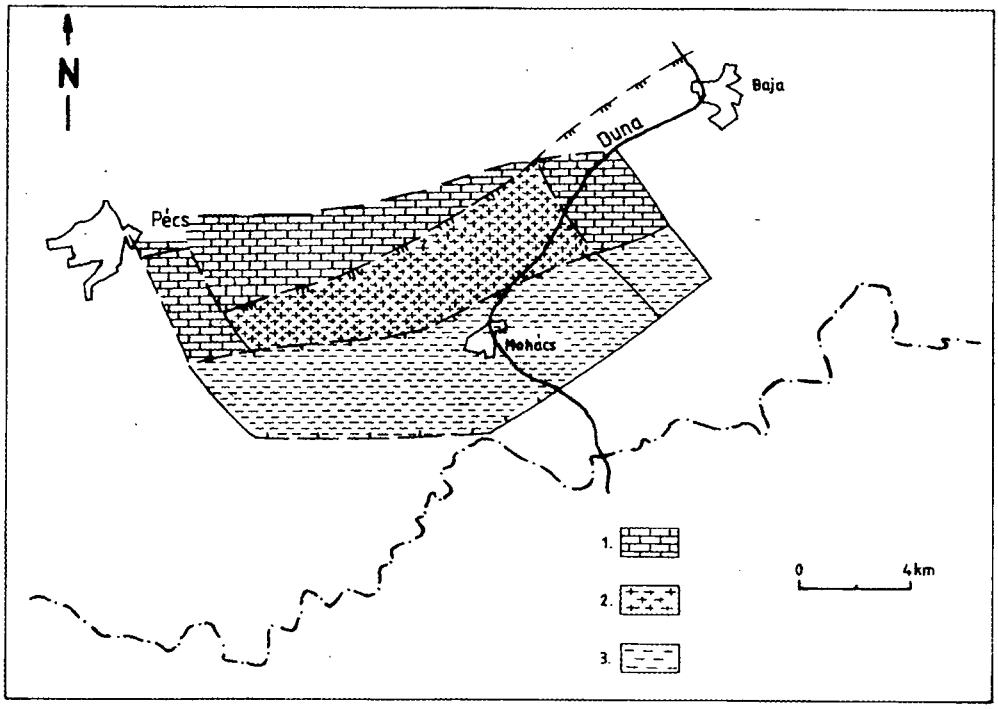

Fig. 2. Uncovered geological sketch map of SE Transdanubia
Legend: 1: Middle Triassic carbonate formations, 2: Máriakéménd-Báta range, 3: Cretaceous formations

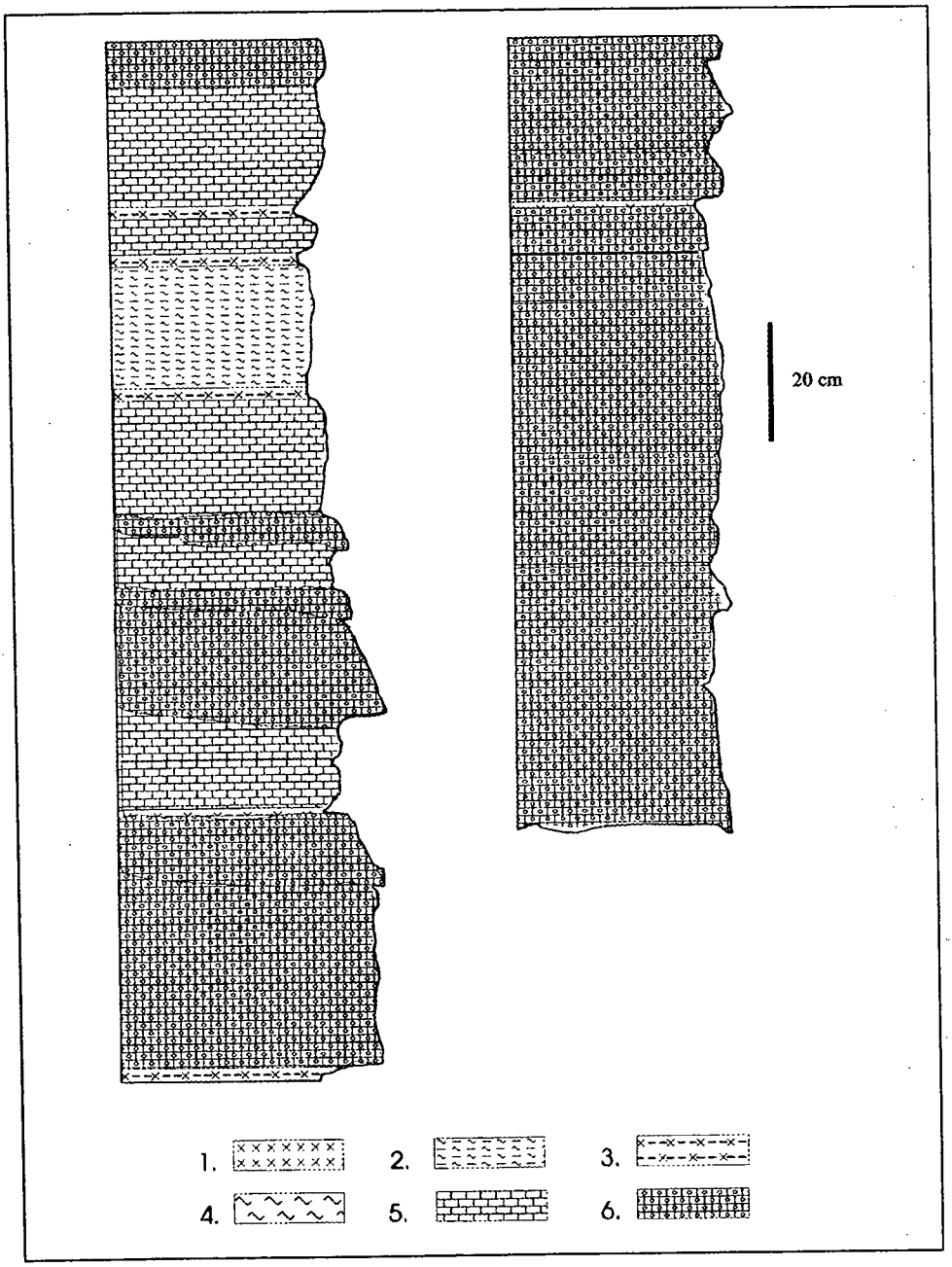

Fig. 3a. Section 1 of the profile
Legend:
1: spongiolite, 2: aleuritic cherty calcareous marl, 3: sericitic clay and clayey marl with spicules
4: clayey aleuritic marl, 5: clayey aleuritic crinoidal limestone, 6: coarse sparry allodapic crinoidal limestone

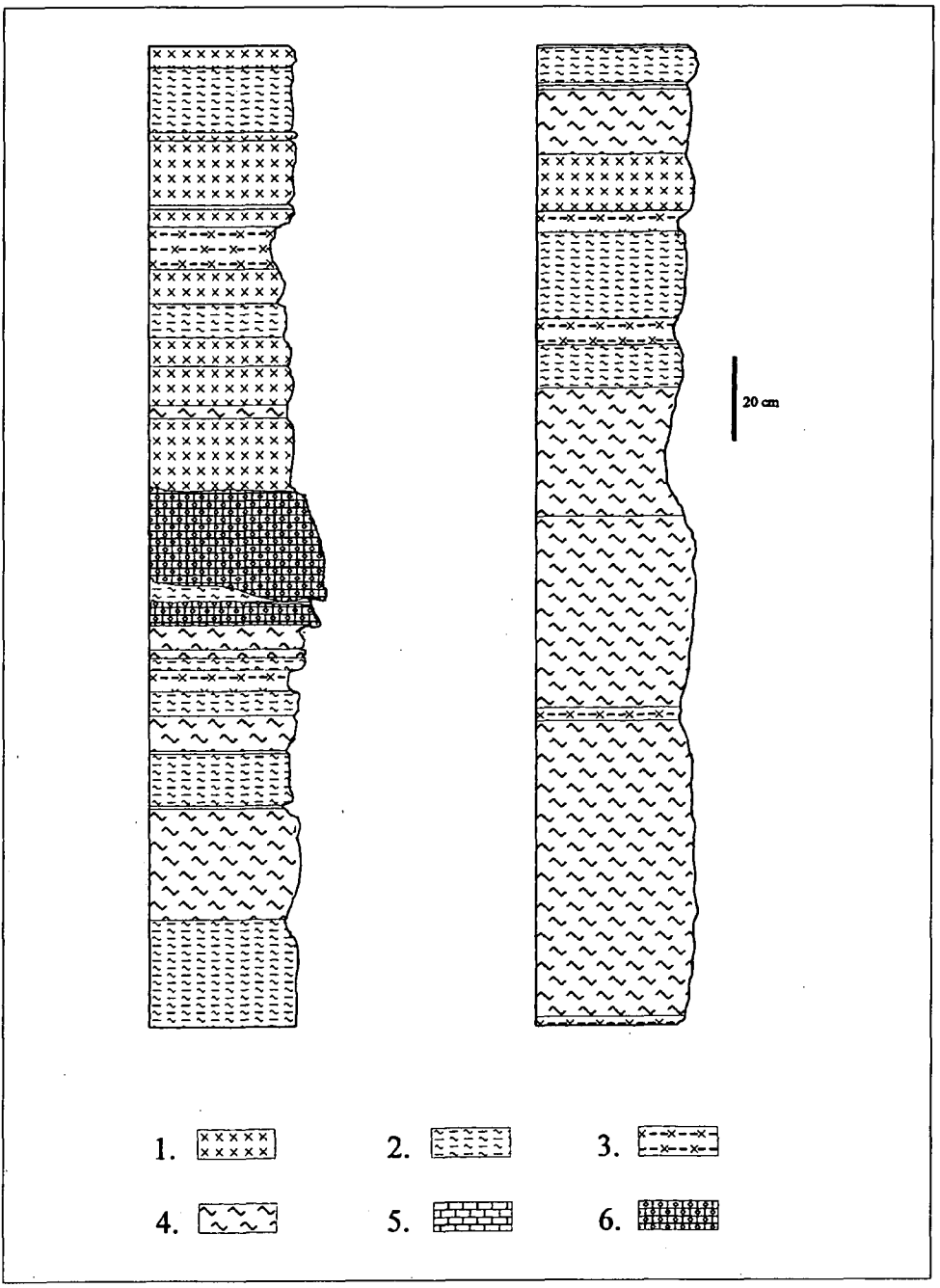

Fig. 3b. Section 2 of the profile
See figure 3a for legend.

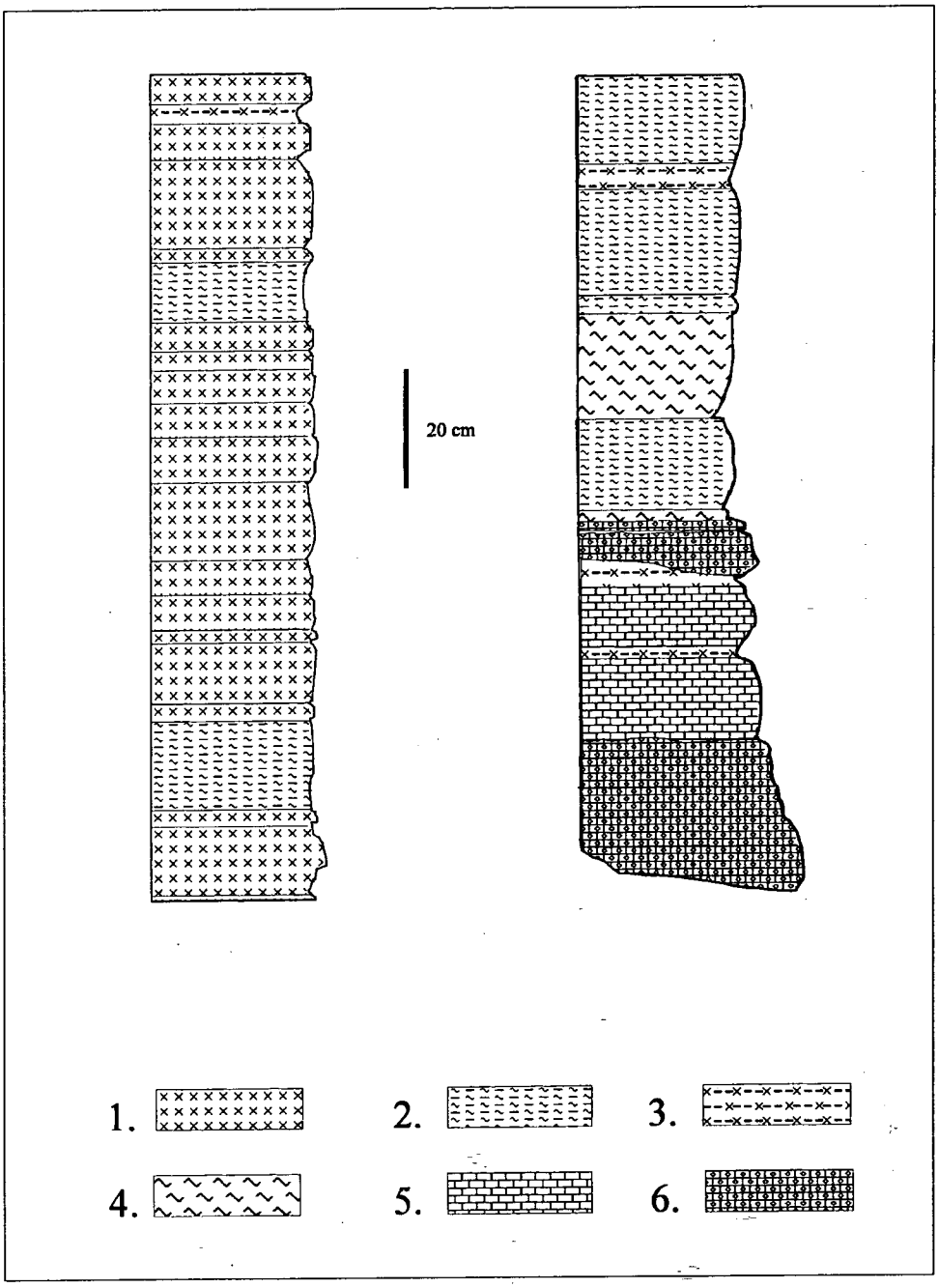

Fig. 3c. Section 3 of the profile
See figure 3a for legend.

PETROGRAPHY

The profile is built up by rocks with undulate bedding surface. Cross-stratification, mechanoglyphs on the underlying or overlying planes have not been mentioned, and I do not notice these features, either. In the lower part of the profile, characteristically over the red, sparry crinoid limestone layers, some allodapic crinoid limestone layers can be found. These layers have strikingly undulate surface, and have laterally extremely varying thicknesses, which can be a stressed diagenetic bedding form. It can not be excluded, however, that these might be diagenetically modified primary "channel" structures. Lack of proper marks, however, directions of flow and transportation can not correctly be concluded.

By macroscopic observation, the following rock types can be distinguished:

a) pale red, slightly sandy and/or aleuritic, coarse sparry, in some places cherty, crinoidal, in some levels allodapic limestone;

b) greenish yellow or brownish red, clayey, aleuritic, in some levels lithoclastic, crinoidal limestone, calcareous marl, allodapic limestone;

c) greenish grey, in altered state porous and white, aleuritic, calcareous marl, marl with chert nodules.

d) grey, in altered state porous spongiolite.

Beds of these rock types are separated from each other by strings of vivid green, sericitic clay and clayey marl. Borders of pure crinoidal limestones and these strings are very sharp, while the transition is gradual in the case of more clayey and cherty layers. Siliceous spicules, foraminifer fragments and aleurite of quartz can be identified in its washing residue.

The column can be divided into three parts on the basis of field observation completed by microfacies analyses:

1) Layers 1-34 belong to the first section ranging from the base to 3.10 m height of the quarry (*Fig. 3a*). Its dominant rock type is a red, sparry crinoidite, which is quite pure at the lower part (*Fig. 4*). At the upper part, it is often slightly (rarely highly) cherty. At some levels, the rock contains more clayey, greenish lithoclasts of millimetres (*Fig. 5*).

Microfacies of this section is characterised by the following types:

Echinoderm grainstone occurs at the base of the section, which did not show mark for gravitational redeposit in thin sections. Its fragments are well-rounded or subrounded, middle sorted bioclasts. Beside echinoderms it contains some percents siliceous spicules and mollusc fragments. Syntaxial sparry cementation can be observed around the skeletal elements (*Fig. 6*). All samples contain about 5 % unrounded quartz grain. In the more cherty samples, the sparry cement may be substituted by calcedony (chert). It can be observed in several cases that sandy echinoderm grainstone and foraminifer, spicule, bositra packstone touch with each other along a sharp border. Echinoderm grainstone totally composes of lower sorted crinoid skeletal elements cemented by syntaxial calcite. In the cases of sharp boundary surface between echinoderm grainstone and with clayey limestone of packstone texture, gradation of echinoderm grainstone can be observed, which suggests allodapic origin of the calcarenite (FLÜGEL 1978 *Fig. 7*).

Directly above the purest crinoidites, the lithoclastic crinoidal limestones generally has packstone texture. Some samples can be regarded as calcareous marl because of the higher clay content. In some samples it can be observed that the sparry grainstone texture groundmass and the packstone micrite one occur together, and they include the darker,

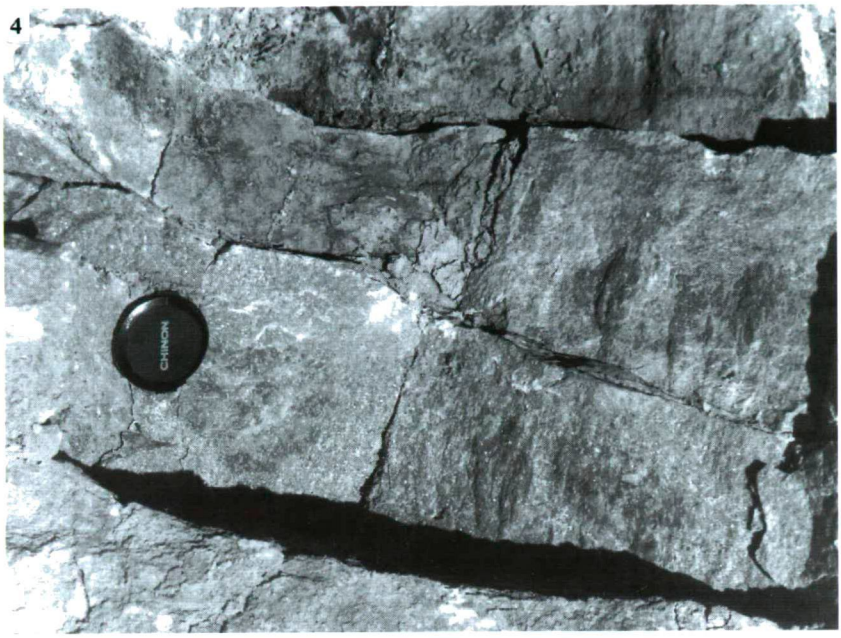

Fig. 4. Crinoidite

Fig. 5. Lithoclastic calcareous marl

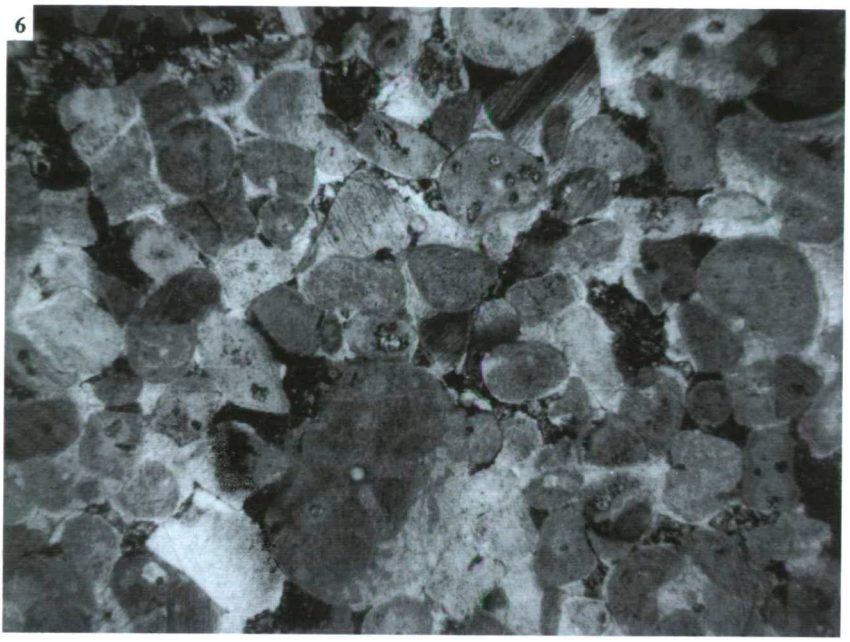

Fig. 6. Echinoderm grainstone

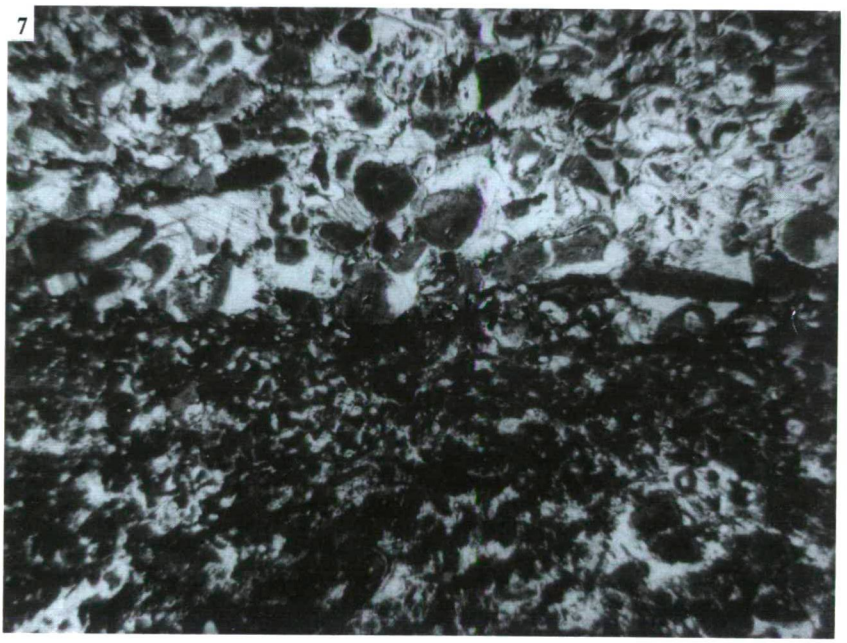

Fig. 7. Allodapic echinoderm grainstone deposited on clayey packstone

more clayey, irregularly elongated or regular lenticular lithoclasts (*Fig. 8*). Texture of the lithoclasts is characterised by echinoderm, but ratio of spicules and bositras considerably increases, too. Radiolarians also appear in the highest layers of the section. It should be noted that unrounded quartz grains of aleuritic size are enriched in laminas of some tenth mm size for some echinoderm packstone samples. Their origin is not certain; role of turbidite flows (Bouma-T_b interval) or that of floor streams can not be excluded, either (SEILACHER 1982).

2) Crinoidal limestone layers are subordinated in this section (layers 35-79). In general, 3-8 cm thick, brown, siliceous nodular, aleuritic limestone, calcareous marl, which contains crinoidal columns and lithoclasts, is characteristic. Greenish grey spongiolite layers appear, and intermediate space of layers becomes to be more thick. Thickness of this section is 4,56 m. (*Fig. 3b*)

Several samples contain echinoderms, although pelagic facies is dominant in its microfacies.

Lithoclastic microfacies described above can also be found in this section. Besides these, echinoderms biomicrite or biosparite of packstone or grainstone texture and foraminifer bositra, spicule biomicrite without sharp boundary are very frequent (*Fig. 9*). Syntaxial cement of echinoderm packstone is substituted by calcedony in several cases. Packstone (rarely wackestone) echinoderm spicule biomicrite (in which bositra and radiolarians are the characteristic accompanying forms) is a frequent microfacies, too (*Fig. 10*). In general, spicules and bositras are oriented; the latter ones form lumachelle-like texture (*Fig. 11*), while the texture shows wackestone character in other parts of same samples, therefore, the rock has a laminated appearance. Echinoderms are well-rounded, terrigenous quartz may occur at most very subordinated amount. The greyish green spongiolite, one of the dominant rock types of the section, appears in this section, too. Its microfacies is a radiolarian spicule biomicrite (*Fig. 12*). Orientation of siliceous spicules can also be observed in this section.

3) This 2,83 m thick section (layers 80-115) started from repeated appearance of red crinoidal limestone (*Fig. 3c*). There is red crinoidal allodapic limestone at its deeper part. Finer grained cherty crinoidal limestone and calcareous marl alternate with greenish cherty marl in the upper part. Dominant rock of the section is greenish grey spongiolite (*Fig. 13*). These rocks also occur in the two lower sections, and characterisation of their microfacies can be found there.

CONCLUSIONS

Microfacies studies on the profile indicate the following environment of formation:

Echinoderm grainstone belongs to the type 12 and zone 6 of the Wilson's standard microfacies zones. This facies occurs in marginal platform environment, near the shallow marine crinoid fields. Biogene elements were transported; medium of high energy, probably above the wave base, washed out the fine micritic calcareous mud from the skeletons, hence, sparry cement could be formed.

According to Wilson, spongiolite belongs to the SMF type 1. It is also suggested by the pelagic planktonic forms. The clayey calcareous mud refers to medium of low energy.

Fig. 8. Echinoderm packstone with lenticular lithoclast

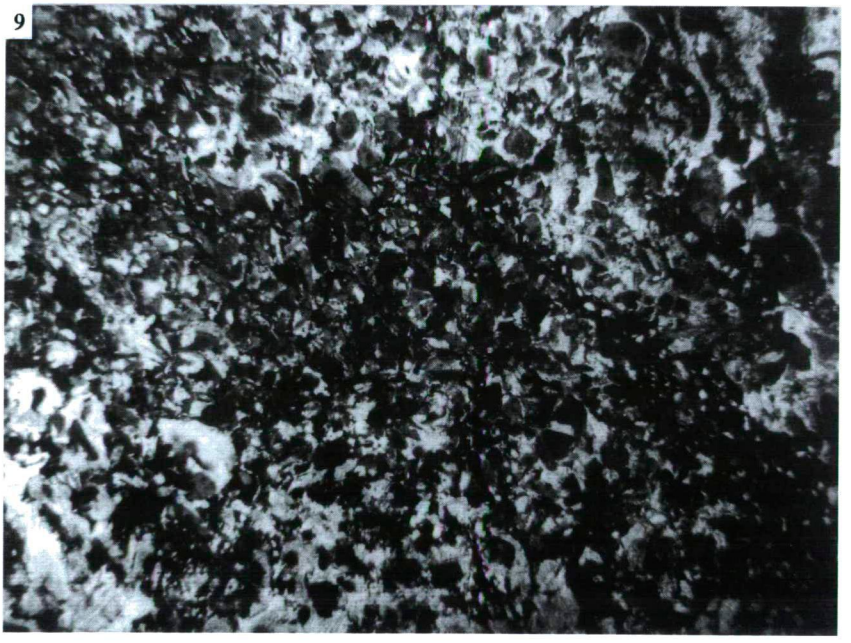

Fig. 9. Echinoderm packstone/ foraminifer bositra, spicule packstone

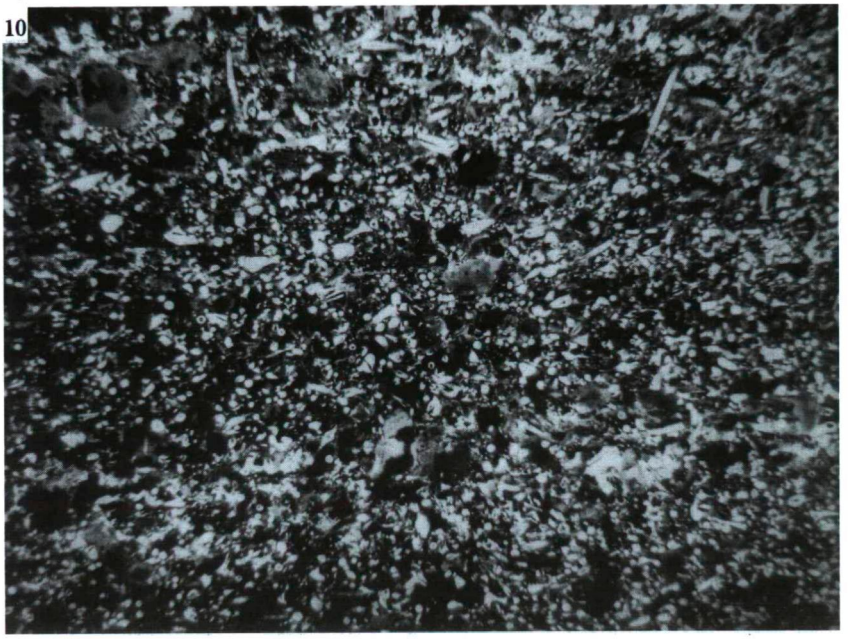

Fig. 10. Spicule biomicrite with bositra, radiolarian and echinoderm

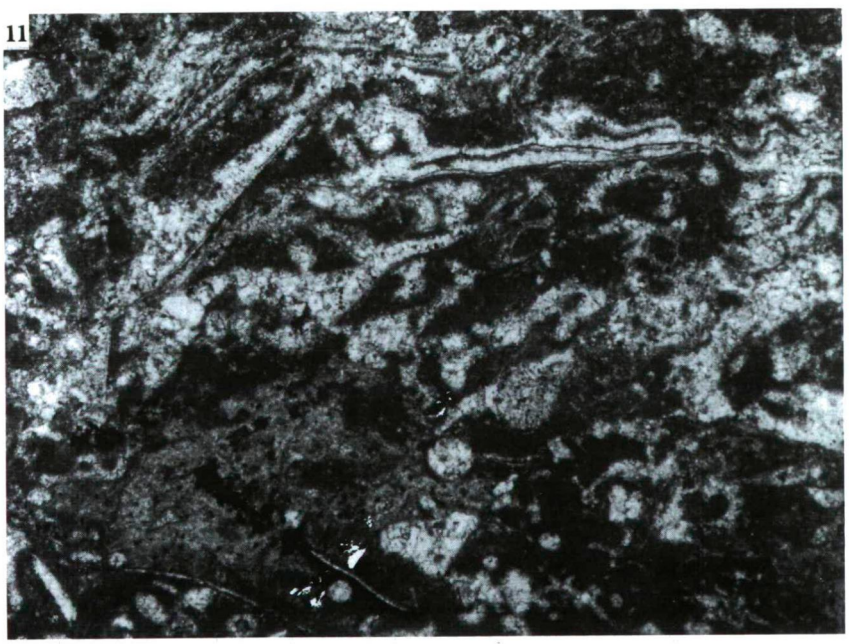

Fig. 11. Lumachelle-like oriented bositras

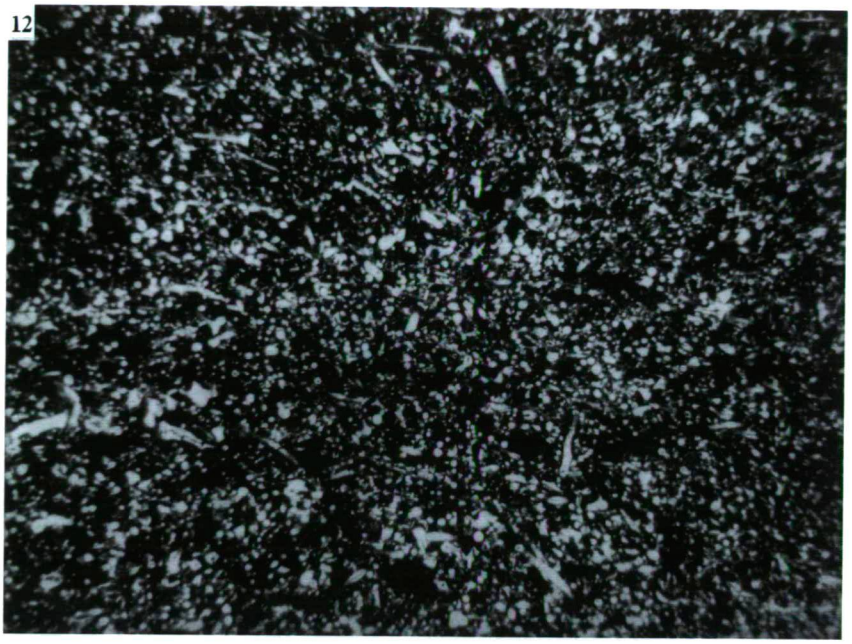

Fig. 12. Spicule biomicrite with radiolarians

Fig. 13. Spongiolite

The all other microfacies types are classified into the Wilson' SMF type 4 (slope facies). It is sure that the original deposition environment of echinoderm packstone was in a relatively shallow marine and near the biotope of crinoids. Energy of the water low, however, was not sufficient to wash out micritic matrix from the grains. Vicinity of this deposition environment, coarser grainy material moving down the slope either ripped open and included calcareous mud deposited in deeper and more quiet water as intraclasts or deposited on to it with allodapic character and sharp ravinement surface. Part of the crinoid debris rushing down the slope that reached farther appears as an echinoderm-poor microfacies of micritic matrix dominated by pelagic forms.

On the basis of study on the profile it can be stated that it is almost entirely formed by slope facies formations. Presumably, there was a sub-aerial, shallow marine facies (it is shown by terrigenous sand and silt in the material, and, perhaps, by kaolinite occurring generally but in low amount in the clay intercalations) that supported the bioclast material (first of all the crinoid calcarenite) getting the slope. Pelitic sediment characterised by siliceous sponge and pelagic plankton was formed during the periods of rest between the sediment transports.

Two zones can be identified in the profile that could be formed by intensive gravitational transport: at the deeper part of section 1 where calcareous marl and limestone appear above the pure crinoidal limestones, and at the base of section 3 where allodapic limestone can be found. Slope facies is dominant in the other parts of the profile, however, more off-shore, pelitic sediment is also important because of less intensive transport. It can not be excluded that these more intensive periods of the carbonate formations have eustatic reasons, since shelves were drowned during the relative highstands periods. In this way, if other factors do not prevent it, greater amount of biogene carbonate can be formed in the euphotic zone, and can be resedimented to slopes and basin surrounding the platform (SCHLAGER and GINSBURG 1981).

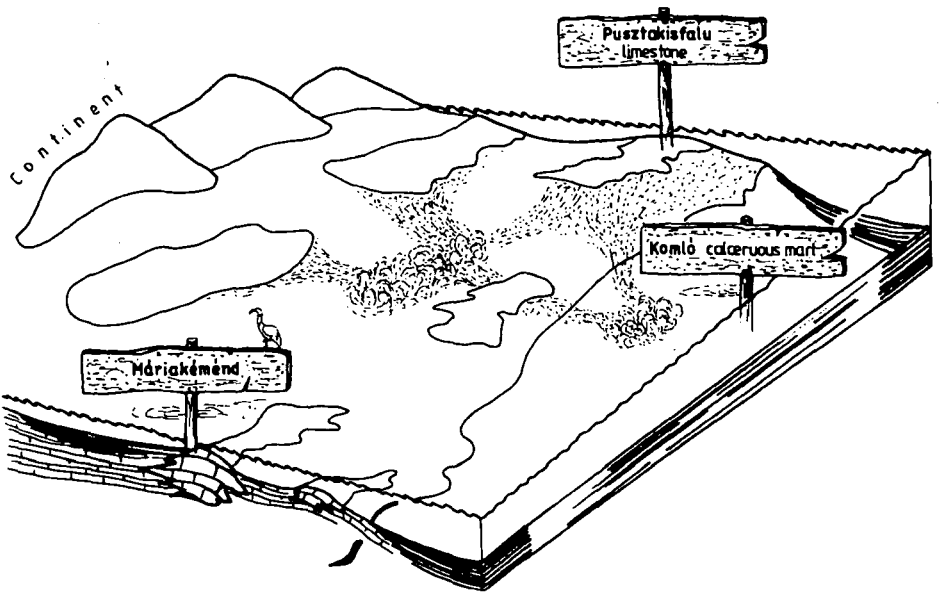

Fig. 14. Facies model of the Jurassic sequence near Máriakéménd village

Study on the surface of the profile confirms Schlemmer's opinion (SCHLEMMER 1984) that the plateau facies Pusztafakisfalu Limestone, the basin facies Komló Calcareous Marl and the intermediate facies between them coexisted for a long time in the Upper Jurassic - Lower Dogger, and interdigitation and closed connection of their formations are characteristic for this period (*Fig. 14*).

Study of the only one reference point, however, does not give an answer the question what connection is between sequence of Mecsek affinity situated on the Máriakéménd-Báta range, which tectonically belongs to the Villány zone, and that of the Mecsek zone of the same age as well as hiatus occurring in the Jurassic sequence of the Villány Mountains.

ACKNOWLEDGEMENT

The author thanks TIBOR SZEDERKÉNYI, JÁNOS HAAS and SÁNDOR KOVÁCS for their valuable consultation and significant help.

REFERENCES

BARABÁS, A. et al. (1964): Results of geophysical research of the Mecsek and Villány Mountains. A Magyar Állami Eötvös Loránd Geofizikai Intézet Évkönyve **I**, 1-126. (in Hungarian)

BARANYAI I. and JÁMBOR Á. (1962): Utilisation of complex geophysical researches and geological studies in the research of the basement in the SE Transdanubian area. Magyar Geofizika. 3, 3-4. 166-176. (in Hungarian)

HETÉNYI R. et al. (1972): Geological map of the Mecsek Mountains. 1: 10000 series. Ófalu. (in Hungarian)

KASZAP A. (1963): Mesozoic island blocks in S Baranya. Földtani Közlöny. **93**, 440-450. (in Hungarian)

KÖRÖSSY L. (1982): Review of geological structure of Hungary. Általános Földtani Szemle. **17**, 21-72. (in Hungarian)

Ifj. LÓCZY L. (1912): Geological condition of southern mountainous area of Baranya County. A Magyar Királyi Földtani Intézet Évi Jelentése. 171-182. (in Hungarian)

Ifj. LÓCZY L. (1915): Monograph of Callovian ammonites of the Villány Mountains. Geologica Hungarica. I. fasc. 3-4. (in Hungarian)

PATAKY N. et al. (1982): Jurassic sequence of the Szén Valley near Ófalu village. Földtani Közlöny. 112, 383-394. (in Hungarian)

SCHLEMMER K. (1984): Microfaciological and sedimentological studies on Jurassic sequence of the boreholes Somberek No. 1 and Máriakéménd No. 3. Manuscript. Department of Petrology and Geochemistry, Eötvös University. (in Hungarian)

SZABÓ J. (1867): Geological notes on the Batina-Bán and the Mohács island. Magyar Királyi Földtani Intézet Évi Jelentése. 336-352. (in Hungarian)

VADÁSZ E. (1935): The Mecsek Mountains. 1-180. (in Hungarian)

VADÁSZ E. (1960): Geology of Hungary. Akadémiai Kiadó, Budapest. (in Hungarian)

WEIN Gy. et al. (1966): Explanation of the geological map series of Hungary. 1:200000 series. L-34-XIII-Pécs. (in Hungarian)

WEIN Gy. (1967): Connections of the orogenic structure zones of SE Transdanubia in the ancient Alpine cycle. Földtani Közlöny. **97**, 286-293. (in Hungarian)

Manuscript received 2. Sep. 1996.

Acta Mineralogica-Petrographica, Szeged, XXXVII, 181–187, 1996

SUBVOLCANIC BASALTIC DYKE FROM BEREMEND, SOUTHEAST TRANSDANUBIA, HUNGARY

S. MOLNÁR[1], T. SZEDERKÉNYI[1]

Department of Mineralogy, Geochemistry and Petrology,
University of Szeged

ABSTRACT

Penetrating Aptian limestones (Nagyharsány Limestone Formation) a narrow subvolcanic body (dyke) has been found in the quarry of Beremend Cement-Plant. Based on its bulk composition this rock can be ranged into the basalt group in general and its low alkaline content suggests a picrobasaltic character. K/Ar age determination (from the whole rock) show a Late Cretaceous subvolcanic event, but the petrochemical data suggest a conection with Miocene basalts and andesito-basalts from Podravska Slatina and Popovac Hill.

INTRODUCTION

Brecciated volcanic body was found by MANGULT (1995) in the Aptian limestone of quarry of Beremend Cement-Plant (*Fig. 1.*) with about 180° strike in perpendicular position. The lava rock terminates 12 m below the surface. Two narrow vein-like fractured zone join to it filled by clay minerals running up to the surface (*Fig. 2.*). Thickness of the dyke does not exceed 2 m accompained by several dm thick contact zones, wich latters are represented by weathered ankerite-siderite enrichment (*Fig.3.*). Rock material of the lava body is also weathered in some degree.

PETROGRAPHY

Brecciated subvolcanic rock macroscopically may be subdevided into two types, as follows: (1) a fine-grained, compact black rock with dense carbonatic veinlets and (2) green-coloured highly altered rock without any visible minerals. This latter group forms xenolites in the first one.

Microscopically the black rock type shows a tipical micro-holocrystalline porphyric texture (*Fig.4.*) with microcrystalline groundmass (about 50%) and 100-150 μm large porphyric clinopyroxene crystals. A fairly low portion of the porphyric ingredients are euhedral (?) labradorites measuring 50-100 μm size. This rock is rather rich in accessories, mostly rutiles and magnetites and/or ilmenites. The light green-coloured type does not contain microscopically determinable minerals. By X-ray measurements it consists of predominant calcite and fairly big portion saponite minerals. *(Fig. 5)*.

[1] H-6701 Szeged, P. O. Box 651.

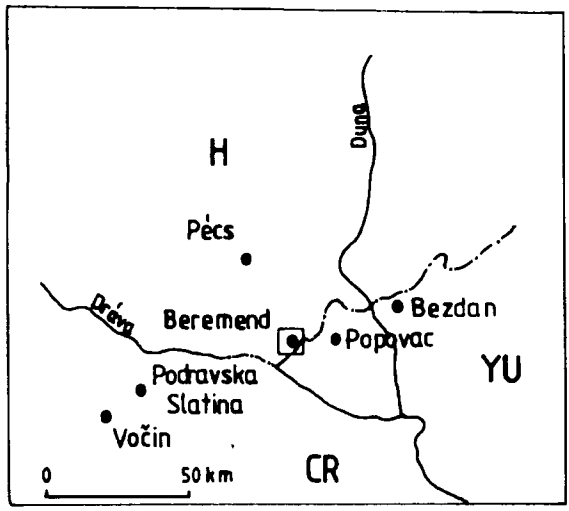

Fig. 1. Site of Beremend occurence.

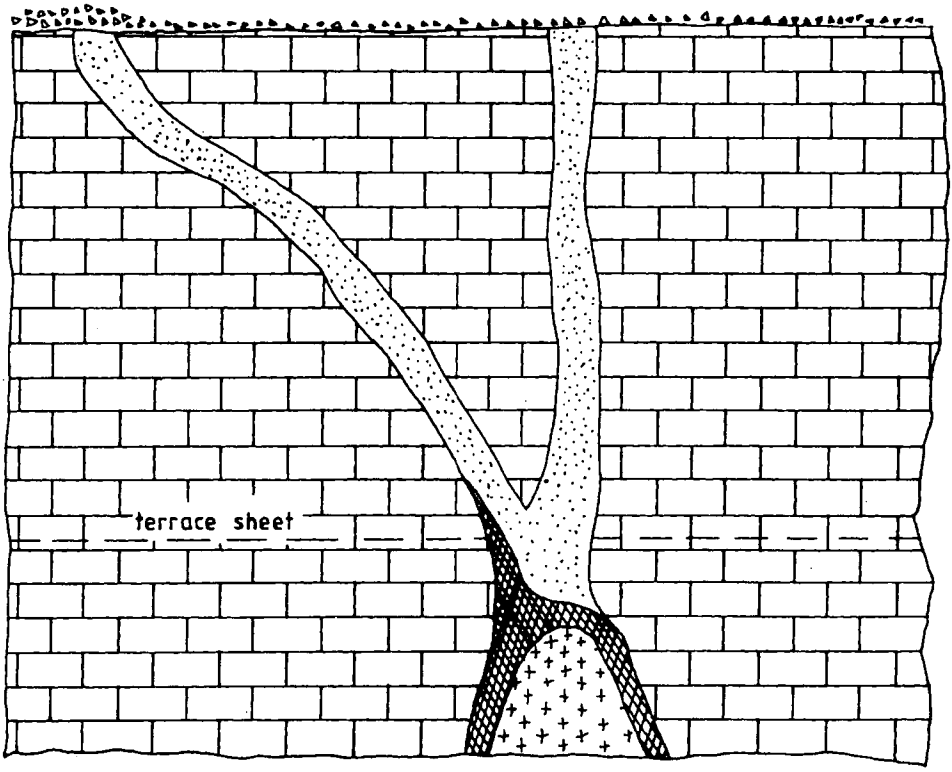

Fig. 2. A sketch about volcanic body and its continuation (MANGULT 1995).
1. Vein-like fractured zone. 2. Contact zone. 3. Aptian limestone. 4. The volcanic body. 5. Recent sediments.

Fig. 3. The volcanic body in Aptian limestone
1. The volcanic body. 2. The Aptian limestone

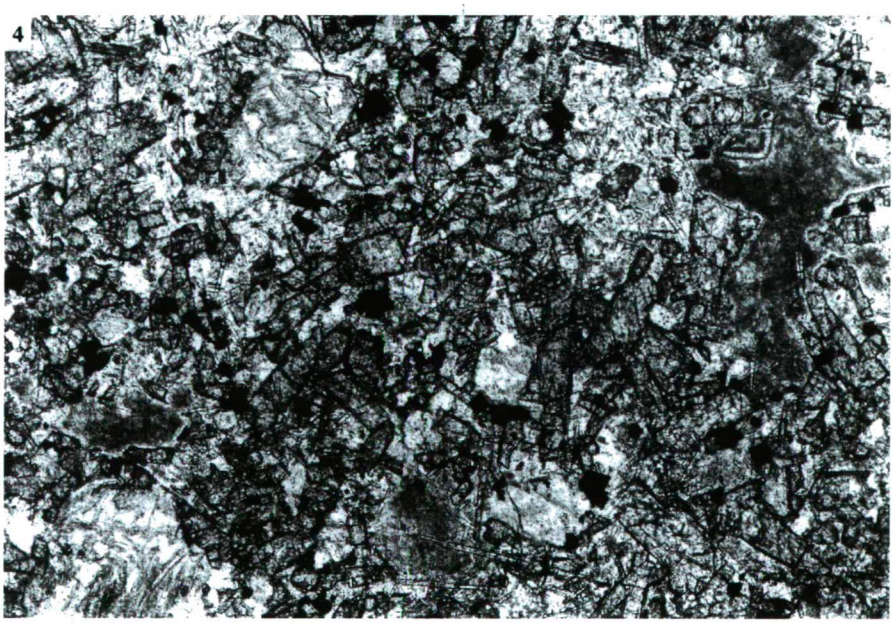

Fig. 4. Texture of the basalt xN n=36

CHEMICAL CHARACTER

Representing mainly of inner part of the dyke the chemical analyses are prepared from the first type (black, relatively fresh) of subvolcanic rock and two ones were made from the xenolites (Table 1.). Most conspicuous chemical characteristics of this bulk compositions are as follows:

– extraordinarily low SiO_2, Al_2O_3 and alkalines and extremly high CaO, CO_2 and H_2O content,

– approximately high Fe_2O_3 + FeO, MgO, P_2O_5 and H_2O content (the last may be faulty).

Taking into account the carbonatic environment, the high CO_2 and CaO content are understandable. Excess of Fe_2O_3 versus FeO is also acceptable in this oxidative surroundings. X-ray measurements show a lack of dolomite in the samples, so the MgO content belongs to the rock-forming minerals, really. Calcite occurs in a fairly big quantity everywhere. Nevertheless, discounting the Ca quantity bound in the calcite, the remaining CaO content is still considerably high may be due to the assimilation. Using the TAS diagram (LE BAS et al. 1986, *Fig. 6.*) this rock in its present state can be classified as picrobasalt, by STRECKEISEN method it is basalt and andesito-basalt.

TABLE 1

The bulk composition of the rocks

	1 ÁGK-6819/a	2 ÁGK-6819/b	3 ÁGK-6819/c	4 ÁGK-6817/a	5 ÁGK-6817/b
SiO_2	36.90	35.00	35.70	22.20	27.40
TiO_2	1.91	1.74	1.77	0.03	0.11
Al_2O_3	10.70	10.20	10.10	1.54	3.10
Fe_2O_3	8.79	7.86	8.12	3.69	4.32
FeO	1.99	2.29	2.24	0.50	0.72
MnO	0.10	0.13	0.13	0.09	0.05
MgO	7.16	7.38	7.57	5.46	5.98
CaO	15.80	17.40	17.60	35.80	31.50
Na_2O	0.61	0.78	0.77	0.04	0.09
K_2O	0.95	0.92	0.94	0.06	0.07
H_2O^+	5.41	5.79	5.94	2.73	2.48
H_2O^+	4.17	2.86	2.75	2.40	2.33
CO_2	3.99	5.66	5.10	25.50	22.10
P_2O_5	1.39	1.22	1.21	n. d.	0.05
Sum.	99.87	99.23	99.94	100.04	100.30

Analysed by FARKAS, J. Hung. Geol. Survey 1996.

AGE AND VOLCANIC CONNECTIONS

Two K/Ar isotopic age determinations were carried out in the Nuclear Research Institute, Debrecen by BALOGH KAD. Age of the black rock (measured from whole rock) proves to be a 76-3 Ma, i.e. younger than that of Nagyharsány Limestone Formation, but this datum requires further confirmation. Age of green-coloured xenolite (also from whole rock) is 129,5-14.2 Ma. Due to very-low radiogene potassium content this datum particularly requires further confirmation.

Fig. 5. Rutiles in the gruondmass 1N n=7O

Regarding possible areal connections of this subvolcanic body it is clear, that nearest Upper Cretaceous magmatite occurence can be found in Hungarian Bácska (Kunbaja No. 5 borehole) belonging to so-called Banatite Association (SZEDERKÉNYI 1984). But the Beremend volcanics are not granitoids, so, there are no any relationships between them. Moreover, no traces of Upper Cretaceous magmatic events are pointed out in the area of Tisia Terrane, except banatites. Thus, it needs to take into consideration some possible connections with Miocene volcanism took place in the vicinity. E.g. basalts and andesites from Popovac Hill (GOLUB 1957), and basalts and andesito-basalts from Podravska Slatina and Vočin (LUGOVIĆ, 1983, GOLUB and MARIĆ 1968, PAMIĆ 1986, 1987, LUGOVIĆ et al. 1990), which show fairly close petrogenetic relationships with the Beremend basalt.

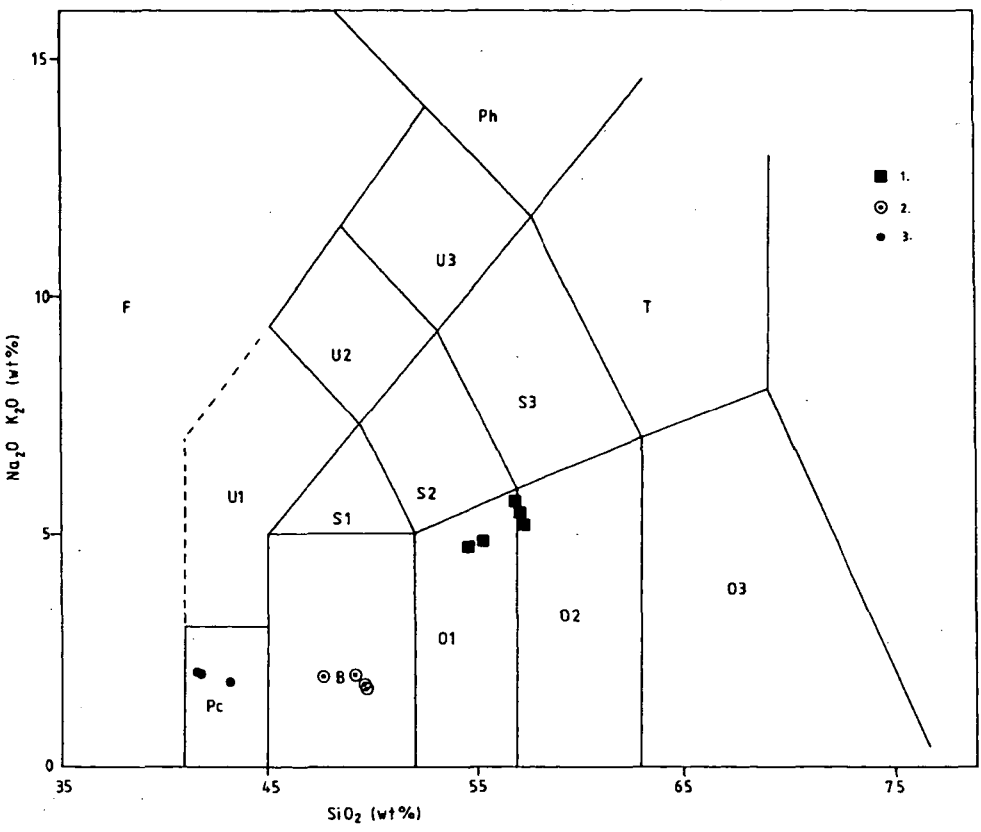

Fig. 6. The TAS diagram for Beremend basalt (LE BAS et al. 1986)
F=Foidite; Pc=Picrobasalt; B= Basalt; U1= Tephrite/basanite; U2= Phonotephrite; U3 = Tephriphonolite; Ph = Phonolite; S1 = Trachybasalt; S2 = Basaltic trachyandesite; S3 = Trachyandesite;
T= Trachyte/trachiandesite; 01 = Basaltic andesite; 02 = Andesite; 03 = Dacite . 1. Andesito-basalts from Pdravska Slatina (LUGOVIĆ et al. 1990) 2. Basalts from Popovac Hill. (GOLUB 1957) 3. Picrobasalts from Beremend.

REFERENCES

GOLUB, L. (1957) : Basalto-andesite near Popovac (in croatian) Geol. Vjesnik **10**, 111-112.

GOLUB, L., MARIĆ, L. (1968): Quarz-trachiandesite from Lučarski Vis. Geol. Vjesnik. **21**, 255-271.

LE BAS, M. J., LE MAITRE, R.W., STRECKEISEN, A., ZANETTIN, B. (1986): A chemical classification of volcanic rocks based on the total alkali-silica diagram. J. Petrol. **27**, 745-750.

LUGOVIĆ, B. (1983): Effusive rocks in the NW-part of Papuk Mts. Geol. Vjesnik (in Croatian). **30**, 135-156.

LUGOVIĆ, B., MAJER. V., STUMPFL, W. (1990): Geochemical Characteristics of Basaltic Andesites from Baranja (Croatia, Yugoslavia). Geol. Vjesnik **43**, 135-142.

MANGULT, I. (1995): Terepi jelentés a beremendi vulkanitról (Field report from Beremend volcanics, in Hungarian) Manuscript.

PAMIĆ, J. (1986): Magmatic and metamorphic complexes of the adjoining area of the Northernmost Dinarides and Pannonian Mass. Acta Geol. Hung. **29/3-4/**, 203-220.

PAMIĆ, J. (1987): Miocene basalts from Budim, on the northen flanks of Mt. Papuk south of Podravska Slatina in Slavonia. RAD Yugoslovenska Akad. Znanosti i Umjetnosti. Tom. **431**, 53-67.

SZEDERKÉNYI, T. (1984): Crystalline basement of the Great Plain and its relationships. Acad. Doct. Thesis (in Hungarian). MTA Library, Budapest.

Manuscript received 16. October 1996.

Illustrations

Figures should be used only where they are essential to elucidate text.

The illustrations should be numbered according to their sequence in the text, and in the text references should be made to each figure.

All illustrations should be given separately, not stuck on sheets and not folded. The number of the figure and the authors name should be noted on the reverse side of the photographs and on the lower frontside of drawings, indicating at the same time the top of the figure where it necessary.

Captions for all figures should be given typewritten on a separate list at the end of the manuscript. Drawn text in the figures should be kept to a minimum.

Drawings should be made on tracing paper by Indian ink. The thickness of the lines and the size of the lettering should enough to allow a necessary reduction.

Photographs of good contract and intensity on glossy paper are only acceptable. Colour photographs or drawings cannot be accepted.

Use bar scale on all illustrations instead of numerical scales that must be changed if reductions are necessary.

References

All references to publications made in the text should be made by quoting the author's name (without initials) and year of publications in paranthesis.

The list of references at the end of the manuscript should be arranged alphabetically by author's names and chronologically per author.

If the referred publications are written by more than two authors, in the text only the name of the first author should be indicated, the other co-authors are denoted by "et al.", however, in the list of references the names of authors and all co-authors should be mentioned.

In the list of references all references should be written, e. g. Balogh, K., A. Barabás (1972): The Carboniferous and Permian of Hungary. Acta Miner. Petr. Szeged, XX/2, 191–207.

At references to books beside the author's name, year of publicaton, title and the publishing house should also be mentioned.

In the case of references for symposium volumes, special issues or multi-authors books, the following system should be used: Roser, B. P., C. W. Childs, and G. P. Glasby (1980): Manganese in New Zealand. In: I. M. Varentsov and Gy. Grassely (Editors): Geology and Geochemistry of Manganese, Vol. II. Akadémiai Kiadó, Budapest, 199–211.

Manuscripts that are not adequately prepared will be returned to the authors(s).